Évolution de l'évolution de l'occupation du sol (1950-2025) et impacts sur l'érosion du sol dans un bassin versant méditerranéen

Hari Gobinda Roy

THESE

présentée devant

l'Université de Nice - Sophia Antipolis

en vue de l'obtention du

DIPLÔME DE DOCTORAT

(arrêté ministériel du 30 mars 1992)

Spécialité : Géographie

par

Hari Gobinda ROY

Long term prediction of soil erosion (1950-2025) in a Mediterranean context of rapid urban growth and land cover change

Evolution de l'évolution de l'occupation du sol (1950-2025) et impacts sur l'érosion du sol dans un bassin versant méditerranéen

Soutenue le 15 septembre 2016

Membres du Jury :

Pr Pierre CARREGA	Examinateur
Pr Dennis FOX	Directeur
Pr Catherine MERING	Rapporteur
Pr Laurent RIEUTORT	Rapporteur
Pr Yves BAUDOUIN	Examinateur

UMR ESPACE 7300 CNRS

Equipe Gestion et Valorisation de l'Environnement
Université de Nice – Sophia Antipolis, 98 Blvd Edouard Herriot, 06204 Nice

ABSTRACT

The European Mediterranean coastal area has experienced widespread land cover change since 1950 because of rapid urban growth and expansion of tourism. Urban sprawl and other land cover changes occurred due to post-war economic conditions, population migration, and increased tourism. Land cover change has occurred through the interaction of environmental and socio-economic factors, including population growth, urban sprawl, industrial development, and environmental policies. In addition, rapid expansion of tourism during the last six decades has caused significant socioeconomic changes driving land cover change in Euro-Mediterranean areas. Mediterranean countries from Spain to Greece experienced strong urban growth from the 1970's onwards, and a moderate growth rate is projected to continue into the future. Land cover change can result in environmental changes such as water pollution and soil degradation. Several previous studies have shown that Mediterranean vineyards are particularly vulnerable to soil erosion because of high rainfall intensity and the fact that vineyards are commonly located on steeper slopes and the soil is kept bare during most of the cultivation period (November to April) when precipitation is at its highest.

To date, few Euro-Mediterranean studies of land cover change explicitly explore spatial constraints on land cover change patterns. Many modeling tools have been developed to explore and evaluate future land cover change possibilities, and time scales have varied greatly from one study to another. Most LUCC models relate change to physical and socio-economic factors in a grid of cells.

The main objective of this thesis is to predict long-term soil erosion evolution in a Mediterranean context of rapid urban growth and land use change at the catchment scale. In order to achieve this, the following specific aims have been formulated: (i) to analyze the spatial dynamics of land cover change from 1950 to 2008; (ii) to compare the impact of historical time periods on land cover prediction using different time scales; (iii) to test the impacts of spatial extent and cell size on LUCC modeling; and (iv) to predict the impact of land cover change on soil erosion for 2025.

The study area of approximately 235 km² is situated in the Var, a department located in southeastern France near the Gulf of St. Tropez. The western and higher part of the watershed,

consisting of about 70% of the catchment, is mostly pine and oak forest; the topography is uneven with the highest elevation at about 650 m. The eastern and lower part of the catchment is a gently sloping alluvial plain. The catchment area is characterized by a Mediterranean climate with hot, dry summers and cooler, rainy winters. Land cover maps were screen-digitized from digital orthorectified aerial photographs (1950, 1982, 2003, 2008, & 2011) purchased from the Institut Géographique National. In order to determine past land cover change patterns, surfaces were classified into five land cover categories based on visual interpretation, namely forest, vineyard, grassland, urban, and suburban. To analyze the spatial dynamics of past land cover change and create a model to predict future land cover change, surfaces were simplified into four categories, namely forest, vineyard, grassland, and built area. (Urban and suburban areas were combined into built area due to their small amount of coverage compared to other land cover categories.) Finally, soil erosion was predicted for the vineyard category.

The aerial photographs from 1950 were the first high-quality post-Second World War photographs available when the area was still largely rural. An intermediate date of 1982 was selected between 1950 and the most recent photographs. Aerial photographs from 1982 represent land cover conditions at the beginning of rapid urban sprawl. Cell size of all digitized maps was changed from 1 m to 25 m to make land cover layers compatible with the 25 m DEM used for the creation of topographic and distance variables.

Land cover change was analyzed using the Land Change Modeler (LCM) and CROSSTAB modules of IDRISI (Eastman, 2012). Explanatory variables were selected through Cramer's coefficient. Land cover maps for 2011 were predicted using three different time scales, namely 1950-1982, 1982-2003, and 2003-2008. These predictions were then compared to the actual digitized land cover map from 2011 to evaluate model accuracy. Major topographic and distance variables were identified including the following: slope, altitude, distance from roads, distance from built area in initial year, and distance from streams. In addition, three constraints and incentives-- forest to built area, vineyard to built area, and grassland to built area-- were included in the prediction process. These were created from the *Plan Local d'Urbanisme* (PLU) and the *Schéma de Cohérence Territoriale* (SCOT). Kappa index and confusion matrix were used to evaluate the model's accuracy. LCM of IDRISI was used to predict land cover in 2011.

LCC dynamics, both in terms of absolute and relative change, were first analyzed using intensity analysis. Then land cover was predicted for 2011 for large (79.1 km²) and small (36.6 km²) windows using cell sizes of 25 m, 50 m, 100 m. Spatial resolution effects were also analyzed by upscaling from 25 m to 50 m and 100 m and then downscaling back to 25 m. Here spatial extent is equivalent to increasing the proportional area of a dormant category. Two spatial extents (36.6 km² and 79.1 km²) and three resolutions (25 m, 50 m and 100 m) were tested. The 50 m and 100 m resolutions were downscaled back to 25 m. Land cover maps dated from 1950, 1982, 2003 and 2011, and LCM was used to predict 2011 cover. Finally, RUSLE was used to predict soil erosion for different years: 1950, 1982, 2003, 2011, and 2025 (predicted).

This study found that land cover changes were concentrated mainly in the alluvial plain and adjoining foothills. Forest remained the dominant land cover in the catchment, changing only slightly from around 86% to 85% in 1950-2008. However, forested areas underwent significant swapping with vineyard and grassland areas. The catchment experienced a marked decrease in vineyard (-28%) and a substantial increase in grassland (about +50%). Urban and suburban areas remained a minor component of the catchment (about 3%), but showed a dramatic relative increase (more than 20 times initial cover). Built areas grew at the expense of vineyards, and grassland also increased on former vineyards. Losses in vineyard were offset in part by growth of vineyard on previously forested foothills close to the alluvial plain. This finding differs from other Mediterranean studies that have shown agriculture (i.e. vineyard cultivation), in the face of urban pressure, moving to steeper marginal slopes, while abandoning fertile plain soils to grassland and forest. Topography (altitude, slope) and distance variables (from roads, streams, built area, and the sea) strongly influenced land cover change dynamics in the catchment between 1950 and 2008. Vineyard located near streams was converted mainly to grassland. Built areas were strongly dependent on roads and former built areas for expansion but expanded little near streams due to flooding risks. Finally, the rate of change was greater during the latter part of the study (1982-2008) than in the earlier period (1950-1982).

Kappa index and confusion matrix were used to evaluate the model's accuracy. Altitude, slope, and distance from roads had the greatest impact on land cover changes among all variables tested. Good to perfect level of spatial agreement and perfect level of quantitative agreement were observed in long to short time scale simulations. Kappa indices (Kquantity = 0.99 and Klocation

= 0.90) and confusion matrices were good for intermediate and best for short time scale. The results indicate that shorter time scales produce better predictions. Time scale effects have strong interactions with specific land cover dynamics; for example, stable land cover categories are easier to predict than rapidly changing ones, and overall quantity is easier to predict than specific location over longer time periods.

Spatial extent had a major impact on land cover change dynamics as absolute and relative values of gains/losses were inverted when dormant category increased. It also improved Cramer's V values (1.3 to 1.5 times greater) and disagreement values artificially improved (twice as good) in change prediction; this resulted from an increase in the number of correctly classified persistent cells. Upscaling/downscaling revealed that coarser cell sizes lose considerable predictive power (1.5 to 2 times greater allocation errors), despite validation statistics. In future studies, dormant category area should be minimized and upscaling/downscaling should be done if data are modeled at coarser resolutions than original cell size.

Land use changes were found to have a significant impact on soil erosion rates in different years. Between 1950 and 2003, soil erosion prone areas increased in the eastern and central parts of the study area; there was decreased soil erosion in the north and western parts of the catchment due a shift from vineyard to built area in the alluvial plain area. Vineyard decreased in the alluvial plain land, and increased in the upland valley and foothills. Therefore, mean and median slope values increased moderately in the same time period. A positive relationship between slope gradient and erosion rates in different years (1950, 1982 & 2003) was observed in this study.

Table of Contents

List of Tables

List of Figures

GENERAL INTRODUCTION

PURPOSE OF THE STUDY

The issue of land cover change has become important throughout the world in recent years, not only for researchers, but also for urban planners and environmentalists advocating and planning for sustainable land use in the future. In Mediterranean Europe, land cover patterns have changed greatly since the Second World War due to intensive human activities, population growth, and urban sprawl. The rapid growth in industrial and tourism activities has accelerated land cover changes in the Mediterranean coastal area in particular. Moreover, in recent decades, urban population growth and expansion of tourism have occurred more in the French Mediterranean coastal area than the average for European Mediterranean coastal areas (Blue Plan Papers, 2001). The increasing number of secondary homes and sport harbors along the Mediterranean coastline of southeast France—"La Côte d'Azur" (the French Riviera)—has transformed the pattern of land cover in the French Mediterranean coastal area (Benoit and Comeau 2005, EAA 2011). French Mediterranean cities have become popular destinations for affluent people from France and other countries to buy vacation and retirement properties. This has resulted in significant land cover change in this region, yet very few studies describing land cover change in this particular area have been conducted to date.

Most of the previous studies on land cover change in the Mediterranean area have highlighted one particular issue and/or described one specific type of land cover change. Few studies have taken into account multiple changes concurrently. In addition, spatial patterns of land cover change and identification of driver variables influencing change have sometimes been considered, but these studies have focused mainly on altitude and slope. For example, Fox et al. (2012) analyzed the impact of land cover change on total runoff between 1950 and 2003 in the upper part of the study catchment area. They noted a small increase in runoff due to a complex pattern of land cover change, but much of the lower alluvial plain, where most changes have occurred, was ignored, and spatial controls on these changes were not examined.

At the outset of this study, 27 recent studies involving land cover change analysis and modeling using CA-Markov and Multi-Layer Perceptron (MLP) with multiple land covers and

urban areas were examined. No studies were found on the comparison of different time scale simulations and the impact of historical time period on land cover prediction using different time scales. Thus, in this study, land cover change has been predicted using different time scales to assess the impacts of historical time period in predicting the land cover map of 2025.

Spatial extent refers to the overall size of a particular area (Turner et al., 1989, Qui & Wu, 1996, Wu, 2004). The review of 27 recent studies (2001-2014) using CA-Markov and MLPNN modeling tools reveals that spatial extent ranged from 114.4 km² to 20,000 km², with mean and median values of 3,056.3 km² and 1,200 km², respectively. If land cover change is distributed homogeneously throughout space, then spatial extent probably has little impact on model prediction outcome. However, many areas have cores of evolving land covers surrounded by less active categories. Increasing spatial extent can introduce new land cover change dynamics (Kok & Veldkamp, 2001) or land cover categories (Turner et al., 1989), but in this study, larger spatial extent will be considered synonymous with increasing the proportional area occupied by a relatively dormant category.

Dietzel & Clarke (2004) proposed guidelines for urban simulation models on spatial resolution (10 m to 1,000 m) in four spatial extents, and found that finer resolutions of less than parcel size (≤ 10 m) in land cover simulation may increase error by creating small and false changes. This lower limit is well below the most frequently used 30 m resolution. At the upper limit, Chen & Pontius (2011) showed that predicted built area accuracy increased with increasing spatial resolution from 30 m to 1,920 m. Moreover, the explanatory power of driving variables can also increase with coarsening spatial resolutions (minimum resolution was 15 km²) (Kok & Veldkamp, 2001). Geri et al. (2011) found that the model's performance increased to a perfect level of agreement with increasing cell size. Spatial extent and cell size may affect the analysis of spatial patterns of land cover change separately or together (Wu, 2004). However, few studies found tested the influence of these parameters in identifying the best cell size and spatial extent for a catchment level land cover change simulation.

Land cover change has a significant impact on land degradation including soil erosion. The Mediterranean area experiences high storm intensity on dry soil in summer and autumn; at this time, vineyard areas remain almost bare and a high rate of erosion can occur (Blavet et al. 2009,

Wainwright 1996, Ramos and Martínez-Casasnovas 2006). Mechanical tillage, chemical weeding, and intensive use of pesticides are the most common practices in vineyard cultivation systems in the Mediterranean area, in which soil remains bare during the whole year (Novara et al. 2011, Salome et al. 2014). These practices may result in higher crop yield and better quality grapes, but soil in these vineyards is particularly vulnerable to erosion, depletion of organic matter, chemical pollution, and loss of biodiversity (Coulouma et al. 2006, Raclot et al. 2009). Several studies found a high rate of soil erosion during the storm season (Martínez-Casasnovas et al. 2005, Wainwright 1996). Most of the studies dealing with the prediction of soil erosion focus on croplands elsewhere in the world, whereas vineyards in the French Mediterranean area have been much less studied.

STATEMENT OF PROBLEM

The principal aim of this thesis is to predict long-term soil erosion evolution in a Mediterranean context of rapid urban growth and land cover change at the catchment scale.

To achieve this, the following three specific objectives were formulated:

1. To identify the spatial dynamics of land cover change patterns in a Mediterranean catchment, namely the Giscle catchment in Southeastern France.
2. To determine the impact of temporal scales, spatial extent, and cell size on land use and land cover change (LUCC) modeling to predict land cover change accurately.
3. To determine past soil erosion patterns (1950, 1982, 2003, 2011) and predict them for the future (2025) based on projected land cover for 2025.

ORGANIZATION OF THE THESIS

This dissertation consists of seven parts, including four chapters of original research. This introductory section outlines the motivations for and goals of the study, as well as the methods of investigation. The first chapter presents a literature review of previous studies dealing with related research topics. The next four chapters of this thesis present new research findings from this study. The dissertation concludes with a final section providing a synthesis of the findings, a

discussion of the limitations of this study, and suggestions for future research. These are summarized below:

- Chapter 1 presents an extensive literature review covering previous academic studies on land cover change dynamics and land cover change modeling. These studies come from every corner of the world and date from 1994 to 2014.
- Chapter 2 analyzes the land cover change patterns in the study area, and identifies explanatory variables for land cover change modeling by quantifying the impacts of topographic and distance variables on land cover change for each land cover category. Land cover maps were screen digitized from digital orthorectified aerial photographs. Surfaces were classified into five categories based on visual interpretation: forest, grassland, vineyards, urban, and suburban areas. Land cover change was quantified using the cross tabulation matrix of the CROSSTAB module and the Change Analysis module of the Land Change Modeler (LCM) of IDRISI Selva version 17.02 (Eastman 2012). After creating land cover maps of 1950, 1982, and 2008, land cover changes in three temporal periods were investigated: 1950-1982, 1982-2008, and 1950-2008. The land cover change determining method proposed by Pontius et al. (2004) was applied for all temporal periods to quantify persistence, gains, losses, total change (addition of gains and losses), net change, and swapping. Then, the impact of spatial variables such as altitude, slope, distances from roads, streams, sea, and built area are presented.
- Chapter 3 deals with the impact of temporal scales on land cover change modeling. Land cover maps of 2011 were predicted from different time scales (1950-1982, 1982-2003, and 2003-2008) using the Land Change Modeler (LCM), and compared with the digitized land cover map of 2011 to measure the model's accuracy. Spatial variables - namely, altitude, slope, and distances from roads, streams, and built area were used in land cover prediction. These variables were tested using Cramer's V coefficient, and identified according to the analysis in Chapter 2. Topographic explanatory variables with several spatial and planning components were used to simulate land cover change without taking into account any particular spatial agent. Therefore, an agent-based modeling approach was not appropriate. The MLPNN-Markov model option of LCM-IDRISI, which was originally designed for land cover change evaluation and managing impact on

biodiversity, was used to simulate temporal and spatial patterns of change in land cover for both short and long time periods.

- Chapter 4 tests the impact of spatial extent and cell size on the perception of land cover change dynamics and land cover prediction. Spatial extent and cell size are interrelated. They can have a great impact, not only on land cover prediction, but also on perceived quality of the prediction, since calculated agreement/disagreement statistics depend on the number of cells present in the study area grid, and this depends directly on cell size and spatial extent. Change dynamics in terms of absolute and relative change were first analyzed using intensity analysis, and then land cover was predicted for 2011 for large (79.1 km²) and small (36.6 km²) windows using cell sizes of 25 m, 50 m, and 100 m. Spatial resolution effects were also analyzed by upscaling from 25 m to 50 m and 100 m and then downscaling back to 25 m.

- Chapter 5 measures the degree of soil erosion, identifies the impacts of land cover changes on soil erosion, and predicts soil erosion in vineyards for 2025 at the catchment scale using RUSLE. Chapter 3 and 4 are essential steps towards identifying the parameters for predicting land cover for the future (2025) and to see how land cover change impacts on soil erosion. Different parameters were measured. The rainfall erosion index (R) was estimated from average rainfall in the 1975-2005 period following Torri et al. (2006). The soil erodability factor *K* was calculated following the equation proposed by Wischmeier and Smith (1978). Based on previous studies, a cover management factor of 0.3 was used on different land cover types and vineyards conservation practice factor P is valued at 0.7 except terraces. According to field studies in the catchment area, terraces are found in most of the vineyards at slopes above 10%. Therefore, vineyards at all slopes above 10% are considered as terraced and valued at 0.2, because terraces reduce erosion by more than 50%. Soil erosion maps were predicted for 1950, 1982, 2003, 2011, and 2025. Predicted soil erosion maps were simplified into three categories: low (<10 t/ha), medium (10-25 t/ha), and high (>25 t/ha) soil erosion, respectively. For estimated erosion rates in 2025, transition potential maps were created for all possible transitions based on actual historical changes during the 1982-2003 period and explanatory variables using the MLPNN algorithm of IDRISI (Eastman, 2012). However, only transition potentials with an accuracy rate greater than 70% were included in land cover prediction, since that approach yielded better final results than

one which included all potential transitions. Accuracy rates greater than 70% consisted of the following: forest to vineyard, forest to grassland, forest to built area, vineyard to built area and grassland to built area. Validation values were weaker when all transitions were included, but the trends with regards to spatial extent and cell size were consistent.

CHAPTER 1

LITERATURE REVIEW ON LAND COVER CHANGE DYNAMICS AND LAND COVER CHANGE MODELING

1. Land cover change

Land cover is the physical and biological cover over the surface of the land including water, vegetation, bare soil, and manmade structures (Ellis, 2011). Land use is a more complicated term that refers to the human activities such as agriculture, forestry, building construction and any other function that alters the land surface or land cover. Land cover is determined by the interaction between human activities and environmental factors such as soil characteristics, climate, topography, and vegetation.

Land cover changes are among the most important human alterations of the Earth's land surface (Lambin et al. 2001) and land cover conversion processes have accelerated since the Second World War (Antrop 2005, Geri et al. 2010, Serra et al. 2008). Moreover, land cover patterns of Mediterranean Europe have changed a lot since the Second World War (Fox et al. 2012) due to intensive human activities (Geri et al. 2010). Land cover change has occurred by the interaction of environmental (physical) and human (socio-economic) characteristics: population growth, urban sprawl, industrial development, and political and environmental policy. In addition, rapid expansion of industrial and tourism activities during the last six decades has caused important socioeconomic changes in rural areas of the Mediterranean area (Dunjó et al. 2003). According to Geri et al. (2011), land cover in Mediterranean areas has been changed by socio-economic development such as industrial and urban activities since the 1940s. Land use / cover change (LUCC) has a great influence on the current global change phenomena in both physical and human environments. It affects world bio-diversity and ecosystems, food security, human health, urbanization, and global climate change (Falcucci et al. 2007, Geri et al. 2011), Sala et al. 2000). It is also responsible for environmental change, water pollution and soil degradation (Dunjó et al. 2003). LUCC has resulted in the abandonment of marginal hillside

terraces and has shifted farm cultivation to better soils to increase profits. Three common major land cover changes in the Mediterranean area are the following: the expansion of tourism along the coastline that results in rapid urbanization, intensification of agriculture on alluvial plains and low lands, and abandonment of agricultural terraced land in mountainous steep slopes leading to their transformation to forest area (Falcucci et al. 2007).

Antrop (2005) conducted a study on landscape dynamics in Europe and divided three periods of time to show historical landscape changes in Europe: pre 18th century, 19th century to the Second World War, and post-World War II. According to the study, traditional landscape changes occurred in the first period but many new landscapes were generated upon the traditional ones in the second period. Urbanization and globalization were identified as effective factors of landscape change in the post war period. In Antrop's (2005) study, landscape was defined as natural, rural, and urban area and characterized by the interaction of natural and human factors. Several driving forces of landscape change in Europe such as accessibility, urbanization, globalization and the impact of calamities were also discussed in the study, but not all of these driving forces are common in the Mediterranean area. Antrop (2005) also mentioned that population growth and technological advantages were associated with urbanization.

1.1 Major trends in Euro-Mediterranean land cover change

Land cover changed greatly in the Mediterranean coastal area after the Second World War because of the industrial and agricultural revolutions. Slope and elevation, soil conditions, and other environmental factors were taken into consideration by farmers in the first part of the 19th century to establish agricultural farms, but this changed after the Second World War when human factors became more influential than environmental factors for land cover change because of high demographic pressure and socio-economic development in the Mediterranean area. Urbanization increased rapidly along the coastline, with resident population doubling every 30 years and tourism every 15 years (Falcucci et al. 2007).

According to different studies (Geri et al. 2011, Nunes et al. 2011), two general trends of land cover change took place in recent decades in the coastal Mediterranean area. Firstly, dry farming

and forest land cover decreased in alluvial plains while reforestation occurred in hilly area. Secondly, urbanization occurred rapidly in most of the coastal plains where the tourism industry flourished. Development of infrastructure, communication networks, and technological advances resulted in socio-economic development that was the main reason for agricultural land abandonment on marginal lands. Population growth and socio-economic development caused agricultural intensification that increased irrigated crops. Different studies have been carried out to identify the factors and spatial patterns of land cover at various scales (Kok and Veldkamp 2001, Verburg et al. 1999). According to Serra et al. (2008), the expansion of tourism in the coastal Mediterranean area, environmental protection of certain areas, and common agricultural policy in Alt Empordà county (north west of Catalonia, Spain), caused important land cover changes in 1977-1997: "*Agrarian abandonment has caused the depopulation of inland hill and mountain areas, whereas tourist activities have resulted in substantial population increases along the coastal zone*" (Serra et al. 2008).

In the 1960s, agricultural activities were influenced by natural climatic conditions, such as rainfall. About 50% of the total agricultural area in Portugal was utilized for non-irrigated cereal cultivation (sown between October to November to make use of precipitation) and unseeded fallow rotation (Nunes et al. 2011). But the scenario changed in the latter half of the 20th century; agricultural activities became less important in the Mediterranean area due to natural barriers: relief and uneven topography, poor soil quality, and uncompetitive farm structures such as small, scattered plots. "*Nowadays, shrub land cover and vine and olive tree patches are the most typical vegetation of the physiognomy and ecology of Mediterranean environments, leading to a whole homogeneous landscape and the consequent loss of biodiversity*" (Dunjó et al. 2003).

Fox et al. (2012) conducted a study to analyze the impact of land cover change on total runoff in a Mediterranean catchment between 1950 and 2003 in the context of river management. Factors and patterns of land cover change were also explained briefly in the study. According to the study, land cover of the study area is strongly influenced by topography and most of the land cover changes occurred in the alluvial plain and foothills (about 29% of the catchment). Forest occupied about 90% of the gauged catchment and most of this was situated in upper hilly area. Vineyards and grassed areas covered the most area after forest and had a high tendency to

transform into urban areas. Some forested area also converted to vineyard in the study period but it was less than the area transformed from vineyard to forest.

Falcucci et al. (2007) measured land cover changes in the Italian peninsula between 1960 and 2000. According to the study, land cover/use changes occurred all over the Italian peninsula, particularly in Apennines and Mediterranean coastal areas from 1960s. Forest area roughly doubled in the Alps and Apennines as it gained land from agricultural areas. Agriculture area decreased in hilly and coastal areas but expanded in the rest of the country where traditional cultivation was transformed to modern technology based intensive cultivation. Land cover change was also related to population density which increased in plains and coastal areas because of tourism, agriculture and urbanization.

Geri et al. (2010) analyzed land cover change in a Mediterranean catchment (Siena province, Italy) in 1954-2000. They observed the direction and rate of land cover change and focused on the effects of human activity/disturbance in a Mediterranean environment. Forest and agricultural areas were more stable whereas semi natural areas were unstable in their study area. About 6% forest cover changed to agricultural land, and 12% and 3.5% of crop land converted to forest and semi natural area, respectively. But 55% and 35% of semi natural area transformed to forest and agricultural area, respectively. The study revealed that losses of forest area occurred mainly at higher elevations and conversion of agricultural land (both crop land and semi natural) occurred at lower altitudes.

Sluiter and de Jong (2007) conducted a study on land cover change in Peyne, France. According to the study, intensification of vineyards increased due to the expansion of the worldwide wine market and on automatic harvesting system. They found that about 90% of land abandonment occurred before 1940s, and was located further away from urban areas and roads. They also mention that intensification and modernization of agriculture were major factors of such change at the time of the "Green revolution". Recent abandoned agricultural areas were near urban areas because most of recent abandonment occurred due to urban sprawl and industrialization.

Alemayehu et al. (2006) analyzed land cover change in the context of demographic desertification in Tabernas (Almeria, Spain) and the study area represented a Mediterranean region where a combination of extreme environmental and land cover changes occurred in the last decades. The study showed that 32 % (2,507 ha) of dry farming areas were changed into different land cover types in 1956-2000, of which 57.7% (1,447.7 ha) changed to irrigated farmland (twice the irrigated area in 1956), 34% (857 ha) were abandoned, and about 8.3% (202 ha) changed to urban and industrial development structures. The study also revealed that land abandonment and the transformation of dry farming land to irrigated crops increased soil erosion, salinization and pollution.

Cori (1999) explained that rapid growth of the tourism industry increased dramatically in the last few decades and influenced land cover change on the northern shores of the Mediterranean area. According to the study, rapid growth of population, tourism activities, change of settlement system, and industrial development were the main causes of land cover change. It was reported that agricultural land decreased and non-agricultural land increased in the Spanish, French, and Italian Mediterranean regions. It also demonstrated that the agricultural areas were affected due to the spread of tourism and traffic infrastructure such as urban structure, hotels, roads etc. In the study, several spatial planning policies were discussed and new plans were introduced to conserve the Mediterranean environment, particularly in Spain, France and Italy.

Van Eetvelde and Antrop (2004) analyzed the characteristics and mechanism of land cover change in southern France (Tavernes) in 1960-1999. They explained how structural and functional changes influenced new landscape formation in their study area. They also identified three main trends of land cover change in Mediterranean areas: development of transportation and infrastructure, urban sprawl, and rapid expansion of the tourism industry in the Mediterranean coastal area. According to the study, little land cover change occurred in the Tavernes basin in 1979-1993. A particular pattern of transition was noticed from vineyards to olive groves. Most of the changes occurred on the foot slopes in the northern and eastern edge of the basin.

Serra et al. (2008) reported that mass tourism on the coast, the development of irrigation projects, environmental reserve areas and common agricultural policy (CAP) subsidies for

irrigated crops were the main causes behind land cover and land cover changes in the Mediterranean area. They revealed that irrigated maize, fruit trees, shrub lands, deciduous forest, and urban areas increased significantly in coastal plain areas. Besides, vineyards and olive trees decreased in the mountainous areas and transitional sub regions that resulted in land abandonment and increased shrub land area.

Koulouri and Giourga (2007) conducted a study in Lesvos Island, Greece. They considered three land cover "types" such as cultivation, short-time abandonment, and long-time abandonment to describe the relationship of land abandonment and soil erosion that occurred by the changes in agricultural practices and soil resource management. Significant land cover change occurred on steep slopes (≥ 25 %). The study revealed that soil erosion increased significantly on steep (≥ 25 %) to very steep slopes (≥ 40 %) because of loss of densely protective plant cover and increase in shrub cover. In addition, increased bare soil area was also described as another major cause of soil erosion.

1.2 Factors affecting land cover change

Land cover change occurs under the pressure of a variety of socio-economic factors that interact with the natural environment to determine the nature and location of land cover change. The list below is not exhaustive but lists the major factors currently referred to in the scientific literature for the Mediterranean area.

1.2.1 Demographic pressure and urban sprawl

Population growth and urbanization have occurred in Mediterranean coastal areas as in other parts of the world. About 60% of the world's population resides in a 65 km wide belt close to the coastline because of its beauty, natural resources and economic activities (Vallega, 1998). Urbanization is a major driving force of land cover change, though it occupies a very small fraction of the Earth's land surface (less than 2%). About 51 % of the world's population were living in urban areas in 2010 (http://data.worldbank.org/topic/urban-development) and about 60%

will be living in urban areas by 2030 (UNFPA 2004). Urbanization affects urban fringe areas which are progressively transformed into full urban areas. Brauch (2003) estimates that the population of Southern European countries doubled in 1950-2000, and the urbanization rate has been projected to increase from 44.2 % in 1950 to 75.2% by 2030; in addition, urban population will reach 71.6 % in Greece, 76.1% Italy, 81.6 %, in Portugal, 82.2 %, in France, and 84.5 % in Spain by 2030, respectively. In Southern Europe, the population of some major Mediterranean coastal cities (Athens, Barcelona, Naples, and Marseille) increased 1.1 to 1.8 fold from 1950 to 2000 and should stabilize around 2015.

The population density in the Mediterranean coastal area (69 inhabitants/km2) is more than double the density of population of the region as a whole (47 inhabitants/km2) (Benoit 2001, Cori 1999). According to Benoit (2001), Mediterranean coastal regions are more urbanized than countries as a whole, and urban and total population in Mediterranean area increased by 2.7 and 1.9 times, respectively, in 1950-1995. Total population growth rates in 1950-1995 were 0.54% and 0.29% in France and Spain, respectively, but population growth rates in Mediterranean coastal regions of these countries were 0.76% and 0.49%, respectively. According to Falcucci et al. (2007), a decrease in population was observed in the Apennines, Alps, and in the central and mountainous part of Sicily and Sardina of Italy in 1960-2000 while an increase was noted along the coastal areas due to rapid growth of economic activities.

Urbanization is a continuous process that was initiated in Europe during the industrial revolution in the nineteenth century (Antrop 2005). Socio-economic development and population growth were two main factors behind it. In Mediterranean Europe, many large cities experienced strong growth rates between the 1950s and the 1980s (Catalán et al., 2008). However, the presence of many small and medium-sized urban centers near large cities contributed to knit together metropolitan regions (Benoit, 2001). For example, urban sprawl is growing rapidly in the Mediterranean area, as in Madrid, Marseilles, and some other cities of southern Europe. According to Benoit (2001), the European Mediterranean coast is now almost completely urbanized where average distance between urban areas was about 10 km, 17 km, and 18 km in Italy, Spain, and France, respectively, in 1995. Moreover, the number of urban areas also increased dramatically in the European Mediterranean basin in 1950-1995 (Benoit, 2001). The

number of urban areas was 296, 676, and 350 in France, Italy, and Spain, respectively, in 1950, and increased to 433, 769, and 415, respectively, in 1995. Urban growth expanded along the periphery at the expense of agricultural or forest areas.

According to Benoit and Comeau (2005) Mediterranean countries from Spain to Greece experienced strong urban growth until the 1970s, and their current moderate growth rates are projected to continue. Land cover change has been affected by newly developed artificial areas: for example, total built area, roads & car parks, and non-built artificial area (gardens, lawns and construction sites) increased by 12%, 10%, and 17%, respectively, in France between 1992 and 2000 (Benoit and Comeau, 2005). About 34% of Spanish Mediterranean coastal areas have been urbanized since 1999 and this figure was 43% for the Italian coastline (Serra et al. 2008). As a result, only 4.7% of primary vegetation in Mediterranean Europe remains unchanged (Geri et al. 2010). In addition, migration from other European countries tends to concentrate in the Mediterranean coastline area due to the quality of life in Mediterranean cities (Cori 1999). Aging population in Europe has a typical migration trend towards the Mediterranean coastal zone (Van Eetvelde and Antrop 2004).

1.2.2 Tourism

The Mediterranean is the world's leading tourist destination where tourism is a major industry in terms of economic activity (MAP 2008), and tourism is one of the most important sources of income for most Mediterranean countries. Though tourists tend to visit mainly in summer, infrastructures such as housing, roads, and entertainment facilities are built permanently, contributing to accelerate urban growth. According to Enne et al. (2005), the Mediterranean region attracts more than 30% of world tourism. Benoit (2001) predicts an average 250 million visitors per year for 2025 in Euro-Mediterranean coastal areas. According to the report of MAP (2008), the number of tourists in the Mediterranean coastal area will increase by about 80% between 2000 and 2025.

Significant human pressure on the Mediterranean coast is caused by the expansion of tourism related to seaside resorts. Van Eetvelde and Antrop (2004) explain that natural, cultural and

scenic values of Mediterranean landscapes were important factors for developing the tourism sector, and new infrastructure developments based on tourism have changed the traditional form of land cover and socio-economic conditions. France received 60 million tourists in 1996 and over 80 million 2007, representing almost 11% of world tourism at the time (Wikipédia, http://fr.wikipedia.org/wiki/Tourisme_en_France). France is the first tourist destination in the world with the third highest income from tourism (after the U.S.A. and Spain). In addition, the World Tourism Organization (WTO) predicted about 100 million foreign tourists will visit France in 2015. Every year, millions of tourists gather in summer in coastal cities to enjoy the Mediterranean Sea and the rugged topography of the Southern Alps, because the dominant climatic regime is typically Southern Mediterranean with mild winters and dry summers. Mediterranean France has a very rich mixed environment, and it presents many of the typical features of Mediterranean tourism, especially in coastal areas, where strong urban development is related to tourism.

According to Cori (1999), Mediterranean countries provide at least 25% of the world's hotel accommodation. Coastal regions of other Mediterranean countries such as Turkey, Cyprus, and Morocco have also been influenced by expansion of the tourism industry. These coastal areas are more urbanized due to the rapid development of local tourism. Greece and Croatia are the leading countries in northeastern Mediterranean with their high potentialities to attract international tourism. Greece has the combined appeal of its archeological and artistic heritage with the traditional sea-sun-shore. The expansion of tourism on the coastal plains and even in the inner mountainous forest areas has reduced the natural and cultural biodiversity, and the degradation of former traditional agricultural landscapes has increased forest fires and soil erosion (Serra et al. 2008).

As described by EAA (2011), the number of secondary homes increased by 10% between 1990 and 1999 in France, creating intensive pressure on the environment, especially in coastal and mountain zones. There is a sport harbor every 3 km and most of these harbors are accompanied by urban development operations in the Mediterranean coastline of southeast France - "La Côte d'Azur" (Benoit 2001, EAA 2011). According to the report of EAA (2011), almost 335,000 new secondary homes were built during the past two decades, occupying 22 km²

of land. In the 1990s, Mediterranean beaches attracted people of central and Eastern Europe as well as the inland population from the Southern side of the Mediterranean basin (Benoit 2001), and both domestic and external tourism are increasing. Moreover, retired population from home and abroad (many from Northern Europe, and African and Arabian elites) have a tendency to buy property and houses in a Mediterranean city. According to (Cori 1999), half of total secondary homes in France are situated in the Mediterranean coastal area.

1.2.3 Intensification of agriculture

Fine grained rural landscape structures are being replaced by large scale ones leading to loss of regional diverse cultural landscapes due to the intensification of agriculture (Van Eetvelde and Antrop 2004). Intensive agriculture can be defined as a cultivation system that uses high input such as labor, fertilizer, pesticides, herbicides, fungicides and capital to obtain maximum yield per unit of land (Lambin et al. 2001). Intensive agriculture requires less land area than extensive agricultural farms but it needs high efficiency machinery for planting, cultivating, harvesting, and producing a similar profit. Generally, farmers use greater farm areas in intensive cultivation for sustainable use of their capital investments and equipment to get higher profit. Nowadays, this type of agriculture is practiced throughout the developed world to increase food production for a rising population. But the pattern of agricultural landscape has changed in Europe since the Second World War because of agricultural and economic development (Geri et al. 2011). Modern intensive agricultural practices ensure food security, increased income, and improved farmer's living standards in both developed and developing countries. The intensification of agriculture occurred mainly based on technological advances and improvements in agricultural materials and machinery, and it has reduced corresponding production costs. Optimum use of organic and chemical fertilizer, development of irrigation, and practice of advance technology in agriculture and animal husbandry increased productivity of land and crop yields per unit area. The "Agri-Basin" of Italy has experienced the relocation of profitable agricultural activities from uplands to plains due to rapid intensification in agriculture (Quaranta, et al. 2001). In addition, profitable

crops such as high yielding varieties are cultivated over huge areas due to increased investment in irrigation.

Two patterns of agricultural land cover change in European Mediterranean areas over the last fifty years can be defined (Baldock et al. 1996).

- Suitable and more productive land cover was converted to more intensive agricultural uses since the 1950s, often with an expansion of arable land at the expense of permanent grassland, wetlands, and forest.
- Marginal areas with physical and socio-economic barriers such as steep slopes, small terraces, wet areas without drainage systems, and remote mountain regions have been abandoned or replaced by specialized farming systems, plantation forestry or natural succession.

1.2.4 Land abandonment

"*Land abandonment can be defined both qualitatively (as a description of the land condition) and quantitatively (as years without use)*" (Moravec and Zemeckis 2007). The concept of land/farm abandonment is applied to the land where traditional or recent agricultural use has stopped. There is no well-defined and commonly accepted definition for land abandonment because there is confusion over the term "abandoned farmland". Sometimes apparently abandoned land often is not truly abandoned, but merely temporarily out of use/cultivation and awaiting a new owner or tenant. In the European Mediterranean, legal owners of much of the abandoned farmland live in a town or city, and they bought their farmland as an investment. The statistical survey of France separates abandoned land from fellow land, but there is no specified duration when fallow land converts to abandoned land (Moravec and Zemeckis 2007).

Dunjó et al. (2003) described the land abandonment process in a typical Mediterranean environment (North East Spain) during the last century. They divided four different land cover types according to the duration of land abandonment such as cultivated fields (vineyard and olive trees, 0 years), recent abandonment (densely and cleared shrubs, 5 years), mid-abandonment

(cleared cork trees and dense olive trees, 25 years) and early abandonment. Most of the studies (Geri et al. 2010, Koulouri and Giourga 2007, Sluiter and de Jong 2007, Van Eetvelde and Antrop 2004) about land abandonment in Mediterranean Europe show that mountainous or semi mountainous hillside areas were abandoned because small plots of vineyards and olive trees were not profitable. Land abandonment is also a common scenario in Mediterranean France because of technological, social, and economic change (Geri et al. 2010, Sluiter and de Jong 2007). Intensive agriculture and long term abandonment started around the 1850s and increased to a high rate after 1900 in 'Peyne', Southern France (Sluiter and de Jong 2007). But it is difficult to understand the real condition or measure changes that occurred because of complex transitions between vegetation and agricultural land. Van Eetvelde and Antrop (2004) describe how land abandonment and urbanization have been occurring simultaneously in their study areas - Tavernes, le Flexi and Montfaucon of southern France. Most of the changes took place in the last few decades because of urbanization and agricultural intensification.

There are different causes of agricultural land abandonment and according to Baldock et al. (1996) and land abandonment may take place in the following ways:

Temporarily out of use

- Farmland which is under irregular management or waiting a new owner or tenant may seem abandoned.
- Farmland which is converting to non-agricultural use seems abandoned, typically in urban fringe areas.
- Farmland which is temporarily set aside under the Common Agricultural Policy (CAP) arable regime may also appear abandoned.

Permanently abandoned

- Land which is under long term set aside schemes, such as habitat creation under Regulation 2078/92 and subject to conservation management.

Converted to other uses

- Land which has undergone a planned conservation to another use, typically forestry, reservoirs, natural or hunting reserves or urban development.
- Land which has converted to another use due to spontaneous abandonment (such as grazing by itinerant livestock).

Environmental factors, geographic location, agricultural structures, social factors, and government and regional policy need to be considered for land abandonment (Baldock et al. 1996). Farmlands which are situated near urban areas have a high probability of being abandoned as a result of high income potentiality of urbanization. Moreover, physical conditions such as soil fertility, slope, altitude and availability of land for farming are important factors. In addition, sometimes land abandonment also occurred due to technological change of farming systems and policies for commercialization.

Common environmental factors are soil, climate, water availability, topography, and altitude, which have a fundamental influence on the agricultural potential of an area (Baldock et al. 1996). Moreover, soil productivity depends on fertility, soil structure, and soil depth. Sometimes fertile soil may be abandoned due to lack of rainfall. Besides, steep slopes and high altitudes may be abandoned because of obstacles to mechanized farming and to the short growing season (Baldock et al. 1996). Moreover, very dry or wet soils are unsuitable for tractors and are likely to be abandoned (Moravec and Zemeckis 2007).

Geographical location is a very important factor for agricultural abandonment. Selling goods and buying inputs for farms depend on communication networks such as roads and trains. Farming in mountainous areas may have poor access that results in higher input costs and reflects the characteristics of Less Favored Area (LFA) according to Baldock et al. (1996).

Holding size of less than 10 ha represents 35.2% of total Utilized Agricultural Area (UAA) in France and this figure is about 67.5% for the whole EU-15 countries (Eurostat- Farm Structure Survey 2005). A small number of large and relatively efficient farms are economically profitable and commercially viable, there are also numerous small and marginal holdings. Besides, most of the owners of small holdings and farms are involved in agriculture as a part time and marginal

activity with little interest. Sometimes, they cultivate their land as a hobby, so these small farms have a high probability to change or be abandoned.

In many typical Mediterranean areas, some social factors have an important influence on land abandonment. Firstly, elderly farmers without successors are a common scenario of mountainous rural agricultural practice. An aging population, uncompetitive farm structures, and lack of alternative employment opportunities cause abandonment of traditional subsistence systems. In addition, abandonment can occur by converting arable land to tree crops (olives, almonds, orange, and carobs) in both upland and lowland areas (Koulouri and Giourga 2007). Some arable cultivation, vines and tree crops survive traditional practices but most of the systems are closed or neglected (Caraveli 2000). Rural population shows a declining trend in the Mediterranean area that creates a scarcity of labor necessary for subsistence agricultural in upland areas. Finally, lack of important social and entertainment facilities in rural areas such as education, health, and sport facilities affect land abandonment.

1.2.5 Economic factors

Land abandonment in the Mediterranean region accelerated due to increasing market demand and competition with the highly productive agriculture of Northwestern Europe. According to (Baldock et al. 1996), relevant economic factors behind land abandonment include the following:

- competition from other agricultural areas, other land covers and production systems;
- rising living costs and income aspirations;
- alternative employment possibilities;
- relative costs of inputs and outputs;
- alternative demands for farm products;
- use of modern technology in agricultural farm land;
- availability of capital/ loans and subsidies.

Other factors, such as “urban fringe”, tourism, forestry, reservoirs, and natural management also influence land abandonment in the Mediterranean.

1.2.6 Policy and planning

The European Union took several unique agricultural policies in the early 1960s and reformed it in 1992 to provide financial support and to encourage the use of modern technologies for farming (www.wwf.org.uk/filelibrary/pdf/ag_in_the_eu.pdf); the main objectives were the following:

- ensure the availability of agricultural goods according to market demand;
- increase agricultural productivity;
- increase the living standard of the agricultural community;
- stabilize the market price and ensure that supplies reached consumers at reasonable prices.

Nunes et al. (2011) describe how the environment and forest areas have benefited from the reform of the CAP in 1992. The CAP provided irrigation subsidies for planting high yielding crops that reduced the production of winter cereals in Spain. Moreover, this agricultural policy also encouraged large farming enterprises and cultivation of subsidized crops in bigger fields. As a result, partial and permanent abandonment of agricultural land increased. Abandoned less favorable areas for commercial farming went under afforestation policies to reduce desertification and soil erosion (Nunes et al. 2011). According to the Service of Agrarian Recognition and Management (SROA) 1970 statistics, about 55% of the total area of the Guarda district, Portugal, was occupied by cereal crops in 1950s and this decreased to 10% for the same crops in 2000 ((Nunes et al. 2011).

1.2.7 Results of land abandonment

Decreasing landscape diversity and complexity and increasing vulnerability of certain hazards such as forest fire, floods, and droughts can be considered as some of the results of intensification and abandonment of land cover/use (Serra et al. 2008). Environmental degradation in connection with forest fires and hydro-geological changes are common phenomenon due to land abandonment in Mediterranean Europe (Moravec and Zemeckis 2007). In addition, land

abandonment also influences biodiversity by changing the habitat of forest and other typical biomes. Moreover, rates of soil erosion depend on the history of agricultural activities of an abandoned land, regeneration process, and composition of vegetation (Sluiter and de Jong 2007). While Koulouri and Giourga (2007) observed some positive impacts of land abandonment, such as decreased soil erosion due to regeneration of vegetation which improved soil structure by adding organic matter and protecting the soil from erosion.

1.3 Land cover change conclusions

Significant land cover changes have been observed in Euro-Mediterranean coastal areas since the Second World War. There are several factors and trends of land cover change in the Mediterranean area some dominant factors, trends, and patterns are similar for the region. Plain and gently steep lands have transformed to intensive agriculture practices and human settlement due to urban sprawl. Agricultural activities in mountainous areas and on steep slopes have been abandoned and reforested. Moreover, the tourism industry has also flourished rapidly and this has influenced land cover change in the coastal area which has been subject to intense

2. Land cover change modeling

Land use / cover change (LUCC) is a major issue for researchers and managers including urban planners, conservationists, ecologists, economists, and resource managers because of its relation with global environmental change and sustainable development (Dietzel and Clarke 2006, Guan et al. 2011, Lambin et al. 2001). LUCC is associated with the interaction between human activities and the natural environment, and land cover change models are the supporting tools to analyze the causes and consequences of land cover changes (Verburg et al. 2004). Land cover change models quantify land cover change patterns and relationships between the human and ecological systems (Veldkamp and Lambin 2001). In particular, land cover change models are able to identify location and quantity of change, to predict land cover change considering past changes and test explanatory variables. For this reason, many interdisciplinary research projects have been initiated for land cover change modeling, measuring regional and global land cover change, forecasting future conditions, and planning for sustainable development (Verburg et al. 1999). As a result, researchers have created a large set of operational modeling tools to implement prediction and exploration of possible land cover change trajectories, and land cover planning and policy in recent years (Verburg et al. 2006).

Land cover change, urban growth, and spatial modeling have drawn considerable interest in the last two decades due to increased computing power, availability of spatial data, and the need for innovative planning tools for decision support (Dietzel and Clarke 2006) . Advanced urban and land cover change modeling techniques have been included in many GIS software programs and have enriched modeling techniques in geographical research. Different studies of land cover change can be summarized as three main core issues: land cover dynamics, driving forces, and modeling global or regional land cover change. Most studies are on spatiotemporal urban dynamics and urban growth prediction (Batty et al. 1999, Clarke et al. 1997, Dietzel and Clarke 2006, Engelen et al. 1999, Li and Yeh 2000). Some studies considered socioeconomic issues to explain unban expansion (Barredo et al. 2003, Jokar Arsanjani et al. 2013). Other studies considered environmental, ecological, and land cover change dynamics (White and Engelen 1993). Very few studies are on land cover change modeling in the Mediterranean area (Geri et al. 2011, Oñate-Valdivieso and Bosque Sendra 2010, Petrov et al. 2009). Land cover change has

great influence on soil erosion, runoff, deforestation, forest fires, and other natural risks, which have direct and indirect impacts on environmental change (Dunjó et al. 2003, Koulouri and Giourga 2007, Nunes et al. 2011).

This chapter presents an overview of land cover change modeling and the justification of our choice of LCM as a modeling tool for our study. An overview of land cover change modeling is provided and Cellular Automata (CA) models are described in detail. This is followed by a more detailed description of data types, sources, and processing methods of the SLEUTH, MOLAND, and Urban Expansion Dynamic (UED) models in sub-sections. The Markov model is then presented and a review of Markov chain modeling and the Land Change Modeler (LCM) of IDRISI are discussed. After this, a brief description of Agent Based Modeling (ABM) in geography is presented. The literature review ends with a discussion of the suitability of the LCM model to analyze and simulate land cover change in the context of our study and a summary conclusion.

2.1 Land cover and land use change models

Different modeling techniques have been designed to analyze present land cover patterns using biophysical potentials and socio-economic characteristics (Guan et al. 2011, Kamusoko et al. 2009), to explore the impacts of land cover change, and predict for future changes (Barredo et al. 2003, He et al. 2008). Huang and Cai (2007) classify land cover modeling into non-spatial models, (such as empirical statistical), and spatial simulation models, such as Cellular Automata (CA) models (Clarke and Gaydos 1998), Constrained CA models (Engelen et al. 1997), Conversion of Land Use and its Effects (CLUE) (Verburg et al. 1999), and the SLEUTH model (Clarke and Gaydos 1998). However, Guan et al. (2011) divide models into three classes: empirical and statistical models, dynamic models, and system dynamic or integrated models; they explain that dynamic models are more suitable to predict land cover change in the future than empirical / statistical models. Moreover, an integrated model that is multidisciplinary and combines elements of different modeling techniques will probably be best for improving and understanding land cover change processes (Guan et al. 2011). Agarwal et al. (2002) reviewed spatial and temporal characteristics of 19 land cover change models used over a wide range of

scales, from less than a day to more than 100 years and from less than 1 ha to more than 1 million km^2. They classified 11 models as raster based, 4 were vector based and the remaining were classified as neither. According to the review, six models used statistical/econometric models at county-level data. The other six models used spatially dynamic approaches.

2.2 Cellular Automata (CA)

Automata are mechanisms of processing information according to surroundings and inputs. In this process, surroundings and characteristics of automata are changed over time according to the rules that govern their reaction. "*An automata is a machine that processes information, proceeding logically, inexorably performing its next action after applying data received from outside itself in light of instructions programmed within itself*" (Lavy 1992, p. 15). White (1998) defined a CA as "*a discrete cell space, together with a set of possible cell states and a set of transition rules that determine the state of each cell as a function of the states of all cells within a defined cell space neighborhood of the cell; time is discrete and all cell states are updated simultaneously at each iteration*".

A finite automaton (**A**) can be described by means of a finite set of states **S** = {S_1, S_2, S_3,... ... ..., S_N} and a set of transition rules **T**.

$$\mathbf{A} \sim (\mathbf{S}, \mathbf{T}) \ldots\ldots\ldots\ldots\ldots\ldots\ldots\ldots \text{(I)}$$

A Cellular Automaton (CA) is a spatially located and interconnected finite system. In CA, space is divided into regular spatial cells and an individual cell represents a particular boundary of location of an automaton (Liu 2009). Cells distributed over a grid space represent a finite number of states and time moves forward in discrete steps. The overall behavior of the system is determined by the combined effect of all the transition rules. Transition rules define an automaton's state, S_{t+1}, at the time step ($t+1$) depending on its state, S_t ($S_{t+1} \in S$), and input, I_t, at time step t:

$$\mathbf{T:} (S_t, I_t) \rightarrow S_{t+1} \ldots\ldots\ldots\ldots\ldots \text{(II)}$$

An automaton can be defined by **A,** belonging to a CA lattice as follows:

$$\mathbf{A} \sim (\mathbf{S}, \mathbf{T}, \mathbf{R}) \ldots\ldots\ldots\ldots\ldots\ldots \text{(III)}$$

Where, **R** represents automata neighboring A.

2.2.1 Fundamental components of a CA model

A cellular automaton consists of five fundamental elements (Liu 2009, White et al. 1999). These characteristics are described below.

1- The cell (C) is the basic spatial unit of two dimensional grids or raster forms of cellular automata used in urban growth and land cover change modeling (Liu 2009, White et al. 1999). However, one and three dimensional cellular automata have also been developed to explain linear objects such as urban traffic, and building heights in developed urban area, respectively (White and Engelen 2000).

2- The states (S) represent the attributes of cells, such as land cover type, and define spatial dynamics of the land surface. States can be binary values such as urban or non-urban, qualitative values that represent different types of land cover or land-use, social economic status (Benenson and Torrens 2004, Santé et al. 2010), or quantitative values such as population attributes, population density, rate of development, sediment load in seawater, groundwater levels, and soil moisture (White and Engelen 2000).

3- The time (t) specifies the interval between updates of the states of all cells.

4- The transition rule (**T**) governs the state of cells at any time and determines how automata adapt over time; and it determines the transition probability of cells according to the highest potentiality of change to another state. It defines how the state of one cell transits in response to its current state and the states of its neighbors. Transition potentials of each cell are calculated from the suitability, accessibility, zoning, and neighborhood effects (White et al. 1999).

5- The neighborhood (**R**) of a cell presents the agglomeration of adjacent cells defined by their distance from an individual automaton. For example, nine cells and five cells are used in the Moore neighborhood and in the “Von Neumann” (four cardinal neighbors) neighborhood, respectively.

2.2.2 CA models in Geography

"*Geographical Automata Systems consist of interacting geographic automata of various types*" (Benenson and Torrens 2004). Ulan and Von Neumann developed Cellular Automata (CA) in the late 1940s (White and Engelen 1993, White 1998). Later, Wolfram (1984) described the likelihood model of natural phenomena by CA and laid the foundation for the theory of Cellular Automata (Santé et al. 2010). The CA framework gained more popularity in the 1950s with the development of the first digital computer, and the idea of connecting and interacting spatial units was developed by Nobert Wiener's work on cybernetics (Benenson and Torrens 2004). In CA, space is divided into regular spatial cells and an individual cell represents a particular boundary of location of an automaton (Liu 2009). The first Cellular Automata approach to geographical modeling was defined and proposed by Tobler (1979) (White et al. 1999), and Couclelis (1996) and Takeyama (1996) explored the dynamics of natural space and introduced a common modeling language for dynamic spatial modeling at all scales within a GIS framework (White 1998). Dietzel and Clarke (2006) illustrated two general approaches of CA in land cover change dynamics: the first group of models treats an urban system as a basic entity consisting of urban and non-urban components, and the second approach comprises multiple land covers. (Yeh and (Li 2003) demonstrated three main types of urban CA for urban simulation: firstly, to test urban theories and hypotheses without using real data (Li and Yeh 2000); secondly, to simulate and predict the direction and the pattern of urban development using real data sets (Barredo et al. 2003, Clarke and Gaydos 1998, White and Engelen 2000); thirdly, to simulate different urban forms based on planning objectives (Yeh and Li 2003).

Many CA-based urban models have been developed in the last decade due to technological advantages in CA modeling (Dietzel and Clarke 2004, Wu et al. 2009) and these have been widely used in the last few years (He et al. 2008), especially in urban studies to simulate urban expansion (Clarke and Gaydos 1998, Liu 2009, Santé et al. 2010, White 1998, White and Engelen 2000). CA models have also been implemented in various land use models to simulate multiple land use types, to show the dynamic nature of land use change, and to analyze local and regional urban growth and sprawl (Jantz et al. 2004). The "Constrained CA model of land use dynamics" approach of White and Engelen (1993) has widened CA modeling of urban dynamics and

reduced its limitations (Benenson and Torrens 2004). Later, White et al. (1997) modeled urban growth using their constrained CA modeling tool to create a decision support system for urban planning, in which cell states represented land covers, and the transition rules expressed the temporal potentiality of each land cover type. In addition, road network, water bodies, and railways were used as spatial constraints for urban land use development. Li and Yeh (2000) applied a CA model to simulate sustainable urban planning based on land suitability by incorporating local, regional, and global constraints; the objective of their study was to simulate sustainable urban development based on constraints that included environmental conservation issues and planning.

2.2.3 The SLEUTH model

SLEUTH generates dynamic spatial patterns by applying growth rules to a grid of cells, each of whose land use state is dependent upon local factors (e.g. roads, existing urban areas, and topography), temporal factors, and random factors. In addition, non-urban land cover transitions (such as range land to agricultural land) can be simulated assuming urbanization as the driver. Annual maps of forecasted change are generated allowing for animated display of forecasts over time as well as integration in GIS databases for further spatial analyses.

Clarke and Gaydos (1998) proposed the SLEUTH model to simulate the historical urban growth of San Francisco and the Washington/Baltimore region. The SLEUTH model is also known as the Clarke Cellular Automata Urban Growth Model or the Clarke Urban Growth Model (Jantz et al. 2004). SLEUTH is an acronym from the six types of data inputs: Slope, Land use, Exclusion, Urban, Transportation, and Hill shading. It is a CA based model that has been widely applied (Dietzel and Clarke 2006, Dietzel and Clarke 2007, Jantz et al. 2004, Silva and Clarke 2002, Wu et al. 2009), and has shown its capabilities for predicting landscape changes. The model emphasizes historical changes of urban growth processes that can help predict future urban growth trends (Jantz et al. 2004), forecast land use change at different scales (Silva and Clarke 2002), and simulate the transition from non-urban to urban land use using historical trends as well as land use dynamics (Liu 2009, Wu et al. 2009). Dietzel and Clarke (2006) presented the SLEUTH model as an appropriate hybrid model that includes both approaches of urban and land

use change dynamics, but the model focuses mainly on simulation of urban changes. Silva and Clarke (2002) applied the SLEUTH model to Lisbon and Porto and demonstrated that the model could be applied to European cities.

Jantz et al. (2004) describe four types of urban simulation (spontaneous growth, new spreading center growth, edge growth, and road influenced growth) that are controlled by the interactions of five growth coefficients: dispersion, breed, spread, road gravity, and slope. These five growth coefficients determine the probability of urban growth by calculating each cell's potentiality of urbanization. The implementation of the model occurred in two general phases: calibration (simulation of historical growth pattern) and prediction (projection of historical growth pattern for future).

Wu et al. (2009) presented some limitations of the SLEUTH model: it gives priority to the edge growth transition rule that deprives the model to simulate urban development process of origin or city center; calibration is time consuming, subjective, and user sensitive; and the randomness and cumulative probability of the model affects its performance. The model does not explicitly deal with population, policies, and economic impacts on land cover change except in terms of growth around roads or those that can be expressed in permissive/controlled growth zoning. Jantz et al. (2004) demonstrate several other limitations: sensitivity to cell size, better simulation from shorter time series with consistent data, and the calibration method Lee and Salles metric influenced by the short time series. They also found that when the Lee and Salle statistic was high, urban growth was low, and when the slope coefficient was high, no urban growth was observed. Moreover, low density development was ignored, proving the limitation of the ability of the model to simulate other urban development. The SLEUTH model is completely scalable to the input model unit. It has been applied at regional (8 states), 1 km, and 30 m scales. All data must be in a raster format. Historical urban data from at least four time periods is required for calibration.

2.2.4 The MOLAND model

The land Management Unit of the Institute for Environment and Sustainability (MOLAND) has developed an integrated modeling framework based on the CA developed by White et al.

(1997) to assess, monitor, and model past, present, and future spatial, urban, regional, and sustainable environment management policies in Europe. Several geo-referenced datasets consisting of five types of digital maps must be input: actual land use types, accessibility of the transport network, inherent suitability for different land uses, zoning status or institutional suitability, socio-economic characteristics (Petrov et al. 2009). The model determines the transition potentials considering the characteristics of individual parcels and can be applied at the global, regional, and local levels. According to Lavalle et al. (2004), the model calculates transition potentials for "each cell and function" on the basis of four factors: physical suitability, zoning or institutional suitability, accessibility, and dynamics at the local level. The objective of this model is to simulate future land cover by taking into account existing spatial plans and policies, and to create alternative planning and policy scenarios in terms of their effects on future land use development (Barredo et al. 2003). Barredo et al. (2003) simulated future urban land cover scenarios for Dublin over 30 years (1968–1998) to show that city built up area had increased considerably over the study period. To do the urban simulation, 22 land cover classes were grouped into residential, industrial, and "other" built up areas. The model was calibrated using visual interpretation, comparing the land use pattern distribution through relatively abstract measures like fractal dimension, and using quantitative matrix methods. Urban simulation was compared with the actual map of 1998 and was found similar based on visual interpretation. Moreover, the comparison matrix was presented using simulated and actual maps of 1998 with a kappa value of 0.73, showing a good match. Petrov et al. (2009) used the MOLAND model for Algarve, Portugal, to determine land cover change due to rapid expansion of the tourism industry, and to take sustainable land management decisions. The study detected two main driving factors: increased demand for housing due to population growth and tourism, and the intensity of economic activity. They found 'scattered' urban development rather than 'compact' development due to urban policy.

Twumasi et al. (2008) illustrated some limitations of the MOLAND model related to the practical implementation, and these included the following: customization of the transition rules, lack of conflict resolving rules, and problems with zoning implementation. Moreover, Twumasi et al. (2008) presented two limitations of MOLAND model to assess and simulate biodiversity.

According to the study, MOLAND is unable to support cell sizes less than 2500 m^2, which is too large to consider for small scale studies where massive loss of information can be incurred. In addition, MOLAND cannot deal with more land cover types, which are essential for biodiversity analysis. However, they presented this model as a potential decision support tool for spatial planning.

2.2.5 The Urban Expansion Dynamic (UED) model

He et al. (2008) presented the Urban Expansion Dynamic (UED) model by incorporating a potential model into a CA model. They implemented this model to determine past urban development and to predict future expansion of the Beijing municipality (total area 16,808 km^2), China. The objective of the UED model was to explain the process of urban expansion considering the individual cell evolution, overall urban pattern, and the spatial interaction of population and capital. The potential model influences transition rules of a CA to locate new urban cells not only considering the function of the states of neighborhood cells in the urban expansion process but also calculating the probability of conversion of a non-urban cell to a new urban cell by considering spatial interaction of distribution and flow of capital and population. According to the study, a rapid urban growth observed in 1991-2004 and the projected urban patterns for 2015 show that about 746 km^2 of non-urban land will be occupied by encroaching on green space and cultivated land. The result also revealed that steady population growth and fast economic development strengthened the urban expansion process. To calibrate the UED model, an ‘adaptive Monte Carlo approach’ was used to avoid subjective or empirical determination of weights in transition rules of the CA model. The UED model can be a useful tool to assist the understanding of urban expansion process and support urban planning and management.

2.2.6 Advantages and limitations of CA models

CA urban models have several benefits: they are interactive, potential outcomes can be visualized and quantified, they can be closely linked with GIS, and raster-based spatial data derived from remote sensing platforms are easily incorporated into the CA modeling environment

(Jantz et al. 2004). According to White and Engelen (2000), CA models are attractive for the following reasons:

1) they are basically spatial, are defined on the raster cell space and are compatible or can be made compatible with most spatial data sets;
2) they are dynamic and capable of representing spatial processes directly;
3) they are adaptable and can be set up to represent a wide range of situations and processes;
4) they are rule-based, and can thus capture a wide variety of spatial behaviors;
5) they are simple, and thus computationally efficient;
6) they can exhibit extraordinarily rich behavior due to their simplicity.

CA models have gained increasing attention from researchers as a powerful modeling tool in simulating geographical phenomena (Macmillan and Huang 2008) as well as predicting spatial patterns of urban development. Most CA models have been successful in urban development studies such as simulation of urbanization, urban density, defining driving factors, and evolution of urban spatial structures over time (White and Engelen 2000, Murayama and Thapa 2011, Li and Liu 2008). However, they have some limitations in analyzing urbanization processes and defining variables (Yeh and Li 2003) and are difficult to calibrate with multiple land use categories (Li and Yeh 2002) and complex urban growth processes (Verburg et al. 2004). Traditional CA models have some limitations to analyze the influences of human factors such as governments, residents and investors, and urban dynamics, and to deal with mobile objects such as pedestrians, migrating households, or relocating firms (Benenson and Torrens 2004). To overcome these problems Li and Yeh (2002) utilized CA in combination with Artificial Neuron Network (ANN).

2.3 Markov chain modeling

The Russian mathematician Andrei Andreyevich Markov (1856-1922) developed the "Markov chain" published in 1907 (Balzter 2000, Basharin et al. 2004). Markov chain modeling is basically a simulation technique that is also known as Markov modeling or Markov analysis. The application of Markov analysis was introduced in geography in 1965 to study the movement of central city rental housing areas by Clark (1965). Development in remote sensing and GIS

techniques have widened the Markov model as well as other modeling tools. Markov chain analysis has been applied in different geographical and environmental studies: vegetation dynamics (Balzter 2000), urban studies such as suburbanization, neighborhood analysis and urban land cover change, land cover impact assessment of large public investments such as dams, the analysis of historical dynamics of urbanization in agricultural areas (Muller and Middleton 1994), and the assessment of the impacts of land cover and land cover change on local climate. Markov models create the statistical relationship between land cover change and environmental factors (Benenson and Torrens 2004). In particular, this process identifies the quantities of conversion area or the amount of change on the basis of immediate preceding states, which are inputted as initial conditions (from time 1 and time 2), and make probability matrices for the future from many possibilities (conversion probabilities). Finally, Markov analysis of land cover change has been combined with GIS to generate a tool for projecting different categories of land cover change (Weng 2002).

Markov chain analysis is an analytical method of stochastic or random processes (Briassoulis, and Balzter 2000, and Lopez et al. 2001). Some specific characteristics of Markov chain analysis differ from other analyses of stochastic processes. The Markov process can be described as a set of states, $S = \{S_1, S_2, \ldots\ldots S_n\}$ where one state changes successively to another state with some probability at each time step (Zhang et al. 2011). This is a characteristic assumption of Markov processes. The probability of moving from one state to another state is called a transition probability that can be calculated from two land use maps of different dates without considering neighborhood influence (Benenson and Torrens 2004, Jokar Arsanjani et al. 2013). If the initial state is S_i, and it moves to state S_j in time period t, then the transition probability can be denoted by P_{ij} and it is given for every ordered set of states. These probabilities can be represented in the form of a transition matrix, P, as shown below:

$$P = (P_{ij}) = \begin{bmatrix} P_{11} & P_{12} & .... & P_{1n} \\ p_{21} & P_{22} & .... & P_{2n} \\ ... & ... & ... & ... \\ p_{n1} & P_{n2} & .... & P_{nn} \end{bmatrix}$$

The Markov chain method is simple and convenient for complex patterns of change, and multiple category land cover change modeling (Eastman 2012). Weng (2002) investigated land cover change dynamics of the Zhujiang Delta in China using satellite remote sensing data, GIS, and Markov chain modeling technique. The result of the study displayed that the Markov chain process is able to predict simple trend land cover change. In Zhang et al. (2011), the transition probability of the Markov process simulation was determined to predict wetland type distribution area in Yinchuan Plain in 2006. The results of the study revealed that integrating remote sensing (RS) and GIS technology with the Markov model resulted in a feasible output that can be useful for wetland ecological system restoration and environmentally sustainable development planning of the study area. The study suggested that high-precision data through remote sensing mapping may help to get an accurate transition probability matrix to establish reliable prediction.

2.4 Markov – CA models

A Markov-CA model is a combination of two modeling approaches, in which the Markov chain process determines the temporal changes among land cover types over time based on transition probability matrices (López et al. 2001) and the CA controls the spatial pattern of change through neighborhood rules depending on the transition potential of each pixel (Araya and Cabral 2010, He et al. 2008).

Guan et al. (2011) tested a "Markov-CA model using seven natural and socioeconomic factors: slope, elevation, distance to the nearest road and distance to the nearest river, population density, GDP per capita, and land price were selected for creating transition potentials. Then spatial distribution of land use was simulated on the basis of the transition rules of the CA model. Finally, they used the Markov-Cellular Automata model to predict future land use changes of Saga city, Kyushu Island, Japan. Kamusoko et al. (2009) combined physical and socioeconomic data with the Markov–CA model to simulate future land use change. Different validation analyses showed that agriculture, woodland and mixed rangelands were relatively well simulated, but the model did not successfully forecast the location of the bare land class due to the shortage of spatial data. Kamusoko et al. (2009) predicted future land cover change (up to 2030) in Masembura and Musana, Zimbabwe, based on the Markov-CA model. Transition probability

matrices were created from Landsat-derived land cover maps using Markov chain analysis, and transition potential maps were generated using a multi-criteria evaluation procedure from biophysical and socioeconomic data. They simulated land cover maps for 2030 using the transition matrix in 1989-2000. Simulation for 2030 revealed that with no development policies in the study area, current trends of land cover change will probably continue and severe land degradation will occur.

In Araya and Cabral (2010), the CA-Markov model of IDRISI Kilimanjaro software was applied to identify and analyze urban change patterns within the Setúbal and Sesimbra municipalities in 1990-2006. The study revealed an intensive urban sprawl in 1990-2006, where urban area increased by more than 90%; and prediction presented the vulnerability of reserved Natural Park and agricultural land. Validation of the model carried out by Kappa index and overall accuracy of simulation for 2006 calculated 83%.

Jokar Arsanjani et al. (2013) used a hybrid model which included a logistic regression model, Markov chain, and CA to improve the standard logistic regression model; it was implemented on the Tehran metropolitan area to analyze and simulate urban growth, and environmental and socioeconomic variables were included to create transition potentials of land cover categories. The model could integrate environmental, socioeconomic, and spatial factors to assess its influence on urban sprawl. The results presented a positive influence on urban expansion of the Central Business District (CBD), demography, population density, vicinity of buildings, parks, roads, farm lands, and open space. However, surroundings of existing city centers and parks were found more probable to be developed, while steeper slopes had less probability to change. The model was validated using ROC, calibrated land cover map 2006, and the model achieved a satisfactory result with a match of 89% between simulated and actual maps of 2006.

Cabral and Zamyatin (2006) utilized CA-Markov, CA-Advance, and GEOMOD models to explain the urban dynamics of Sintra-Cascais municipalities (Portugal) and compared their findings. Kappa indices were calculated to validate their models, and they found that both CA-based models produced better simulation results. However, CA-Markov presented some limitations to simulate small land cover changes for long term forecasting where the other two models presented better simulations with different dynamics according to location.

2.5 IDRISI Land Change Modeler (LCM) model

LCM is an ecological analysis module in IDRISI software that was developed by Clark Labs. Developers recommended it for predicting and assessing the impact of land cover and land cover change on biodiversity. LCM consists of modules to analyze historical change, predict future change, validate the model, and calculate the estimated Green House Gas (GHG) (Figure 1.1). The Reducing Emissions from Deforestation and forest degradation (REDD) project tab was added to LCM of the IDRISI 17.02 edition as an extension to implement a climate change mitigation strategy focusing on forest conservation policy (IDRISI). LCM creates bar graphs and maps based on land cover changes of individual or all land cover categories, and calculates transition potentials between two historical input images.

An Artificial Neural Networks (ANN) is a non-linear statistical method defined as a complex mathematical function that converts input data to a desired output and consists of a connected network of processing units created on the basis of the human brain neuron network (Eastman 2012). ANNs have been successfully applied to numerous domains and have proven their suitability to solve various problem (Mas et al. 2004). In IDRISI, the Multi-Layer Perceptron Neural Network (MLPNN) calculates transition potentials of multiple land covers based on information from training sites by using multiple output neurons applying a back propagation algorithm (Li and Yeh 2002). It has several advantages such as the capability to model group transitions and complex relationship between numerous variables and multiple land covers (Eastman 2012, Li and Yeh 2002). The MLPNN contains one input layer (blue circles in Figure 1.2), one output layer (green circles in Figure 1.2) and one or more intermediate hidden layers (red circles in Figure 1.2) where each layer contains nodes (or neurons) and layers are connected through connecting weights. The performance of MLPNN depends on its architecture (number of hidden layers and nodes) and on the training parameters (learning rate, momentum, and number of iterations in the case of a back-propagation learning algorithm). The accuracy of the training rate is displayed in percent (Eastman 2012, Pérez-Vega et al. 2012). An HTML file is displayed

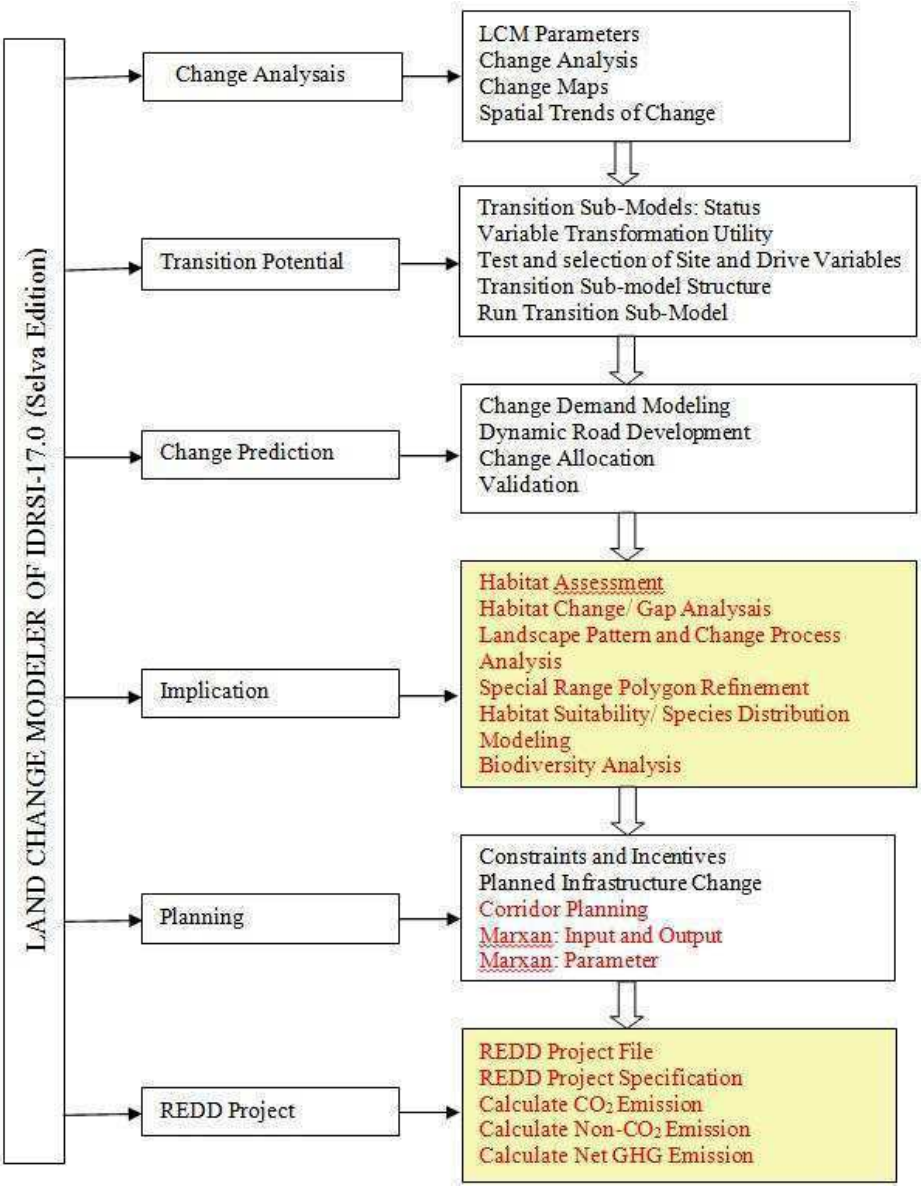

Figure 1.1: Different sub-modules and panels of LCM (red colored sub-modules have not used in the study).

with information on the training process, including the relative power of the explanatory variables used after completing the training process, and transition potential maps can be created (Eastman 2012). However, transition potentials with a high accuracy rate (more than 80%) are recommended to use for future prediction to achieve better simulation results.

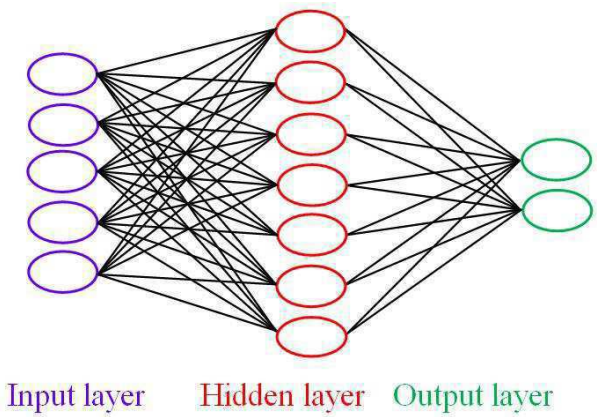

Figure 1.2: Structure of a Multilayer Perception Neural Network (MLPNN) model.

Figure 1.2 presents the simple structure of a MLPNN that is a feed-forward neural network (Mas et al. 2004). The basic processing units are neurons or nodes that are indicated as circles and connecting weights are presented by lines. The number of neurons (n) in the input and output layers are the same and the hidden layer contains 2n+1 neurons (Li and Yeh 2002). Li and Yeh (2002) suggested that 2n+1 hidden neurons can assure perfect simulation and reduction in the number of neurons may lead to increased inaccuracy.

2.5.1 Literature review on IDRISI-LCM

Oñate-Valdivieso and Bosque Sendra (2010) conducted a study to analyze land cover changes in the Catamayo-Chira Binational Basin, Spain, to identify explanatory variables, and to explain the relationship among the explanatory variables using the LCM module of IDRISI. Land cover changes were analyzed following the methodology proposed by Pontius et al. (2004) to calculate interchanges among the categories, persistence, loss, and gain. The explanatory variables were evaluated through the Cramer's V coefficient. In this model, six explanatory variables were considered: elevation (DEM), slope, total annual precipitation, distance to watercourse, distance to the initial location of the cover, and the type of land. After selecting variables, transition potential maps were created through both logistic regression and MLPNN that are available in LCM using land cover maps of 1986 and 1996. The land cover map of 2001 was then predicted through Markov chain. The confusion matrix, Kappa index, and the relative operating

characteristic (ROC) (Pontius and Schneider, 2001) were used to evaluate the accuracy of the model. According to their observation, logistic regression provided slightly better results than MLPNN.

Mas et al. (2012) conducted a study to compare simulated land cover map patterns generated using two different models (DINAMICA and Land Change Modeler). They used land cover maps of 1986 and 1994 and five explanatory variables to simulate a land cover prediction map for 1994. Land cover changes were analyzed using a Markov matrix which is the common method in DINAMICA and LCM. Transition potential maps in IDRISI were created using MLPNN and five explanatory variables: distance from urban areas, distance from roads, slope, distance from disturbance, and elevation. The weights of evidence method was employed in DINAMICA. The findings of the study revealed that deciduous mature forest, savanna, Amazonian mature forest, and woodland savanna transformed to anthropogenic disturbed area during the study period. The results also showed that LCM generated land cover changes mainly in edges of previous patches of anthropogenic disturbance while the changes are scattered in maps generated from DINAMICA.

Pérez-Vega et al. (2012) reported an assessment of transition potential maps produced by two LUCC models DINAMICA and LCM based on the same explanatory variables using the weights of evidence method and neural networks, respectively. Three different techniques were employed to compare outcome maps from the models: visual interpretation, ROC and an index of Difference in Change potential, and they found better results at the per transition level using DINAMICA while LCM produced more accurate transition potential maps for overall change.

Silva and Tagliani (2012) conducted a study to identify recent land cover dynamics of the landscapes surrounding the Patos Lagoon of Brazil to analyze land cover changes in 1987-2000, identify driving factors of change, and predict land cover for 2015. Socioeconomic indicators such as population, social accountability, standard of living index, income and occupation level in agriculture, and government development plans were considered to identify driving variables. LCM of IDRISI Taiga was performed to analyze and predict land cover change in the study. Transition potential maps were created using land cover maps of 1987 and 2000, distance from road, distance from urban areas, geomorphology, and a zoning map incorporated as a constraint.

About 480 km^2 of forest areas transformed to agricultural which was the largest change in 1987-2000. Urban area increased by 170 Km^2 (20% of urban area in 1987) in the same time interval. The model had an overall accuracy of 83%.

Johnson (2009) conducted a study to evaluate the structure and accuracy of LCM for ArcGIS using the data set of the CONWR case study. In addition, different levels of resolution (1 m, 10 m, 30 m, 60 m, 90 m, and 120 m) were used to determine the sensitivity of LCM to multiple levels of resolution. According to the study, dramatic increases in water, developed, and forested areas were observed in 1938-1971. The creation of the lake under the Crab Orchard Creek Project was responsible for the increase in the water body, and the forest cover increased due to the tree plantation project for reducing soil erosion in the early 1940s. Moreover, much abandoned and shrub land area converted to forest. The study highlighted some limitations of LCM, such as the wrong tabulation of the .rdc file, confusion in the measurement units, and insufficient quantitative data output. Later, recommendations were offered to improve the ability to view numerical data in tabular form, improve the capability for exporting tables, matrices, and change graphs, and increase the ability to modify the color, axes, and legend of graphs.

Tewolde and Cabral (2011) analyzed urban expansion and its impact on agricultural areas and forest cover of the Greater Asmara Area (GAA), the capital of Eritrea, in 1989-2009. In addition, they also identified major variables of rapid urban growth, loss of agriculture and forest cover, and showed the effect of built-up sprawl in the near future using ArcMap and LCM of IDRISI Andes. The built up area increased by about 200% from 1,464 ha (7%) to 3,172 ha (15%) in 1989-2000, and further increased to 5,905 ha in 2009 which resulted in loss of urban agricultural land and forest area. Moreover, high population growth (>5%) after independence of the country (1991) and return of refugees from neighboring countries are identified as main causes of land cover change and urban sprawl. The model was validated using the Kappa index of IDRISI's VALIDATE module and the it achieved 80% accuracy.

Aguejdad (2009) presented urban sprawl simulation of Rennes (France) using LCM. They utilized several variables, and applied MLPNN to create transition potential maps. A simulation map was created for 2006 and validated with a Kappa index of 0.98. Short term prediction using LCM achieved better goodness of fit. Aguejdad and Houet (2008) conducted a study to simulate

urban sprawl of Rennes France, using Logistic Regression of LCM. Several distance variable (distance from existing urban area, distance from the village center, and distance from major road), topographic variables, Land Use Plans (POS) and Local Urban Development Plans (PLU) were used as explanatory variables; urban constraints were also added to simulate urban change for 2020 using 2000 and 2005 maps as initial inputs.

2.6 Agent Based Modeling (ABM) in Geography

Simulation modeling has become an efficient way of analyzing complex theoretical and empirical studies using agent based modeling (ABM) and cellular automata (CA) in a common computer program (Wu et al. 2009). "*An autonomous agent is a system situated within and a part of an environment; that senses that environment and acts on it, over time; in pursuit of its own agenda and so as to effect what it senses in the future*" (Franklin and Graesser 1996 in Benenson and Torrens 2004. p. 154). Multi Agent Simulation (MAS) consists a set of agents that interact between themselves and their environment to fulfill user's goals using information and the states of the objects in the environment (Ligtenberg et al. 2004). The SLEUTH (Dietzel and Clarke 2007) and CLUE (Verburg et al. 1999) models are the most recently used agent based land cover change simulation models. Applications of agent-based modeling in land cover change are usually spatially explicit, and agents represent, for example, households that are relocating their homes or individuals using transport systems (Miller et al., 2004). Nowadays, agent-based modeling has gained popularity in population, immigration and residential mobility studies, and in land cover change modeling research. Agent-based approaches allow modelers to represent different individual agents that interact with each other and on the system under consideration (Macmillan and Huang 2008, Haase et al. 2010). Moreover, hybrid agent based system (ABS) and CA modeling tools are developing day by day where ABS represents mobile agents and CA represents environmental characteristics. Hybrid models are designed to simulate complex, dynamic and stochastic patterns and, to analyze the interactions between human activities and the environment (Wu et al. 2011).

Utilization of agent-based or multi-agent system tools for the human environment modeling has been increasing among researchers during the last decade. An agent-based model of land

cover change consists of two key components (Wu et al. 2011): the first is a cellular model that represents the study area and may draw on a number of specific spatial modeling techniques such as CA, spatial diffusion, and Markov models. The second component is an agent-based model (ABM) that represents human decision making and interactions consisting of a number of human agents that interact with each other and with their environment. According to Wu et al. (2011), an agent may represent land cover characteristics, component and quality of soil, topographic condition, and an assessment of the land management choices of neighbors (the spatial social environment) to calculate a land cover decision. Some models seek to link human and natural systems at different spatiotemporal scales to understand changes in land cover (Haase et al. 2010). Macmillan and Huang (2008) focused on the economic and demographic issues linked in multi-agent modeling. Haase et al. (2010) used the RESMOBcity model to simulate the pattern of residential mobility in Leipzig, Germany. In this model, they used household types and the population based on demographic transition and spatial location of housing. It was also able to simulate urban population growth and residential mobility. Wu et al. (2011) used a hybrid agent-based and CA6 model to analyze the evolution of China's population. They used ABM to simulate the behavior of individual migrant members. CA was used to simulate the geographic environment in raster format. They used a "population system" and three other sub-systems: climate, social and agricultural systems, which influence the total population system. Climate has a direct influence on agricultural and social systems, causing migrations that influence the population system. Verburg et al. (1999) used the CLUE (the Conversion of Land use and its Effects) modeling framework to calculate changes in demand for agricultural products taking into account population growth that influenced the spatial distribution of land cover types related to agricultural production. The calculations were based on the trends of the past and projections for the future. Verburg and Overmars (2009) introduced a modeling approach named 'Dyna-CLUE' with an application for European land cover where interactions between changing demands for agricultural land and vegetation processes lead to the re-growth of natural vegetation on abandoned farmland. The Dyna-CLUE model is an adapted version of the CLUE model (Verburg et al. 1999) which is based on the spatial allocation of demands for different land cover types to individual grid cells. This version combines the top down allocation of land cover change to grid

cells with a bottom-up determination of conversions for specific land cover transitions. They divided the land cover types into two groups: those driven by demand at the regional level, and those where the demand at the regional level cannot be determined. According to the model, the spatial allocation module allocates the regional level demand by considering location suitability, neighborhood suitability, conversion elasticity and competitive advances. However, the results of this model depend on the specific study area, spatial and temporal scale, and the purpose of the study (Verburg and Overmars 2009).

Evans and Kelley (2004) presented how outcomes from an agent-based land cover change model vary with different scales. Results from different model outcomes show that the finest resolution produced the most useful results, overall fit was best at this spatial resolution, and the model produced a more diverse set of agent types. They suggested using a variety of spatial scales to explore the scale dependence of the model outcomes for agent-based models of land cover change with a similar household/parcel framework.

2.7 Model choice

Advantages, disadvantages, and application of different modeling approaches have been discussed in the above sections. CA modeling, concerned mainly with urban growth simulation, has shown limitations in multiple complex land cover prediction. Several studies have done well with acceptable calibration and validation using CA-Markov chain modeling approach in different scales and environments in recent years (Araya and Cabral 2010, Guan et al. 2011, Jokar Arsanjani et al. 2013, Kamusoko et al. 2009). Recently, agent based models or multi-agent modeling systems have been used to explain and simulate interactions between human action and spatial components. In agent-based models, socioeconomic, demographic, and all other spatial attributes can be used with a spatial component to describe and simulate a particular issue.

In this study, we used topographic explanatory variables with several spatial planning components to simulate land cover changes without taking into account any particular spatial attribute such as population or socioeconomic data. Therefore, we did not use any agent based modeling approach. We used Land Change Modeler (LCM) of IDRISI, a CA-Markov based model, to simulate temporal and spatial patterns of change in land cover for both short and long

time periods. Several studies were described briefly in the above review, and LCM proved to be a powerful modeling tool to simulate change with a variety of land cover types, including urban growth simulation studies. Implication analysis (habitat analysis and assessment such as habitat and biodiversity change pattern, and modeling) and planning (constraints and incentives, planning infrastructure change, corridor planning) tools are included in the LCM model for a variety of applications (Eastman 2012). Multi-Layer Perceptron Neural Network (MLPNN), Markov chain, and regression models are fully integrated in LCM. MLPNN is a very powerful modeling approach, a non-linear system based on human brain function, is able to take into account complex relationship between inputted variables (Mas et al. 2004).

Pérez-Vega et al. (2012) conducted a study to compare the performance of LCM and DINAMICA revealed that potential maps of LCM generated by using neural networks are more accurate than individual probabilities obtained through the weights of evidence method of DINAMICA. (Fuller et al. 2011) projected deforestation of Central Kalimantan, Indonesia for 2020, compared results from three different models Dinamica EGO, GEOMOD, and the LCM, found the last modeling tool simulated the highest accurate result for allocation of changes. LCM model proved to be more powerful than CURBA (California Urban and Biodiversity Analysis Model by Landis 1998) and CUF (California Urban Futures by Landis 1995) models because LCM can be used for change prediction with a variety of land cover types, including urbanization growth simulation studies (Khoi 2011). Khoi (2011) analyzed and predicted deforestation of the *Tam Dao National Park* (TDNP) region in Vietnam using Multi-Layer Perceptron Neural Network-Markov chain (MLPNN-M) approach of LCM. Ahmed and Ahmed (2012) used Stochastic Markov, CA-Markov, and LCM to compare simulated land cover of Dhaka city for 2009, and they found the last method was most appropriate. Tewolde and Cabral (2011) applied LCM to analyze urban expansion and its impact on agricultural areas and forest cover of the Greater Asmara Area (GAA) and achieved 80% accuracy from kappa index. Aguejdad and Houet (2008) used LCM to simulate short term urban sprawl of Rennes, and the results suggested that LCM could be used to simulate both urban growth and multiple land cover changes of any environment.

2.8 Conclusion

Studies of the temporal and spatial distribution of land cover change have become an important issue due to the rapid conversion of land cover and its impact on environmental change. Modeling of land cover change and urban growth has been initiated in the last decades to predict and simulate future land cover conditions. Several computer modeling techniques associated with GIS have been developed and they have improved simulation accuracy. CA modeling, developed in the 1950s, was the first stage of modeling on spatial and geographical simulation. Markov chain modeling and CA-Markov modeling were developed and combined with GIS to generate a tool for projecting land cover and spatial changes. Nowadays, agent based modeling has gained popularity in population, immigration, residential mobility and communication sectors. LCM in IDRISI has proven to be a powerful land cover change modeling tool capable of dealing with complex multiple land cover categories.

CHAPTER 2

SPATIAL DYNAMICS OF LAND COVER CHANGE IN A EURO-MEDITERRANEAN CATCHMENT (1950-2008)

(Article published in the Journal of Land Use Science, 2015, vol. 10:277-297, in Appendix)

1 Introduction

Land cover changes represent major human alterations of the Earth's land surface (Lambin et al. 2001) and land cover conversion processes in Europe have accelerated since the Second World War (Antrop 2005, Geri et al. 2010, Serra et al. 2008). Land cover change has occurred through the interaction of environmental and socio-economic characteristics, including population growth, urban sprawl, industrial development, and political and environmental policies. In addition, rapid expansion of tourism during the last six decades has caused important socioeconomic changes (Dunjó et al. 2003) driving land cover alterations in Euro-Mediterranean areas (Geri et al. 2011). Land cover changes affect biodiversity and ecosystems, food security, human health, urbanization, and global climate change (Falcucci et al. 2007, Geri et al. 2011, Sala et al. 2000). They can also be responsible for environmental change, water pollution and soil degradation (Dunjó et al. 2003).

Several studies have described land cover changes in the Mediterranean area. Mediterranean countries from Spain to Greece experienced strong urban growth from the 1970's onwards, and a moderate growth rate is projected to continue (Benoit and Comeau 2005), (Serra et al. 2008) reveal that about 34% of Spanish Mediterranean coastal areas were urbanized between 1989 and 1999. In France's Provence Alpes Côte d'Azur region (SE France), about 40% of shorelines were built in 2006 (IFEN 2012). Migration from other European countries tends to concentrate in the Mediterranean coastline area (Brunetta and Rotondi 1996) since the quality of life in Mediterranean cities seems to be greater than average in European countries (Cori 1999). Aging population in Europe has a typical migration trend towards the Mediterranean coastal zone (Van Eetvelde and Antrop 2004). In addition, internal migration also favors coastal areas, increasing urban pressure land cover changes in these areas (IFEN 2009). For example, (Van Eetvelde and Antrop 2004) analyzed the characteristics and mechanisms of land cover change in southern France (Tavernes) and identified a pattern where arable land decreased in foothills while urban

areas expanded near the coast. They also found that residential and secondary houses occupied traditional terraced foot slopes.

Traditional Mediterranean agriculture was comprised mainly of vineyards, olive trees, and wheat grown in the nearby hinterland, often on terraces. (Serra et al. 2008) reported that vineyards and olive trees decreased in mountainous areas and transitional sub-regions, resulting in land abandonment and increased shrub land area. Vineyard area decreased near roads and urban areas due to urban sprawl and industrialization in moderately mountainous to flat valley areas in Peyne, France (Sluiter and de Jong 2007). Under these conditions, farmland is sacrificed to urban expansion (Martínez-Fernández et al. 2013). (Nainggolan et al. 2012) identified several biophysical and socioeconomic factors (demography, markets, and subsidies on agriculture) responsible for the change in Torrealvilla catchment of South-eastern Spain: population decreased in 1960-1980 due to migration from villages to the coastal area and rain fed agricultural, the main landscape feature in 1940-1960, was abandoned. However, in 1980-2005, intensification of agriculture occurred on flat to gentle slopes and near main roads due to subsidies for agriculture and the European highway infrastructure. Other authors have found that land cover change affected the overall environment, resulting in deforestation (Kepner et al. 2006), land abandonment (Serra et al. 2008), and increased runoff and soil erosion in Portugal and Greece (Koulouri and Giourga 2007, Nunes et al. 2011).

From a spatial point of view, (Falcucci et al. 2007) describe three common major land cover changes in the Mediterranean area of Italy: the expansion of tourism that promotes rapid urbanization along the coastline, spatial concentration of agriculture on alluvial plains and low lands (except in the coastal area) due to urban sprawl, and abandonment of agricultural terraced land in mountainous steep slopes resulting in their transformation to forest. Four general trends of land cover change took place during the last decades in the coastal Mediterranean area (Geri et al. 2011, Nunes et al. 2011). Firstly, dry farming and forest land cover decreased in alluvial coastal plains while reforestation occurred in hilly areas. Secondly, urbanization occurred rapidly in most of the coastal plains where the tourism industry flourished. Thirdly, population growth and socio-economic development caused agricultural intensification that increased irrigated crops. Fourthly, the development of infrastructure, communication networks, and technological advances resulted in socio-economic development that was the main reason of agricultural land abandonment on marginal lands.

Most of the studies on land cover change in the Mediterranean area highlight a particular issue or describe an individual land cover change such as forest, agriculture, or urban expansion (Calvo-Iglesias et al. 2009, Pelorosso et al. 2009), and few studies take into account all these changes concurrently. In addition, spatial patterns of land cover change and identification of driver variables influencing change are sometimes taken into consideration, but they tend to focus mainly on altitude or slope (Geri et al. 2010, Serra et al. 2008) and few authors (Sluiter and de Jong 2007) take distance variables into account. Urban population growth and expansion of tourism occurred more in the French Mediterranean coastal area than on average for European Mediterranean coasts in the last decades (Benoit 2001). This resulted in significant land cover change in this region, but very few studies describing land cover change in the area can be found. (Fox et al. 2012) conducted a study to analyze the impact of land cover change on total runoff between 1950 and 2003 in a context of river management. They noted a small increase in runoff due to a complex pattern of land cover change, but spatial controls on these changes were not examined.

The first objective of this study is to quantify land cover change patterns in terms of gains, losses, total change and swapping in a Mediterranean catchment with a strong vineyard activity in proximity to a coastal area well known for its tourism. The second objective is to quantify the impacts of topographic and distance variables on land cover change for each land cover category.

2. Methods

2.1 The study area

The Giscle watershed has a surface area of about 235 km² and is situated in the Var department of SE France near the Gulf of St. Tropez (Figure 0.3). It is characterized by a Mediterranean climate with hot dry summers that extend from June to August, and cooler rainier winters. Average temperatures range between 22°C to 26°C in summer and 5°C to 10°C in winter. The mean annual rainfall is about 900 mm, and the main rainy season is from October to January and in April (Fox et al. 2012). The study area includes two topographic units: the hilly upper part of the catchment (roughly 70% of the catchment) is made up of metamorphic rocks, mostly schists and gneiss, while the lower part of the catchment, located near the gulf, is a gently sloping alluvial plain (Fox et al. 2012).

The western (upper) part of the watershed is mostly forest (pine and oaks) and the topography of the area is uneven with the highest elevation at about 650 m. Vineyard and moderate to dense urban areas are the dominant land cover types of the lower part of the catchment. The region became a major tourist destination of Mediterranean France in the second half of the twentieth century, with the "Côte d'Azur" development, and this generated a strong growth in urbanization. Three main municipalities are located within the catchment: Cogolin, Grimaud and La Môle (Figure 0.3). Cogolin and Grimaud are situated in the eastern part of the catchment, about 5 km from the Mediterranean coast. They represent the main populated areas with total populations of around 11,000 and 4,000, respectively (INSEE 2011). La Môle is a small urban area with a total population of around 950 (INSEE 2011). The total population of the catchment increases by several times (perhaps as many as 10) in the summer due to tourism and secondary homes. Unlike many Mediterranean coastal areas, the sea front is confined by the gulf and topography, and land cover change is restricted to the inner near coastal area.

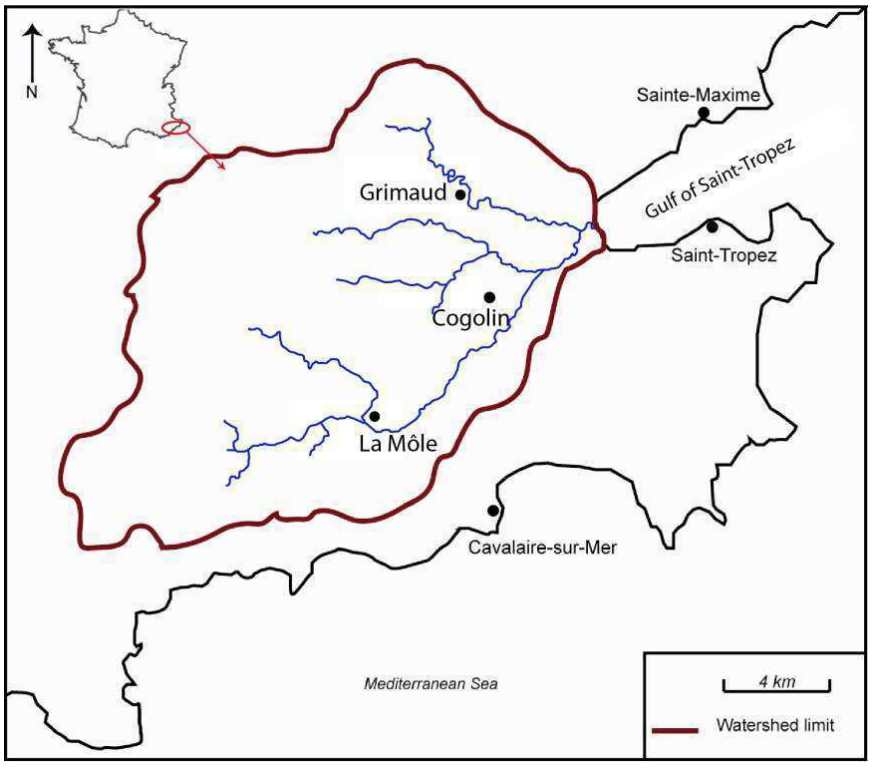

Figure 0.3: Location of the catchment.

2.2 Data description and land cover classification

Land cover maps were screen digitized from acquired (Institut Géographique National) digital orthorectified aerial photographs (1950 and 1982 were panchromatic; 2008 was color) using ArcGIS (Dangermond 2012). Initial spatial resolution for all aerial photographs was 0.5 m, and this was reduced to 1 m to facilitate data manipulation. The aerial photographs of 1950 were the first high quality post-Second World War photos available when the area was still strongly rural; an intermediate date (1982) was selected between 1950 and the most recent 2008 photographs. Aerial photographs of 1982 may represent land cover conditions at the beginning of rapid urban sprawl (Baccaini and Sémécurbe 2009, Salvati et al. 2013).

Surfaces were classified into five categories based on visual interpretation: forest, prairie or grassland, vineyards, urban and suburban areas. High density urban, industrial and commercial areas were classified as urban, and moderate density to low density built areas were classified as suburban. Urban and suburban areas were distinguished by the density of buildings and other infrastructures as described below. Isolated housing was ignored. To avoid creating a small isolated category, the Verne water dam (built in 1989-1991) was ignored and left as forest; its surface area is negligible compared to total forest cover. Similarly, a small recreational port built on the sea at the outlet of the catchment was ignored, and the limit used for the catchment was the 1950 seashore. After digitization, land cover maps were imported into IDRISI (Eastman 2012). Main roads and stream networks were then digitized from the aerial photographs of 2008. Main roads were about the same in aerial photographs of 1982 and 2008, so this layer did not change over time. Cell size of all digitized maps was changed to 25 m to make land cover layers compatible with the 25 m DEM used for the creation of topographic and distance variables.

Land cover layers were identified visually. Examples of each land cover type are presented in Figure 0.4. Most of the forest areas found in the aerial photographs were evergreen, and were clearly identified by their deep grey color in the black and white aerial photographs (1950 and 1982) and deep green color in color aerial photographs (2008) (Figure 0.4a). Vineyards were differentiated by their blocky, geometric shapes and linear texture created by the rows of planted vines (Figure 0.4b). Unmanaged or abandoned agricultural areas, new shrub lands with small and scattered trees, and pasture land for sheep and horses were all classified as grassland even though some of it could more appropriately be called shrubland (Figure 0.4c). Densely to moderately built areas, including residential, commercial, and industrial areas, were identified as urban.

Urban areas (Figure 0.4d) were distinguished from suburban (Figure 0.4e) by the density of buildings and absence of trees and open area. Suburban area is essentially low density residential housing. Some small denser communities were considered suburban areas. The presence of trees and open spaces were common in the suburban area. Land cover classification was facilitated by numerous field visits.

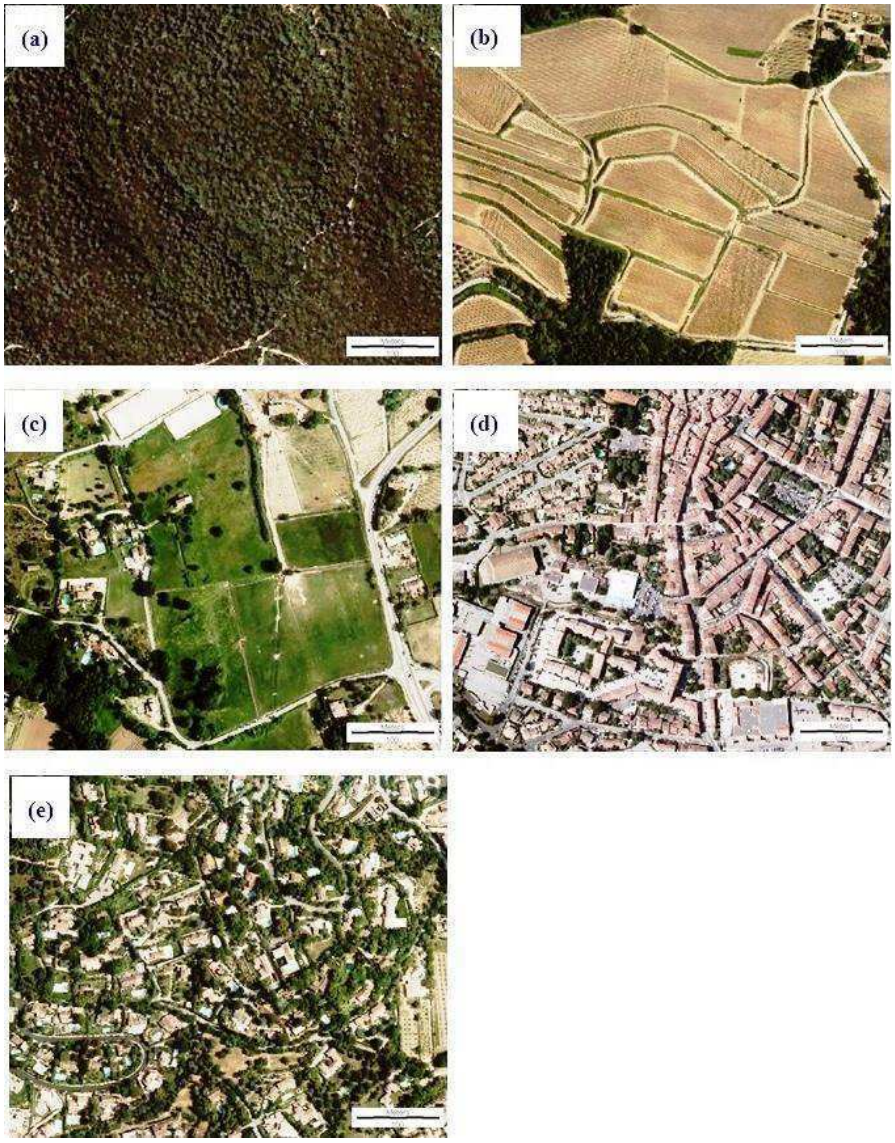

Figure 0.4: Examples of (a) Forest, (b) Vineyard, (c) Grassland , (d) Urban area, (e) Sub-urban area.

2.3 Cross tabulation analysis in 1950-1982, 1982-2008, and 1950-2008

Land cover change was quantified using the cross tabulation matrix of the CROSSTAB module and the Change Analysis module of the Land Change Modeler (LCM) of IDRISI Selva

(version 17.02 (Eastman 2012). The cross tabulation matrix is a fundamental process in land cover change analysis (Pontius Jr et al. 2004) to show land cover changes between two images of different dates. Persistence and pixel numbers of each category from earlier to later classified images are displayed through images and tables. After creating land cover maps of 1950, 1982, and 2008, land cover changes in three temporal periods were investigated: 1950-1982, 1982-2008, and 1950-2008. Cross tabulation of 1950-1982 represents the historical land cover change shortly after the Second World War; 1982-2008 represents more recent changes in land cover from the beginning of the urban sprawl period. The net 58 year change is provided by the 1950-2008 analysis. The land cover change determining method proposed by (Pontius Jr et al. 2004) was applied for all temporal periods to quantify persistence, gains, losses, total change (addition of gains and losses), net change, and swapping (exchanges between land cover classes, equal to the difference between total change and absolute net change).

2.4 Spatial dynamics

To describe spatial dynamics in land cover change, surfaces were simplified into four categories: forest, vineyard, grassland, and built area. Urban and suburban areas were combined into built area due to their small individual coverage compared to other land cover categories. Although data was available for all time periods cited above, maps of losses and gains for individual categories were simplified to show the spatial pattern of net 1950-2008 change since spatial patterns did not vary significantly between 1950-1982 and 1982-1950. Histograms were used to display quantitative losses and gains of each land cover class as a function of topographic (altitude, and slope) and distance (from streams, roads, built area, and the sea) variables for the 1950-1982 and 1982-2008 periods. Altitude and slope were obtained from a 25 m Digital Elevation Model (DEM). Only main roads (created by screen digitization) were taken into consideration and smaller roads and dirt paths were ignored. Main stream channels were also digitized manually due to errors in the automatic tracing of the hydrologic network from the 25 m DEM: in the plain, where topography is nearly flat, errors of up to 300 m could be observed between the modeled and actual channels. Finally, for changes in land cover occurring in 1950-1982, distance from built area in 1950 was used. For changes taking place in 1982-2008, distance from built area in 1982 was calculated.

3. Results

The steps in describing the results are the following: overall trends in land cover change over the study period, detailed analysis of land cover change patterns for three periods (1950-1982, 1982-2008, 1950-2008) using CROSSTAB, spatial trends of land cover change, and topographic and distance controls on land cover change.

3.1 Areal trends in land cover change

Figure 0.5 shows land cover maps digitized from the air photos, and Table 0.1 provides the corresponding surface areas and changes in surface area for each category and time period. Forest remained by far the dominant land cover in the catchment (Figure 0.5), accounting for more than 85% of land cover at all times (Table 0.1). Forest cover decreased by more than 200 ha in 1950-1982, and although this was the largest absolute change in cover, it represents only about 1% of its cover due to its large initial surface cover. A further 1.2% loss was experienced in 1982-2008. Vineyard was the second dominant land cover and it too declined from about 2,241 ha to 2,089 ha (a loss of almost 7%) between 1950 and 1982 (Table 0.1). This trend accelerated in 1982-2008 to about 1,616 ha (almost 23% lost). Over the 1950-2008 period, vineyard lost more than a quarter of its initial cover. Grassland was the third dominant cover in 1950, though its surface area amounted to less than a third of vineyard. Contrary to forest and vineyard, grassland increased significantly during the study period, showing an overall 50% increase between 1950 and 2008. These first three land cover categories covered 97% (in 2008) of the catchment (Table 0.1). Rapid changes occurred in built area (both urban and suburban), which increased steadily to over 700 ha in 2008 from below 50 ha in 1950 (Table 0.1). Moreover, urban and suburban areas each covered only 0.1% of the catchment in 1950, and they increased to about 1.7% and 1.3% of the catchment in 2008, respectively.

Table 0.1: Surface area of land cover types for 1950, 1982, and 2008, and changes in area for 1950-1982, 1982-2008, and 1950-2008.

Land cover type	**Surface area in ha (% of catchment)**			**Change in surface area in ha (% of initial cover)**		
	1950	**1982**	**2008**	**1950-1982**	**1982-2008**	**1950-2008**
Forest	20538 (87.2)	20336 (86.3)	20091 (85.3)	-202 (-1.0)	-245 (-1.2)	-447 (-2.2)
Vineyard	2241 (9.5)	2089 (8.9)	1616 (6.9)	-152 (-6.8)	-473 (-22.6)	-625 (-27.9)
Grassland	754 (3.2)	872 (3.7)	1140 (4.8)	118 (15.6)	268 (30.7)	386 (51.2)
Urban	19 (0.1)	146 (0.6)	402 (1.7)	127 (668.4)	256 (175.3)	383 (2015.8)
Suburban	13 (0.1)	122 (0.5)	316 (1.3)	109 (838.5)	194 (159.0)	303 (2330.8)

As can be seen in Figure 0.5 most of the changes occurred in the eastern part of the catchment. This area corresponds to the alluvial plain where altitudes and slopes are gentler. For the vegetation land covers (forest, vineyard, grassed areas), the rate of change, expressed as % of initial cover, was greater in 1982-2008 than 1950-1982 (Table 0.1). Calculated on an annual basis, the difference would be even greater since the latter period showed greater change in a shorter time, 26 years versus 32 for the initial period. Although the contrary appears to be true for urban and suburban categories, where % change was greater in 1950-1982 than in 1982-2003, it should be noted that the latter period experienced greater absolute change, and small absolute differences in 1950-1982 generate an artificially large % change due to the very small initial area. The built categories showed the greatest % change of all land cover types during the 1950-2008 study period with an increase of more than 2,000% each.

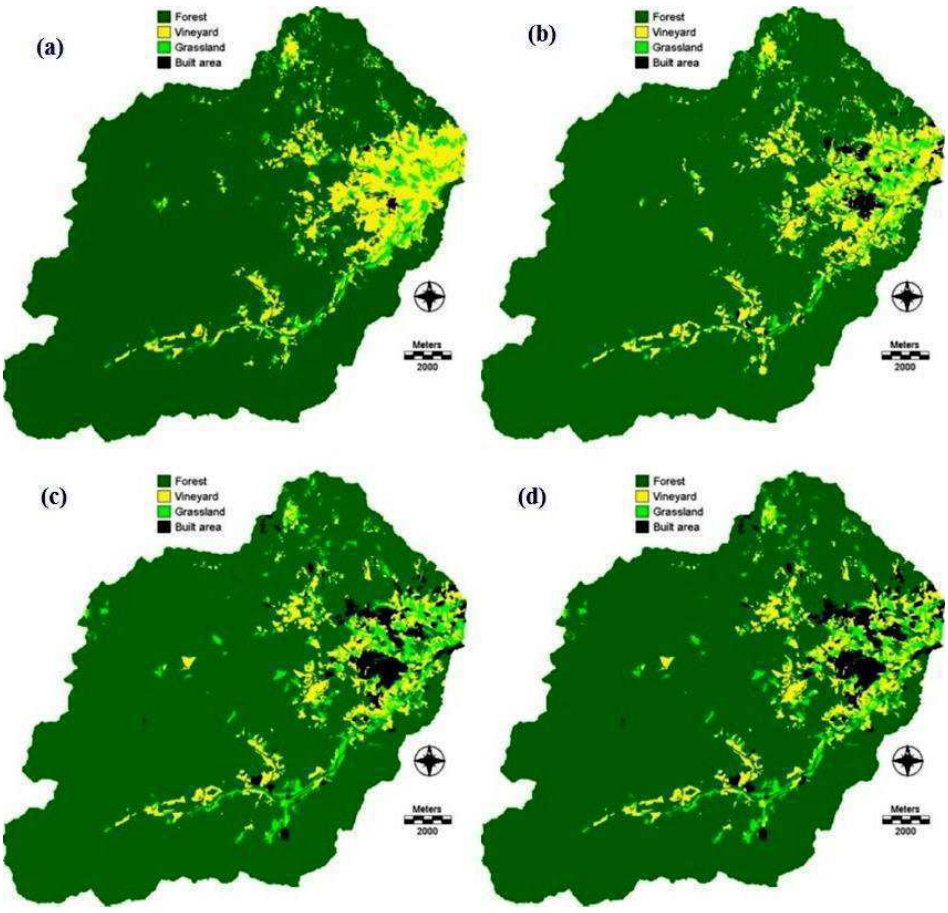

Figure 0.5 : Land cover maps of (a) 1950, (b) 1982, (c) 2008, (d) 2011.

3.1.1 Cross tabulation analysis 1950-1982

Cross tabulation for 1950-1982 (Table 0.2) was used to explain persistence, losses, and gains in land cover. In this table, columns display time 1 (1950) and rows display time 2 (1982). Persistence represents the amount of unchanged land cover between 1950 and 1982; this is highlighted in bold in diagonal and values are presented in both ha, and % of initial (1950) area in parentheses. As for % change, persistence is often correlated with initial land cover, where extensive land covers tend to have greater persistence (Pontius Jr et al. 2004). The sum of each column shows total area in 1950 for each land cover type. The sum of each row shows total area in 1982. The cross section of each column-row shows the area converted from one land cover to another between 1950 and 1982. For example, 407 ha were converted from forest to vineyard between 1950 and 1982; in terms of losses/gains, this therefore corresponds to a loss of 407 ha of forest to vineyard and a gain of 407 ha of vineyard from forest.

Table 0.2: Cross-tabulation of land cover in 1950 (columns) and in 1982 (rows). Values are in ha, persistence (diagonal) is also expressed in % of total area in initial year (1950).

	Forest	**Vineyard**	**Grassland**	**Urban**	**Suburban**	**Total**
Forest	**19918 (97.0)**	234	184	0	0	20336
Vineyard	407	**1502 (67.0)**	180	0	0	2089
Grassland	164	362	**346 (45.9)**	0	0	872
Urban	12	88	22	**19 (100.0)**	5	146
Suburban	37	55	22	0	**8 (61.5)**	122
Total	20538	2241	754.0	19	13	23565

Forest had the greatest persistence (97.0%) and most of its loss was conversion to vineyard. Vineyard, on the other hand, had moderate persistence (67.0%) and its greatest loss was conversion to grassland. In this initial period (1950-1982), the dominant trends among the vegetated land covers are a conversion from vineyard to grassed areas (362 ha) and forest to vineyard (407 ha). This apparent compensation in vineyard loss is only partial since there is also considerable loss of vineyard to forest (234 ha). Among the different land cover types, swapping is greatest for forest and vineyard. Although grassland gained in surface area, it had low persistence and greater susceptibility to change, showing high losses to both forest and vineyard as well as significant gains from these two land cover types, especially from vineyard (362 ha). The urban category reflects an “end state” which cannot easily evolve into another land cover type, though suburban can evolve into urban. Both urban and suburban gained from all vegetated

land cover types. The greatest gains in the built categories were from vineyard. Therefore, although all land cover types contributed to the growth of urban and suburban areas, the major trend was expansion of built area on vineyard.

Table 0.3 summarizes the gains, losses, absolute value of net change, total change, and swapping expressed as a percentage of the catchment for each category (Pontius Jr et al. 2004). Absolute net change is the absolute value of the difference between % of catchment in 1982 and in 1950. Total change is the sum of the absolute value of gains and losses for each category. Swapping is the surface area exchanged between land cover categories; this corresponds to the difference between total change and net change for each category. For example, equal gains and losses between categories 1 and 2 would provide a net change of 0% but could correspond to a substantial total change and high swapping if significant areas of category 1 were converted to 2 and vice versa.

As described above, forest, vineyard and grassland experienced the most significant gains and losses (Table 0.1 and Table 0.2). Among these, vineyard underwent the greatest total change within the catchment (Table 0.3), even though its initial surface area in 1950 was only about 11% that of forest (2,241 ha vs 20,538 ha). It also exhibited the highest rate of swapping, demonstrating extensive exchanges with other land cover types, especially forest and grassland. Of the 5 land cover types, vineyard was the most active, gaining and losing the most area and exchanging the most land with other land covers. Built areas had low total change, but especially very low swapping since these land covers tend to gain from others but not lose in exchange.

Table 0.3: Summary of land cover changes (1950-1982) expressed as % of catchment.

Land cover type	**Gains**	**Losses**	**Absolute net change**	**Total change**	**Swap**
Forest	1.77	2.63	0.86	4.40	3.54
Vineyard	2.49	3.13	0.64	5.63	4.98
Grassland	2.23	1.73	0.50	3.96	3.47
Urban	0.54	0.00	0.54	0.54	0.00
Suburban	0.48	0.02	0.47	0.51	0.04
Total	7.52	7.52	3.00	15.04	12.04

3.1.2 Cross tabulation analysis 1982-2008

As can be seen in Table 0.4, trends during 1950-1982 continued in 1982-2008. Forest area decreased slightly but maintained high persistence (96.6%) due to its high surface area. A large

area of vineyard continued to convert to grassland (445 ha), but during this period the compensating effect of forest to vineyard was weaker than in 1950-1982 (237 ha vs. 407 ha), and vineyard persistence decreased (61%). The conversion of forest to grassland was greater in 1982-2008 than in 1950-1982 (298 ha vs. 164 ha). As in 1950-1982, urban expansion occurred mainly at the expense of vineyard. However, during the latter period, suburban growth took place on forest cover before vineyard. Grassed area showed the lowest persistence as significant areas converted to forest or vineyard.

Table 0.4: Cross-tabulation of land cover in 1982 (columns) and in 2008 (rows). Values are in ha, persistence (diagonal) is also expressed in % of total area in initial year (1982).

	Forest	**Vineyard**	**Grassland**	**Urban**	**Suburban**	**Total**
Forest	**19649 (96.6)**	202	240	0	0	20091
Vineyard	237	**1275 (61.0)**	104	0	0	1616
Grassland	298	445	**397 (45.5)**	0	0	1140
Urban	53	105	64	**146 (100.0)**	34	402
Suburban	99	62	67	0	**88 (72.1)**	316
Total	20336	2089	872	146	122	23565

Table 0.5 summarizes the dynamics of land cover change for the 1982-2008 period. During this time, grassland surpassed vineyard in both total change and swapping, even though it still accounted for only 4.8% of the catchment in 2008 (Table 0.1). The significance of grassland changes will be discussed below. Total change in 1982-2008 was greater than in 1950-1982 for all categories except vineyard, though vineyard had the greatest net change (-2.01%) (Table 0.5). This was particularly true of urban and suburban areas for which total change in 1982-2008 was more than double the values for 1950-1982. Overall, the 1982-2008 period experienced more land cover change than in 1950-1982 (17.03% of catchment (Table 0.5) compared to 15.04% (Table 0.3).

Table 0.5: Summary of land cover changes (1982-2008) expressed as % of catchment.

Land cover types	Gains	Losses	Absolute net change	Total change	Swap
Forest	1.87	2.90	1.03	4.77	3.75
Vineyard	1.45	3.47	2.01	4.92	2.91
Grassland	3.13	2.01	1.12	5.14	4.02
Urban	1.09	0.00	1.09	1.09	0.00
Suburban	0.96	0.14	0.82	1.11	0.29
Total	8.51	8.52	6.07	17.03	10.96

3.1.3 Cross tabulation analysis 1950-2008

Table 0.6 shows the results of almost 60 years of land cover change in the catchment (1950-2008). Forest remained the dominant category by far and had high persistence (95.3%) but large areas of forest were converted to vineyard (458 ha) and grassland (320 ha). These losses were only partially compensated by gains from vineyard (331 ha) and grassland (191 ha). Vineyard is the land cover type that contributed most to all others, and more particularly to grassland (518 ha). The majority of urban expansion occurred on vineyard while suburban growth took place more or less equally on vineyard and forest. Overall, 3 land cover types showed low persistence: vineyard (45.3%), grassland (40.1%), and suburban (40.1%), where the low persistence of suburban can be explained by its conversion to urban.

Table 0.6: Cross-tabulation of land cover 1950 (columns) and land cover 2008 (rows) (ha)

Land cover type	Forest	Vineyard	Grassland	Urban	Suburban	Total
Forest	19569 (95.3)	331	191	0	0	20091
Vineyard	458	1015 (45.3)	144	0	0	1616
Grassland	320	518	302 (40.1)	0	0	1140
Urban	69	241	66	19 (100)	8	402
Suburban	123	137	51	0	5 (40.8)	316
Total	20538	2241	754	19	13	23565

The net result of land cover changes between 1950 and 2008 is summarized in Table 0.7. The greatest land cover change was experienced by vineyard which lost an equivalent of 2.65% of the catchment (or 625 ha, Table 0.1) in the 58 year time frame. This, however, was not a simple loss in land but corresponds to a complex pattern of exchanges with other land cover types since vineyard has the greatest swapping value (5.11%) of all land cover types. The great majority of these exchanges were with forest and grassland, where forest experienced high total change (6.33%) and loss (4.11%); grassland, on the other hand, progressed significantly within this context of land cover swapping. Total and net change were smallest for urban and suburban land covers, but these values are high for land covers which had very low initial values (Table 0.1). Urban and suburban area increased by about more than 20 times in 1950-2008.

Table 0.7: Summary of land cover changes (1950-2008) expressed as % of catchment.

Land cover types	Gains	Losses	Absolute net change	Total change	Swap
Forest	2.21	4.11	1.90	6.33	4.43
Vineyards	2.56	5.20	2.65	7.76	5.11
Grassland	3.55	1.92	1.64	5.47	3.83
Urban area	1.63	0.00	1.63	1.63	0.00
Suburban area	1.32	0.03	1.29	1.35	0.07
Total	11.27	11.27	9.09	22.54	13.44

3.2 Spatial dynamics influencing land cover change

The spatial dynamics of land cover change will be investigated in two steps. In the first, land cover change maps will be used to highlight specific locations. In the second, the impact of spatial variables (altitude, slope, distances from roads, streams, sea, and built area) will be presented. As described in the methods, urban and suburban are grouped together into a single 'built' category.

3.2.1 General spatial trends

Although the rates of change between 1950-1982 and 1982-2008 were different, spatial patterns for losses and gains were similar, so only the net 58 year (1950-2008) differences are shown here. Gains and losses for each land cover type are shown in Figures 2.5-8; low altitudes are portrayed in white while higher values are in black. Losses and gains in forest (Figure 0.6) indicate that much of the lost land was in foothills in proximity to the alluvial plain (white patch in eastern part of catchment). Area lost was almost twice the area gained (Table 0.7). Gains in forest occurred mainly in the south-eastern portion of the alluvial plain.

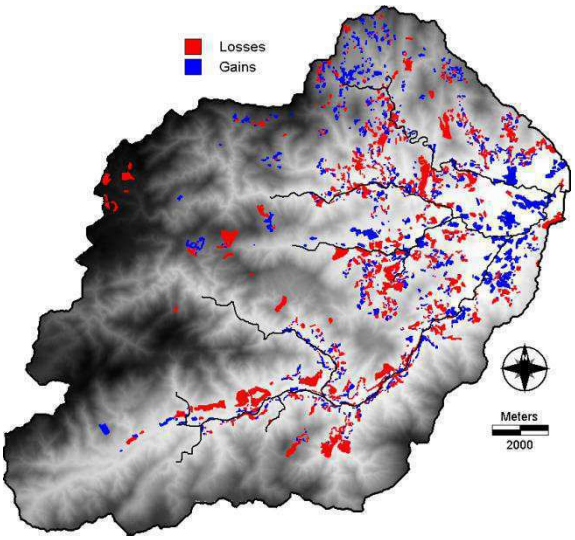

Figure 0.6: Forest change in 1950-2008

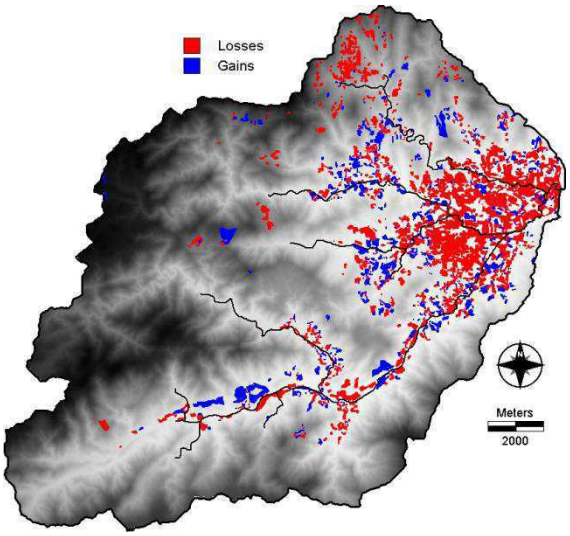

Figure 0.7: Vineyard change in 1950-2008

Whether in terms of % of initial area (Table 0.1), absolute area (Tables 2.1 and 2.6), or % of catchment area (Table 0.7), vineyard was the major loser of all land cover types. Lost area clearly outstrips gains and was concentrated almost entirely in the alluvial plain (Figure 0.7). Only about half the land lost was compensated by gains elsewhere, and these tend to be found outside the eastern alluvial plain area, either in nearby foothills or on alluvial soil to the extreme SW of the catchment.

In terms of absolute area and % of catchment (Table 0.1 and Table 0.6), grassland gained the most land, just ahead of urban areas. There is no strong spatial pattern to the gains and losses in grassland (Figure 2.6) with gains and losses both occurring in the alluvial plain. There is a weak tendency for grassland losses to be absent from higher altitudes (Figure 2.6).

The combined gains in urban and suburban covers outstrip individual gains and losses of all other land covers (Table 0.1, Table 0.6, and Table 0.7). Built area expansion (Figure 0.9) occurred almost exclusively in the alluvial plain and much of it was in close proximity to the core city centers of Grimaud and especially Cogolin (Figure 0.3, 2.3c).

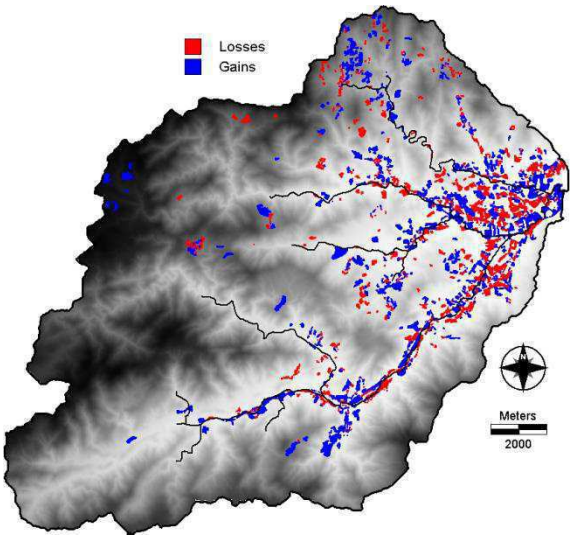

Figure 0.8: Grassland change in 1950-2008

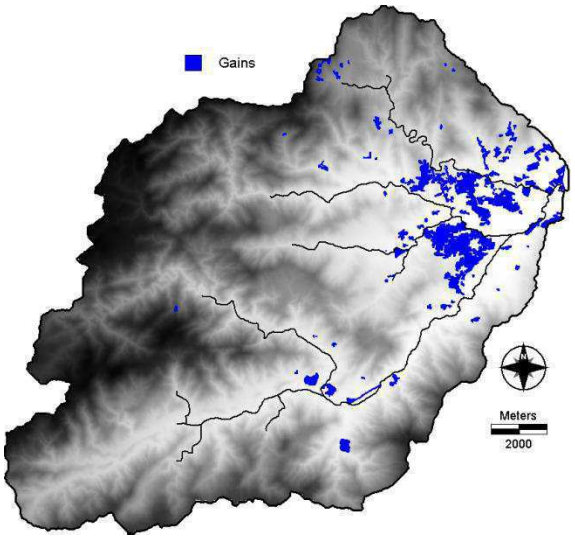

Figure 0.9: Built area change in 1950-2008

3.2.2 Altitude

The impact of altitude on total change for each land cover type is shown in Figure 0.10a and 8b, respectively. Total change is distinguished into gains and losses for each time period and land cover type in Figures 8c-8f. Total change in all land cover types decays exponentially with increasing altitude (Figure 0.10a and Figure 0.10b). The decrease in change with increasing altitude is the least pronounced for forest, for which about 30% of total change occurs in the 0-25 m range in both time periods. For the other land cover types, the 0-25 m range accounts for about 50 to 65% of total change according to the specific cover and time period. Grassland has the highest percentage of total change in the 0-25 m for both periods: 64.4% and 58.4% for 1950-1982 and 1982-2008, respectively.

The relationship between gains and losses in forest cover and altitude over time is complex (Figure 0.10c). In both time periods, gains outstrip losses in the lowest altitude range (0-25 m); this corresponds to the overall increase in forest noted in Figure 0.6 in the SE portion of the alluvial plain. At greater altitudes, losses are greater than gains, and in intermediate altitudes (50-100 m), lost forest area tends to be greater in 1982-2008 than in 1950-1982. Unlike the other land cover types, losses in forest cover tend to increase slightly at the highest altitudes (great than about 200 m). This loss tends to benefit grassland and then vineyard most.

Vineyard changes (Figure 0.10d) tend to be the opposite of forest trends noted above. For both time periods, the 0-25 m altitude experienced significant loss in vineyard cover. Although

gains at greater altitudes (≥ 25 m) compensate a small part of the losses in vineyard in 1950-1982, this is no longer true in 1982-2008 where losses remain significantly greater than gains in the 25-50 m range.

Grassland gains and losses with altitude (Figure 0.10e) are quite different from both forest and vineyard. In 1950-1982, gains are slightly greater than losses for all altitude ranges. Although the trend remains the same in 1982-2008, the gap between gains and losses is greater. Finally, built area (Figure 0.10f) increases at all altitudes and more particularly in the lower range, as for the other land cover types. The 1982-2008/1950-1982 gain ratio is substantially greater in the intermediate altitude range (25-75 m) than in the 0-25 m range, indicating that higher altitudes were preferentially built in the latter time period.

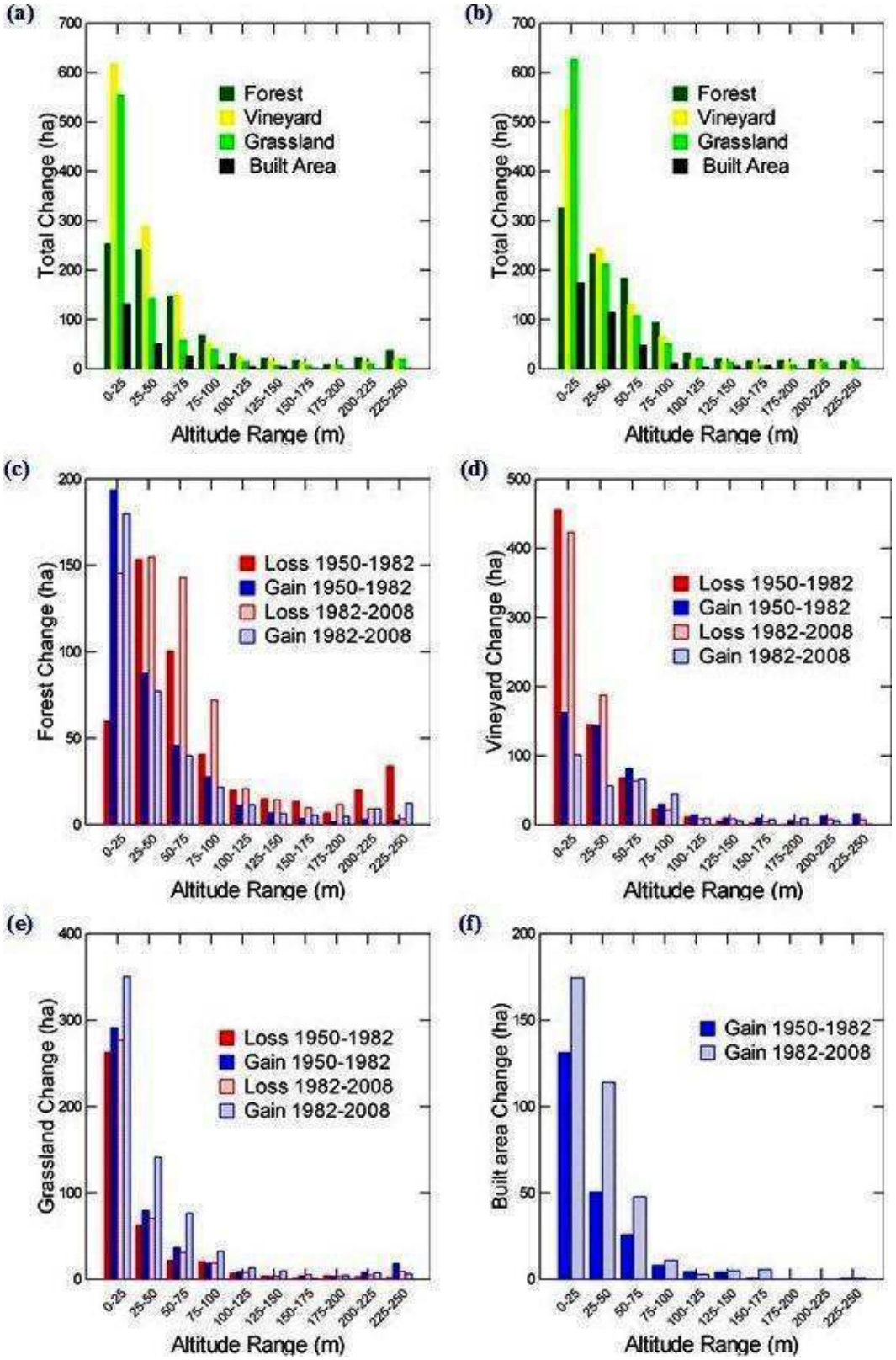

Figure 0.10: Land cover changes with altitude in (a) 1950-1982, (b) 1982-2008, (c) Forest, (d) Vineyard, (e) Grassland, and (f) Built area.

3.2.3 Slope

Slope and altitude are correlated in the catchment as higher altitudes tend to have steeper slopes. Changes in land cover as a function of slope (Figure 0.11a-f) are therefore similar to the trends with altitude and only noteworthy differences will be highlighted here. Overall trends are sensitive to the choice of range and in this case, there is an intermediate range (5-15%) where values in 2 categories (5-10% and 10-15%) remain constant (Figure 0.11a-b); there seem to be no significant exceptions to this trend (Figures 9c-f). Roughly 30% of changes in forest occur on slopes less than 5%, and this value ranges from about 50% to 60% for the other land covers. For slopes less than 10%, these values increase to about 50% (forest) and 60% to 70% (others), respectively. Changes in land cover for the 0-25 m altitudes (Figures 2.8a-f) correspond closely to values for the 0-5% slope range (Figures 2.9a-f).

Unlike altitude, where forest cover loss increased at higher altitudes (Figure 0.10c), there is no increase in land cover loss on steepest slopes (Figure 0.11c). Thus, the loss experienced at higher altitudes corresponds to level ground or top slope convexities with low slopes.

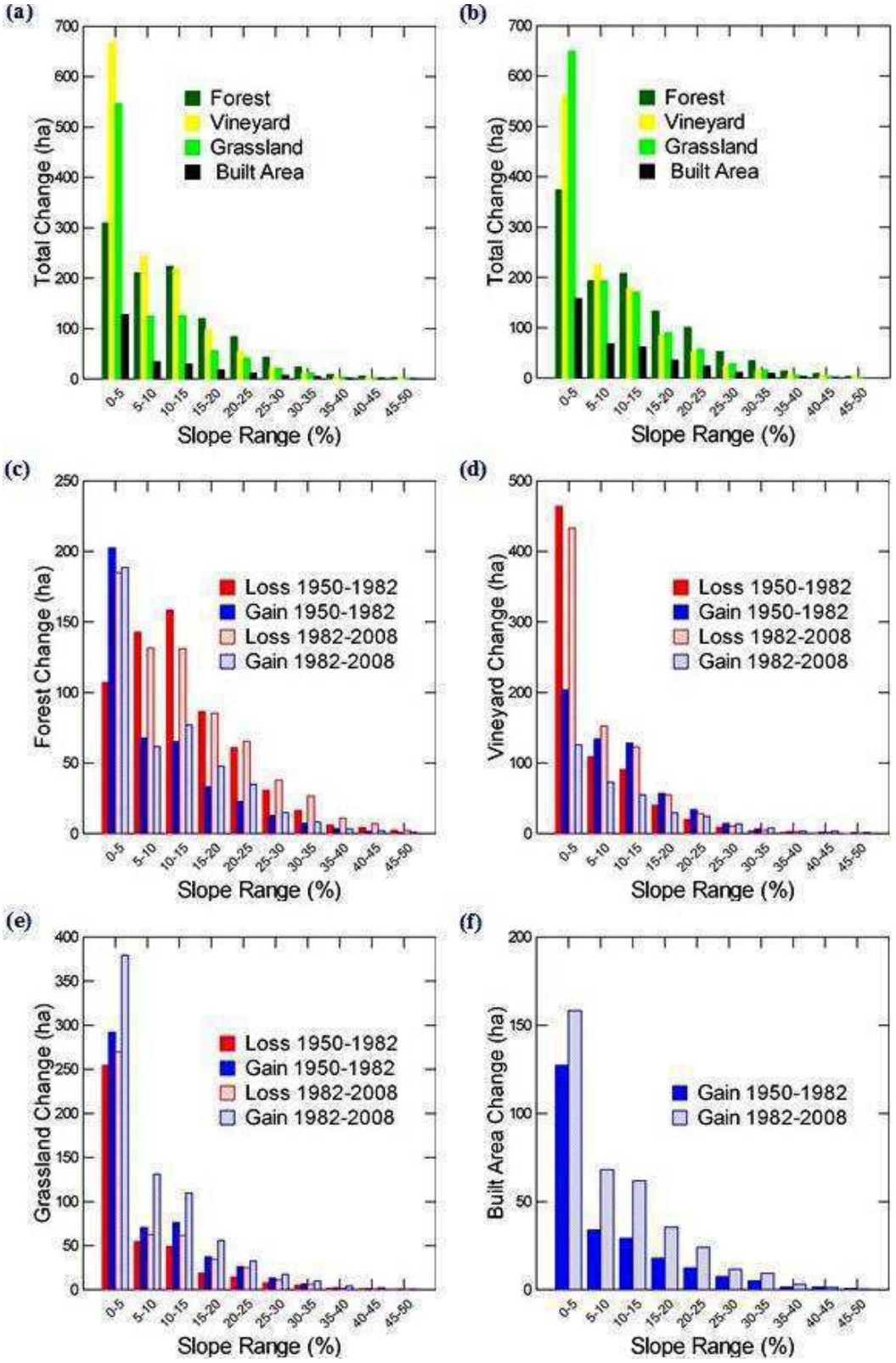

Figure 0.11: Land cover changes with slope in (a) 1950-1982, (b) 1982-2008, (c) Forest, (d) Vineyard, (e) Grassland, and (f) Built area.

3.2.4 Distance from streams

Total change in the vegetation covers (forest, vineyard, and grassland) all decrease exponentially with distance from streams (Figure 0.11a-b). In the initial period (1950-1982), the greatest total change near streams concerns vineyards most, and this continues on into intermediate distances of up to about 900 m (

Figure 0.12a). In the latter period, grassland experiences the greatest total change near streams, but there is little difference with vineyard or forest beyond about 100 m and 200 m, respectively (

Figure 0.12b). The relationship between total change in built area and distance from stream (

Figure 0.12a-b) is unlike any other so far: very little change close to the stream, moderate change at intermediate distances (roughly 100-800 m), and then little change again at greater distances.

In 1950-1982, forest gains more than twice the surface lost close to streams, but this trend is reversed in 1982-2008 (

Figure 0.12c). For all other distances and in both periods, forest generally loses more land than it gains. In the initial period (1950-1982), lost land tends to peak at about 200-300 m from streams whereas it is greatest close to streams in 1982-2008 and decreases with distance. Vineyard loses more land than it gains at all times and distances, except for the 1950-1982 period when gains are slightly greater than losses at distances greater than about 800 m (

Figure 0.12d). At intermediate distances in 1950-1982 (100-400 m), the difference between losses and gains is progressively minimized by greater gains, but this no longer holds in the 1982-2008 period.

Trends in grassland (Figure 2.10e) are the general opposite of those noted for forest (Figure 10c), though the gains in grassland cannot be accounted for entirely by forest and significant areas of vineyard (Figure 2.10d) must have contributed to grassland growth close to streams. The greatest gains in grassland close to streams (< 400 m) occur in 1982-2008 (

Figure 0.12e). Before then, gains and losses are roughly equivalent except at intermediate distances (400-600 m) where gains are greater than losses. In the latter period (1982-2008), gains become greater than losses again at distances beyond about 1,000 m (Figure 2.10e).

Built area gains relatively little land immediately next to streams (< 100 m) (Figure 10f). Gains in built area are then relatively stable between distances of 100-700 m and 100-800 m for 1950-1982 and 1982-2008, respectively. For almost all distances, gains in 1982-2008 were

greater than in 1950-1982, with the exception of roughly equivalent values in the 500-700 m range.

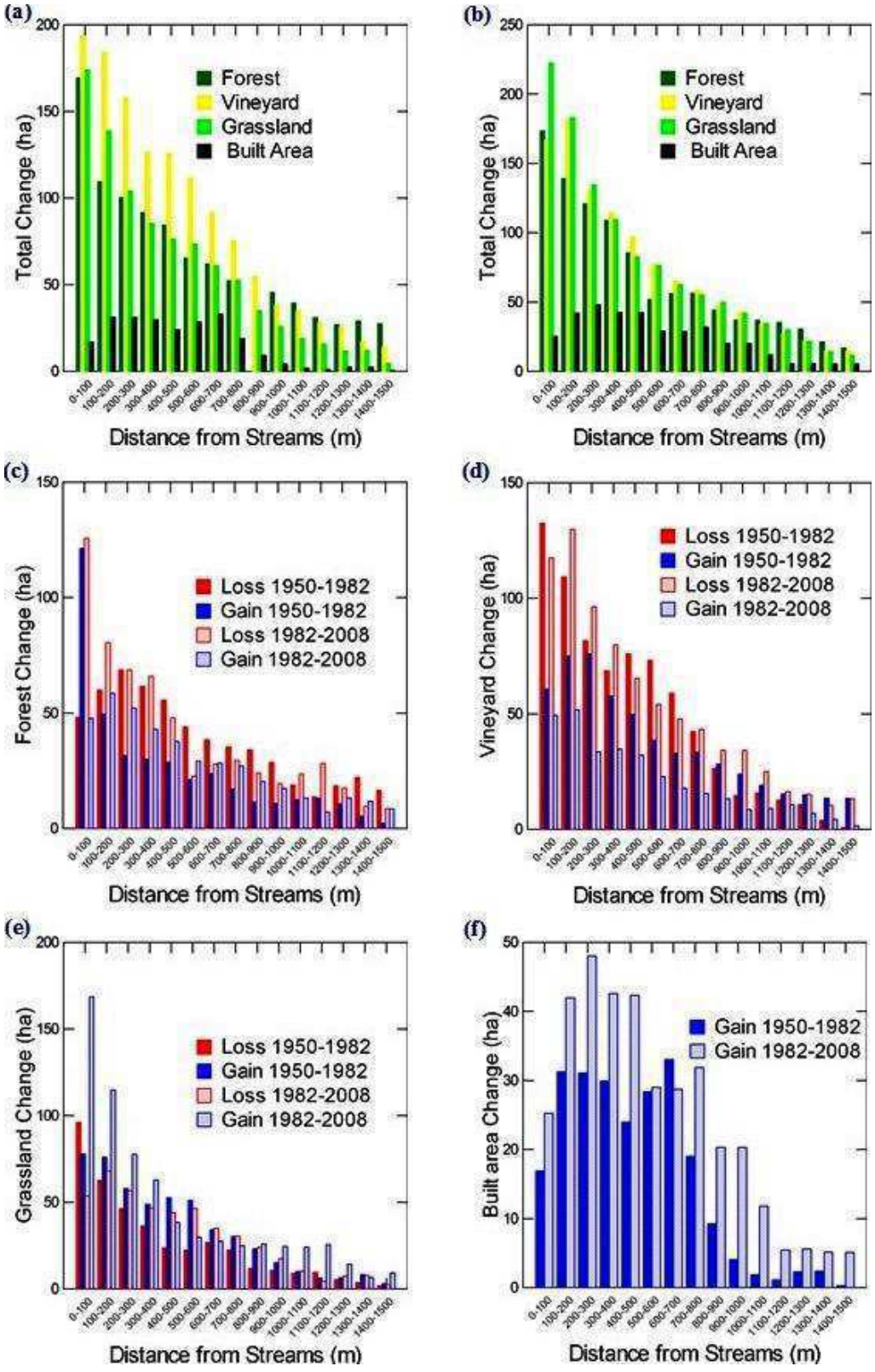

Figure 0.12: Land cover changes with distance from streams in (a) 1950-1982, (b) 1982-2008, (c) Forest, (d) Vineyard, (e) Grassland, and (f) Built area.

3.2.5 Distance from roads

Total change in land cover with distance from roads (Figure 0.13a-b) follows the decaying exponential trend of most variables taken into consideration. Roughly 40% to 50% of total change in forest, vineyard, and grassland occurred within 100 m of a road. This value was greater than 95% for built area. In 1950-1982, vineyard was most affected close to roads (0-100 m), but in 1982-2008, vineyard and grassland were approximately equal.

For both time periods and almost all distance ranges, loss in forest cover was greater than gains, and the greatest overall difference was in the 0-100 m range in 1982-2008 (Figure 0.13c). Vineyard trends are similar to forest but greatly exaggerated (Figure 0.13d). Losses outweigh gains significantly close to roads (0-100 m), but differences are small beyond this distance. Grassland gains are greater than losses at all distances, though the land gained and lost decreases with distance from roads (Figure 0.13e). Major gains are registered more particularly in the 0-100 m range for 1950-1982 and in the 100-300 m range for 1982-2008. Built area clearly distinguishes itself from the other land cover types since almost all of its gain occurs within 100 m of a road (Figure 0.13f).

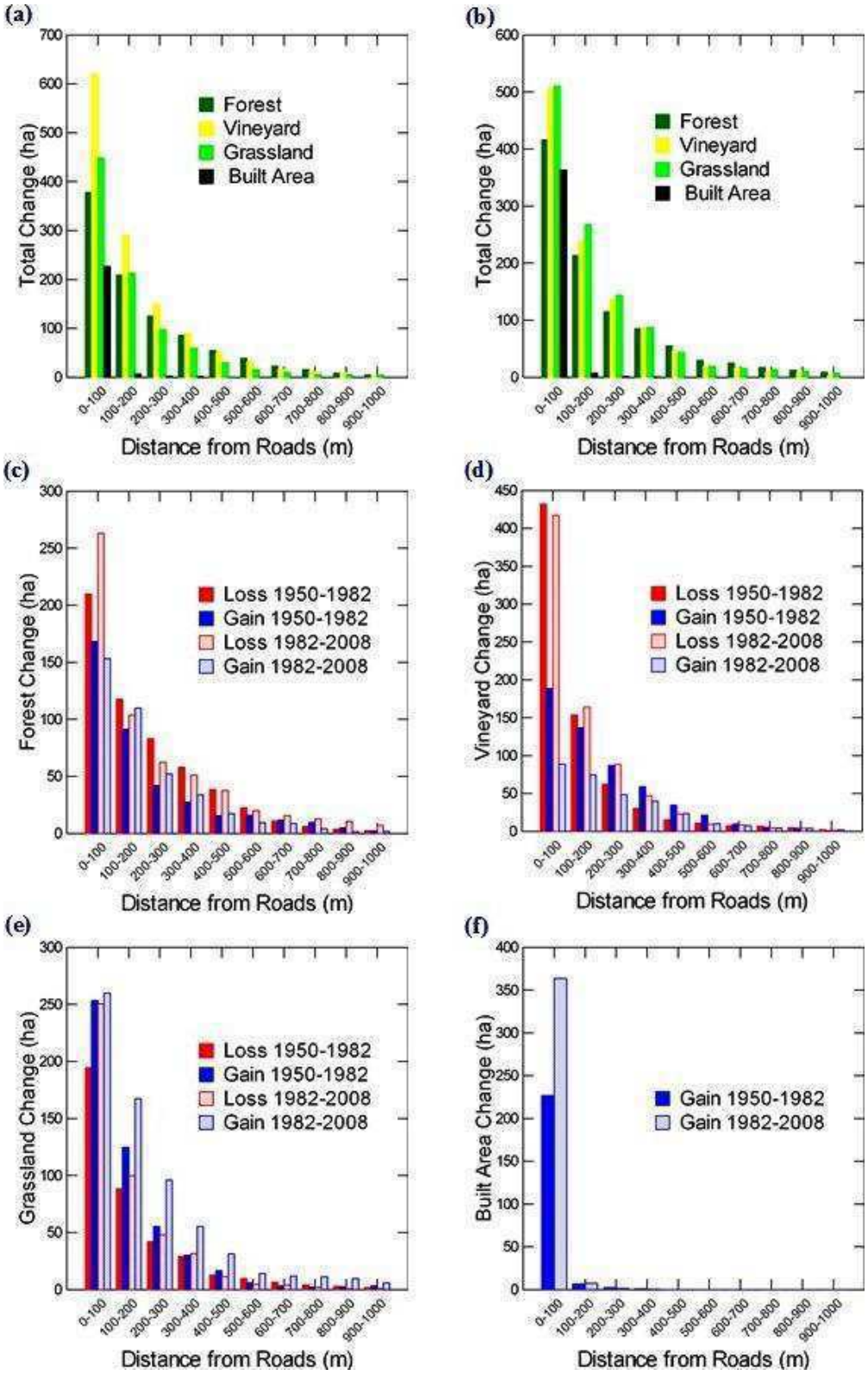

Figure 0.13: Land cover changes with distance from road in (a) 1950-1982, (b) 1982-2008, (c) Forest, (d) Vineyard, (e) Grassland, and (f) Built area.

3.2.6 Distance from built area

The relationship between total land cover change and distance from built area (Figure 0.14a and b) is strongly time dependent. In 1950-1982 (Figure 0.14a), there is little evolution in land cover change with distance from built area despite a tendency for the vegetation covers (forest, vineyard, grassland) to show greater change at intermediate distances (300-1300 m) and built area to change more close to earlier built area (0-100 m). In 1982-2008, the pattern is totally different (Figure 0.14b). For vineyard and grassland, total change first increases with distance from built area, peaks at about 100-200 m and then decreases with further distance from built area. Total change in forest cover is roughly constant between 0-300 m before decreasing with greater distances. Built area change is greatest within 0-100 m, where more than 50% of total change takes place in 1982-2008. For comparison, the value for the other land cover types in this distance range is approximately 15%. It should be noted that built area was limited to only 32 ha in 1950 and expanded to almost 270 ha in 1982 (Table 0.1); built area expansion was particularly important in the 1982-2008 period (Figure 0.14f and Table 0.1and Table 0.5).

Gains and losses in forest vary with time (Figure 12c): in 1950-1982, gains and losses are relatively small and tend to occur far from built area. In 1982-2008, forest land is lost close to built area (within 200 m) and gained at intermediate distances (200-500 m). Vineyard clearly loses significant area near built area (Figure 0.14d). The trend is particularly strong in 1982-2008 within about 300 m to 400 m from built area. In this range, losses are 3 to 10 times greater than gains. Although total changes are similar for vineyard and grassland (Figure 0.14b), the relationship with distance from built area is quite different (Figures 12d and 12e for vineyard and grassland, respectively); in grassland, losses and gains are better balanced in the estimation of total change. In the 0-100 m range, grassland experiences a net loss, but beyond this distance, grassland gains are generally greater than losses, even though losses can remain substantial, especially in the 100 m to 400 m range. Where vineyard systematically lost area, grassland both lost and gained land. Built area expansion in 1982-2008 occurred close to former built area, as can be seen in Figure 0.14f. Almost 75% of the land gained in 1982-2008 was located within 200 m of 1982 built land.

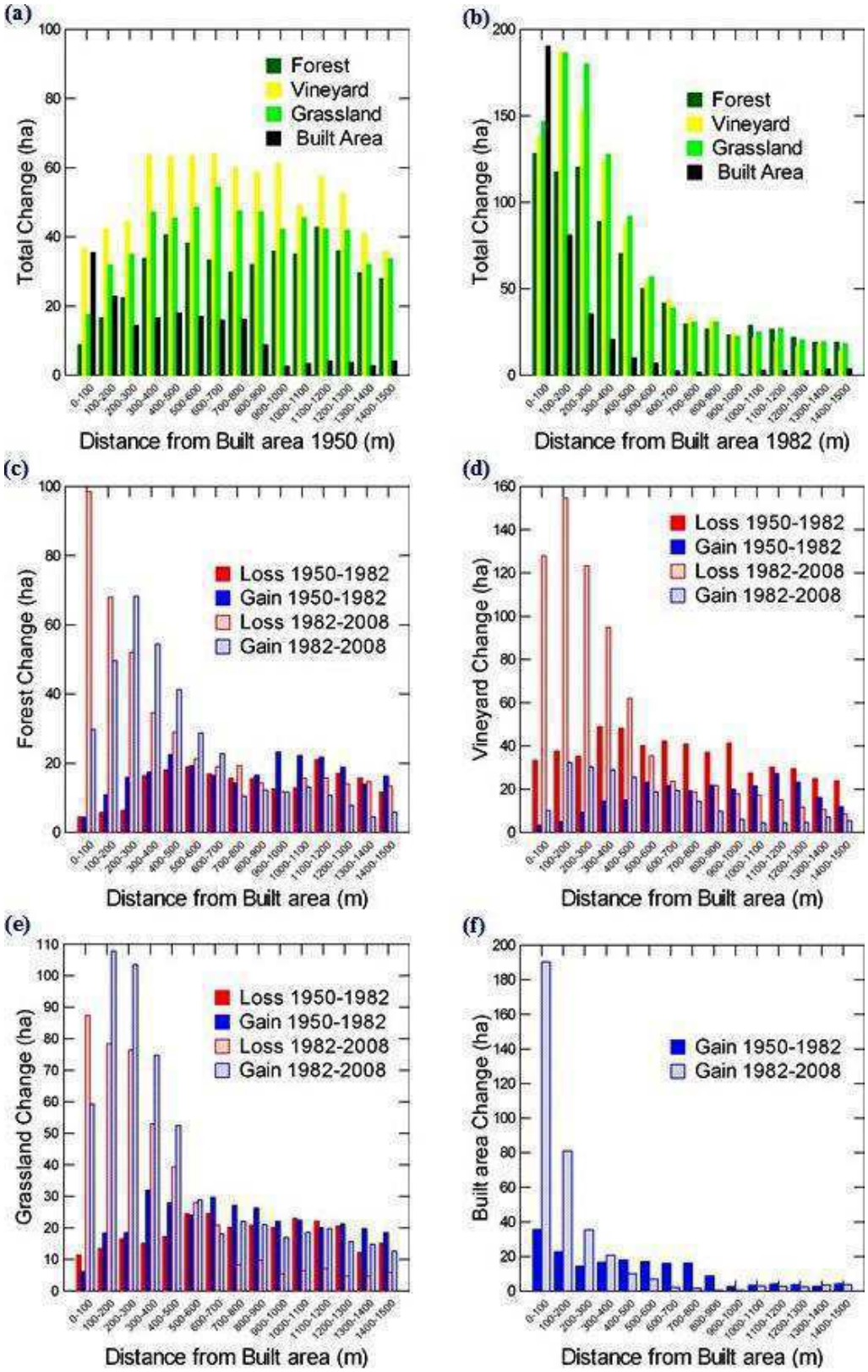

Figure 0.14: Land cover changes with distance from built area in (a) 1950-1982, (b) 1982-2008, (c) Forest, (d) Vineyard, (e) Grassland, and (f) Built area.

3.2.7 Distance from sea

Trends for changes in land cover with distance from the sea are distinct from all other patterns examined thus far. Before examining these, it should be noted that the catchment sea front is restricted to a narrow band near the outlet into the Gulf of St Tropez (Figure 2.1). Total change in vineyard, grassland and built area covers tends to be greatest at about 3 to 5 km from the sea front in 1950-1982 (Figure 0.15a). This distance corresponds roughly to the centre of the alluvial plain and is close the city cores of Cogolin and Grimaud (Figure 0.3). Changes in forest cover peak at a greater distance (about 7-9 km) and this corresponds roughly to a secondary peak in change for vineyard and grassland. This distance is situated near the foothills peripheral to the alluvial plain described in Figure 0.6-7.Finally, there appears to be a third smaller peak in change around 10-12 km and this corresponds roughly to the area near the town of La Môle (Figure 0.3). Trends for 1982-2008 (Figure 13b) are generally similar to 1950-1982 (Figure 13a), but changes in forest are concentrated within closer distances to the sea, vineyard changes are less great at intermediate distances (5-9 km), grassland peaks are greater at both near (3-5 km) and intermediate (7-9 km) distances, and built area changes are significantly greater in the 1-4 km range especially.

Forest gains and losses are sensitive to distance from the sea (Figure 0.15c). Gains outweigh losses close to the sea (within about 2-3 km for both periods and 3-4 km for 1950-1982), but losses are generally greater beyond about 5 km. The greatest difference in gain-loss occurs at about 7-9 km. Vineyard losses and gains (Figure 0.15d) are strikingly simple. Losses outstrip gains at all distances up to 6 km, and gains outweigh losses at all distances beyond 6 km. Peak lost land is situated about 3-5 km from the sea and the peak gained land occurs at a distance of around 6-9 km. Grassland trends (Figure 0.15e) are more complex and vary less systematically as a function of either time period or distance. Three approximate distance peaks can be identified. The first is in the 2-5 km range: here, grassland gains more land than it loses in 1950-1982, but the trend is reversed in 1982-2008. The second is in the 7-9 km range: gains are greater than losses for both time periods. The third is in the 10-13 km range where land gained is also greater than lost. Finally, the major peak in gained land for built area (Figure 0.15f) is about 3-5 km from the sea in 1950-1982 and 2-6 km in 1982-2008. For the initial 1950-1982 period, significant gains were made close to the seafront but these do not persist in 1982-2008. Finally, built area shows growth in the distant (11-13 km) range in the latter period.

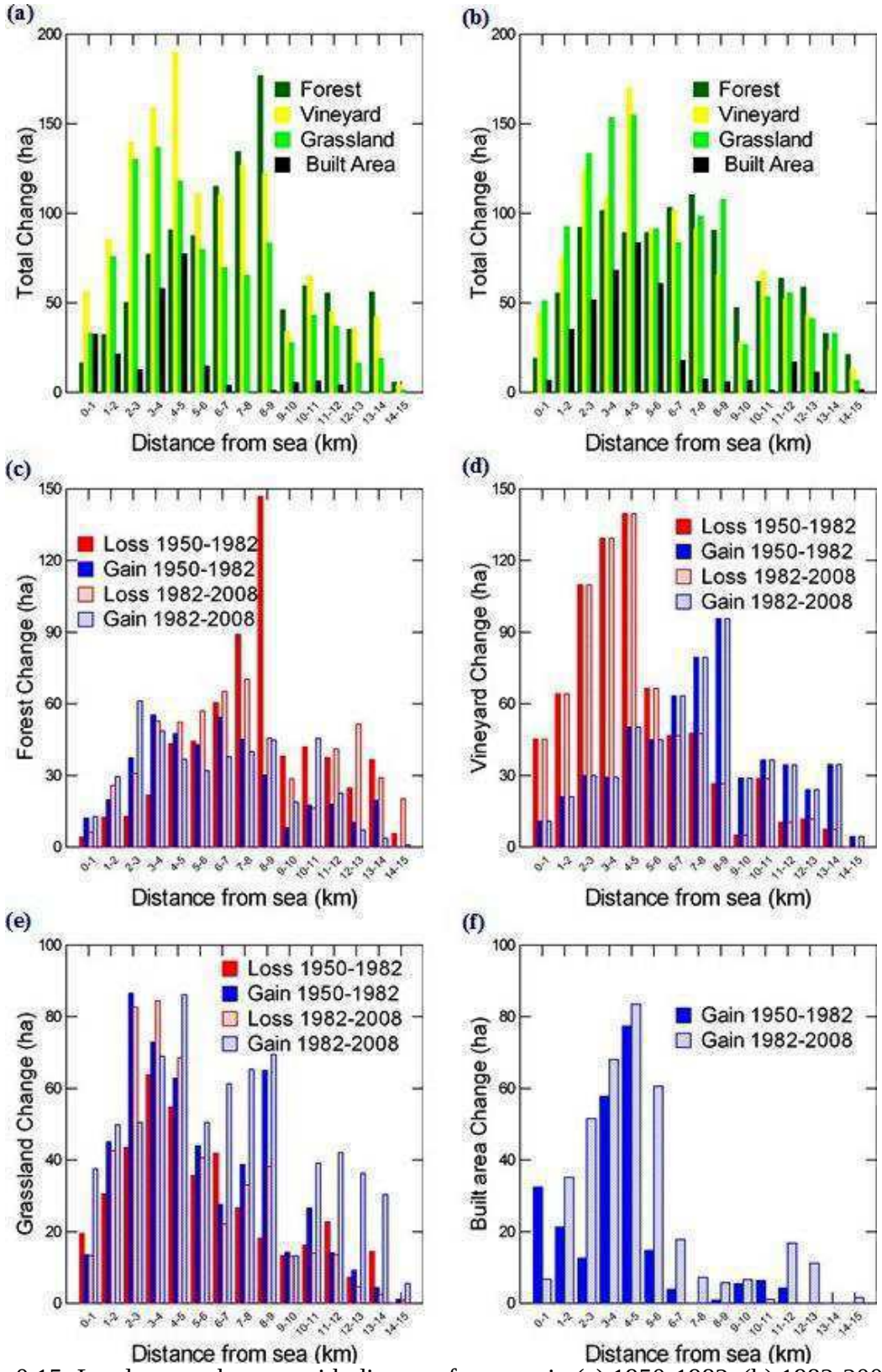

Figure 0.15: Land cover changes with distance from sea in (a) 1950-1982, (b) 1982-2008, (c) Forest, (d) Vineyard, (e) Grassland, and (f) Built area.

4. Discussion

The results above detail land cover changes for the 235 km² Giscle catchment over 2 time periods and describe spatial patterns and topographic/distance variables influencing these changes. The spatial and temporal dimensions create a complex pattern of change that will be simplified in the discussion to highlight the major findings of the study. Before this, it should be noted that the topographic and distance variables are often correlated, but may have distinct impacts. Altitude and slope are correlated and both reflect a greater distance from the sea; in addition, slope influences building costs as it is cheaper to build on flat land than steep slopes. Distance from the sea also reflects the impact of built area, as described in the results. The major cities of Ste Maxime and St Tropez are located on either side of the Gulf of St Tropez, so distance from the sea also represents distance from larger urban centers, seafront tourism, and major road and rail transportation networks. Behind all these variables are economic considerations that are impossible to isolate and quantify.

Perhaps the most frequently cited land cover transition in Mediterranean regions in the scientific literature is the abandonment of agricultural practices on marginal land and its conversion to forest (Falcucci et al. 2007, Geri et al. 2010, Parcerisas et al. 2012, Pelorosso et al. 2009, Serra et al. 2008). This was not observed in this catchment. On the contrary, marginal lands on steeper slopes were converted from forest to vineyard, as can be seen in Figure 0.16 showing vineyard terraces on foothills above the alluvial plain. A forest fire in the catchment in 2003 (Fox et al. 2006) revealed extensive terracing on steep slopes, but marginal subsistence farming was probably abandoned in the region before 1950, as was the case elsewhere in Mediterranean France (Sluiter and de Jong 2007). The Maures mountains (‘Massif des Maures’) are highly prone to forest fires and this clearly explains the prevalence of cork oak (*Quercus suber*) as the dominant tree species in the catchment. The thick bark of cork oak protects the heart of the tree from intense heat, and most trees survive even high severity fires. Exceptions are the very young or old trees, and trees which have recently been harvested for their cork bark. Pine (*Pinus pinaster*) trees, on the other hand, are systematically killed by high severity fires. With regard to vineyards, large areas in the plain were converted to grassland, built area, and some forest. This was compensated in part (but only partially since the net result is a 28% loss in vineyard cover between 1950 and 2008) by planting on steeper slopes in proximity to the plain. These fields

therefore find themselves at the interface between the extensive forest on one side and the plain on the other. During the large fires of 2003, vineyards served as effective fire breaks; as forest fires penetrated into the vineyard, the lack of combustible vegetation extinguished the fire after the first few vine rows were burned or dried out.

A second common trend cited is the intensification of agriculture on plains (Falcucci et al. 2007, Geri et al. 2010, Van Eetvelde and Antrop 2004). The term 'intensification' is ambiguous as it can imply either the clearing of land to plant crops or an increase in mechanization in crop production. The latter is true here; wine producers are more mechanized and most harvest grapes mechanically and no longer manually in the catchment, as has been the trend elsewhere in southern France (Sluiter and de Jong 2007). However, the first interpretation of land clearing does not hold since vineyard experienced the greatest loss (-27.9%, Table 0.1) in the alluvial plain of all land cover types. Much of this was to built area as urban centers expanded onto adjoining land. The tendency for cities to grow onto agricultural land is common throughout the world and the Mediterranean area (Serra et al. 2008, Sluiter and de Jong 2007). However, the conversion of vineyard to grassland in conjunction with urban expansion is less common (Falcucci et al. 2007, Serra et al. 2008). In this case, abandoned vineyard fields generally belonged to owners who did not produce their own wine but brought their grapes to a wine making cooperative. Grape production was therefore not necessarily central to their livelihood as it is for the wine making "domaines". Furthermore, when land is passed on from one generation to the next, grape production can be abandoned but the land retained. Property values are known to increase in the region, so land represents a secure financial investment. This explains some of the conversion from vineyard to grassland and accounts for the paradoxical situation of agriculture conquering marginal lands on steep slopes while abandoning fertile land in the plain to grassland and then forest.

The shift in agriculture from the alluvial plain to fields located on bedrock soils is probably specific to vineyard production since vines adapt better to cultivation on steeper slopes than most crops. In addition, steeper slopes with thin soils brought into cultivation are generally terraced, and soil depths are significantly improved by terracing. Upland slopes are dominated by schist and gneiss which tend to generate slightly acidic sandy soils. In an unpublished analysis of 24 soil samples from vineyards from both the plain and foothills, there was very little variation within the catchment in texture and pH. Clay contents were low for all samples (mean and

median of 7.6% and 6.6%, respectively), coarse sand contents were high (mean and median of 45.3% and 48.4%, respectively), and pH values were all slightly acidic (mean and median of 6.6 and 6.7, respectively). Hence, soil attribute differences generated by different geological substrates were minor, and the French notion of'terroir' in wine production can be considered preserved despite the move of some fields from the plain to the foothills. It is, however, probable that the alluvial plain soils benefit from better soil moisture conditions in the summer, but there are no data available to support this.

Grassland dynamics are particularly complex in the catchment. As discussed above, some of the growth in grassland is due to land abandonment in the fertile alluvial plain. However, several other factors come into play. One is the conversion of vineyard to grassland (mostly pasture) along stream channels (Figures 2.10d-e) and this is probably related to flooding risks (Figure 0.17) where lowland areas along stream channels experience regular flooding. This probably also accounts for the relatively low gains in built area close to stream channels (Figure 10f). With time, abandoned vineyard evolves into grassland (or shrubland) first (Serra et al. 2008), then forest afterwards, accounting for grassland-forest transitions and the increase in forest area in the alluvial plain in 1982-2008 (Figure 0.6). Although the reverse is intuitively impossible, clearing of forest to create fire breaks was a priority after the 2003 fire that ravaged >4,000 ha, and some fire breaks were present before then. Finally, some of the vineyard-grassland transition is related to the creation of horseback riding activities in recent years. Tourism is a major local industry and the proximity of large expanses of forest with paths and dirt roads makes horseback riding an attractive tourism activity. (Cori 1999) explains that rapid growth of the tourism industry increased dramatically in the last few decades and influenced the land cover change on the northern shores of the Mediterranean. He reported that agricultural land decreased and non-agricultural land increased in the Spanish, French, and Italian Mediterranean regions due to the spread of touristic activities. And Nainggolan et al. (2012) found significant land cover change over 72 % of their study area in a Mediterranean catchment due biophysical and socioeconomic factors, most of which were associated directly or indirectly with rapid urbanization and tourism. The combination of all these dynamics explains the high swapping of land between forest, vineyard and grassland (Table 0.3, 5, and 7).

Figure 0.16: Clearing and terracing of foothills for vineyard.

Figure 0.17: Flooding in vineyard close to stream channel.

Built area increased substantially between 1950 and 2008. During the initial period, about 236 ha were added to the catchment in 32 years (7.4 ha y^{-1}); this value increased to 450 ha in 1982-2008 (17.3 ha y^{-1}). Other authors (Antrop 2005, Salvati et al. 2013) have also found that urban sprawl accelerated in Euro-Mediterranean countries in the 1980's. Permanent population for the 3 main cities grew faster in 1982-2007 (about 296 pers. y^{-1}) than in 1962-1982 (about 229 pers. y^{-1}), but built area growth in the region probably depends as much on the non-permanent population. Many new secondary homes were built during the past two decades occupying 22 km^2 of land (EAA 2011) near Mediterranean beaches to attract European and French populations (Blue Plan Papers, 2001). In addition, French and immigrated foreign retirees tend to settle in Mediterranean cities or use their coastal house as a secondary home. According to Cori (1999), half of total secondary homes in France are situated in the Mediterranean coastal area. Spatially, previous built area had a stronger impact on new built area location in 1982-2008 than in 1950-2008, and urban expansion occurred almost exclusively within 100 m of roads and was concentrated mainly at low altitudes and on low to intermediate slopes. This agrees well with the findings of (Schneider and Woodcock 2008) on the growth trends in 25 cities across the World in 1990-2000.

5. Conclusion

As in much of Mediterranean Europe, significant land cover changes occurred in 1950-2008. Forest remained the dominant land cover at all the times, and relative changes in forest cover were small for several reasons: its large surface (more than 85% of the catchment) and location at higher altitudes and on steeper slopes. Despite this, forest swapping with vineyard and grassland was high. Vineyard lost considerable area. It was converted mainly into grassland, urban, and

suburban land covers. Grassland was highly dynamic and experienced large losses and gains due to vineyard abandonment and the creation of fire breaks and pasture land. Grassland expanded mainly on abandoned vineyards. Most land cover changes occurred at lower altitudes and flat to gently sloping areas in the eastern part of the catchment. All distance variables (from streams, roads, built area, and the sea) had significant impacts on land cover change dynamics.

CHAPTER 3

PREDICTING LAND COVER CHANGE IN A MEDITERRANEAN CATCHMENT AT DIFFERENT TIME SCALES

(Article published in the Proceedings of the Ninth International Conference on Geographical Analysis, Urban Modeling, Spatial Statistics, Geog-and-Mod 2014, 30 June–3 July, 2014, Guimaraes , Portugal., in Appendix)

1. Introduction

1.1 Land cover change modeling

Land cover is changing rapidly throughout the world, and it has become an important issue for urban planners, ecologists, economists, and resource managers to evaluate environmental change and establish sustainable development planning (Dietzel and Clarke 2006, Guan et al. 2011, Lambin et al. 2001). Land cover change models are able to identify location and quantity of change, predict land cover change considering past changes, test explanatory variables, and simulate management policies. For this reason, many interdisciplinary research projects have been initiated for land cover change modeling, measuring regional and global land cover change, forecasting future conditions, and planning for sustainable development (Verburg et al. 1999). As a result, researchers have created a large set of operational modeling tools to implement prediction and exploration of possible land cover change trajectories and land cover planning and policy in recent years (Verburg et al. 2006). Moreover, land cover change, urban growth, and spatial modeling have drawn considerable interest in the last two decades due to better computing power, availability of spatial data, and the need for innovative planning tools for decision support (Dietzel and Clarke 2006). Advanced urban and land cover change modeling techniques have been included in many GIS software package.

1.2 The role of time scale in land change prediction

The selection of prediction and validation time intervals has a great impact on prediction accuracy (Chen and Pontius 2010). Prediction accuracy can depend on the rate and process of transitions in both time intervals. Modeling of land cover change using a coarser temporal scale may fail to understand landscape change patterns properly and can hamper model performance (Álvarez Martínez et al. 2011), so most studies on future land cover change use short to intermediate historical time scales (5–15 years). Many studies on urban land cover change

modeling use short time scales that achieve better prediction (Ahmed and Ahmed 2012, He et al. 2006, Li and Yeh 2002, Sang et al. 2011). Some studies use intermediate time scales (Huang and Cai 2007, Jenerette and Wu 2001, Kamusoko et al. 2009, Oñate-Valdivieso and Bosque Sendra 2010, Silva and Tagliani 2012, Tewolde and Cabral 2011, Mhangara 2011, Guan et al. 2011, Pérez-Vega et al. 2012) and very few studies use long time scales to simulate urban land cover (Bohnet and Pert 2010) and multiple land cover change (Guan et al. 2011, Pérez-Vega et al. 2012).

Very few studies were found on the comparison of the impact of historical time periods on land cover prediction using different time scales. To investigate the impact of time interval on prediction accuracy in Gorizia-Nova Gorica (Italy), urban area was predicted for different years (2005 to 2010) from initial conditions in 1985 and 2004 (Chaudhuri and Clarke 2014). The authors found that prediction accuracy increased with decreasing prediction time period.

Table 0.8 presents historical and prediction time periods of several studies on land cover change. Historical time period is accounted from the interval of initial (T1) and second time (T2), and the prediction time period is measured from the interval of the second time (T2) and the prediction time (T3). In this Table, recent studies on land cover change analysis and modeling for the future using CA-Markov and Multi-Layer Perceptron (MLP) with multiple land cover are included. Average historical and prediction time periods are about 10 and 12 years, respectively, analyzing 25 recent studies on land cover change using CA-Markov and Multi-Layer Perceptron (MLP).

Table 0.8: Temporal scales of different studies. (V- Year of validation, F- year of future prediction)

Authors	**Study area**	**Time scale**	**Prediction date**	**Historic Interval**	**Predict Interval**
Ahmed and Ahmed, 2011	Dhaka city, Bangladesh	1989-1999	2009 (V) 2019 (F)	10	10
Álvarez Martínez et al., 2011	La Sierra d'Ancares, Spain	1991-2004	Land cover change analysis	13	-
Araya and Cabral, 2010	Setúbal and Sesimbra in the Lisbon Metropolitan Area, Portugal	1990-2000	2006 (V), 2020 (F)	10	20
Berberoglu and Akin, 2009	The Cukurova Deltas, Turkey	1985- 1993 1985-2005	Land cover change analysis	8, 20	_
Bohnet and Pert, 2010	Cairns, Queensland, Australia	1952-2008	2031 (F)	56	23

Authors	Study area	Time scale	Prediction date	Historic Interval	Predict Interval
Bracchetti et al., 2012	Central Apennines, Italy	1955-1978 1978-2006	Land cover change analysis	28	_
Dadhich and Hanaoka, 2012	Jaipur, India	1989-2000	2002 (V)	11	2
Dewan and Yamaguchi, 2009	Greater Dhaka, Bangladesh	1975-1992,1992-2003, and 1975-2003	Land cover change analysis	17, 11, and 28	_
He et al., 2006	Beijing, China	1997, 2000 and 2004	2004 (V), 2020 (F)	3	20
Huang and Cai, 2007	Shiqian County, China	1988, 2001	2001(V), 2014 (F)	13	13
Jenerette et al., 2001	The central Arizona - Phoenix region of the United States	1975-1995	2015 (F)	20	20
Kamusoko et al., 2009	Bindura district, Zimbabwe	1973-1989	2000 (V), 2010 (F), 2020, 2030	16	20
Koi 2011 (Ph. D. thesis)	Tam Dao National Park Region(TDNP), Vietnam	1993-2000	2007 (V), 2014 (F), 2021	17	14
Li and Yeh, 2002	Dongguan city, China	1988, 1993	2005 (V)	5	12
Liu et al., 2008	Guangzhou, in thePearl River Delta of China	1988, 1993	2002 (V)	5	9
Lo´pez et al., 2001	Morelia city, Mexico	1960, 1975, 1990	1990 (V)	15	15
Moghadam and Helbich, 2013	Mumbai, India	1973, 1990, 2001, 2010	2010 (v), 2020 (F), 2030	11	10
Pérez-Vega et al., 2012	The state of Colima, the western part of Mexico.	1986-1993, 2002	2002 (V) Comparison	7	9
Sang et al., 2011	Beijing, China	2001, 2006	2008 (V), 2015 (F)	5	9
Silva et al., 2012	The Rio Grande do Sul coastal plain, Brazil	1987-2000	2015 (F)	13	15
Tewold and Cabral, 2011	Greater Asmara Area (GAA), Eritria	1989-2000	2009 (V), 2020 (F)	11	9
Valdivieso et al., 2010	Catamayo Chira basin south-west borderline region between Ecuador and Perú	1986-1996, 2001	2001 (V), 2012 (F)	10	16
Verburg et al., 2002	Sibuyan Island, Philippines	1997	2017	-	20
Vliet et al., 2009	The Greater Vancouver Regional District (GVRD), Canada	1996, 2001	2001 (V)	5	
Wang and Li,	Shenzhen City, China	2000, 2005	2010 (V)	5	10

Authors	Study area	Time scale	Prediction date	Historic Interval	Predict Interval
2011					
Wang et al., 2011	City of Calgary, Canada	1985, 1992, 1996, 2001 and 2006	2006 (V)	5	5
Wang et al., 2012	Changping District, Beijing	1988-1995	2000 (V)	7	5
Wu et al., 2006	Beijing, China	1986, 1991, 1996, 2001; 1986-2001	2021 (F)	15	15
Xin et al., 2012	Changping, a district of Beijing, China	1988-1998	2008 (V)	10	10

1.3 Objectives

The objective of this paper is to explore the impact of temporal scales on land cover change modeling for predicting land cover change in a Mediterranean catchment in SE France. Land cover maps of 2011 were predicted from different time scales (1950-1982, 1982-2003, and 2003-2008) and compared with the digitized land cover map of 2011 to measure model accuracy. The study is part of a larger program to evaluate the impacts of land cover change on runoff and soil erosion at the catchment scale.

2. Methods

Study area, land change modeling steps, and data are discussed in this section.

2.1 Site description

The study area (about 235 km²) is situated in the Var department of SE France near the Gulf of St. Tropez. The western part of the watershed (about 70% of the catchment) is forest (mostly pine and oaks), and the topography is uneven with the highest elevation at about 650 m. The lower part of the catchment is a gently sloping alluvial plain. The catchment area is characterized by a Mediterranean climate with hot dry summers, and cooler rainier winters. Average temperatures range between 22°C to 26°C in summer and 5°C to 10°C in winter. The mean annual rainfall is about 900 mm, and the main rainy season is from October to January (Fox et al. 2012). Several tributaries flow into the Giscle main channel, including the Môle, the Grenouille,

the Tourre, and the Verne. Three main municipalities are located within the catchment: Cogolin, Grimaud, and La Môle (Figure 0.18).

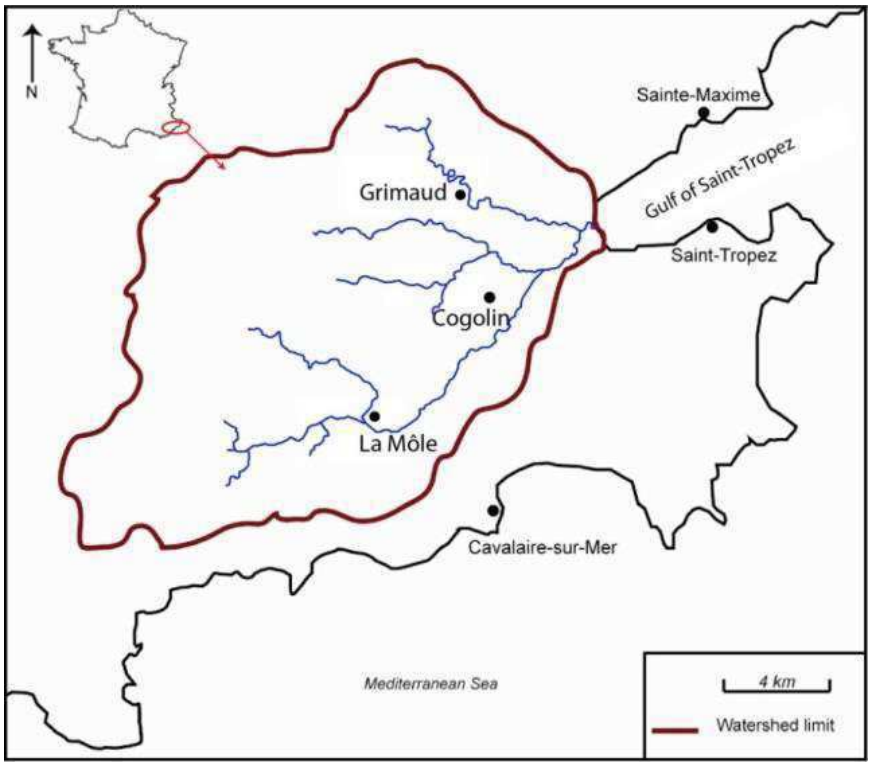

Figure 0.18: Location of the catchment.

2.2 Land change modeling procedure

Land Change Modeler (LCM) was originally designed to manage impacts on biodiversity, and analyze and predict land use and land cover changes. Only thematic raster (byte or integer value 1-265) images with the same land cover categories listed in the same sequential order can be inputted in LCM for analysis, and background areas must be identified on maps coded with 0. LCM evaluates land cover changes between Time 1 (initial time) and Time 2 (second time). It calculates the changes, and displays the results with various graphs and maps. Finally, it predicts future (Time 3) land cover on the basis of relative transition potential maps. LCM was used in this study to identify explanatory variables, create transition potentials, and predict future land cover maps. Figure 0.19 presents all major steps of the LCM-IDRISI model (Eastman 2012) that have been used in the study. Three major steps: data input, results and validation are presented in this flow chart with relevant module name that are used in the study. Digitization of land cover maps, creation and selection of explanatory variables, constrains, and transition potentials are

shown in the data input section. Results and validation sections are presented with associated modules which are incorporated to predict land cover maps and to validate the accuracy of the predicted land cover maps.

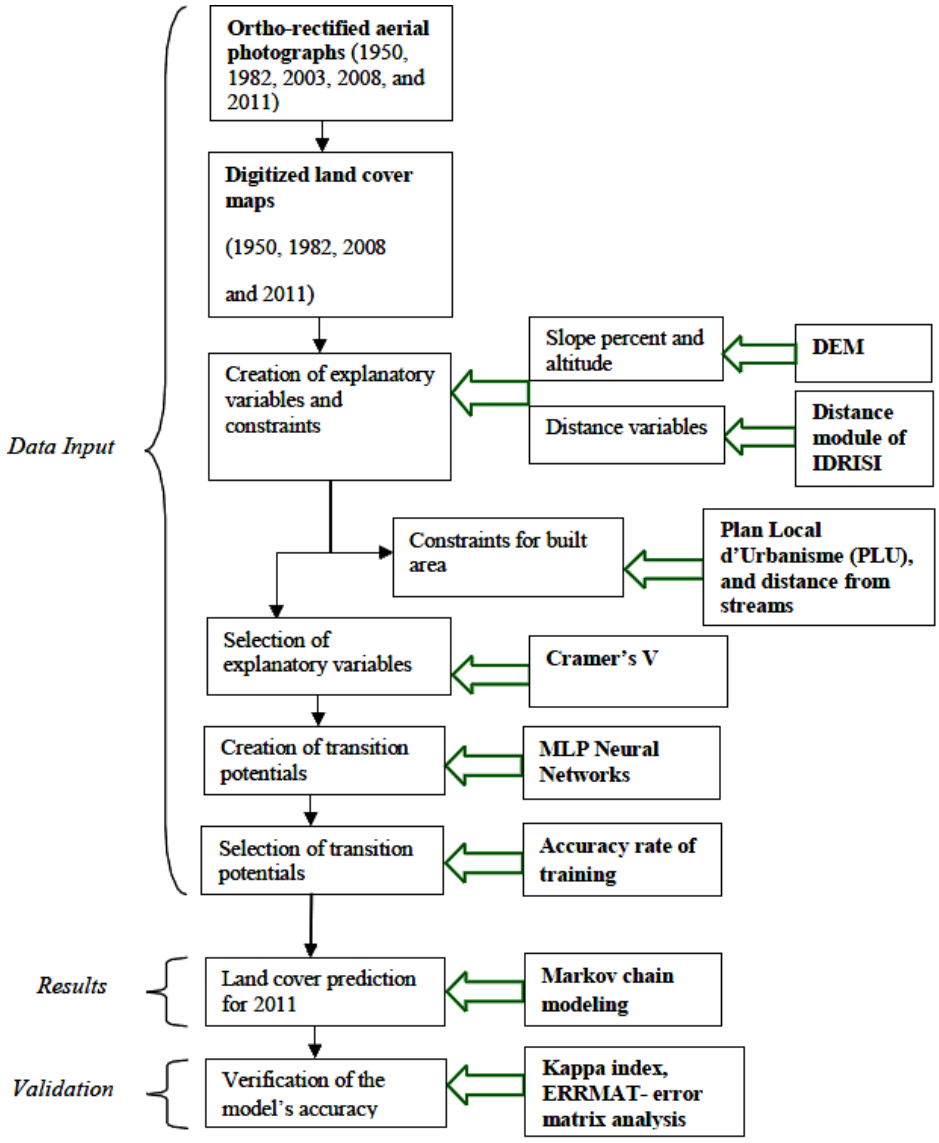

Figure 0.19: Flowchart of the model

2.2.1 Digital data and land cover categories

Land cover maps were digitized from grey scale ortho-rectified aerial photographs of 1950 and 1982, and color ortho-photos of 2003, 2008, and 2011. Spatial resolution for all aerial photographs was reduced to 1 m from 0.5 m to facilitate data manipulation during digitization. Surfaces were initially characterized into five categories: forest (F), vineyard (V), grassland (G),

urban (U) and suburban (S), but the last 2 categories were collapsed into a single built area (B) class to improve category attribution as described below (Table 0.9). Methods of land cover digitization, classification, and characteristics of land cover classes were discussed in (Roy et al. 2014b). Land cover classification was facilitated by numerous field visits, and validation was carried out through a group of 15 third year Geography students of the University of Nice Sophia Antipolis. Each student was provided with a sample of 20 selected cells to identify land cover class; each sample had a roughly equal number of cells in each category, and there were 5 students for each year (1950, 1982, and 2003). This was the students' first contact with digital air photos, so the validation is considered a worst case scenario.

Slope was created from a 25 m Digital Elevation Model (DEM). Road and stream networks were screen digitized from the aerial photographs of 2008. Only major roads were taken into account, so road network was considered constant for all time periods. In order to make the land cover maps compatible with the explanatory variables, cell size was converted to 25 m.

Table 0.9: Characteristics of the different land cover classes

Final land cover categories	Description
Forest	Natural forest area including dense shrubland and scattered housing.
Vineyard	Vineyards are identified by their blocky, geometric shapes, and linear texture created by the rows of planted vines.
Grassland	Abandoned agricultural land, new shrubland with small and scattered trees, and pasture land for sheep and horses.
Built area	Densely to low developed areas including some small denser communities: residential, commercial, and industrial.

2.2.2 Explanatory variables and constraints

Topographic and distance variables have been used to simulate land cover change studies throughout the world (Khoi 2011, Li and Yeh 2002, Mas et al. 2012, Oñate-Valdivieso and Bosque Sendra 2010). In an earlier study (Roy et al. 2014b), major topographic and distance variables were identified. These include the following: slope, altitude, distance from roads, distance from built area (initial year), and distance from streams. In addition, three constraints and incentives (forest to built area, vineyard to built area, and grassland to built area) were

included in the prediction process. These were created from the “Plan Local d’Urbanisme” (PLU) and “Schéma de Coherence Terrtoriale” (SCOT) (Figure 0.20). The PLU is the local urban plan in France; it determines land use guidelines. The SCOT integrates different policies regarding urban planning: social and private housing, communication infrastructure and public transport, commercial infrastructure, and environment protection. Constraints and incentives are multiplied by the corresponding transition potential during modeling. In this study, values of 0 on the map were used to define absolute constraint, and 1.1 was used for incentives to emphasize the expansion of built areas in suitable selected zones for development according to the regional plan. In addition, distance from streams was also added with above mentioned constraints. Disincentive areas situated within a distance from streams of 0-25 m, and 25-50 m were defined by values of 0.6 and 0.8, respectively to maintain the historical trend of less urbanization near stream networks in the study area according to (Roy et al. 2014b).

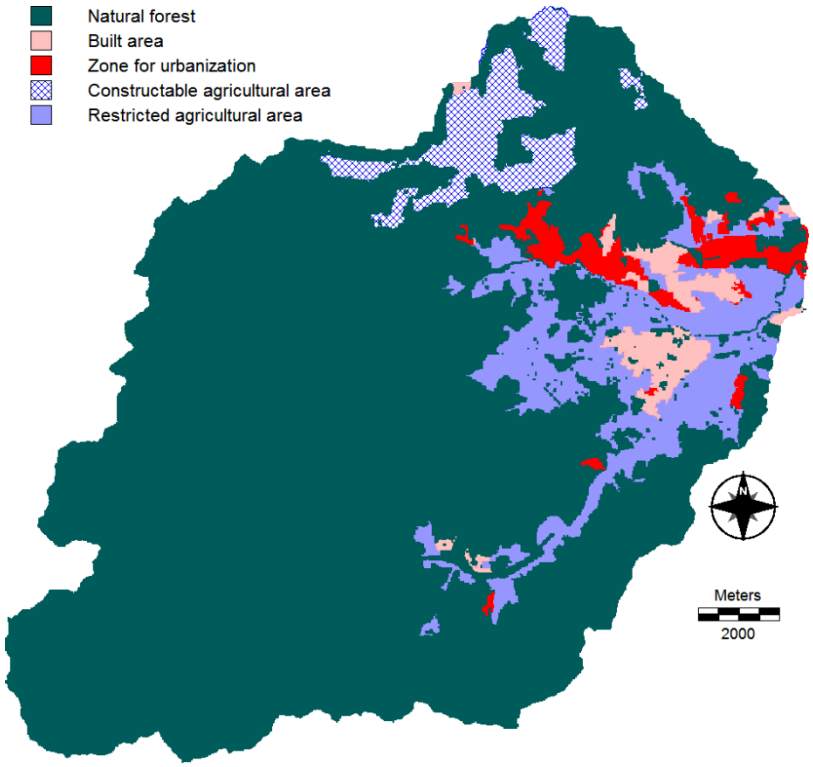

Figure 0.20: PLU and SCOT map of the study area.

2.2.2.1 Selection of explanatory variables

The simulation of multiple categories of land cover change depends on several explanatory variables (Li and Yeh 2002). Explanatory variables that were drivers of past land cover change are expected to be an influential force in future changes and are selected based on available data and their explanatory abilities. DEM, slope, and distance from road represent the accessibility of a neighborhood, and distance from built area highlights the proximate location of urbanization. The significance of explanatory variables was tested using Cramer's V which measures the strength of association between two categorical variables based on Chi-square statistics (Pérez-Vega et al. 2012). In this study, land cover change in a historical time period and explanatory variables are taken into account to test Cramer's V for a particular variable. LCM calculates Cramer's V automatically and displays the association level of explanatory variables with land cover categories. Variables with greater values are considered more important than other variables. Cramer's V values of ≥ 0.4 and ≥ 0.15 are considered good and useful, respectively; and values <0.15 should be removed from the model (Eastman 2012).

Two topographical variables (slope and altitude) and three distance variables (roads, streams, and built area) have significant impacts on land cover change in the study area (Roy et al. 2014b), and these are employed in the model. Distances from roads and streams were developed from the digitized road and stream layers, respectively. Distance from built area was measured using built area of the initial year of the corresponding historical time period.

2.2.3 Transition potentials

Transition potential maps were created for each transition possibility (F to V, F to G, F to B, V to F, V to G, V to B, G to F, G to V, and G to B) based on historical changes and selected explanatory variables. The Multi-Layer Perceptron Neural Network (MLPNN) algorithm of IDRISI (Eastman 2012) was employed to create transition potentials. Each transition potential was modeled individually using the same explanatory variables, but only transition potentials with an accuracy rate greater than 70% were utilized for land cover prediction.

For all transitions at different time periods, 10,000 iterations were selected. The minimum number of cells that transformed into a particular time period for a particular transition is selected as the sample size per class, in which 50% of these cells are used for training and another 50% of these cells use for testing purposes to measure the calibration of this transition potential (Eastman

2012). For example, if 'x' cells of forest converted to vineyard in 1982-2003; this (x) is the maximum/total cells that converted from forest to vineyard in 1982-2003. 'The minimum cells that persisted' also displays the persistence of a land cover in that particular time period for all possible transitions.

2.2.4 Land cover prediction and time scales test

Land cover change prediction has two aspects: the quantity of change is provided by the Markov change model matrix and the spatial distribution of change is given by MLPNN. LCM provides the quantity of change by evaluating the Markov matrix comparing the initial (T1) and second land cover (T2), and then predicts the future land cover (T3) using a transition probability matrix for the future. The transition probability matrix displays the probability of each land cover category changing into another category. A value close to 0 indicates a low conversion probability, and 1 indicates a high conversion probability for the target land cover. Transition probabilities can be modified manually and saved but all rows must sum to one (Pontius 2000, Eastman 2012). The probability matrices provide the potential for change of each category without any spatial distribution of change; this is provided by the transition potential maps generated using MLPNN. Land cover maps were predicted for 2011 using transition potential maps from several historical time periods (1950-1982, 1982-2003, 2003-2008) (Table 0.10). The same variables and constraints were incorporated in all simulations.

Table 0.10: Historical time periods, prediction and validation dates for different scales.

Historical time period	Prediction date	Historical time interval	Validation time interval
1950-1982	2011	32	29
1982-2003	2011	21	8
2003-2008	2011	5	3

2.2.5 Land cover prediction validation

Validation of a model is needed in order to assess its accuracy. To do this, simulated land cover maps of 2011 created using different time scales were compared with a digitized map of the same year. Both quantitative and location errors were calculated in the study. The quantitative error is the difference between the quantity of cells in a particular land cover category in one map

(predicted) and the quantity of cells in that category of the other map (actual), and the location error is the spatial deviation of a category in one map from same category in another map (Eastman, 2012). The accuracy of quantity and location indicates totally different aspects. 100% accuracy rate of quantity can be 0% for spatial accuracy. However, the greatest (100%) spatial accuracy and the least (>0%) quantitative accuracy are impossible to find in the same simulation for a particular land cover category because spatial accuracy considers spatially wrong overestimated and underestimated area where quantitative accuracy only consider the difference area in simulated and actual map for a particular category.

Kappa indices and error matrix analysis are incorporated in the study for model validation. The standard 'Kappa index' is a comparative analytical process that measures spatial and non-spatial aspects between predicted and reference maps (Eastman 2012). Kappa index was first introduced by (Landis and Koch 1977), though their guidelines were not accepted by all, and they propose the following levels of agreement with a corresponding range of kappa (Table 0.11). Kappa values were characterized as excellent over 0.75, 0.40 to 0.75 as fair to good, and below 0.40 as poor (Eastman 2012).

Table 0.11: Level of agreement associated with Kappa values by (Landis and Koch 1977)

Strength of agreement	Landis and Koch, 1977
Poor	<00
Slight	0.00 - 0.20
Fair	0.21 - 0.40
Moderate	0.41 - 0.60
Substantial	0.61 - 0.80
Almost perfect	0.81 - 1.00

Kappa indices for different components are developed by (Pontius 2000) to assess the reliability of a model which can be expressed by the following equation:

$$\text{Kappa Index} = \frac{\text{Po}-\text{Pc}}{\text{Pp}-\text{Pc}} \qquad (2)$$

Where Po is the observed proportion correct, Pc is the expected proportion correct due to change, and Pp is the proportion correct when the classification is perfect (100%). In equation (2), if classification is perfect, Po−Pc=Pp−Pc≠0, then Kappa=1

$$\text{If} \qquad \text{Po} > Pc, then\ Kappa > 0$$

$$\text{If} \qquad \text{Po} = \text{Pc}, \text{then Kappa} = 0$$

$$\text{If} \qquad \text{Po} < Pc, then\ Kappa < 0$$

Pontius (2011) shows several components of Kappa indices: Kappa standard ($K_{standard}$), Kappa for location ($K_{location}$), Kappa for quantity ($K_{quantity}$), and Kappa for no spatial and quantity information (K_{no}). (Pontius and Millones 2011) defines "*$K_{standard}$ as an index of agreement that attempts to account for the expected agreement due to random spatial reallocation of the categories in the comparison map, given the proportions of the categories in the comparison and reference maps, regardless of the size of the quantity disagreement*". K_{no} depends on randomly selected quantity and spatial allocation of categories in the comparison map. $K_{quantity}$ is a ratio of quantitative difference between the categories in the comparison map and reference map, and $K_{location}$ is the spatial allocation agreement between them.

The confusion matrix was analyzed using the ERRMAT module of IDRISI (Eastman 2012) to assess the fitness of spatial cell allocation between predicted and true values. ERRMAT outputs an error matrix containing a tabulation of the number of cells found in each possible combination of true and mapped categories, and a summary of statistics (Eastman 2012). Error of omission estimates the proportion of the area of a particular land cover that is omitted by the model and total area of the same category of the reference image. Error of commission represents the proportion of wrongly attributed land cover of a particular category that is overestimated by the model for each category. Commission and omission errors were calculated according to the following formulae:

$$\text{Commission error} = \frac{\text{Total area of a particular category in } \textbf{projected map - Persistence}}{\text{Total area of that category in } \textbf{projected map}}$$

$$\text{Omission error} = \frac{\text{Total area of a particular category in } \textbf{reference map - Persistence}}{\text{Total area of that category in } \textbf{reference map}}$$

ERRMAT also presents the overall and per category Kappa Index of Agreement (KIA) values. This module is executed for different predictions that were generated using different time scale.

3. Results

3.1 Land cover change analysis during different time periods

The classification validation procedure revealed that classifying land cover into five categories was difficult from grey scale photographs and simpler for the 2003 color air photos. For 1950, classification error was 27%, and sources of error were either a confusion between vineyard and grassland or urban and suburban. The classification error decreased to 20% when urban and suburban were collapsed into a single built category. For 1982, category error was 10% and 20% for 4 and 5 categories, respectively. Finally, for 2003, the error was only 4% for 4 categories, down from an initial 15% due to confusion between urban and suburban classes (by one student). It should be noted that the exercise was for unexperienced undergraduates just introduced to digital air photos. The actual classification was carried out by an experienced user over several months and verified thoroughly by a second experienced user, so the actual classification accuracy can be considered much greater than the values cited above.

Figure 0.21 a-d show land cover maps (1950, 1982, 2003, and 2008) digitized from the air photos. Most of the land cover changes occurred in the alluvial plain (East), where most of the vineyard, grassland and built areas are concentrated.

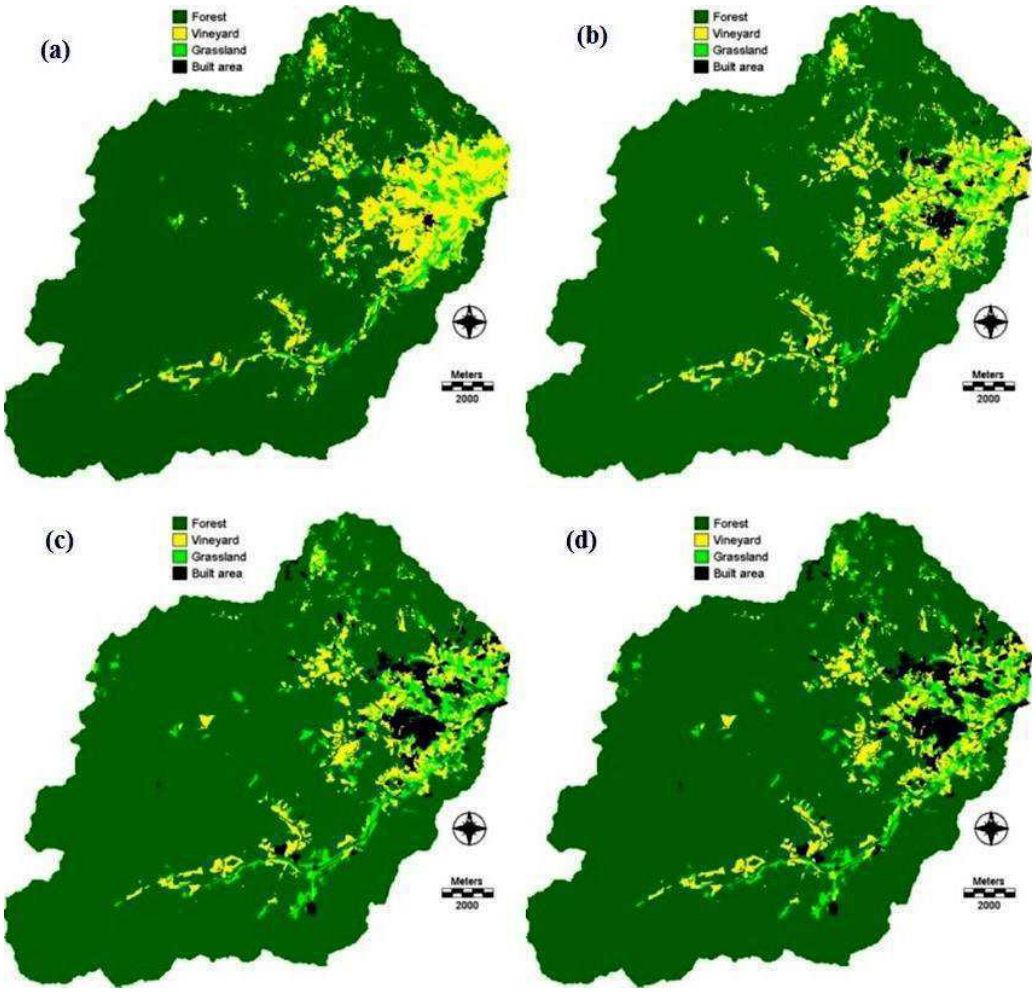

Figure 0.21: (a) Land cover map of 1950, (b) 1982, and (c) 2003, and (d) 2008.

Figure 0.22a-d present land cover changes (ha) in all categories of the study area, and Table 0.12 shows the percentage of total surface area of each land cover category in different years. Two general trends can be identified in land cover change since 1950: forest and vineyard decreased while grassland and built area increased. Some changes in forest occurred in 1982-2003 as it lost about 120 ha (Figure 0.22). A marked decrease was observed in vineyard (28% of the initial year) that lost 854 ha between 1950 and 2003 (Figure 0.22). Then, it increased 67 ha in 2003-2008 and resumed its decreasing trend in the last time period 2008-2011. Vineyard was 10.4% of the catchment in 1950 and decreased to 6.6% in 2003 and then remained more or less stable till 2011. A clear increase was observed in grassland (50%). However, some fluctuations are also observed in grassland change after 2003. Grassland increased from 3.4% to 5.4% of the catchment in 1950-2003 and decreased slightly to 4.9% in 2011. It increased greatly (383 ha) in

1982-2003, decreased 122 ha in the next time period (2003-2008) but resumed the increasing trend again in 2008-2011 (Figure 0.22). Built area remained a minor component of the catchment, and increased rapidly from only 0.1% to 3.2% of the catchment during the study period (Table 0.12).

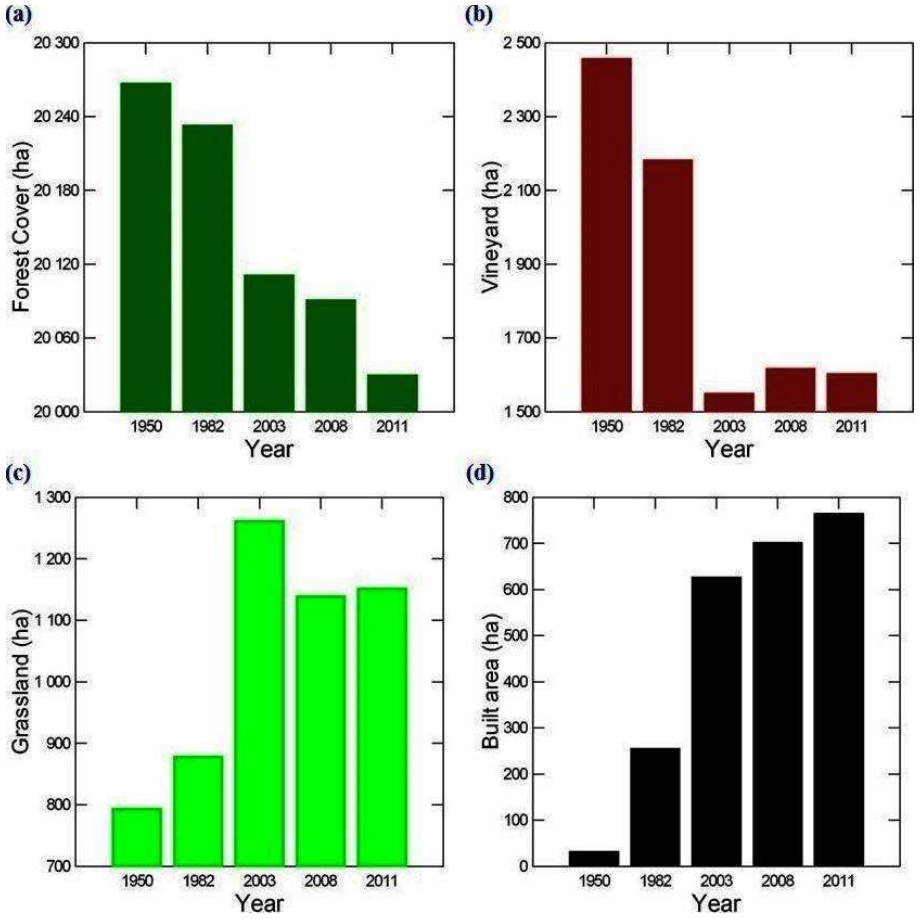

Figure 0.22: (a) Forest change in 1950-2011. (b) Vineyard change in 1950-2011. (c) Grassland change in 1950-2011 (d) Built area change in 1950-2011.

Table 0.12: Percentage of the catchment area for each category

	Total surface area (% of the catchment)				
	1950	1982	2003	2008	2011
Forest	86.1	85.9	85.4	85.3	85.1
Vineyard	10.4	9.3	6.6	6.9	6.8
Grassland	3.4	3.7	5.4	4.8	4.9
Built area	0.1	1.1	2.7	3.0	3.2

Figure 0.23 summarizes the mean rate of change of each land cover category in the different time periods. Forest loss was -1.1 ha yr^{-1} and -5.8 ha yr^{-1} in 1950-1982 and 1982-2003,

respectively, it lost -10.1 ha yr^{-1} in the recent time period 2003-2011. The average forest depletion rate was -3.9 ha yr^{-1} in 1950-2011. The greatest rate of vineyard loss was -30.1 ha yr^{-1} in 1982-2003, and the average overall rate of vineyard depletion was -14 ha yr^{-1}. The rate of grassland expansion was 2.7 ha yr^{-1} in 1950-1982; it increased to 18.2 ha yr^{-1} in 1982-2003, and then to 13.8 ha yr-1 in 2003-2011. Grassland gained an average of 5.9 ha yr^{-1} in the study period. The rate of built area expansion was 7 ha yr^{-1} in 1950-1982 and increased to 17.6 ha yr^{-1} in the recent time period 2003-2011. So, the average rate of built area expansion was 12 ha yr^{-1} in 1950-2011.

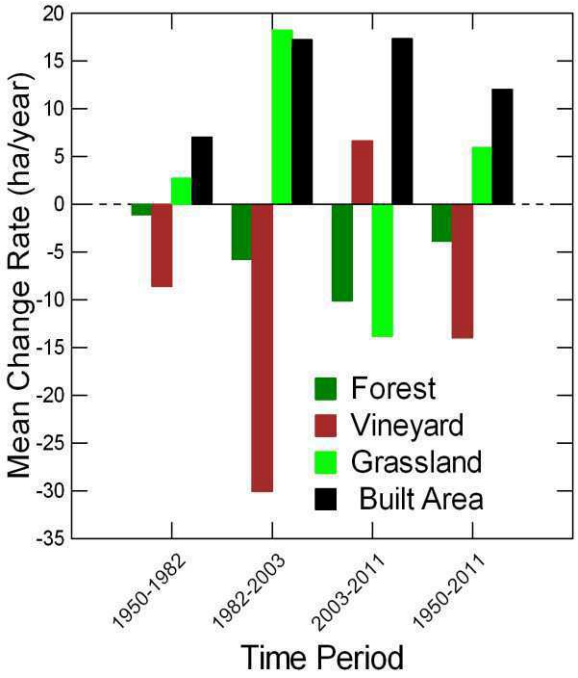

Figure 0.23: Mean rate of land cover changes (ha) in different time periods

3.2 Selection of explanatory variables

Figure 0.24a-e present all explanatory variables utilized in the study to predict future land cover changes using different time scales. It can be seen in these Figures that most of the eastern part of the catchment is a plain with low altitudes and gentle slopes. In addition, distances from roads, streams, and built areas are than the remaining catchment. As was described in (Roy et al. 2014b), most of the changes in land cover occurred in the alluvial plain area.

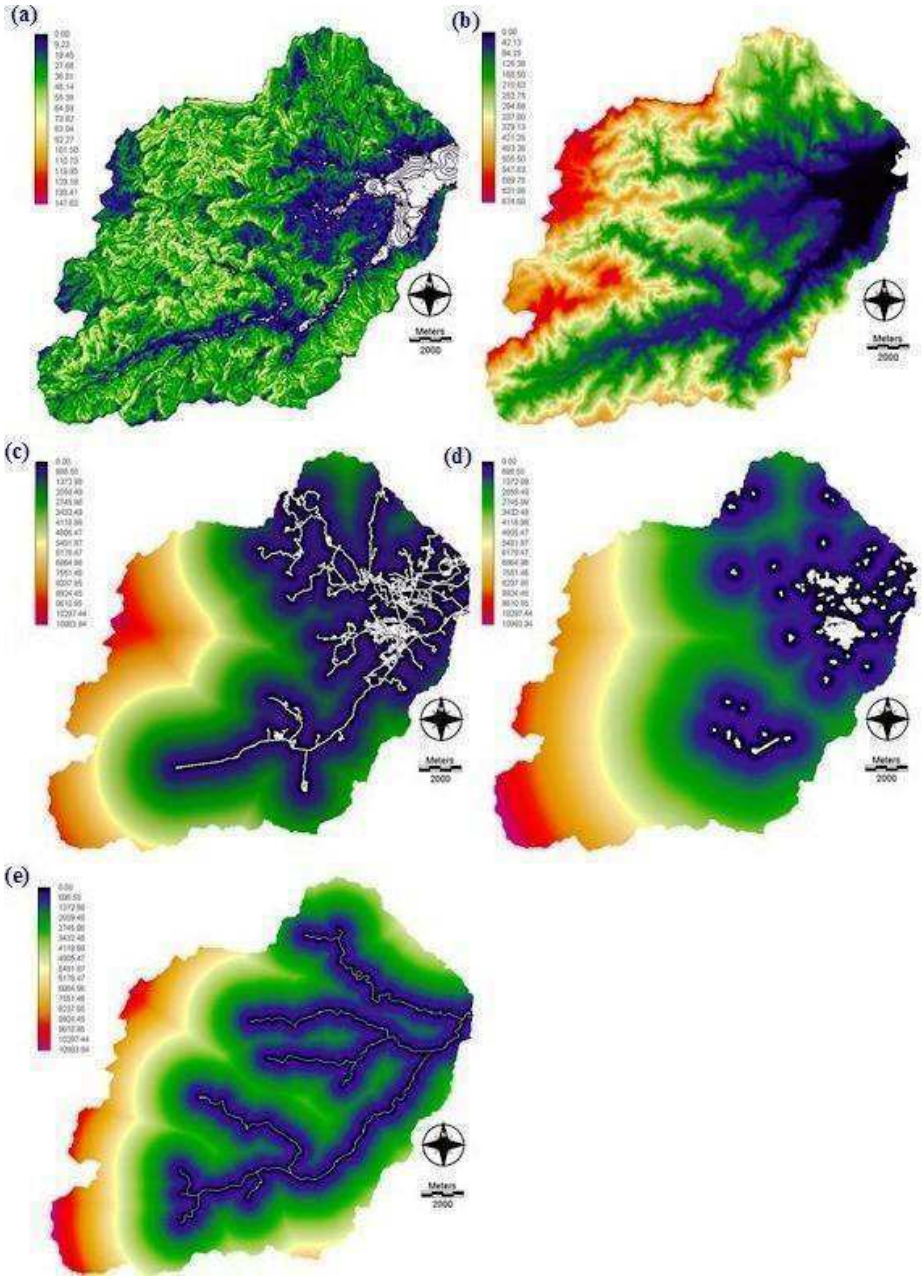

Figure 0.24: (a) Slope. (b) Altitude. (c) Distance from road. (d) Distance from built area. (e) Distance from streams.

The association level between explanatory variables and land cover types in different time periods is shown in Table 0.13. It is measured through Cramer's V. All variables have a Cramer's V value ≥0.15 with all land cover types except forest in the long time period (1950-1982).

The strongest explanatory variable is altitude, which has a good association level (Cramer V ≥0.40) with all land covers except forest for all time periods. A good association level is also observed in slope with all land covers in all time periods, especially with vineyard and grassland.

Distance from roads shows a high association level with vineyard in all time periods, and has good association level with forest and grassland in the intermediate (1982-2003) and long (1950-1982) time periods, respectively. Distance from built area also has a good association level with forest and vineyard in all time periods. Distance from streams is the weakest variable; it shows comparatively limited association with existing land covers and has only a good level of association with vineyard in all time periods. The lowest association is observed for forest with all variables except distances from road and built area, indicating that the dominant forest category (about 85%) is less influenced by topographic variables.

Table 0.13: Cramer's V coefficient (relationship between land cover change and explanatory variables). Values ≥ 0.40 are highlighted in bold.

Time period		Altitude	Slope	Dist. Road	Dist. Built area	Dist. stream
1950-1982	Forest	0.20	0.15	0.31	**0.40**	0.12
	Vineyard	**0.69**	**0.65**	**0.59**	**0.46**	**0.41**
	Grassland	**0.52**	**0.50**	**0.44**	0.33	0.32
	Built area	0.39	0.36	0.28	0.22	0.20
1982-2003	Forest	0.30	0.22	**0.49**	**0.60**	0.16
	Vineyard	**0.67**	**0.63**	**0.59**	**0.59**	**0.41**
	Grassland	**0.40**	**0.40**	0.36	0.33	0.27
	Built area	**0.44**	**0.42**	0.30	0.30	0.25
2003-2008	Forest	0.30	0.22	**0.49**	**0.64**	0.16
	Vineyard	**0.67**	**0.62**	**0.59**	**0.60**	**0.41**
	Grassland	**0.41**	**0.41**	0.36	0.34	0.27
	Built area	0.39	0.38	0.27	0.29	0.25

3.3 Transition potentials

Transition potentials for different time periods present similar patterns and the same explanatory variables were used in all simulations for the different time scales. Therefore, only transition potentials for the intermediate time period (1982-2003) are displayed in Figure 6a-i. High potential areas for all transitions are found mostly in the alluvial plain (Figure 0.25a-h). Most of the lower altitude and gentle slope areas have shown high potentiality of change from forest to vineyard and grassland. The same trend is observed in grassland change, where most of the grassland far away from streams and roads have a higher potentiality to transform into forest, and grassland in lower distance from roads and streams have the higher potentiality to convert into vineyard.

Figure 0.25a and b display transition potentials from vineyard and grassland to forest, respectively. In the vineyard to forest transition, some scattered vineyard at the edge of the existing built area have shown higher potentiality of change to forest, and the rest of the vineyard in the plain land has lower potentiality to change into forest, and most of the grassland far away from streams and roads have a higher potentiality to transform into forest. Most of the lower altitude and gentle slope areas have shown high potentiality of change from forest to vineyard, and grassland in lower distance from roads and streams have the higher potentiality to convert into vineyard (Figure 0.25c-d). Transition potentials to grassland from forest and vineyard are shown in Figure 0.25e and 6f, respectively. Most of the lower altitude and gentle slope areas have shown high potentiality of change from forest and grassland (Figure 0.25e). Some scattered vineyards at the edge of the existing built area have shown higher potentiality to convert into grassland, and have higher potentiality to transform into grassland (Figure 0.25f). Transition potentials to built area from all other land covers are presented in Figure 0.25g-i. The plain land near road and the existing developed area are more vulnerable to change into built area. Transitions from all land cover categories to built area are selected areas near the road network and existing built area particularly, huge forest area is shown vulnerable to convert into built area Figure 0.25g.

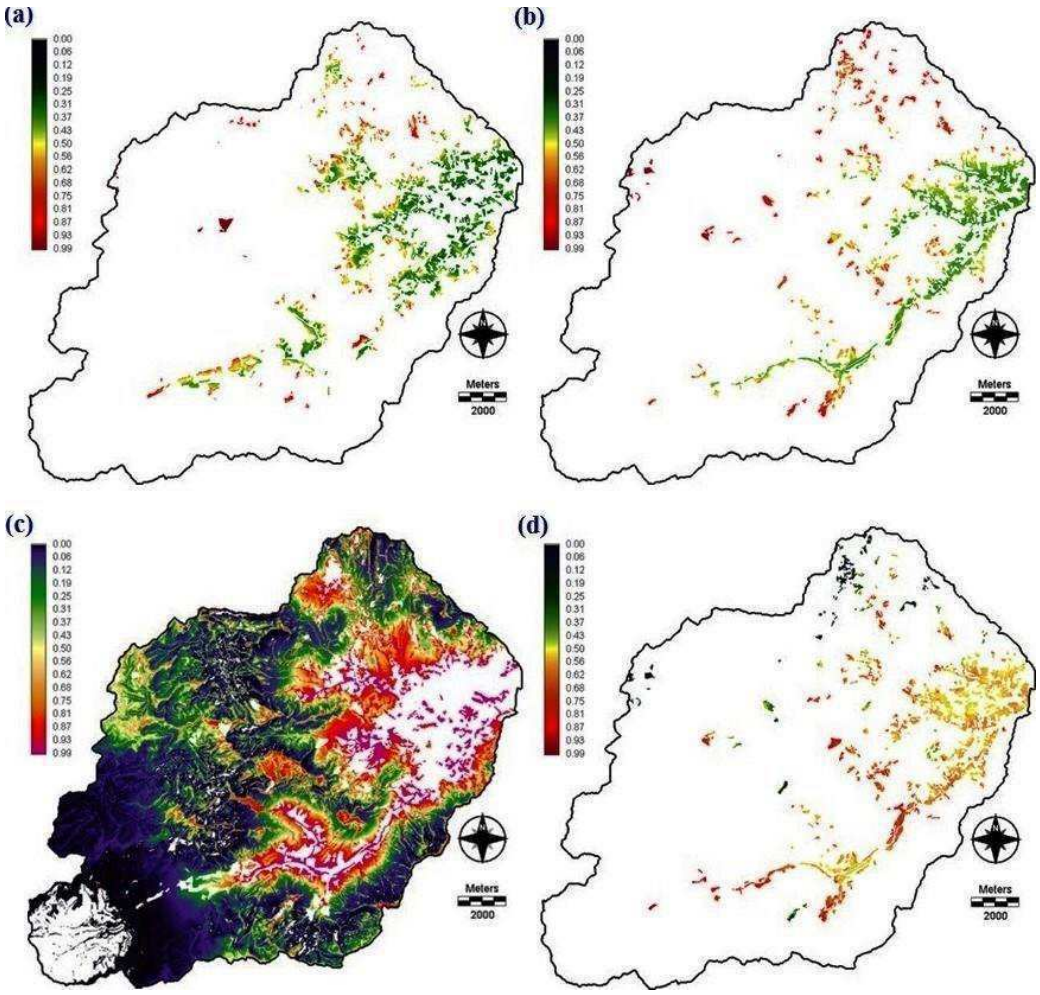
(a)
(b)
(c)
(d)
0.00
0.06
0.12
0.19
0.25
0.31
0.37
0.43
0.50
0.56
0.62
0.68
0.75
0.81
0.87
0.93
0.99
Meters
2000

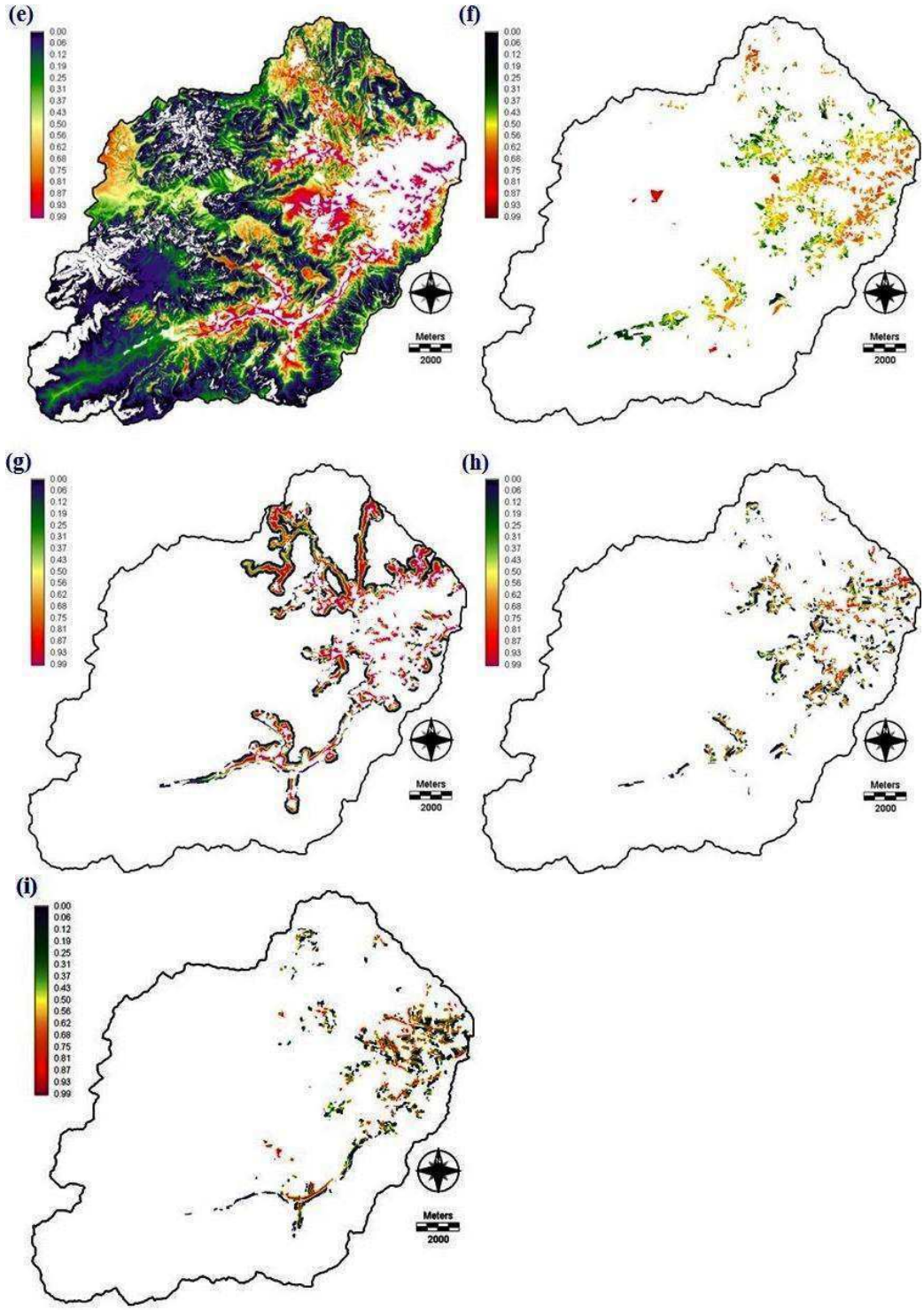

Figure 0.25: (a) Transition potential from vineyard to forest. (b) Transition potential from grassland to forest. (c) Transition potential from forest to vineyard. (d) Transition potential from grassland to vineyard. (e) Transition potential from forest to grassland. (f) Transition potential from vineyard to grassland. (g) Transition potential from forest to built area. (h) Transition potential from vineyard to built area. (i) Transition potential from Grassland to built area.

Table 0.14 presents the accuracy rate of all transition potentials for different time periods. Accuracy rate presents the agreement between a particular transition and selected explanatory variables. A high accuracy rate is observed for several transitions in all time periods: forest to all other categories, and vineyard and grassland to built area. Transition from vineyard to forest in 2003-2008 also shows high accuracy. Therefore, transition potentials from forest to all and vineyard and grassland to built area are good. All transitions from vineyard and grassland to other land covers except built area have low to intermediate accuracy rate.

Table 0.14: Accuracy rate (%) of transition potentials in different time periods (F-Forest, V-Vineyard, G-Grassland, B-Built area).

	Accuracy rate (%)								
Time period	F-V	F-G	F-B	V-F	V-G	V-B	G-F	G-V	G-B
1950-1982	85	86	99	64	58	97	63	58	97
1982-2003	83	81	97	64	60	85	62	57	83
2003-2008	91	97	98	100	63	85	63	64	82

3.4 Prediction of land cover change using different time scales

The transition probability matrices for all time periods are presented in Table 0.15 where 4 × 4 matrices are presented for three time periods, the row represents the second year of the initial time period (T2) and the column represents the simulation year (T3). Expected transition area (diagonal) is also expressed in ha. The Markov transition probability matrices show the transition probability of each land cover category, are calculated based on historical land cover changes during the periods 1950-1982, 1982-2003, and 2003-2008. The probability of expected amount of unchanged land cover represents expected persistence in predicted time period are presented in ha in diagonal and in parentheses. The off-diagonal values indicate the probability of a land cover change may occur from one land cover category to another.

The transition probability matrix can be expressed as the % of a particular land cover in the year T2. For example, the probability of forest 0.97 can be expressed as 97%, which indicates that most of its coverage will remain unchanged due to its imputed coverage in the catchment. For the initial 1950-1982 time period, probabilities of 0.02 and 0.01 exist for vineyard and grassland, associated with a transition of 404 ha and 202 ha from forest, respectively. A probability of 0.72 is associated with the persistence of vineyard, displays its vulnerability of change to other land cover. While, a probability of 0.51 indicates the lowest persistence of

grassland, indicates its instability, and shows the highest possibility of change to other land cover in 1982-2011. Built area remained constant and it has no probability of change into other land covers.

Transition probabilities based on the intermediate time period shows that the trend of land cover change probabilities based on the long time period (1950-1982) has continued for this time period but the probabilities of land cover changes have decreased for this 8 year time period (2003-2011). Markov matrix of this time period indicates that built area and forest were the most stable land cover categories with the probabilities of 1.0 and 0.98, respectively. However, transitions of large area are observed in forest, vineyard, and grassland. A transition probability of 0.01 is equivalent of a transition area 201 ha associated with deforestation and conversion of forest into vineyard and grassland. A probability of 0.18 is equivalent to a transition of 227 ha from vineyard to grassland, is associated with vineyard abandonment. While transition probabilities of 0.14 and 0.07 are associated with transition of 177 ha and 108 ha of grassland into forest and vineyard, respectively. It has shown the probability of interchanges between vineyard and grassland. Built area has no probability to transform into other land cover categories.

Transition probabilities based on the short time period presents transition probabilities of land cover changes in 2008-2011 on the basis of changes in the earlier time period 2003-2008. The transition probabilities of all land cover categories are the lowest among all time periods due to the short time scale. However, the same trend of conversion continued from the history to recent time for both long and short time scales. The highest probability of persistence is observed for all land cover categories that actually going to predict almost as the same of its initial year.

Table 0.15. Land cover transition probabilities in 1982-201, 2003-2011, and 2008-2011, using different time periods 1950-1982, 1982-2003, and 2003-2008, respectively. Expected transition area or change area matrix is also expressed in ha in diagonal, accounted from the total area in initial year (T2).

Initial time period	Land cover types	Forest	Vineyard	Grassland	Built area
1950-1982	Forest	**0.97 (19,626)**	0.02 (404)	0.01 (202)	0.00 (0)
	Vineyard	0.08 (174)	**0.72 (1,571)**	0.15 (327)	0.049 (109)
	Grassland	0.21 (184)	0.23 (202)	**0.51 (448)**	0.048 (43)
	Built area	0.00 (0)	0.00(0)	0.00(0)	**1.000 (255)**
1982-2003	Forest	**0.98 (19,709)**	0.01 (201)	0.01 (201)	0.00 (00)
	Vineyard	0.01 (15)	**0.79 (1,224)**	0.18 (227)	0.02 (31)
	Grassland	0.14 (177)	0.07 (108)	**0.73 (458)**	0.06 (76)
	Built area	0.00 (0)	0.00(0)	0.00(0)	**1.000 (627)**
2003-2008	Forest	**1.00 (20,091)**	0.00 (0)	0.00(0)	0.00 (0)
	Vineyard	0.00 (0)	**0.98 (1,585)**	0.14 (11)	0.01 (16)
	Grassland	0.02 (23)	0.05 (81)	**0.91 (639)**	0.02 (23)
	Built area	0.00(0)	0.00(0)	0.00(0)	**1.000 (702)**

3.5 Validation of predicted land cover

Simulations for 2011 were executed using transition potentials from 1950-1982, 1982-2003, and 2003-2008, respectively. Simulated and actual land cover maps of 2011 are presented in Fig. 7a-d. Dissimilarities are observed mainly in the plain land of the eastern part of the catchment where most of the conversion took place as described in (Pontius and Millones 2011). Visual interpretation (Figure 0.26 a-c) suggests the simulated maps from intermediate (Figure 0.26b) and short (Figure 0.26c) time scales are reasonably similar to the actual map of that year (Figure 0.26d).

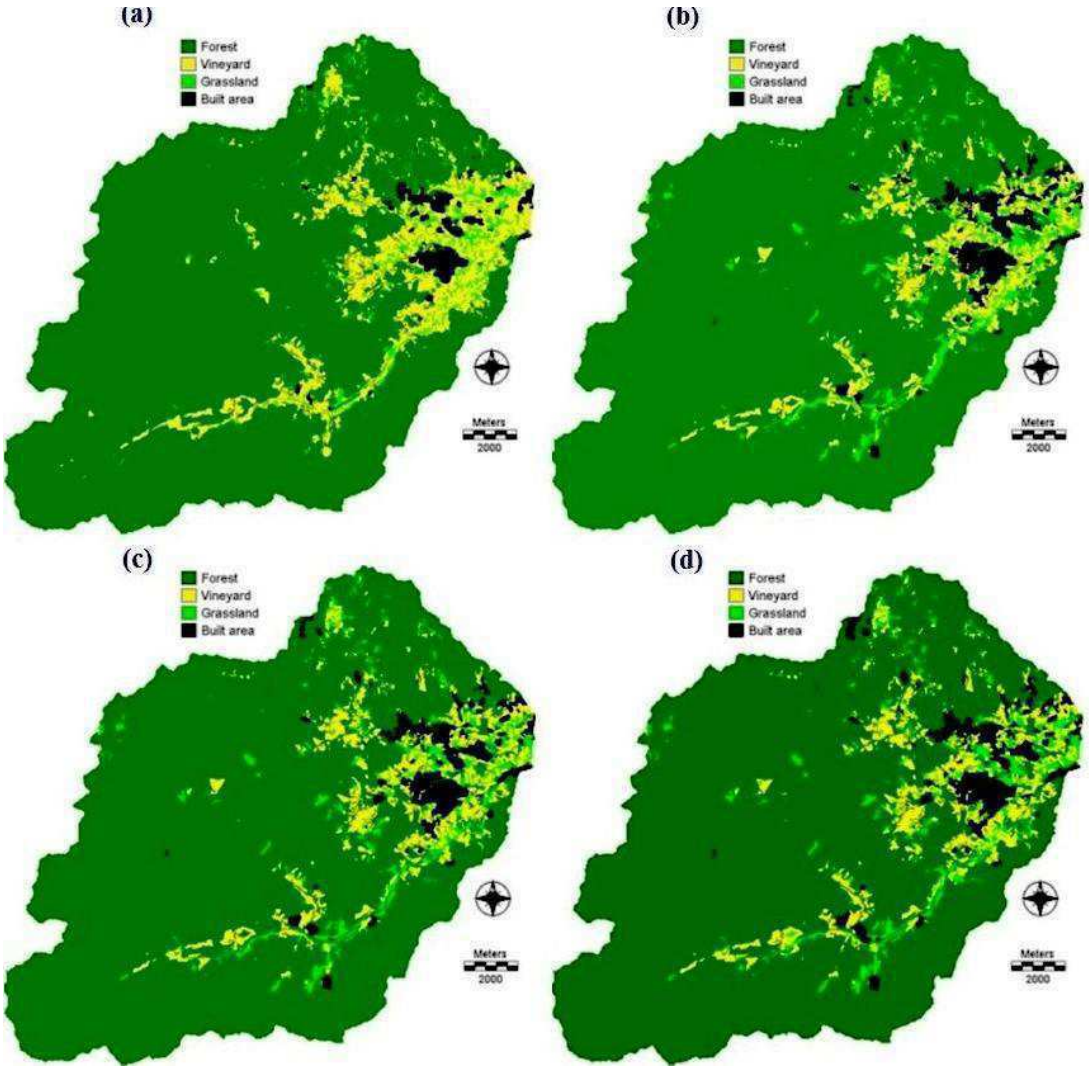

Figure 0.26: (a) Predicted land cover map of 2011 from transition potentials 1950-1982. (b) Predicted land cover map of 2011 from transition potentials 1982-2003. (c) Predicted land cover map of 2011 from transition potentials 2003-2008. (d) Land cover map 2011 (actual)

3.5.1 Kappa index analysis for predicted land cover from different time periods

The summary of the Kappa indices at different time scale simulations is presented in Table 0.16. These indices are acquired from the VALIDATION module of IDRISI (Dietzel and Clarke 2006) and can also be obtained using the Pontius matrix following (Pérez-Vega et al. 2012). Results show that all kappa components increase with decreasing time scale up to the near perfect level of agreement for the short time scale. However, simulation from long time scale also achieved a perfect level for $K_{quantity}$, and a reasonable level of agreement for $K_{location,}$ and $K_{standard}$.

Values of $K_{quantity}$ were observed in the perfect level of agreement in all three simulations, and these values were increased a little from 0.95 to 1.00 for long to short time scale simulation. $K_{location}$ gives the overall spatial accuracy of a simulation. Spatial accuracy was difficult to achieve from the long time simulation. Values of $K_{location}$ varied greatly from long to short time scale though the simulation for the long time scale also had good levels of agreement (0.75); these increased to 0.87 and 0.94 for intermediate and short time simulation, respectively. The greatest changes were also observed in $K_{standard}$ for different time scales which increased from 0.66 to 0.94 with decreasing time scale.

Table 0.16: Summary of Kappa indices

	Initial time period		
	1950-1982	1982-2003	2003-2008
$K_{quantity}$	0.95	0.99	1.00
$K_{location}$	0.75	0.90	0.94
$K_{standard}$	0.66	0.87	0.94

3.5.2 Error matrix analysis for predicted land cover from different time periods

Table 0.17 presents the error matrix analysis of actual land cover map 2011 (column) against predicted land cover (row) for different time scales. The table contains three 6 x 6 matrices for the 1950-1982, 1982-2003, and 2003-2008 time periods. In addition to overall errors, this table also shows where the errors occur. For example, 158 ha of vineyard is wrongly attributed to forest, and 438 ha of vineyard is omitted that should be forest.

Errors for all land covers decreased with decreasing time scales. The lowest commission and omission errors were observed in forest for all time scales and these decreased slightly with decreasing time scales. Errors of commission and omission were 2.6% and 3.8%, respectively for forest in the long time scale prediction, and these decreased to 0.7% and 1.6% in the intermediate and 0.5% and 0.4% in the short time scale prediction, respectively. High error of commission (45.3%) was observed in vineyard in the long time scale where the greatest amount of vineyard (1,082 ha) was wrongly attributed, and commission error decreased markedly in intermediate and short time scales. However, error of omission was relatively low in the long time scale simulation for vineyard. The highest errors of commission and omission were observed in grassland in all time scale simulations, particularly the long time scale where errors of commission and omission were 56.6% and 65%, respectively. Errors for this land cover also decreased greatly with

decreasing time scale (Table 0.17). Considerable amounts of vineyard and grassland were wrongly attributed as forest, and considerable amounts of vineyard and grassland were omitted by the model in the long time scale simulation; this occurred mainly due to high swapping of these land covers with forest. For this reason, high errors of commission and omission were generated for vineyard and grassland in the long time scale; errors decreased considerably in the intermediate and short time scale simulations. In long time simulation, errors of commission of built area were lower than for vineyard and grassland due to its smallest coverage in the catchment, and it was wrongly attributed 72 ha of other land cover. However, high error of omission was observed in the same simulation because much built area (388 ha) was omitted.

Table 0.17: Error matrix analysis of actual land cover map 2011 (Column) against predicted land cover from transition potentials for different time periods. Values are expressed in hectares (ha) and error of commission and omission are expressed in % and in bold.

Initial time period		Forest	Vineyard	Grassland	Built area	Total	Error of commission (%)
1950-1982 (long)	Forest	19,277	158	236	113	19,784	**2.6**
	Vineyard	438	1,305	488	156	2,387	**45.3**
	Grassland	295	113	403	118	930	**56.6**
	Built area	20	27	25	378	450	**16**
	Total	20,030	1,603	1,152	765	23,550	
	Error of Omission (%)	**3.8**	**18.6**	**65**	**50.6**		**9.3**
1982-2003 Iinterme-diate)	Forest	19,716	45	52	51	19,864	**0.7**
	Vineyard	68	1,413	80	30	1,590	**11.2**
	Grassland	204	119	965	37	1,326	**27.2**
	Built area	42	26	54	647	770	**15.9**
	Total	20,030	1,603	1,152	765	23,550	
	Error of Omission (%)	**1.6**	**11.9**	**16.2**	**15.4**		**3.4**
2003-2008 (short)	Forest	19,953	30	45	27	20,055	**0.5**
	Vineyard	16	1,496	94	15	1,621	**7.7**
	Grassland	44	68	997	17	1,127	**11.5**
	Built area	16	9	16	706	747	**5.4**
	Total	20,030	1,603	1,152	765	23,550	
	Error of Omission (%)	**0.4**	**6.7**	**13.4**	**7.7**		**1.69**

4. Discussion

Land cover dynamics and changes in individual land cover also have impact on land cover simulation. As it is described in the results, forest is easy to predict, and obtains better level of agreement and the lowest error in all simulations using different time scales due to its dominant coverage in the study area. It covers mostly the reserve forest situated on the high altitude and

steep slope of the study area. While most of the land cover changes in the study area occurred mainly in the alluvial plain. For these reasons, forest is selected as less probable to change in all transition potentials of forest to other land covers, and it is predicted as the same for the future (2011). So $K_{quantity}$ also shows better for all time scales.

Simulations of vineyard and grassland are extremely difficult to predict: accuracy is lower and errors greater due to the dynamic changes in different time periods and high swapping between these covers. Hence, high commission and omission errors are observed in vineyard and grassland simulations, particularly in the long time scale. These errors may occur due to different rates of change in initial and prediction time periods and the selection of transition potentials where transition potentials from vineyard to forest and grassland, and grassland to forest and vineyard were avoided due to their limited accuracy rate (<70%). Simulations of vineyard and grassland may improve using constraints for vineyard and grassland. Vineyard fields belonging to the wine making "domaines" tend to remain stable and convert to other covers less (Roy et al. 2014b), so a "domaine" layer could be used as a constraint for vineyard. This information, however, was not available in this study. In addition, fire breaks, horseback riding, and other tourism related activity zones that are classified as grassland could perhaps be taken as a constraint for grassland.

Accurate prediction of urban expansion is difficult due to the complexity in urbanization which depends on several spatial variables, urban planning, and land use demand (He et al. 2008). The rapid relative rate of urban growth impacted the urban prediction. For example, the model predicts (for 2011) about 40% less built area than the actual map of 2011 using the long time scale because the rate of built area expansion increased by more than double in the latter time period (1982-2011) compared to the initial period (1950-1982) (Figure 0.23). However, intermediate and short time periods perform better since increasing trends in the initial time periods are about the same as in the prediction time periods (2003-2011 and 2008-2011). In addition, several scattered urban areas are developed exceptionally far away from existing built area in the recent year, and these remain difficult to predict because the model is based on historical trends. Earlier trials showed the use of constraints for the transitions to built area from other land covers reduced error in built area in all simulations.

Time scales have a significant impact on land cover simulation. Quantity was predicted better than location, probably due to the dominant forest cover in the study area. Therefore, $K_{quantity}$ is

nearly perfect in all time scales. However, complex land cover changes and swapping between land covers generate less perfect levels of agreement for $K_{location}$ than $K_{quantity}$, and values increase with decreasing time scales.

Although different indexes are used, there is a general trend for Shorter time scales to Produce better prediction results (Ahmed and Ahmed 2012, Kamusoko et al. 2009, Khoi 2011, Mhangara 2011, Oñate-Valdivieso and Bosque Sendra 2010, Pérez-Vega et al. 2012, Sang et al. 2011), as found in this study was. The values of $K_{quantity}$ and $K_{location}$ are in acceptable ranges for different time scales in this study. Maximum commission and omission errors observed in crops and grassland (Oñate-Valdivieso and Bosque Sendra 2010) were also noted in this study since complex changes in grassland and vineyard are difficult to simulate.

5. Conclusions

Studies of the temporal and spatial distribution of land cover change have become an important issue due to the rapid conversion of land cover and its impact on environment change. Time scale has a significant impact on prediction. Near perfect quantitative accuracy is achieved in all time scales but spatial accuracy varies with different time scales. High quantitative and location accuracy are found in forest prediction due to its large surface area, in which changes are relatively small and swapping does not impact the prediction. Prediction of vineyard and grassland are difficult due to high swapping with one another and forest, and prediction of built area is difficult due to dramatic relative growth that increases in the recent time periods and the emergence of urban lots far from historic centers. Cell size and catchment area may also impact land cover change simulation and this is under study now.

CHAPTER 4

PREDICTING LAND COVER CHANGE: DORMANT CATEGORY AND CELL SIZE EFFECTS ON THE PERCEPTION OF CHANGE DYNAMICS AND MODEL PERFORMANCE

(Article manuscript accepted with modifications in Cybergeo, 25 April, 2016; currently being corrected)

1. Introduction

Land cover change is rapidly changing the environment and spatial organization of societies. Globally land cover change is driven by population growth rates, migration, and in many countries by rural to urban transitions; other factors include rising competition for land, conservation policies, and a myriad of socio-economic and political dynamics (Müller and Munroe, 2014; Munroe and Müller, 2007). The Mediterranean area is subject to significant land cover change due to rapid urban growth, tourism, and diverse socio-economic factors (Cori 1999, Geri et al. 2011, Parcerisas et al. 2012, Serra et al. 2008, Van Eetvelde and Antrop 2004). Coastal development and abandonment of marginal lands are frequently cited in the literature as dominant trends (Calvo-Iglesias et al. 2009, Sluiter and de Jong 2007), but other land cover transitions (intensification of agriculture, suburban sprawl) are common (Falcucci et al. 2007, Geri et al. 2011).

In order for land use managers and policy makers to develop future sustainable land use management plans, complex transition processes must be identified (Alo and Pontius Jr 2008). Several modelling techniques have been developed to explore and predict land cover change (Barredo et al. 2003, He et al. 2008), and topographic and socio-economic factors are considered important drivers in understanding and predicting land cover evolution (Munroe and Müller 2007). However, land cover change prediction accuracy depends not only on the relevance of explanatory variables but also on several other variables: type and number of land cover categories, historical and future time intervals (Roy et al. 2014a), and spatial extent and resolution (Chen and Pontius 2011).

Spatial extent refers to the overall size of a particular area (Turner et al. 1989, Wu 2004). A review by the authors of about 27 recent studies (2001-2014) using Ca-Markov and MLPNN

modeling tools reveals that spatial extent ranged from 114.4 km² to 20,000 km² (mean and median values of 3,056.3 km² and 1,200 km², respectively) (Table 0.1). If land cover change is distributed homogeneously throughout space, then spatial extent probably has little impact on model prediction outcome. However, this is frequently, perhaps even generally, not the case, and increasing spatial extent often translates into increasing the surface are of one or two large relatively stable categories, such as forest cover for example, around a core (or cores) of actively evolving land covers. Increasing spatial extent can introduce new land cover change dynamics (Kok and Veldkamp 2001) or land cover categories (Turner et al. 1989), but in this paper, larger spatial extent will be considered synonymous with increasing the proportional area occupied by a relatively dormant category.

Dietzel and Clarke (2004) proposed guidelines for urban simulation models on spatial resolution (10 m-1,000 m) in four spatial extents, and found that finer resolutions of less than parcel size (< 10 m) in land cover simulation may increase error by creating small and false changes. This lower limit is well below the most frequently used 30 m resolution. At the upper limit, Chen & Pontius (2011) showed that predicted built area accuracy increased with increasing spatial resolution from 30 m to 1,920 m. Moreover, the explanatory power of driving variables can also increase with coarsening spatial resolutions (minimum resolution was 15 km²) (Kok & Veldkamp, 2001). Geri et al. (2011) found that all kappa indices increased to a perfect level of agreement with increasing cell size. Spatial extent and cell size may affect the analysis of spatial patterns of land cover change individually or together (Wu 2004). These studies suggest that modelling land cover change be improved using coarser cell sizes while reducing calculation time.

The selection of suitable time intervals, spatial extents, cell sizes is as important for land cover modeling as the modeling strategy and independent variables. Time scale effects for our study area were discussed in Roy et al. (2014b). In this paper, the role of spatial extent (dormant category) and cell size are highlighted using the same explanatory variables and modeling approach. In the same analysis of 27 recent studies (2001-2014) referred to above, cell size varied from 30 m to 1,000 m (mean and median resolutions are 94.8 m and 30 m, respectively. Spatial extent and cell size are interrelated and can have a great impact not only on land cover prediction but also on perceived quality of the prediction since calculated agreement/disagreement statistics depend on the number of cells present in the study area grid, and this depends directly on cell size

and spatial extent. The objective of this study is to test the impact of spatial extent (increased proportional area of a dormant category) and cell size on the perception of land cover change dynamics and land cover prediction for a Mediterranean catchment in SE France. Based on air photos from 1950, 1982, 2003, and 2011, change dynamics in terms of absolute and relative change were first analyzed using intensity analysis, and then land cover was predicted for 2011 for large (79.1 km²) and small (36.6 km²) windows using cell sizes of 25 m, 50 m, 100 m. Spatial resolution effects were also analyzed by upscaling from 25 m to 50 m and 100 m and then downscaling back to 25 m.

It should be noted that although the location and category types used here represent a real case study, the findings with regards to spatial extent and cell size are independent of location and land cover type: replacing the dormant Mediterranean forest category by rice paddies, savannah or tropical forest (and changing the other land cover types as well) would produce the same statistics so long as the number and relative areas of land covers are maintained. Similarly, a range of spatial areas can be concerned by the findings so long as neither new processes nor new land categories are introduced as spatial extent is increased. The approach therefore has global applications even though the demonstration is linked to a specific environment.

Table 0.1: Spatial scales, land cover types, and variables of different studies

Authors	**Model**	**Categories**	**Spatial Unit** **Cell Size** **Surface area**	**Variables**
Ahmed and Ahmed 2012	Ca-Markov MLPNN-Markov (LCM)	• Vegetation • Bare soil • Low land • Fellow land • Water bodies	∗ Administrative ∗ 30 m x 30 m ∗ 446 km^2	Undefined
Álvarez Martínez et al. 2011	Binary logistic regression (BLR)	• Forest • Meadow • Shrub land and heartlands • Rock outcrops • Bare land • Urban • Water	∗ Administrative ∗ 30 m x 30 m ∗ 1,000 km^2	(i) Administrative data: municipality area and number of villages including Natural Park. (ii) Climate: annual minimum, maximum and mean temperature, precipitation and solar radiation derived from monthly data. (iii) Terrain: altitude, slope and curvature. (iv) Socio-economic factor: agricultural and livestock activities,

Authors	Model	Categories	Spatial Unit Cell Size Surface area	Variables
				economy, employment, population growth and urban expansion, tourism and transport.
Araya and Cabral 2010	CA-Markov	• Forest • Urban vegetation • Irrigated land • Non irrigated • Bare land • Urban area • Water bodies	∗ Administrative ∗ 50 m x 50 m ∗ 2,957 km^2	(iii) Terrain: Slope, distance from roads, water bodies, built area, protected area.
Berberoglu and Akin 2009	Undefined	• Sand dune vegetation • Wetland vegetation • Bulrush • Woodland • Afforestation • Sand dunes • Salty plain • Agricultural land • Settlement • Bare soil • Water	∗ Catchment ∗ Undefined ∗ 1,500 km^2	Undefined
Bohnet and Pert 2010	Undefined	• Natural land use • Agriculture • Urban	∗ Administrative ∗ Undefined ∗ 114.4 km^2	
Bracchetti et al. 2012	Markov Chain	• Chestnut plantation • Tree plantation • Cropland • Grassland • Shrub land • Woodland • Bare soil • Human settlement	∗ Catchment ∗ 30 m x 30 m ∗ 168 km^2	Undefined
Dadhich and Hanaoka 2010	MLP and Markov Chain	• Forest • Agricultural land • Bare land • Urban	∗ Administrative ∗ 50 m x 50 m ∗ 1,080 km^2	(i) Administrative data: Road networks. (ii) Terrain: DEM (altitude), slope, hill shade, distance from road, city center, city periphery of 1989.
Dewan and	ERDAS spatial	• Vegetation • Agricultural	∗ Administrative ∗ 30 m x 30 m	(i) Administrative data: municipal

Authors	Model	Categories	Spatial Unit Cell Size Surface area	Variables
Yamaguchi 2009	modeler	land • Urban • Water bodies • Bare land • Wetland / low land	∗ 415.64 km^2	boundaries, road networks, geomorphic units (ii) Terrain: DEM (altitude), slope. (iii) Socio-economic factor: population growth and GDP.
Guan et al. 2011	CA-Markov	• Forest • Agricultural land • Built up land • Roads • Water • Others	∗ Administrative ∗ Undefined ∗ 431.42 km^2	(ii) Terrain: Elevation, lope, distance from nearest river, distance from nearest road, distance from railway. (iii) Socio-economic factor: population density, GDP per capita, and land price.
He et al. 2006	CA-Urban Expansion Scenario (UES)	• Forest • Agricultural land • Shrub land • High density urban land • Low density urban land • Water	∗ Administrative ∗ 30 m x 30 m ∗ 16,808 km^2	(ii) Terrain: Slope, distance from expressway, distance from ring road, distance from railway, distance from highway, distance from airport, distance from central city, distance from sub-cities.
Huang and Cai 2007	CA	• Forest • Farmland • Grassland • Urban area • Bare soil • Water	∗ Administrative ∗ 90 m x 90 m ∗ 1,835 km^2	(i) Terrain: DEM, elevation, slope, distance from stream, distance from road.
Jenerette and Wu 2001	Markov-CA	• Agricultural land • Urban • Undeveloped desert	∗ Catchment ∗ 250 m x 250 m ∗ 6080 km^2	(i) Terrain: DEM (altitude), slope (ii) Socio-economic factors: population growth (iii) An environmental constraint.
Kamusoko et al. 2009	Markov-CA (IDRISI)	• Agriculture • Woodland • Mixed rangeland • Bare land • Water	∗ Administrative ∗ 30 m x 30 m ∗ 525 km^2	(i) Administrative data: ward boundaries. (ii) Terrain: DEM, distance to town Centre, and distance to Rivers. (iii) Socio-economic factors: population density, distance travelled to fetch fuel wood, fuel wood consumption, area under the maize of cultivation, area under the cultivation of groundnuts, total yield of maize produced.

Authors	Model	Categories	Spatial Unit Cell Size Surface area	Variables
Khoi 2011	MLP-LCM	• Primary forest • Secondary forest • Non forest	∗ Administrative ∗ 30 m x 30 m ∗ 1,200 km^2	(ii) Terrain: DEM, slope, proximity to road, water, primary forest, secondary forest, settlement in 2000, settlement in 2007, cropland in 2000, cropland 2007.
Li and Yeh 2002	ANN-CA	• Forest • Cropland • Orchards • Urban area • Construction sites • Water	∗ Administrative ∗ 50 m x 50 m ∗ 2,465 km^2	(i) Administrative data: Administrative boundary, urban centers, roads. (ii) Terrain: Slope, soil types, existing land use types, distance from major urban area, suburban area, and road. Neighborhood function: Amount of cropland, orchards, construction sites, built up areas, forest, and water.
Liu et al. 2008	The kernel-based CA model	• Developed • Non-developed	∗ Administrative ∗ 50 m x 50 m ∗ 445.5 km^2	(i) Terrain: Distance from cite proper, distance from city center, distance from national and provincial highways, distance from roads, distance from railways, distance from expressways, and number of cells in the neighborhood. (ii) Constraints: Altitude, land use, agriculture suitability.
López et al. 2001	Markov matrices and Regression analyses	• Forest • Cropland • Shrubs • Plantation • Shrubs-grassland • Main urban area • Other urban settlement	∗ Administrative ∗ 30 m x 30 m ∗ 200 km^2	(i) Terrain: Altitude, slope (ii) Socio-economic factors: population density.
Shafizadeh Moghadam and Helbich 2013	CA-Markov (IDRISI)	• Forest and green spaces • Open land and cropland • Urban area • Wetlands • Water bodies	∗ Administrative ∗ 30 m x 30 m ∗ 465 km^2	(i) Terrain: Slope (Sigmoid), distance from roads (J-shaped), distance from water bodies (Linear), distance from build-up areas (Linear), land use categories.
Pérez-Vega et al. 2012	DINAMICA 14.0) and LCM IDRISI (version	• Cropland • Tropical deciduous forest (TDF)	∗ Catchment ∗ Undefined ∗ 5,543 km^2	(i) Terrain: Altitude, slope, soils types, and distance from principal dirt roads, distance from secondary dirt road, distance from paved road,

Authors	Model	Categories	Spatial Unit Cell Size Surface area	Variables
	16.05)	• Secondary TDF • Pasture land		distance from human settlements. (ii) Socio-economic factors: Land tenure
Sang et al. 2011	CA-Markov (IDRISI)	• Arable land • Woodland • Urban • Garden • Grassland • Unused land • Water	∗ Administrative ∗ 100 m x 100 m ∗ 1,990 km^2	Undefined
Silva and Tagliani 2012	IDRISI Taiga (LCM)	• Forest • Agriculture • Urban • Wetland • Water • Dunes and beaches • Silviculture	∗ Administrative ∗ Undefined ∗ 20,000 km^2	(i) Terrain: Geomorphology, topography. (ii) Socio-economic factors: (including population, social account-ability, standard of living index, and income and occupation level in Agriculture) and governmental development plan. (iii) Constraints: Silviculture zoning.
Tewolde and Cabral 2011	LCM-MLPNN	• Irrigation • Grazing land • Urban • Plantation • Rain fed • Water	∗ Administrative ∗ 30 m x 30 m ∗ 212 km^2	Undefined
Oñate-Valdivieso and Bosque Sendra 2010	IDRISI Taiga (LCM), Logistic Regration and MLP	• Dry forest • Shrub vegetation • Agriculture/ crops • Grassland	∗ Catchment ∗ 100 m x 100 m ∗ 17,199 km^2	(i) Terrain: Elevation (DEM), slope, soil types, distance to watercourse, distance to the initial location of the coverage and the type of land, distance from cities. (ii) Climate: Total annual precipitation.
Verburg et al. 2002	CLUE-S	• Forest • Grassland • Coconut plantation • Rice field • Others	∗ Administrative ∗ 1 km x 1 km ∗ 456 km^2	(i) Terrain: Altitude, slope, aspect, distance from road, distance from coast, distance from port, distance from streams, erosion vulnerability, geology. Socio-economic factors: Population density.
Vliet et al.	Constrained (CA)	• Forest	∗ Administrative	(i) Terrain: Slope, distance from

Authors	Model	Categories	Spatial Unit Cell Size Surface area	Variables
2009		• Agriculture • Undeveloped area • Residential area • Commercial and industrial area • Extractive industries • Transport and Utilities • Water	∗ 100 m x 100 m ∗ 2,820 km^2	transport network. Constraint: Restricted areas for development.
Wang and Li 2011	Radial Basis Function Neural (RBFN)	• Forest • Orchard • Agriculture • Bare land • Urban area • Water • Beach	∗ Administrative ∗ 100 m x 100 m ∗ 1,952 km^2	(i) Terrain: Slope, elevation, distance from highways, distance from roads, distance from railways, distance from urban center, distance from country centers.
Wang et al. 2011	CA	• Forest • Vegetation • The Tsuu T'ina land • Urban • Water	∗ Catchment ∗ 60 m x 60 m ∗ 600 km^2	(i) Terrain: Distance to river, distance to Calgary City center, and distance to road.
Wang et al. 2012	IDRISI, Markov-CA	• Agriculture • Woodland • Meadow • Urban • Water • Others	∗ Administrative ∗ 30 m x 30 m ∗ 1,352 km^2	(i) Terrain: Slope, soil class, distance from settlements, roads and water.
Wu et al. 2006	Markov-Regression	• Forest • Agriculture • Bare land • Rural residence • Urban • Water	∗ Administrative ∗ 30 m x 30 m ∗ 668 km^2	(i) Terrain: DEM, distance from urban center. (ii) Socio-economic factors: agriculture and non-agriculture population, per capita income.
Yang et al. 2012	Ant Colony Optimization (ACO)-CA-Markov	• Forest • Agriculture • Urban • Water • Other used land	∗ Administrative ∗ 30 m x 30 m ∗ 1,352 km^2	(i) Terrain: Distance from the major urban area, closest town area, closest road, and railway.
Yeh and Li 2003	(Artificial Neural Network) ANN	• Urban and • Non-urban	∗ Administrative ∗ 50 m x 50 m ∗ 2,465 km^2	(i) Terrain: Distance from the major urban areas, suburban areas, closest road, closest expressway, closest

Authors	Model	Categories	Spatial Unit Cell Size Surface area	Variables
	and CA			railway. (ii) Socio-economic factors: Neighborhood development quantity, and agriculture suitability.

2. Methods

Study area, intensity analysis of land cover change procedures, and land cover modelling steps using different spatial areas and cell sizes are explained below.

2.1 Site description

The Giscle catchment (about 235 km²) is located in SE France near the Gulf of St Tropez and includes three cities (Cogolin, Grimaud, and La Môle) (Figure 0.1). Geophysical and topographical characteristics of the catchment are discussed in Roy et al. (2014a). The catchment is typical of many land cover transformation scenarios of the Euro-Mediterranean region where rapid urbanization along the coast and changes in agricultural activities impact the natural ecosystem. The western part of the catchment is forested and has changed little since about 1950 (Fox et al. 2012, Roy et al. 2014a, Roy et al. 2014b), and much of the land cover change has been concentrated in the alluvial plain towards the east near the coast.

The small zone selected for this study is a 33.6 km² square that encompasses the main populated area in the alluvial plain and the core of much of the land cover change in the catchment (Figure 0.1). The large window is a rectangle that includes the small zone and an extension reaching westward to include a large tract of stable forest cover; total area of the large zone is 79.1 km². Mean altitudes for the small and large windows are 42 m and 167 m, respectively; corresponding median values are 32.5 m and 119.5 m, respectively. As expected, mean slope is also gentler for the small window, 10.6% vs. 24.7%; median values are 7.2% and 21.5%, respectively.

The two zones are analogous to a core of dynamic land cover change surrounded by a stable hinterland that allows us to analyse the impacts of spatial extent and the inclusion of a largely

dormant category on our perception of land cover change dynamics. The fundamental characteristic of interest in the context of this study is that most of the change is occurring in the small window, with very little change in the extended zone.

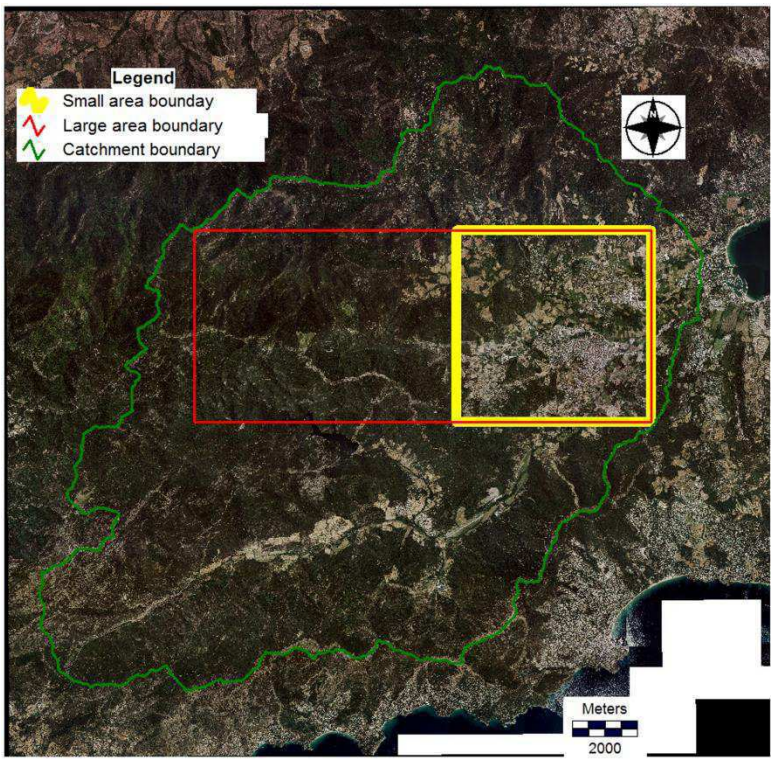

Figure 0.1: Location of the catchment

2.2 Intensity of land cover change

Intensity analysis is an effective method to analyze spatiotemporal dynamics among land cover categories; this method was developed and applied at different levels of land cover change and represents a new mathematical framework in land cover change analysis (Aldwaik and Pontius Jr 2012) which is being increasingly integrated in land cover change studies (Huang et al. 2012 Mallinis et al. 2014). It simplifies the analysis of multiple land cover category changes over consecutive time intervals and facilitates the comparison of land cover gain and losses in order to determine the magnitude and speed of land cover change at different levels (Aldwaik and Pontius Jr 2012). In our case, dynamics that concern spatial extent or cell size effects will be highlighted.

In order to determine the relative rates of land cover change with regards to their surface area, Aldwaik and Pontius (2012) describe the intensity of land cover change at three levels: interval,

categorical, and transition. Change intensity is expressed as the land cover area changed (overall, category gain/loss, transition) divided by the number of years in the historic time interval and area. As will be described below, the area in the denominator varies according to the level under consideration. Units of intensity analysis are expressed as mean annual percentage units since land area converted is divided by the time interval, though this overall mean cannot be interpreted as a specific % rate in a given year. In our case, intensity analysis will be used to investigate the impact of spatial extent and cell size on the perception of land cover change dynamics.

2.2.1 Interval intensity analysis

Interval level intensity analysis considers area converted and rate of change during different time intervals by calculating annual change intensities for each time interval (S_t) and the mean change intensity rate (U) of all intervals combined. Therefore, S_t is the mean annual rate of change in a particular time interval per unit area of a landscape, and U is the average annual rate of all time intervals, so relatively fast or slow periods of change can be easily identified. If $S_t > U$, then the rate of change in this interval is relatively fast; if $S_t < U$, then it is relatively slow. If annual and uniform intensities are the same for all time intervals then the rate of change is constant over time (or stationary) as described by Aldwaik and Pontius Jr (2012).

2.2.2 Category intensity analysis

Category level change can identify relatively dormant or active categories since both time interval and category area are taken into account (Aldwaik and Pontius Jr 2012). It is assumed that categories with large areas change more in terms of absolute area than categories with less area. For this level of analysis, annual gross gains and losses per category are used. The mean annual gross gain intensity of a category is the percentage of gain of the category at the end of the time interval, (T_1 area–T_2 area)/T_2 area. The mean annual loss intensity of a category is the percentage of loss from the beginning of the time interval, (T_1 area–T_2 area)/T_1 area. Category gains and losses can be compared to one another and to the uniform intensity of overall change during each time interval (Aldwaik and Pontius Jr 2012).

2.2.3 Transition intensity analysis

Transition level analysis identifies the intensity of transitions in a particular time interval and shows the relationship between two transitioning categories relative to the total landscape (Huang et al. 2012). Transition matrices were computed for three consecutive time intervals: 1950-1982, 1982-2003, and 2003-2011. Transition level analysis helps to identify the intensity of specific transitions between categories during a time interval. It calculates mean annual intensity of transition from a category (*i)* to a gain category *(n)* during time interval T_1-T_2 (mean annual transition area from *i* to *n* during T_1-T_2/area of *i* at T_1) and the uniform intensity of annual transition from all non-*n* categories during time interval T_1 and T_2 (mean annual gross gain of category *n* during T_1-T_2/area of non *n*-category at T_1). The transition intensity of a loss category *m* to *j* depends on the area of *j* at time T_2 (mean annual transition area from m to j during T_1-T_2/area of *j* at T_2) and uniform transition intensity of a loss category (mean gross loss of category *m* during T_1-T_2/area of non-category *n* at T_2).

The transition intensity level of analysis produces two sets of outputs for each land cover at each time interval: one set analyzes transitions for gains (*n*) and another analyzes transitions for losses (*m*). Since the overall focus of the larger research program and for the sake of brevity, only transitions to and from vineyard will be considered here. As described by Roy et al. (2014a), vineyard is a category that has been particularly active in the study area over the past 60 years.

2.3 Land cover change modelling steps

IDRISI's (Eastman, 2012) Land Change Modeler (LCM) was used to predict land cover for 2011. LCM is a widely tested and used model initially designed to predict land cover change for the analysis and modelling of impacts on biodiversity using multiple land cover categories (Mas et al. 2012, Oñate-Valdivieso and Bosque Sendra 2010, Silva and Tagliani 2012, Tewolde and Cabral 2011). The impact of spatial extent and cell size on land cover prediction was carried out by predicting 2011 land cover from historic changes between 1982 (T_1) and 2003 (T_2) and explanatory driver variables (described below) and comparing the predicted and real images for all spatial extent and cell size combinations. In addition, the 2003 and 2011 maps were compared as recommended by Chen and Pontius (2011), though a full relative operating characteristic (ROC) analysis was not undertaken.

2.3.1 Land cover mapping

Land cover map digitization and classification were described in Roy et al. (2014a) for the entire catchment and are summarized here for the selected study zones. Firstly, land cover maps were digitized from ortho-rectified 1 m aerial photographs of 1950, 1982, 2003 and 2011 using Arc-GIS (ESRI 2012). Land cover was classified into four categories: forest, vineyard, grassland, and built area. Although air photo and digitizing resolution was 1 m, small objects (isolated houses, roads, streams, riperian vegetation…) were ignored, so the actual land cover map resolution is more correctly represented at the 25 m scale, and vector land cover maps were converted into 25 m raster layers. In order to investigate the impact of cell size on land cover change modeling, cell sizes were successively converted to 25 m, and 50 m, and 100 m. Altitude and distance variables were upscaled using pixel aggregation; categorical images such as land cover maps and constraints/incentives were upscaled using the majority-takes-all rule. Subsequently, the 50 m and 100 m cell sizes were downscaled to the original 25 m in order estimate error introduced during upscaling. To investigate the impact of spatial extent, the small window described above and shown in Figure 0.1 was isolated from the larger window, so all predictions were run separately (2 spatial extents (Small, Large) * 5 cell size configurations (25 m, 50 m, 100 m, 50-25 m, 100-25 m)).

2.3.2 Independent variables and constraints

After an initial analysis of land cover change drivers (Roy et al. 2014a), five independent variables were incorporated in the modelling procedure: altitude, slope, and distances from roads, initial built area, and streams. Distance variables (from roads, built area (1982), and streams) were created from digitized roads, streams, and built area in 1982 using corresponding land cover maps in each cell resolution. Constraints and incentives (forest to built area, vineyard to built area, and grassland to built area) were also included in the prediction process to integrate regional and municipal land use zoning laws. The “Plan Local d’Urbanisme” (PLU) and “Schéma de Cohérence Territoriale” (SCOT) were adapted so that a constraint of 0 was used to characterize areas where urban development was completely restricted (reserve forest and agricultural zones) and 1.1 was used for incentives to emphasize the expansion of built areas in zones selected for development according to urban zoning laws. In addition, disincentive (constraint) areas situated within a distance from streams of 0-25 m, and 25-50 m (in original 25 m images before upscaling) were defined by values of 0.6 and 0.8, respectively, to maintain the historical trend of

less urbanization near stream networks in the study area identified in Roy et al. (2014a). Explanatory variable cell sizes were matched to the land cover maps in both upscaling and downscaling. The only exception was the slope layer: to avoid introducing excessively artificial errors, the original 25 m slope layer was used for the two 50 m and 100 m downscaled layers. Other explanatory variables were both upscaled and downscaled, as for the land cover layers.

2.3.3 Explanatory variable and transition potential statistics

Cramer's V was used to evaluate the impact of spatial extent and cell size on the significance of explanatory variables. LCM estimates Cramer's V automatically and displays the association level of explanatory variables with land cover categories. Cramer's V here is an approximation of the impact of the explanatory variable on category change (Eastman 2012) and the Multi-Layer Perceptron Neural Network (MLPNN) algorithm of LCM provides a more complete and rigorous measure of association. However, values from this measure vary according to specific transitions and to which explanatory variables are held constant (all, one, backward regression), so the results are too extensive for this publication where 2 spatial extents, 5 cell size configurations, and 9 transitions per spatial extent * cell size combination are possible (built area cannot transition to another category); a full analysis would therefore require 90 tables. For the purposes of this study, Cramer's V provides an indication of the apparent change in explanatory power induced by altering spatial extent and cell size. Generally, the greater the value of Cramer's V, the greater its impact on land cover change. Cramer's V values ≥ 0.4 and ≥ 0.15 are considered good and useful, respectively (Eastman 2012).

Transition potential (probability of a category changing to another) maps were created for all possible transitions based on historical changes during 1982-2003 and explanatory variables using the MLPNN algorithm of IDRISI (Eastman 2012). However, only transition potentials with an accuracy rate greater than 70% were included in land cover prediction since final results were better than including all potential transitions. As described in Roy et al. (2014a), high spatially random exchanges between vegetation categories (especially vineyard and grassland) made these land cover changes difficult to model. Accuracy rates greater than 70% were the following: forest to vineyard, forest to grassland, forest to built area, vineyard to built area and grassland to built area. Validation values were weaker when all transitions were included, but the trends with regards to spatial extent and cell size were identical.

2.3.4 Land cover simulation

Land cover change was predicted for 2011 for each spatial extent * cell size combination by LCM which uses a Markov chain model. The Markov matrix defines the quantity of expected land cover transition from T_2 (2003) to the predicted date (2011) based on the historical trend between T_1 (1982) and T_2 (2003), and LCM allocates the change according to transition potential values calculated by the MLPNN algorithm described above. There are therefore two validation criteria when comparing predicted versus real maps: quantity and location of change (Pontius & Mallones, 2011).

2.3.5 Validation of predicted land cover maps

Disagreement indices described by Pontius and Millones (2011) were used in the study to validate the model's accuracy for the different configurations and test the impacts of spatial extent and cell size on model performance. Both quantity and allocation disagreement errors are derived from the error matrix and measured in terms of the percent of the landscape; the sum of these errors represents the total prediction error (Chen and Pontius 2011). Both quantity and allocation disagreement errors are expressed as % of landscape (Pontius and Millones 2011).

3. Results

Results will be presented in four sub-sections. The first will summarize land cover characteristics in the two study zones. The second will cover intensity analysis at the interval, category and transitions to and from vineyard levels. The third will consider the impacts of spatial extent (dormant category) on Cramer's V and prediction disagreement. The fourth section will cover the impacts of cell size on the same measures.

3.1 Land cover maps and category areas in the small and large zones

Table 0.2 compares surface areas for the different land cover categories between the small and large zones. In the small zone, forest and vineyard occupy equivalent areas in 1950 (about 43%), though this balance changes substantially over time as vineyard loses ground to other land cover types. In the small zone, built area undergoes a relatively large increase as it changes from only 0.8% in 1950 to 16.5% in 2011. Grassland area remains relatively constant over time, but

this hides high spatial swapping with forest and vineyard as described in Roy et al. (2014a). As expected, forest dominates land cover in the large zone, where it remains stable at about 74%. Since most of the other land cover types are concentrated in the small zone, absolute areas of these land covers in the large window closely follow values for the small zone in Table 4.3; however, percentage values change substantially since total area is greater in the large window. For all categories, values expressed in % area are all smaller in the large zone than for the small window due to the high forest cover in the large window.

Table 0.2: Surface area of land cover types for different years. Values are expressed in ha (% of catchment area is noted in parentheses).

	Category	**1950**	**1982**	**2003**	**2011**
Small	Forest	1,466 (43.6)	1,520 (45.2)	1,507 (44.8)	1,492 (44.4)
	Vineyard	1,455 (43.3)	1,170 (34.8)	824 (24.5)	835 (24.8)
	Grassland	415 (12.3)	482 (14.3)	570 (16.9)	482 (14.3)
	Built area	28 (0.8)	192 (5.7)	463 (13.8)	555 (16.5)
Large	Forest	5,884 (74.4)	5,911 (74.8)	5,885 (74.4)	5,861 (74.1)
	Vineyard	1,544 (19.5)	1,287 (16.3)	912 (11.5)	924 (11.7)
	Grassland	449 (5.7)	515 (6.5)	642 (8.1)	560 (7.1)
	Built area	29 (0.4)	193 (2.4)	467 (5.9)	561 (7.1)

Figure 1.1a-d and Table 0.2 confirm that most of the changes occur in the small window, and the western spatial extension added to form the large window remains dominated by forest cover with little change in vineyard and grassland and virtually no change in built area (values in Table 2 are the sums of gains and losses within each category). Apart from forest in 1950-1982 and 1982-2003, the % of total change occurring in the small window is close to 90% for all categories and time intervals, and values are close to 100% for built area for all periods. Forest has the lowest % change occurring in the small zone (about 78% for the first two transition periods), but even it approaches 90% in 2003-2011. With time, land cover changes in the vegetation categories appear to concentrate even more in the alluvial plain (small zone).

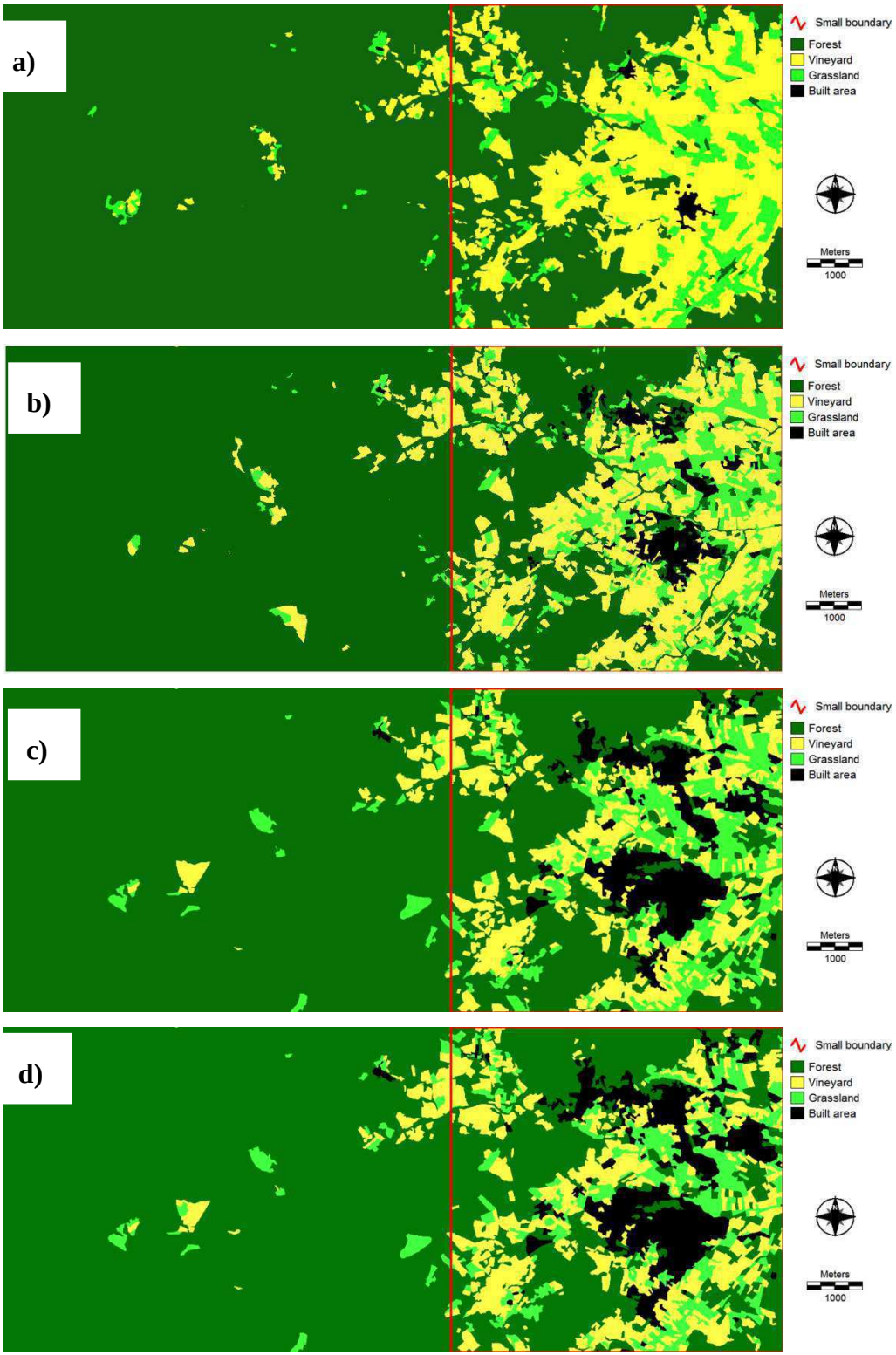

Figure 0.2: Land cover map of 1950 (a), 1982(b), 2003 (c), and 2011(d)

Table 0.3: Category land cover and total change during the different time intervals, and % of change occurring in the small window (equal to 100% everywhere for the top rows).

		Change (ha)			% of change in small window		
	Category	**1950-1982**	**1982-2003**	**2003-2011**	**1950-1982**	**1982-2003**	**2003-2011**
Small	Forest	387	398	137			
	Vineyard	703	550	168			
	Grassland	504	577	231			
	Built area	164	271	93			
	TOTAL	1,758	1,796	630			
Large	Forest	491	514	153	78.8	77.4	89.5
	Vineyard	781	631	180	90.0	87.2	93.3
	Grassland	549	653	246	91.8	88.4	93.9
	Built area	164	274	94	100	98.9	98.9
	TOTAL	1,985	2,071	673	88.6	86.7	93.6

3.2 Land cover change intensity

In this section, all "a" figures show gross change in ha; since the sum of losses of all categories corresponds to the sum of gains in all categories (the loss in a category translates into an equivalent gain for one or several other categories), the observed change is the total change shown in Table 0.2 divided by 2. All "b" figures show change values in % units: in these figures, time interval and spatial area are accounted for as described in the Methods.

3.2.1 Interval intensity analysis

Figures 0.3a-b show total observed change and mean annual change (expressed as percentage of large and small areas, respectively). In addition to site specific historical change dynamics, two factors affect the presentation of results in these figures: time interval and surface area. Time interval was dealt with explicitly in Roy et al. (2014b), so it will only be touched upon briefly here. For similar change dynamics, longer time intervals show more absolute change. In Figures 0.3a, the relatively small observed change for 2003-2011 results primarily from the short time interval (8 years) compared to the other periods (32 and 21 years, respectively), so time interval tends to dominate bar height in Figure 4.3a. However, the greatest absolute change was for the second period (1982-2003) even though it is 11 years shorter than the initial 1950-1982 interval, and this is due to more active change dynamics as discussed in Roy et al. (2014a, 2014b). Figure 3b demonstrates this clearly since it corrects for different time intervals and shows relative rates

of change within each spatial zone. Within each spatial unit, the most active period was 1982-2003, followed by 2003-2011 and then 1950-1982. Displaying results in ha y^{-1} would have compensated for temporal but not spatial differences as is described below.

Absolute change (Figures 0.3a) can only be greater in the large zone, since all changes in the smaller zone are included in the large window. Since most of the change is concentrated in the alluvial plain, trends are inversed in intensity analysis (Figures 0.3b) where rates of change are always greater in the small zone. In the small zone, relative changes are about 2 times greater than in the larger window. Trends with regards to a uniform change are similar within each scale and both scales show a less than average change rate in the initial 1950-1982 period (bar heights are beneath dotted lines for both zones).

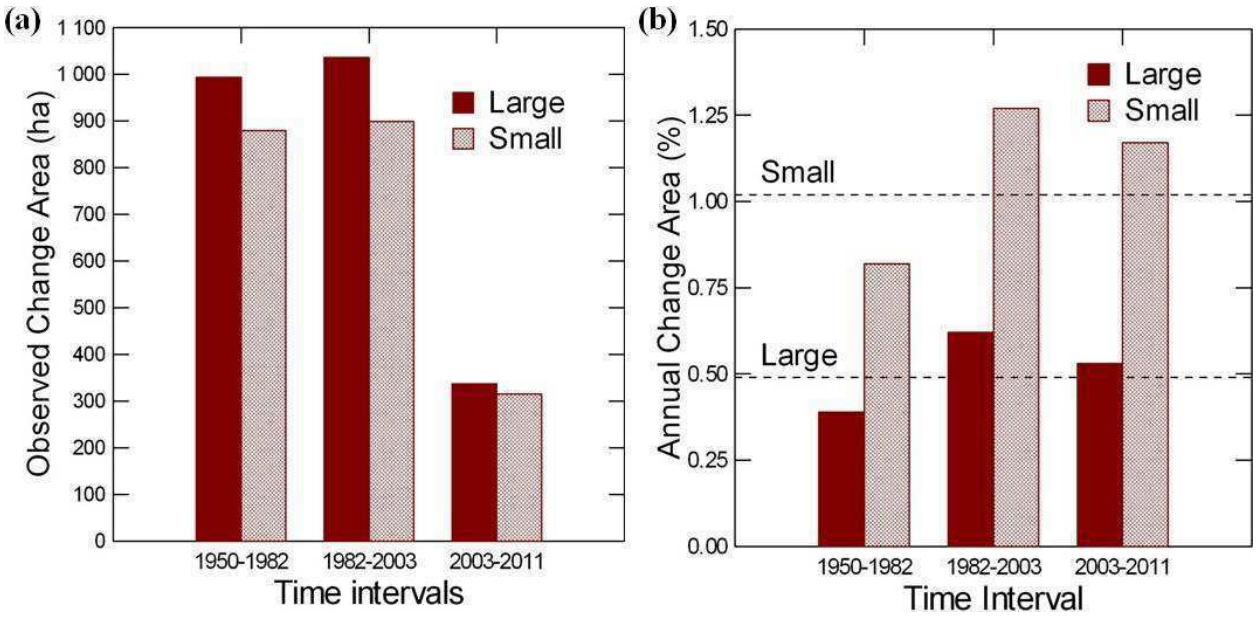

Figures 0.3: (a) Observed change in different time intervals, (b) intensity of different time intervals

3.2.2 Category intensity analysis

Figures 0.4-6 show gross gains and losses (a) and gain/loss intensities (b) per category for the 3 time intervals. As can be deduced from the figures, gains and losses at the categorical level are affected by the same 3 components for interval analysis: gain/loss activity, time interval, and category area. Specific category activity dynamics and time interval effects were examined in

Roy et al. (2014a; 2014b), though intensity analysis was not used in either of these initial publications.

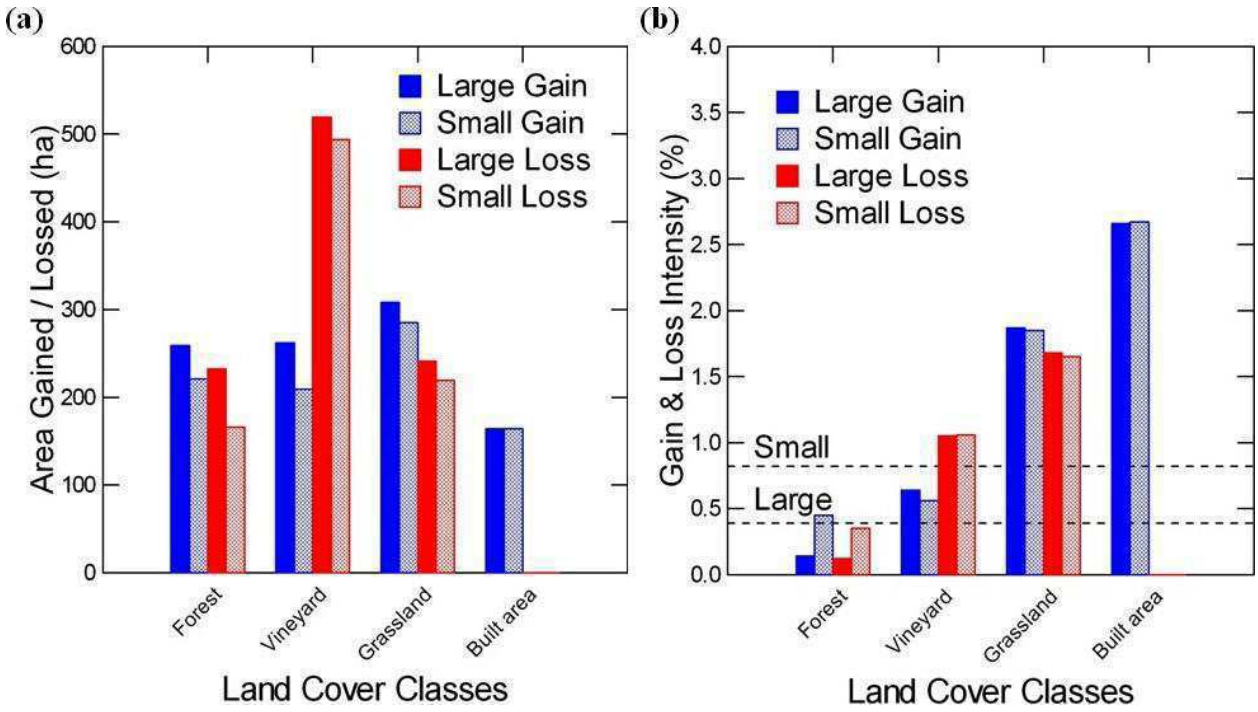

Figures 0.4: Gross gains and losses in 1950-1982 (a) and gain and loss intensity in 1950-1982 (b)

Since the annual rates in Figures 0.4-6b are expressed not as ha y^{-1} but as a percentage of category area, spatial scale impacts are more explicit. Spatial scale impacts are of two types. The first is relative variations between categories due to differences in category area. For example in Figures 0.4-6a, forest has more or less average absolute gains and losses compared to other categories but lower gain and loss intensities than all other categories (Figures 0.4-6b). Built area has the lowest absolute gain in Figures 0.4a but the greatest gain intensity in Figures 0.4b. Considering only absolute gains and losses gives the impression that forest is relatively active while built area is relatively inactive whereas intensity analysis reveals the contrary: forest changes little with respect to its surface area and can be considered almost dormant while built area is the most active of the land cover types in the initial period. Similarly, vineyard losses at both spatial scales in the initial (Figures 0.4a) and intermediate time (Figure 0.5a) periods are greatest among all categories, roughly twice as great as grassland losses, but vineyard loss intensity (Figures 0.4-5b) is less than grassland due to lower initial grassland areas.

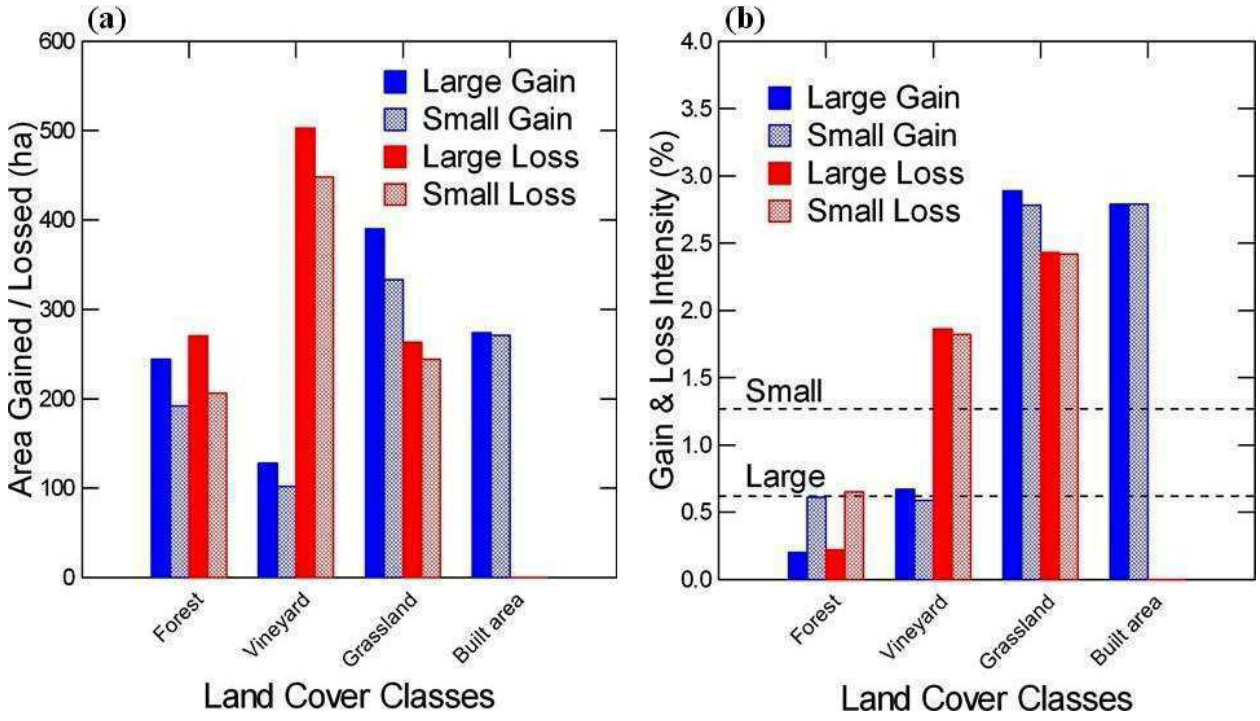

Figure 0.5: Gross gains and losses in 1982-2003 (a) and gain and loss intensity in 1982-2003 (b)

The second spatial extent effect is related to within category differences in study area. In all figures of absolute change (Figures 0.4-6a) gross gains and losses in the large window can only be equal to or greater than in the small zone. This, however, is not the case for gain/loss intensity values, where intensity values in the small zone can be greater than, equal to, or less than in the larger window. Forest is one example where absolute values are greater in the large zone but intensity values are greater in the small window for all time intervals since most of the forest cover is in the extended zone and most of the change in forest is in the small window. Almost all the built area and changes in built area are in the small window, so absolute values are nearly identical in all time intervals. Finally, both observed change in grassland (Figure 0.5a) and intensity rate (Figure 0.5b) are greater for the large zone.

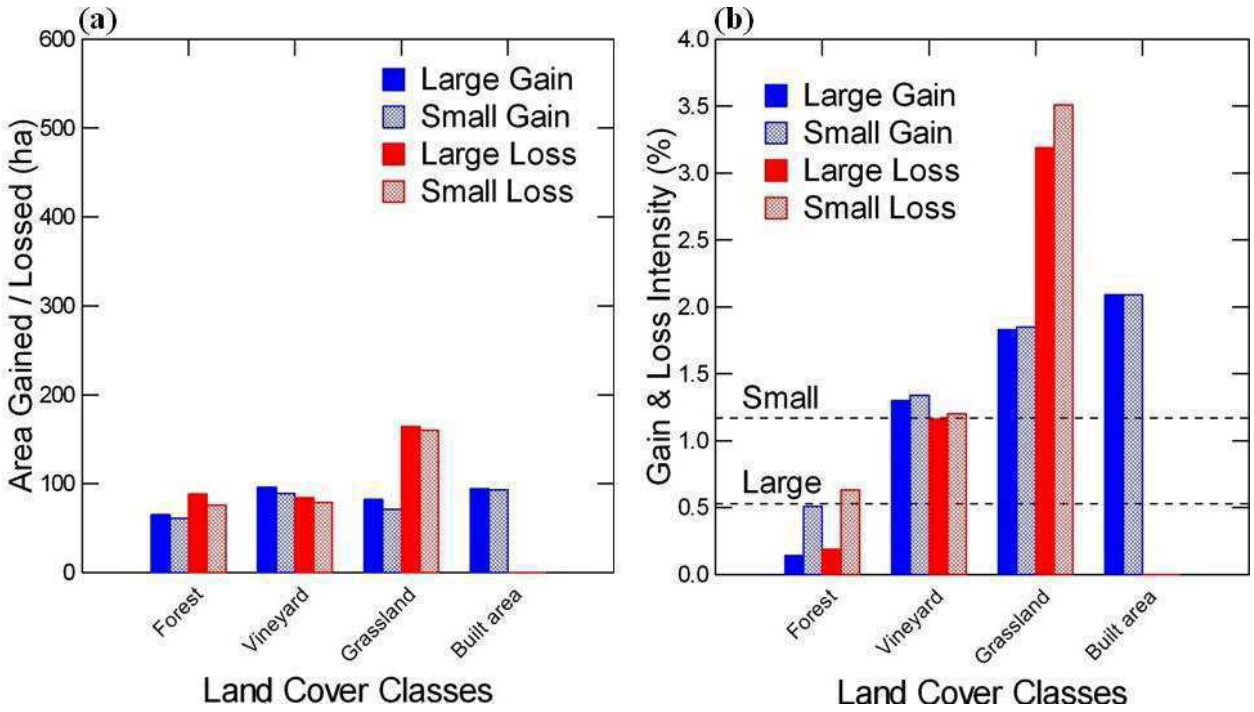

Figure 0.6: Gross gains and losses in 2003-2011 (a) and gain and loss intensity in 2003-2011 (b)

When comparing category dynamics to a uniform intensity (Figures 0.4-6b) at the large scale, only forest is below uniform intensity, all other categories are equal to or above average intensity. At the small window scale, trends are different, even though forest remains below average for all periods: in Figures 0.4b, vineyard gains are greater than uniform for the large zone but less than uniform in the small window; in Figure 0.5b, vineyard gains are close to uniform in the large zone but much less than uniform in the small zone; and finally, in Figure 0.6b, vineyard losses are greater than uniform at the large scale but equal to uniform in the small window.

3.2.3 Transition intensity analysis

Since the larger focus of this research program is on vineyard evolution and its impacts on runoff and erosion, only transition potentials affecting vineyard will be considered in Figure 0.7-9 for conversions to vineyard and in Figure 0.10-12 for changes from vineyard. Y scale values were kept constant for the transitions to and from vineyard to facilitate comparisons. As for the category changes, land converting to or from vineyard at the large scale can only be greater than at the small scale (Figure 0.7-9a). In Figure 0.7-9, built area can never convert to vineyard and is 0 in all figures (included nonetheless to harmonize with Figure 0.10-12). The reverse is not the

case, however, since significant areas of vineyard have been urbanized, as was explained in Roy et al. (2014a) and will be discussed with regards to Figure 0.10-12.

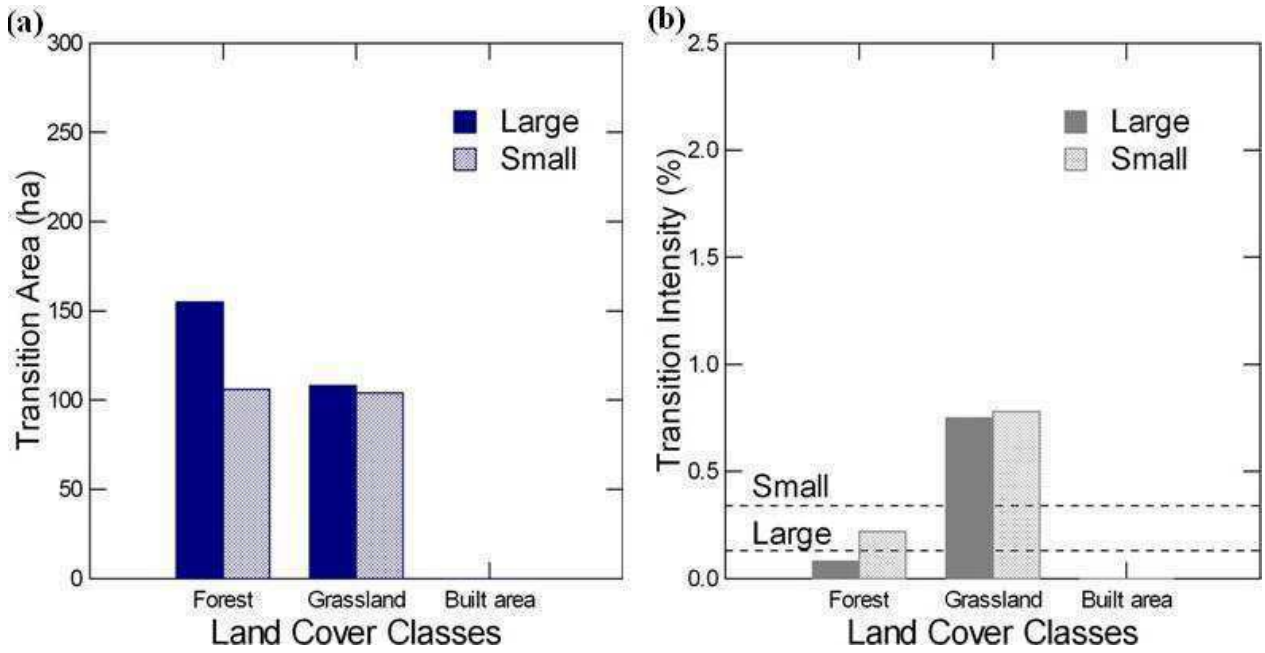

Figure 0.7: Transition area to vineyard in 1950-1982 (a), annual transition intensity to vineyard in 1950-1982 (b)

Conversion of forest to vineyard is greater than grassland to vineyard for the initial (1950-1982) and intermediate (1982-2003) periods, as can be seen in Figure 0.7and 8a, respectively. The reverse is true in the latter period (Figure 0.9a). Since grassland values are similar in all figures, it can be assumed that nearly all the vineyard gains from grassland occur within the small window. Vineyard gains more land from forest than grassland in the initial and intermediate transition periods (Figure 0.7-8a), but much of this change is focused in the small zone, so intensity values (Figure 0.7-8b) are greater for the small window. In contrast to the earlier periods, more land is converted to vineyard from grassland than from forest in the latter period (Figure 0.9a).

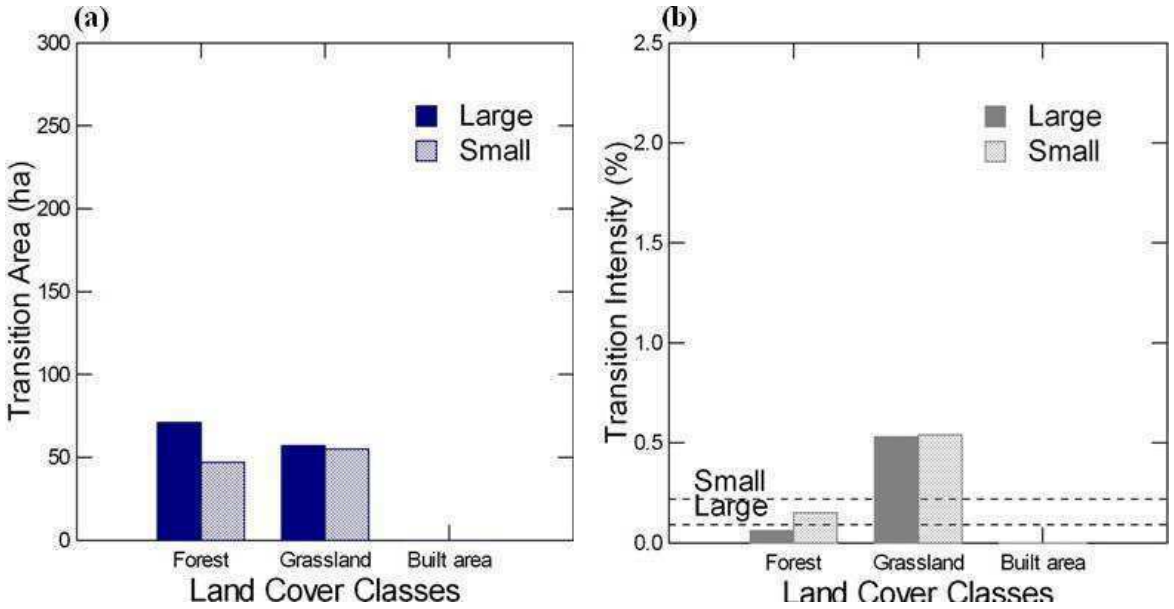

Figure 0.8: Transition area to vineyard in 1982-2003 (a), annual transition intensity to vineyard in 1982-2003 (b)

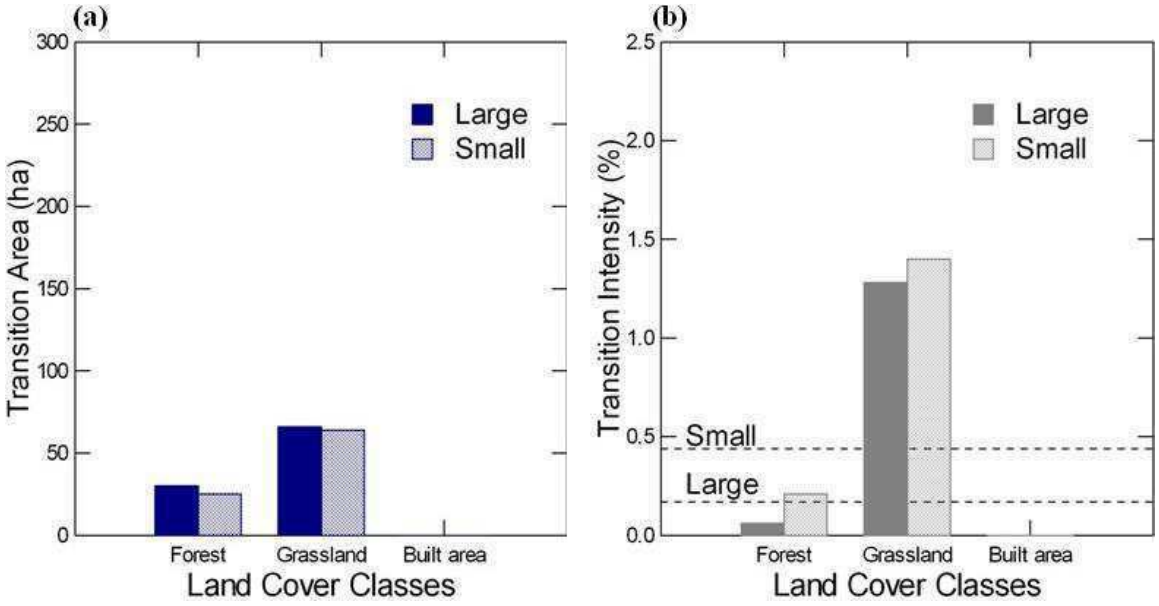

Figure 0.9: Transition area to vineyard in 2003-2011 (a), annual transition intensity to vineyard in 2003-2011 (b)

Transition dynamics from vineyard to other categories (Figure 0.10-12) show some differences from the transitions to vineyard described above (Figure 0.7-9). Transitions from

vineyard (Figure 0.10-11a) to other categories are greater than transitions to vineyard (Figure 0.7-8a) for all time intervals but the last (Figure 0.12a and 9a). The rate of change to vineyard (Figure 0.9b) accelerated in this period while losses from vineyard (Figure 0.12b) slowed after very high loss rates in 1950-1982 (Figure 0.10b) and 1982-2003 (Figure 0.11b). As expected, built area gains from vineyard are concentrated in the alluvial plain, so absolute and relative large/small zone relationships are similar in Figure 0.10-12. Transitions from vineyard to forest are relatively dormant at both spatial extents (Figure 0.10-12b) compared to conversion to grassland and built area despite relatively large areas converted from vineyard to forest in the first two periods (Figure 0.10a and 10b). Transition dynamics with regards to uniform rates are not noticeably affected by spatial extent since below and above average rates are similar at both scales in Figure 0.10-12b.

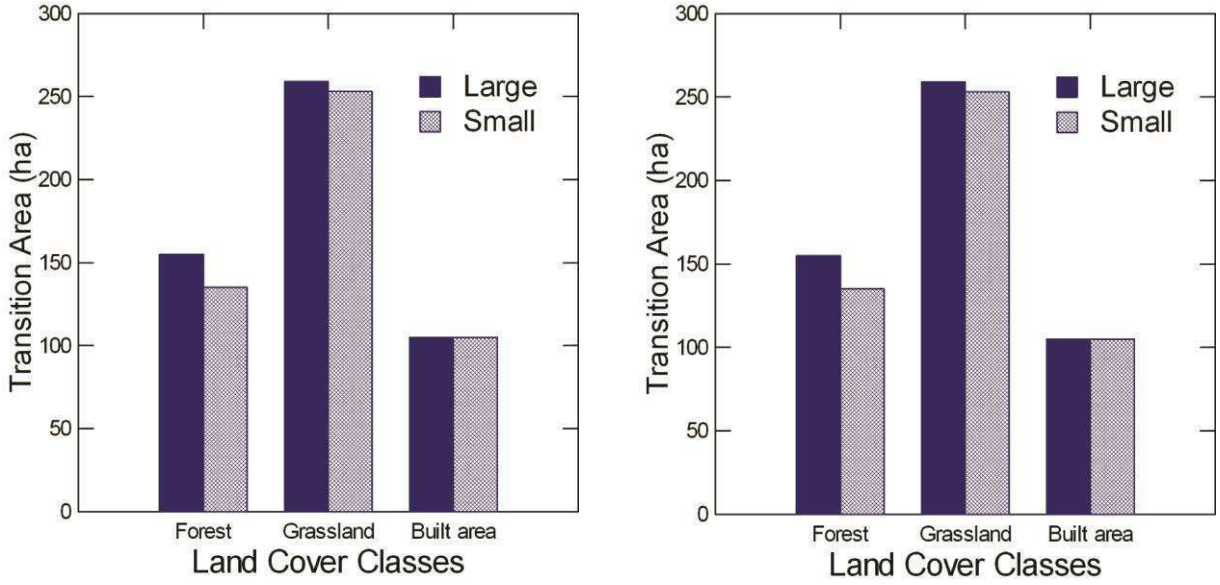

Figure 0.10: Transition area from vineyard in 1950-1982 (a), Annual transition intensity from vineyard in 1950-1982 (b).

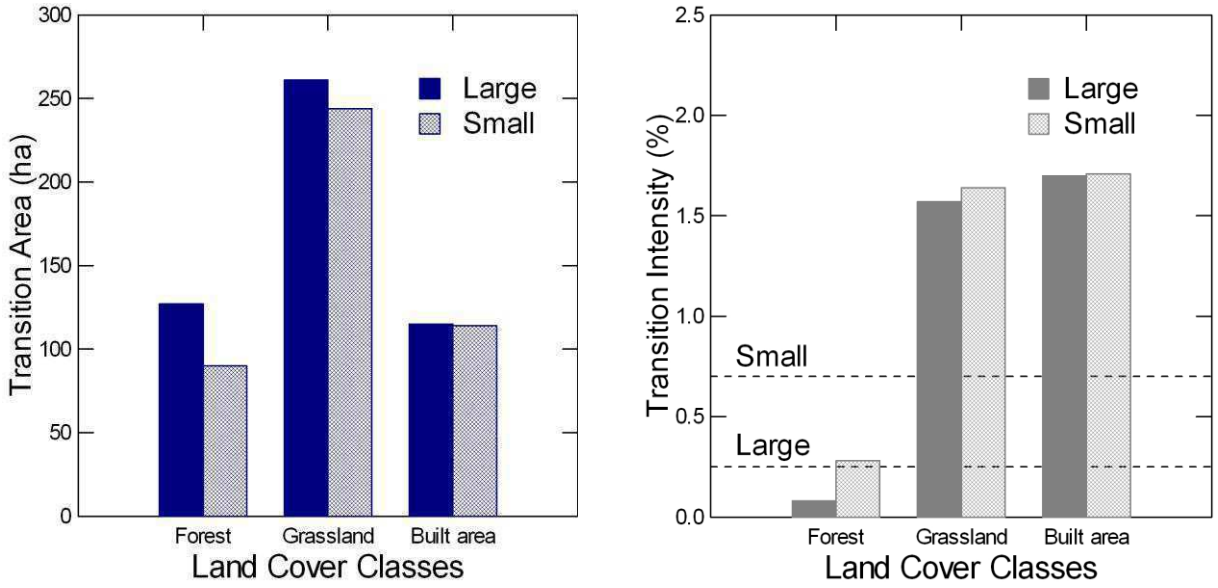

Figure 0.11: Transition area from vineyard in 1982-2003 (a), Annual transition intensity from vineyard in 1982-2003 (b)

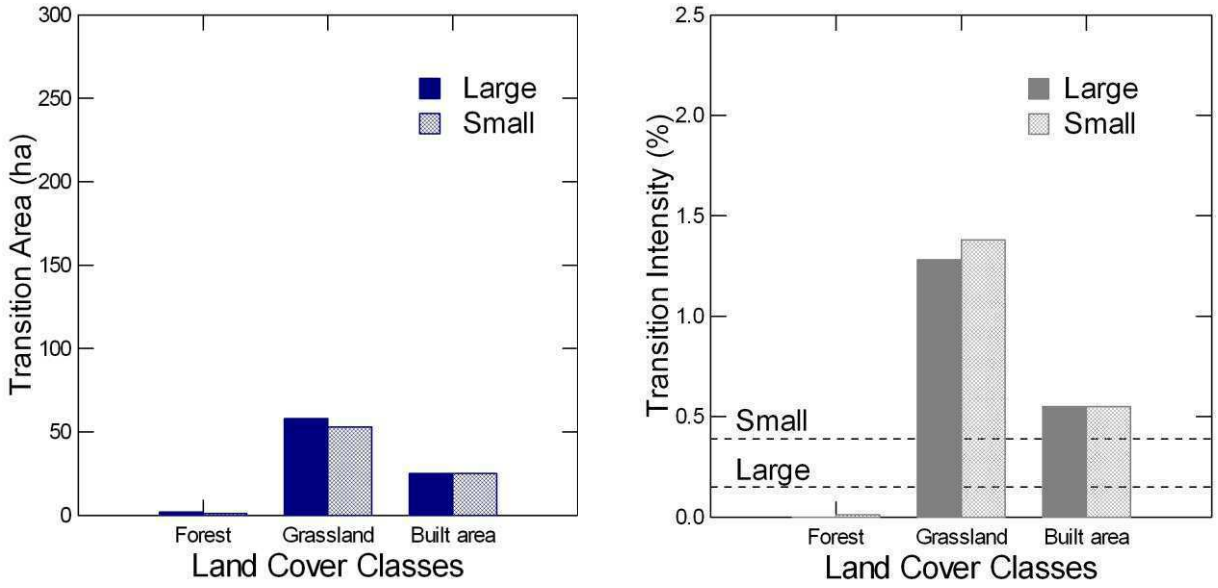

Figure 0.12: Transition area from vineyard in 2003-2011 (a), Annual transition intensity from vineyard in 2003-2011 (b)

3.3 Dormant category impacts on land cover modelling indices

In this section, the impacts of spatial extent of the study area on Cramer's V and disagreement indices are considered. The following tables summarize results for both spatial extent and cell

size effects, so readers are asked to focus on spatial extent at the 25 m resolution only for now. Differences between cell sizes will be considered afterwards.

3.3.1 Cramer's V

Cramer's V is a measure of association between a land cover change driver and a category: the greater the value, the stronger the relationship, Values for the different spatial extents and cell sizes are shown in Table 0.4-7. At this stage, readers should focus on the 25 m cell size (Table 3a) for spatial extent impacts. Spatial extent clearly has a strong impact on Cramer's V values. Mean values are generally 1.3 to 1.7 times greater for the large zone than for the small window, and this holds for all categories and explanatory variables except for built area and the two strongest predictors of built area change (distances from roads and 1982 built area). Since virtually all the change occurs in the small window, increasing spatial extent should have no impact on the capacity to predict category changes. Despite this, for categories with high surface areas and very little change outside the window, Cramer's V values are greater. Similarly, built area Cramer's V values increase for altitude, slope, and distance from streams though no more than 1% of built area is located outside the small window (Table 0.3).

Table 0.4: Cramer's V coefficient for 25 m cell size. Values ≥ 0.40 are highlighted in bold and overall accuracy is in italics

COVER	**ALTITUDE**		**SLOPE**		**DIST. ROADS**		**DIST. BUILT**		**DIST. STREAMS**	
	Small	Large	Small	Large	Small	Large	Small	Large	Small	Large
Forest	**0.50**	**0.70**	**0.51**	**0.66**	**0.44**	**0.67**	**0.41**	**0.64**	0.20	**0.42**
Vineyard	0.23	**0.42**	0.30	**0.42**	0.19	0.39	0.21	0.39	0.14	0.27
Grassland	0.36	**0.42**	0.34	**0.40**	0.16	0.30	0.22	0.32	0.16	0.23
Built	0.17	0.31	0.09	0.24	**0.58**	**0.58**	**0.71**	**0.69**	0.15	0.21
Overall	*0.32*	***0.42***	*0.32*	***0.40***	***0.39***	***0.46***	***0.45***	***0.51***	*0.16*	*0.26*

Table 0.5: Cramer's V coefficient for 50 m cell size. Values ≥ 0.40 are highlighted in bold and overall accuracy is in italics

COVER	ALTITUDE		SLOPE		DIST. ROADS		DIST. BUILT		DIST. STREAMS	
	Small	Large	Small	Large	Small	Large	Small	Large	Small	Large
Forest	**0.50**	**0.70**	**0.51**	**0.66**	**0.45**	**0.66**	**0.41**	**0.64**	0.22	**0.42**
Vineyard	0.23	**0.42**	0.29	**0.41**	0.20	0.39	0.21	0.38	0.14	0.27
Grassland	0.36	**0.43**	0.34	**0.41**	0.17	0.30	0.23	0.32	0.17	0.24
Built	0.17	0.30	0.09	0.24	**0.57**	**0.54**	**0.71**	**0.70**	0.15	0.20
Overall	*0.32*	***0.42***	*0.32*	*0.39*	*0.38*	***0.45***	***0.45***	***0.51***	*0.17*	***0.26***

Table 0.6: Cramer's V coefficient for 100 m cell size. Values ≥ 0.40 are highlighted in bold and overall accuracy is in italics

COVER	ALTITUDE		SLOPE		DIST. ROADS		DIST. BUILT		DIST. STREAMS	
	Small	Large	Small	Large	Small	Large	Small	Large	Small	Large
Forest	**0.50**	**0.69**	**0.50**	**0.63**	**0.47**	**0.65**	**0.42**	**0.63**	**0.25**	**0.41**
Vineyard	0.26	**0.44**	0.31	**0.42**	0.23	**0.40**	0.24	0.39	0.18	0.28
Grassland	0.35	**0.41**	0.33	0.39	0.20	0.28	0.23	0.30	0.17	0.22
Built	0.17	0.29	0.14	0.23	**0.64**	**0.54**	**0.71**	**0.71**	0.18	0.20
Overall	*0.32*	***0.42***	*0.32*	*0.38*	***0.43***	***0.44***	***0.46***	***0.51***	0.19	***0.25***

3.3.2 Prediction validation

With greater Cramer's V values, one would expect improved prediction for the large window and this is apparently the case as shown by the disagreement values in Figure 0.13. Solid fill bars show quantity disagreement while hatched bars show allocation disagreement. Quantity disagreement is 3-4 times smaller than allocation disagreement for both spatial extents. Both quantity disagreement and allocation disagreement are roughly half as great in the large window as in the small window. Land cover prediction therefore appears to be much improved in the large zone. However, predicted land covers for the surface in the small window are the same for both the small and large window predictions.

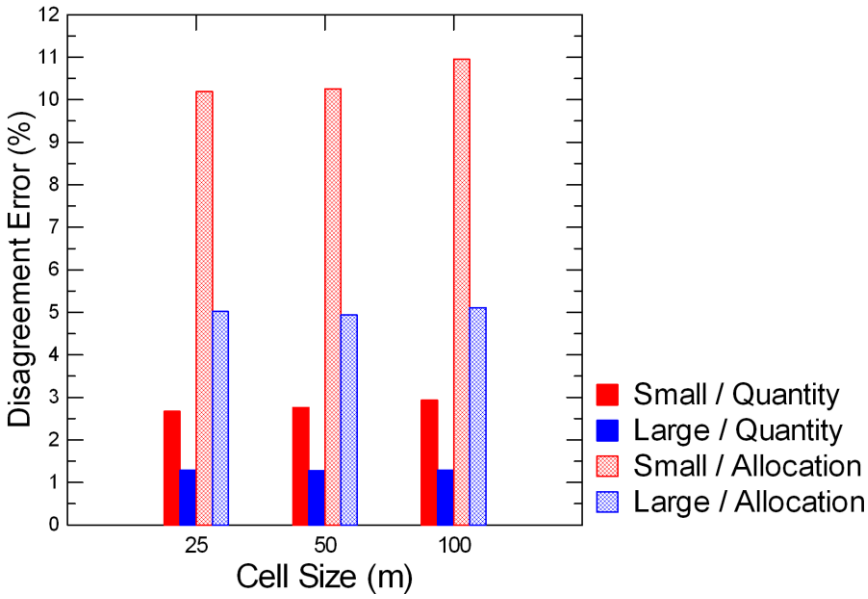

Figure 0.13: Disagreement values according to spatial extent and cell size for 25 m, 50, and 100 m cells sizes

3.4 Cells size impacts on land cover modelling indices

Cell size initially appears to have no impact on Cramer's V as values in Tables 3a-c are nearly identical for the three cell sizes within the two spatial extents. The exceptions are the two explanatory variables most strongly related to built area changes – distance from roads and distance from built area. For these, Cramer's V is systematically greater for built area than for forest in the small window but not in the large window. The explanatory power of distance to roads and distance to built area increases substantially when spatial extent is reduced. When the coarser 50 m and 100 m resolutions are downscaled back to 25 m, the relationships between explanatory variable and category remain the same with no noticeable changes between Table 0.4 (original 25 m), Table 0.7 (50-25 m downscaled), and Table 0.8 (100-25 m downscaled).

Table 0.7: Cramer's V coefficient for 50-25 m upscaling/downscaling cell size. Values ≥ 0.40 are highlighted in bold and overall accuracy is in italics (values are to be compared to Table 3a and 4b)

COVER	**ALTITUDE**		**SLOPE**		**DIST. ROADS**		**DIST. BUILT**		**DIST. STREAMS**	
	Small	Large	Small	Large	Small	Large	Small	Large	Small	Large
Forest	**0.50**	**0.70**	**O.52**	**0.66**	**0.44**	**0.66**	**0.41**	**0.70**	0.21	**0.42**
Vineyard	0.23	**0.42**	0.30	**0.42**	0.20	0.38	0.21	0.38	0.14	0.27
Grassland	0.36	**0.42**	0.34	**0.40**	0.17	0.30	0.23	0.32	0.16	0.24
Built	0.17	0.31	0.09	0.24	**0.57**	**0.55**	**0.71**	**0.70**	0.15	0.21
Overall	0.32	**0.42**	0.32	**0.40**	**0.38**	**0.45**	**0.45**	**0.52**	0.16	0.21

Table 0.8: Cramer's V coefficient for 100-25 m upscaling/downscaling cell size. Values ≥ 0.40 are highlighted in bold and overall accuracy for each explanatory variable is in italics (values are to be compared to Table 3a and 4a)

COVER	**ALTITUDE**		**SLOPE**		**DIST. ROADS**		**DIST. BUILT**		**DIST. STREAMS**	
	Small	Large	Small	Large	Small	Large	Small	Large	Small	Large
Forest	**0.50**	**0.69**	**0.50**	**0.65**	**0.47**	**0.65**	**0.42**	**0.64**	**0.25**	**0.41**
Vineyard	**0.26**	**0.44**	**0.32**	**0.43**	0.23	**0.40**	0.24	0.39	0.18	0.28
Grassland	**0.35**	**0.41**	**0.31**	0.38	0.20	0.28	0.23	0.30	0.17	0.22
Built	0.17	0.29	0.31	0.23	**0.64**	**0.54**	**0.71**	**0.71**	0.18	0.20
Overall	0.32	***0.42***	0.32	*0.39*	**0.43**	***0.44***	**0.46**	***0.51***	0.19	*0.25*

The lack of an impact of cell size on model prediction values is also apparently confirmed by similar disagreement values between the 25 m, 50 m, and 100 m spatial resolutions (Figure 0.13). However, when the downscaled predicted images are compared to the 25 m 2011 reference image, disagreement values respond differently (Figure 0.14). Quantity disagreement varies little, and even improves slightly at 100 m, but allocation disagreement rises sharply for the 50-25 m and 100-25 m land cover predictions for both the small and large study zones. Allocation disagreement for the original 25 m image is about 10%, and this value increases to about 17% and 24% for the 50-25 m and 100-25 m predictions, respectively. The implications of this are discussed below.

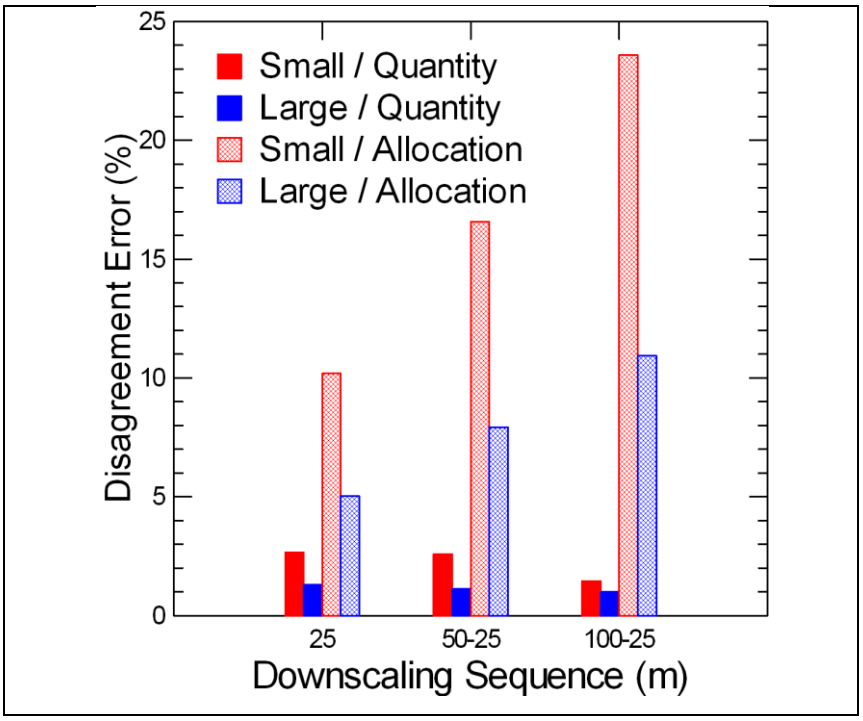

Figure 0.14: Disagreement values for upscaling / downscaling effects for 25 m, 50-25 m, and 100-25 m.

Before moving on to the discussion, the authors would like to point out that although the model results shown in Figure 0.13 are reasonably satisfactory, none of the spatial extent / cell size combinations performed better than simply comparing the 2003 image to 2011, though the spatial extent trends remain the same. Quantity and allocation disagreement values for this comparison are in the order of 3.0% and 6.0% for the small window and 1.3% and 3.0% for the large zone. Although this has no implications for the findings of the study it reinforces the necessity to compare the predicted image to both the synchronous and historical images as described by Chen and Pontius (2011).

4. Discussion

Spatial extent effects on the perception of land cover change dynamics will be considered before discussing spatial extent and cells effects on predictor strength and model validation.

4.1 Perception of land cover change dynamics and spatial extent

The first section of this paper on intensity analysis demonstrates that the perception of category activity depends partly on spatial extent. Based on absolute values of converted land, forest was moderately active at both spatial extents, but in terms of its relative spatial area, it was much less active than smaller categories undergoing less change in terms of absolute area but much greater evolution in terms of % of category area. Vineyard appeared particularly active at the large scale but much less so in the small window (for about the same change) when compared to intensity values of grassland and built area. In this study, both grassland and built area are particularly active with regards to their respective surface areas, and this tends to reduce the relative importance of vineyard changes when much of the dominant, relatively stable, forest category is excluded from the study by passing from the large to the small window. Below or above average activity rates are therefore sensitive to spatial extent and can be quite different when a large dormant category is present, and categories that appear particularly active at the large scale are below average at the small window level.

With respect to spatial extent, three factors come into play in determining category activity variations. Firstly, if all, or nearly all, a land cover category is found within the smaller zone (built area here) then absolute and annual rates will be nearly identical at both scales. Secondly, if a significant amount of a land cover is found outside the small zone, but most of the change is in the smaller window (as for forest), then absolute values will be greater at the large scale, but relative rates will be lower in the smaller window. Finally, for land covers with significant surface areas and important changes outside the small zone, then large/small window tendencies can remain the same for both absolute and relative measures of change (no examples of this in this study). The case of a small stable area extended to include a highly changing zone is excluded because land cover change studies focus on areas undergoing change and not on stable landscapes; nobody purposely studies land cover change in an unchanging landscape while ignoring a nearby rapidly changing zone.

4.2 Spatial extent and land cover change prediction

Predictive power of explanatory variables is strongly affected by spatial extent, and the presence of the persistent forest cover gave the impression that explanatory variables were better predictors at the large scale than for the small window for the same land cover change. Similarly,

disagreement values appeared to indicate a better prediction for the large zone than the small zone. However, the actual prediction is virtually the same for both windows in the small zone, so the lower disagreement values for the large window are somewhat artificial. Adding a large area of persistent land cover appears to reduce quantity and allocation errors. Quantity and allocation disagreements are greater in the small window due to changes in three different values used to calculate these indices: total area, total absolute change, and correctly predicted area. Both disagreement values are calculated as the % of the study area, so values decrease with increasing study area if other components remain constant or change little. Quantity disagreement depends mainly on absolute total change and allocation disagreement relies on the number of wrongly predicted cells. Therefore, both disagreement values are smaller in the large window because denominators (study area) increase more than numerators in calculating both fractions. Lower disagreement (apparent increase in model performance) is related to the number of correctly predicted stable cells. In the small window, about 86% of pixels are correctly predicted persistent cells, and in the large window this value increases to about 91% for all cell sizes. Hence, lower disagreement values for the large window can be attributed to the correct prediction of persistent cells, which are easy to predict in a large expanse of forest with no surrounding cells of other land cover categories. This agrees with observations by Chen and Pontius (2010) and Pontius and Spencer (2005) that persistence is easier to predict than change. Virtually all the change occurs in the small window, and the extended part of the large window is essentially persistent. Actual land cover change prediction is the same for the large and small windows, but the large window provides more satisfying statistics.

Why Cramer's V improves so strongly with spatial extent (for categories other than built area and distance from roads and built area variables) is not clear since about 90% of change for all categories except built (close to 100%) occurs in the small zone. One possibility is that as window size increases, explanatory variable range increases. For example, the ranges in altitude are 237 m and 663 m for the small and large windows, respectively. Similarly, range values for slope are 70.5% and 123%, respectively. Even though little area changes outside the small window, these small differences may have a large impact on the Chi-Square value used to calculate Cramer's V, the way a few outliers can on a correlation coefficient in linear regression.

The selection of spatial extent for modelling land cover change can be driven by process, data constraints, or arbitrary decision. Land cover change modelling using data based on

administrative units is generally restricted by the geographic administrative limits, which may or may not add large areas of dormant land covers. Most land cover studies probably extract somewhat arbitrary rectangular windows from satellite images or air photos. In such a case, scientists should look to minimize the presence of large dormant categories to avoid artificially inflating prediction results.

4.3 Spatial resolution and change prediction

Grid cell size is driven by many factors and can be subject to different interpretations. It can depend on initial cell size of input data (*eg.* 30 m Landsat vs. 10 m SPOT images) or can refer to final cell size after harmonisation, expansion and contraction procedures. Only the second aspect was considered here. It can be assumed that finer spatial and spectral resolutions of source data lead to better category identification and therefore more reliable land cover maps. In this study, 1 m air photos were digitized to represent land cover, but without integrating details at the 1 m scale. Roads, for example, were left out to avoid creating a supplementary category that would only complicate land cover change analysis. The advantage of using such a fine resolution resides mainly in a better classification of land cover types and not necessarily in a more detailed land cover map.

The initial results appear to show that cell size has no impact on land cover change modelling since Cramer's V and disagreement values were unchanged by upscaling. However, the upscaling / downscaling procedure revealed that during upscaling considerable information was lost. The impacts of spatial extent and cell resolution on landscape data are discussed in Turner et al. (1989), in which the probability of small or rare information loss increases with increasing cell size: land cover types with scattered distributions lose area rapidly with coarser cell resolutions whereas clustered land covers disappear more slowly. As cell size increases, detail is lost, isolated pixels disappear, and the landscape becomes both increasingly simpler and less representative of reality. Improved statistics with coarser resolutions (Chen and Pontius 2011, Geri et al. 2011, Pontius et al. 2008) may simply be the result of a landscape becoming increasingly simplified and composed of larger category patches. The simpler the landscape, the better the prediction; in short, the model gets better at predicting a landscape that grows progressively further from reality. Downscaling does not restore the initial information, but it allows the modeler to have some measure of the amount of information lost by changes in the disagreement values. Studies

considering cell size effects should systematically downscale back to the original spatial resolution to avoid the potentially false impression that the upscaled model leads to better prediction.

5. Conclusions

Spatial extent and cell size are two fundamental issues of land cover change modelling which continue to require attention in order to better understand land cover changes dynamics and prediction results. In this study, increasing spatial extent was synonymous with integrating a large dormant category and effects related to adding new categories or processes were not considered. Spatial extent has a major impact on perceived land cover change dynamics, where relatively large dormant categories can mask smaller more dynamic category changes. It is more difficult to model small areas with multiple land cover types undergoing rapid change than larger stable zones, and simply adding significant areas of stable land improves model performance without improving change prediction. Quantity and allocation disagreement are greater in the small window than in the large window because most of the changes occur in the small zone and the extended part of the large window is mostly persistent forest and persistence generates greater prediction accuracy.

CHAPTER 5

EVOLUTION OF SOIL EROSION IN A MEDITERRANEAN CATCHMENT IN 1950-2025

(Article proposal submitted to AgroMed International Conference 2016

December 1-2, 2016 Avignon (FRA) with publication in Land Use Science)

1. Introduction

Soil is a vital non-renewable resource formed through various physical, chemical, and biological processes in the natural environment. Soil degradation due to erosion has become a serious environmental problem throughout the world due to the rapid growth of overgrazing, deforestation, inappropriate agricultural practices, overexploitation of fuel wood, forest fire, and other human activities (Alkharabsheh et al. 2013, Brady and Weil 1999, Terranova et al. 2009). In many areas of the world, soil erosion rates exceed soil formation resulting in serious soil degradation (Toy et al. 2003). About 56% soil degradation is associated with soil erosion by water (Brady and Weil 1999). Soil erosion may cause several environmental and economic problems: loss of agricultural productivity, water pollution (silting in streams, rivers, reservoirs), and biodiversity loss etc. (Lu et al. 2004, Zhang et al. 2014). Martínez-Casasnovas and Ramos (2006) estimate that soil erosion costs about 7-8% of income from grape production in Mediterranean NE Spain.

Brady and Weil (1999) describe three fundamental steps of soil erosion: detachment of soil particles from soil mass, transportation of the detached particles by floating, rolling, dragging, and splashing, and deposition of the transported particles to lower elevations. Three forms of water erosion are also described in Brady and Weil (1999): sheet erosion, rill erosion, and gully erosion. Sheet erosion can be observed when water flow removes soil more or less uniformly; it becomes rill erosion when sheet flow concentrates into small channels. When the volume of runoff further concentrates and flowing water cuts deeper into the soil, gullies can be formed; the size limit distinguishing gullies from rills is when common agricultural tools can no longer erase the trace of concentrated erosion.

The risk of soil erosion varies from case to case depending on several parameters: topography, soil characteristics, local climate, vegetation type and cover, and implemented land

use and management practices (Alkharabsheh et al. 2013). Soil erosion affects the land and its inhabitants in various ways and changes soil physical and chemical properties (Toy et al. 2003). Soil erosion also affects soil formation processes by removing the most fertile upper layer of the soil. It alters the infiltration capacity by the removing nutrient-rich A-horizon and exposing less fertile B-horizon. The infiltration capacity of the A-horizon is generally greater than the B-horizon. Soil erosion also affects transportation and deposition of sediments and associated substances. Transported agricultural pollutants can damage the ecosystems of downstream water bodies. Therefore, soil erosion control is an important issue for researchers in order to maintain soil fertility and establish sustainable soil conservation practices.

Soil erosion by runoff is an important issue for Mediterranean France. Several studies have already been conducted to measure soil erosion and to identify factors of soil erosion for various catchments in the Mediterranean area (Blavet et al. 2009, Kosmas et al. 1997, Ramos and Martínez-Casasnovas 2006, Torri et al. 2006, Wainwright 1996).

1.1 Factors affecting soil erosion

Soil erosion risk depends on different topographic, geographic, and climatic conditions among which land cover type, slope, area, soil characteristics, local climatic conditions, and land use management play important roles (Alkharabsheh et al. 2013). Slope gradient is a key factor for soil erosion which increases significantly on steeper slopes (Fox and Bryan 2000, Liu et al. 2013, El Kateb et al. 2013, Koulouri and Giourga 2007). Slope length is also important but secondary to gradient. Increased soil erosion was observed with increasing slopes, and severe soil erosion was observed on slopes greater than 25° in China (Koulouri and Giourga 2007, Zhang et al. 2014). Therefore, terracing can decrease soil erosion since both gradient and length are reduced (Liu et al. 2013).

In addition to direct effects of slope, topography is intimately related to land cover use and soil properties. Van Rompaey et al. (2002) show that slope played a significant role in arable land and forest conversion during the past 250 years in the Dijle catchment (central Belgium). Arable lands were converted into forest mainly on the steeper slopes in 1774-1990, but the reverse occurred on lower slopes. Forest increased on steep slopes and badly drained soil while deforestation took place in relatively flat and favorable loamy soils with well drained areas.

A significant impact of vegetation and organic matter is noted in Mohammad and Adam (2010). The study found that vegetation coverage (*P. halepensis*) adds organic matter to the soil surface, and this can prevent soil erosion by developing soil structure and improving aggregate stability. Moreover, vegetation cover protects soil surface from rainfall and reduces the runoff energy.

Undistributed forest and dense grass provide the best soil protection followed by relatively dense forage crops (legumes and grasses). Small grains offer intermediate soil protection to surface erosion. Agricultural fields of row crops such as corn, soybeans, and potatoes are more vulnerable to surface erosion (Brady and Weil 1999). El Kateb et al. (2013) observed less runoff and soil erosion in the forest than in grassland, farmlands and tea plantations. This study also revealed that soil erosion is more sensitive than runoff to changes in vegetation cover. In addition, Vineyard is reported to be one of the most vulnerable land covers to soil loss in the European Mediterranean region (Kosmas et al. 1997, Cerdan et al. 2010).

In Alkharabsheh et al. (2013), mean soil loss decreased due to changes in land cover and land cover management where a large cultivated area was abandoned during the study period. Many fields remained abandoned due to the lower productivity that resulted mainly from climate change (decreasing precipitation and increasing temperature). Bakker et al. (2005) identified a good relationship between soil erosion and land use change in the western part of Lesvos, Greece. To identify the relationship, a logistic regression was performed using land use change as the response variable and soil depth, erosion and slope as explanatory variables. They found intense soil erosion and land use change in the marginal area of the study area over the last century.

Vacca et al. (2000) studied soil erosion and runoff in three different land cover types for plots in a Mediterranean catchment. The highest runoff and soil erosion rates were observed under a *Eucalyptus sp*. plantation followed by abandoned grazing and burned macchia. In another study, Nunes et al. (2011) revealed how land cover change affects soil erosion and runoff in a Mediterranean catchment, Portugal. According to the study, soil erosion increased due to a 30% drop in vegetation cover. They found that the Mediterranean region has high soil erosion risk in cereal fields due to unprotected ploughed bare soil in the rainy season (autumn), and it is more than 20 and 500 times greater than abandoned and pasture plots, respectively. In addition, uses of heavy machinery and deep ploughing techniques have also accelerated soil erosion.

1.2 The magnitude of erosion in Mediterranean Europe

Mediterranean areas are particularly vulnerable to soil erosion due to high rainfall intensities, agricultural activities on steep slopes, low organic matter, low nutrient contents, and rapid land-use changes (García-Ruiz 2010, Novara et al. 2011). García-Ruiz (2010) indicated several reasons for accelerated soil erosion in vineyards: soil is bare much of the cultivation period and vineyards are relatively common on steeper slopes. In another study, García-Ruiz et al. (2013) reviewed analyses on the principal environmental and human factors of soil erosion in the Mediterranean area. According to their study, hydrologic and geomorphologic changes occurred near the Mediterranean coasts of Spain, France, and Italy due to urban sprawl. Shrub lands and forested areas increased in abandoned farmland on hilly areas due a shift to more intensive agricultural practices in lowlands.

Kosmas et al. (1997) studied seven different sites in Mediterranean Europe including the Roussillon region located on the Pyrenese footslopes, France. The study revealed that rain-fed croplands in the hilly areas of Mediterranean regions are highly sensitive to erosion due to shallow soil and lack of vegetation cover. During spring and winter, soil surfaces of many Mediterranean vineyards remain almost bare and highly vulnerable to loss due to high moisture content, loose upper layer, and high intensity rainfall events. Moreover, abandonment of farmland, expansion of vineyard in the upland forests and cereal fields has also accelerated soil erosion risk in this area. Similar results were also found by Le Bissonnais et al. (2002), wherein a large area of southwest France was identified as highly threatened by soil erosion due to the steep slopes and high rainfall.

Arnaez et al. (2007) described different factors of soil erosion and used the USLE to estimate erosion for a Spanish Mediterranean catchment dominated by vineyards (La Rioja and Penedès). The study found that slope gradient, rain drop size, infiltration capacity and water storage have direct impacts on erosion processes. The study proposed that soil erosion can be decreased by increasing density of vines, changing tillage system (at right angle to the maximum slope gradient to favor infiltration), and building terraces along the contour lines. This study also took into account the importance of gravel cover on the resistence of soil to erosion in their study. Kouli et

al. (2009) analyzed various factors of soil erosion using RUSLE for 9 different watersheds in southern Greece, and they found that an extended part of their study area was undergoing severe soil erosion.

(Terranova et al. 2009) conducted a study to identify highly affected soil erosion by water in Calabria (southern Italy) using the RUSLE model. Results from this study show that erosion rates decreased from 30 to 12.3 Mg ha^{-1} y^{-1} due to land management actions, such as minimum cultivation methods, practices to avoid stubble wildfires, controlled partial grass regeneration, limiting tilling - harrowing -, increasing in areas with vegetation cover.

1.3 Soil erosion in Mediterranean vineyards

The Mediterranean climate is particularly well suited for quality grapes and wine production, and vineyard is one of the main agricultural land covers. Vineyards in the Mediterranean area have the highest soil erosion rates - greater than rain fed cereals, olives, grassland, and forest cover (Kosmas et al. 1997). The Mediterranean area experiences high storm intensities on dry soil in summer and autumn when vineyards are frequently bare, so high erosion rates occur at this time (Blavet et al. 2009, Wainwright 1996, Ramos and Martínez-Casasnovas 2006). In April, farmers kill grasses using mechanical ploughing and chemical herbicide treatments. Use of tillage and chemical weeding, and intensive use of pesticides are the most common practices in vineyard cultivation system in the Mediterranean area, in which soil remains bare during much of the year (Novara et al. 2011, Salome et al. 2014). Generally, chemical methods keep the fields bare for a longer time and allow less grass to grow in the off-season. Grapes are harvested in August-September, and heavy rainfall starts shortly afterwards and continues from October to March. These practices are popular to obtain high yielding and better quality grapes. The vineyards are vulnerable to erosion, soil organic matter depletion, pollution, and loss of biodiversity (Coulouma et al. 2006, Raclot et al. 2009). Wainwright (1996) studied a particular flash flooding event on 22 September 1992 in the Vaucluse and Drome regions of Southern France where 100 mmh^{-1} rainfall for 3 hours generated soil erosion of 37.5 T ha^{-1}. Another flash flood in the Penedes region, Catalonia, NE Spain in caused soil loss of 342.6 T ha^{1} during the storm with a maximum intensity of 187 mm h^{-1} (Martínez-Casasnovas et al. 2005).

The effect of land use and management on water erosion in a French Mediterranean wine-growing vineyard area was described in Blavet et al. (2009) and the highest erosion rate was

observed in chemically weeded vineyards. This study observed beneficial effects of vegetation cover and mulching and showed that soil organic carbon content can limit runoff and soil erosion. However, these factors are not effective on bare soils of chemically weeded vine plots. The study also found that young grassland had limited protection against runoff, but fallow grassland with good soil aggregate stability and good soil cover had no runoff or soil erosion.

Novara et al. (2011) conducted a study to estimate soil loss in an irrigated vineyard in Sambuca di Sicilia, in southwestern Sicily under conventional tillage. The study estimated an average soil erosion rate of 124.1 T $ha^{-1}y^{-1}$ using the USLE model and the highest erosion rates were observed on the steeper slopes. Ramos and Martínez-Casasnovas (2006) carried out a study to calculate nutrient losses in vineyards and their relation with soil erosion in the Alt Penedès vineyard region (north-eastern Spain). In their study area, 80% of the cultivated area was occupied by vineyards, and soil erosion increased due to intensification and mechanization of vineyard cultivation. Soil loss in the study plot reached 207 T ha^{-1} due to a maximum rainfall intensity 170 mm h^{1} during an event on 10 June 2000 (Ramos and Martínez-Casasnovas 2004). Usón (1998) in García-Ruiz (2010) determined an erosion rate of about 24.25 T $ha^{-1}y^{-1}$ for the same catchment area (vineyards in Catalonia). De Santisteban et al. (2006) reported soil erosion rates (3.6 to 178.5 T $ha^{-1}y^{-1}$) in vineyards of Navarre (spain) that were about double those of cereal crops because of lower vegetation cover and intense rainfall during the rainy season.

Augustinus et al. (1996) studied soil conservation methods in vineyards in Mediterranean France. The study found that most farmers used herbicide or cultivation methods to remove weeds from their vineyard. Therefore, a low permeability crust can form at the soil surface, and this increases runoff. The crust can be completely destroyed several times a year due to weed removal using a cultivator, and the crust can crack due to natural shrinking and swelling. According to the study, the presence of adequate terraces can prevent soil erosion on steep slopes. The impact of contouring on straight slopes and on slopes with concavities and convexities was also found beneficial.

1.4 Soil erosion models

Various erosion models have been interfaced with GIS to assess and predict soil erosion. Frequently cited models include the following: Revised Universal Soil Loss Equation (RUSLE) (Renard et al. 1997) which is a modified version of the empirical Universal Soil Loss Equation

(USLE), Water Erosion Prediction Program (WEPP) hill slope model (Laflen et al. 1991), LandSoil (Ciampalini et al. 2012) and the Soil Erosion Model for Mediterranean Regions (de Jong et al. 1999). Soil erosion models are important to measure and identify the detachment, transportation, and deposition processes of soil erosion using a set of mathematical equations related the rainfall, soil characteristics, topography, vegetation, and soil management of a site (Brady and Weil 1999).

The LandSoil model is based on the Sealing and Transfer by Runoff and Erosion related to Agricultural Management (STREAM) model, and the main distinction of this model is to consider soil characteristics (soil roughness, surface crusting, and vegetation cover evaluation) as the major soil erosion/redistribution process in an agricultural landscape (Ciampalini et al. 2012). Landsoil models soil redistribution processes in different topographic and agricultural landscapes, and it facilitate landscape design at the catchment scale for soil conservation using different land cover types in southern France (Ciampalini et al. 2012).

In the same way, Evrard et al. (2010) identified the impact of rainfall seasonality and land use change on soil erosion over the last 40 years using the STREAM model for a catchment in southern France. The study found that sediment export increased by 168% after land consolidation due to the decrease in the grassland cover and increase in field size.

Water Erosion Prediction Project (WEPP) predicts soil loss and deposition using a spatially and temporally distributed approach and can integrate different land covers (rangeland, forest, agriculture land, and urban area) (Mahmoodabadi and Cerdà 2013). It is also able to describe runoff and erosion processes and to evaluate the impacts of management intervention and environmental change.

The Soil Erosion Model for Mediterranean Region (SEMMED) predicts annual rate of soil erosion considering detached soil particles by raindrops impact and transport of these particles by overland flow, but it does not take into account splash transport and runoff detachment (de Jong et al. 1999). The model includes multi temporal vegetation images, a Digital Terrain Model (DTM), a digital soil map, and a limited amount of soil physical field data.

1.4.1 The use of the RUSLE model in different studies

The USLE model has been used worldwide since the 1970s and it was updated in the early 1990s to create an erosion prediction tool named the Revised Universal Soil Loss Equation

(RUSLE) (Brady and Weil 1999). RUSLE is a factor based model which estimates overall soil erosion rate where each factor quantifies one or more processes and interactions (Millward and Mersey 1999). It is easy to use and convenient to quantify soil erosion by considering rainfall, topography, soil, vegetation, land use, and land management (Zhou et al. 2008). The earlier version of this model was developed for agricultural fields, and the updated recent version is modified based on stream power theory which is suitable for complex topographic conditions (Mitasova et al. 1996, Chakroun et al. 1993). However, this model is unable to consider deposition (Terranova et al. 2009).

The USLE and its improved version, RUSLE, are the most commonly used models to estimate and predict soil erosion for various geographic locations: African (Angima et al. 2003, Bewket and Teferi 2009, Lufafa et al. 2003, Alkharabsheh et al. 2013), Mediterranean (Arnaez et al. 2007, Kouli et al. 2009), North American (Millward and Mersey 1999, Mitasova et al. 1996, Nyakatawa et al. 2001, Royall 2007), Chinese (Zhou et al. 2008), Chilean (Bonilla et al. 2010), and Indian (Prasannakumar et al. 2012) catchments have all been modelled using RUSLE, not to mention several other regions of the world. The model has been used for vegetation (Zhou et al. 2008), maize (Millward and Mersey 1999), vineyard (Arnaez et al. 2007, Blavet et al. 2009, Chevigny et al. 2014, Pacheco et al. 2014), and various land covers (Angima et al. 2003, Nyakatawa et al. 2001, Lufafa et al. 2003). It has also been performed for both plot (Zhou et al. 2008) and catchment (Millward and Mersey 1999) scales.

Angima et al. (2003) evaluated the performance of RUSLE in predicting long term soil loss under cropped land dominated by coffe, banana, and corn bean in a hilly catchment area. The study found that the rate of soil loss varies mostly with changing slope factor, and soil loss was estimated at 134 T $ha^{-1}y^{-1}$ and 549 T $ha^{-1}y^{-1}$for average LS factors of 0-10 and 10-20, respectively. In a different study, Bakker et al. (2005) used the USLE in various crop lands at the Chemoga watershed, Ethiopia. They reported that the model estimated a fairly reliable prediction of soil erosion loss. Kouli et al. (2009) quantified soil erosion factors and predicted annual soil loss of a Mediterranean catchment in southern Greece. The study found results consistent with those of other Mediterranean watersheds and recommends RUSLE for the Mediterranean environment at watershed scales. They predicted a mean annual soil loss of about 200 T ha^{-1} y^{-1} for nine different Mediterranean watersheds in Greece with average annual precipitation 900 mm. In another study. Lufafa et al. (2003) tested the USLE within a microcatchment at the Lake

Victoria Basin (LVB), Uganda. Soil loss was predicted at 93, 52, 47, and 32 T ha^{-1} y^{-1} for cropland, rangeland, banana–coffee, and banana, respectively.

1.4.2 RUSLE model description

RUSLE is designed to predict average annual soil erosion due to runoff from topography, rainfall erosivity, soil erodibility, and management systems (Alkharabsheh et al. 2013, Nyakatawa et al. 2001). It is an equation based on the principal factors that affect soil erosion (Renard et al. 1997). RUSLE calculates the average per unit and patch soil erosion following the equation bellow.

$$\mathbf{A = R. K. LS. C. P} \quad \text{……..equation-i}$$

Renard et al. (1997) describes the equation in the following way:

A is expressed in T ha^{-1} yr^{-1} (or T $acre^{-1}$ yr^{-1} in imperial units) and is the computed spatial and temporal average soil loss per unit area.

R is the rainfall erosivity factor (MJ mm ha^{-1} h^{-1} yr^{-1}).

K is the erodibility factor (T h MJ^{-1} mm^{-1}) that depends on the soil loss rate per erosion index unit for a specified soil for a standard plot.

L is the slope length factor.

S is the slope steepness factor.

C is the cover management factor.

P is the support practice factor.

The R, K, and LS factors determine the erosion rate while the C and P factors are reduction factors ranging between 0 and 1 (Meusburger et al. 2010).

1.4.2.1 Rainfall-runoff erosivity factor (R)

R is the rainfall erosivity factor that represents an average annual value of aggressiveness of rain to cause erosion (Lal, 1990, in (Kouli et al. 2009). It is the total storm energy (E) for the maximum 30 minute intensity (I_{30}) calculated for each rainstorm for a particular period (Kouli et al. 2009, Renard et al. 1997). However, it could be calculated from the average annual rainfall

due to the lack of detailed rainstorm data that is suggested in RUSLE, and mean monthly rainfall amount has also been used in USLE (Renard et al. 1997). This factor is considered as the most influential for soil erosion in different studies using RUSLE throughout the world (Kouli et al. 2009, Wischmeier and Smith 1978). Renard and Freimund (1994) developed the following power relationship to estimate rainfall erosivity as a function of average annual precipitation (mm) for the Continental U.S. (where *R* is the rainfall erosivity factor and *P* is the mean annual rainfall (mm)).

$$\boldsymbol{R = 0.04830\ P^{1.510}}$$

Bewket and Teferi (2009) measured rainfall erosivity using monthly recorded rainfall data from three meteorological stations for a 14 year time period (1993-2007). In their study, the following equation developed by Hurni (1985) was followed to estimate R factor from annual total rainfall:

$$\boldsymbol{R = -8.12 + 0.562P}$$

The R factor was estimated at 1226.4 and 1799.6 MJ mm ha^{-1} h^{-1} y^{-1} for the Therisso and Keritis watersheds, respectively (Kouli et al. 2009). Angima et al. (2003) calculated R factor 8527 MJ mm $ha^{-1}h^{-1}y^{-1}$ for Kianjuki catchment in central Kenya. And Torri et al. (2006) developed the following linear relationship between rainfall erosivity and annual rainfall (mm) in Italy.

$$\boldsymbol{R = -944 + 3.08P}$$

1.4.2.2 Soil erodibility factor (K)

The soil erodibility factor is the soil loss rate per erosion index unit for a specific soil plot, which is 22.1 m in length of with a uniform slope of 9 % continuously in clean tilled fallow (Renard et al. 1997). It reflects the soil detachment process that is generated by the impact of splash or surface flow, and it estimates the influence of soil properties on soil. K depends on soil texture (M), organic matter (OM), soil structure (1<s<4), and permeability or infiltration capacity (1<p<6) (Morschel and Fox 2004, Renard et al. 1997). The value of K factor ranges from 0 to 1 (Bewket and Teferi 2009).

$$\boldsymbol{K = 2.8 \times 10^{-7} M^{1.14}(12 - MO) + 4.3 \times 10^{-3}(s - 2) + 3.3 \times 10^{-3}(p - 3)}$$

Where, **M** is the product of the primary particle size fraction; Wischmeier and Smith (1978) proposed a particle size parameter, M = (% of silt + fine sand) (particles of 0.1-0.002 mm) × (100 – clay (%)), where silt fraction does not exceed 70%. Soil texture has a significant impact on K. Fine textured soils with a high clay contents have low K values, ranging from 0.05 to 0.15, because of their high resistance to detachment. However, coarse textured soils, such as sandy soils have low K values, ranging from 0.05 to 0.2. Medium textured soil such as silt loams have moderate K values, ranging from 0.25 to 0.4. **OM** is the percentage of organic matter. High contents of organic matter can decrease erodibility of soil reducing the susceptibility to $\times 10-7M1.1412-MO+4.3 \times 10-3\ (s-2)+3.3 \times 10-3(p-3)$*s* refers to soil structural class: (1) very structured or particulate, (2) fairly structured, (3) slightly structured and (4) solid. And *p* indicates profile permeability codes: (1) rapid, (2) moderate to rapid, (3) moderate, (4) moderate to slow, (5) slow and (6) very slow (Meusburger et al. 2010).

1.4.2.3 Topographic factor (slope length and steepness – LS)

The LS factor describes the combined effects of slope length (***L***) and gradient (***S***). These factors reflect the effects of topography on soil erosion (Fu et al. 2006). Slope length (***L***) can be measured as the horizontal distance from the origin of overland flow to where deposition begins or runoff becomes concentrated (Wischmeier and Smith 1978, Renard et al. 1997). Renard et al. (1997) describe a practical slope length limit of 122 m in many situation, which can occasionally be longer (up to 305 m). L is estimated with the following equation:

$$\boldsymbol{L = (\lambda / 22.1)^{m}}$$

Where, **22.1** is the plot length in meter, $\boldsymbol{\lambda}$ is horizontal projection of slope length, m is a variable slope-length exponent related to the ratio of rill to interrill erosion and is measured by the following equation:

$$\boldsymbol{m = \beta / (1 + \beta)}$$

Where, $\boldsymbol{\beta}$ is the ratio of rill to interrill erosion which is principally caused by raindrop impact.

$$\boldsymbol{\beta = (sin\theta / 0.0896)\ /\ [3.0(sin\theta)^{0.8} + 0.56]}$$

Where, θ is the slope angle (°).

S is the slope steepness factor which is the ratio of soil erosion from the field slope gradient to soil erosion from a 9 % slope under the same conditions. It represents the effect of slope steepness on soil erosion.

$$S = 10.8 \sin\theta + 0.03 \qquad S < 9\ \%$$

$$S = 16.8 \sin\theta - 0.5 \qquad S < 9\ \%$$

The shape of a slope also affects the average soil loss that can be 30% greater for a convex slope than that for a uniform slope with the same steepness (Renard et al. 1997). The range of the LS factor was calculated for 30 different segments in 5-55% slope gradients for three different land use types and it ranged from 0.8 to 17(Angima et al. 2003). LS ranged from 0 to 118 in Kouli et al. (2009).

1.4.2.4 Cover management factor (C)

C is the land cover management factor which is used in RUSLE to estimate the effects of cropping and management practices on erosion rates (Renard et al. 1997). This factor considers various tillage systems, crop rotations, fertility treatments, and crop residue management (Renard et al. 1997). In addition, it highlights the effect of soil conservation plans and their impact on average soil loss during various conservation and management schemes to decrease soil erosion. The published values of C range from 0.0005 for 100% forest coverage to 1 for bare soil (Meusburger et al. 2010 in US Department of Agriculture, 1977). Novara et al. (2011) calculated the average C factor value, and it ranged from 0.09 to 0.23 for different Sicilian vineyards. C factor values for various land covers in different study are presented in Table 0.1.

Table 0.1: C factor values for different land cover categories

Land cover types	C factor values	References
Corn-bean 1 year rotation	0.415	Angima et al. 2003
Coffee	0.415	Angima et al. 2003
Banana	0.122	Angima et al. 2003
Cultivated land (barley, oats and wheat)	0.150	Bewket and Teferi 2009

Broad-leaved forest	0.130	Kouli et al. 2009
Fruit trees and berry plantation	0.180	Kouli et al. 2009
Mixed forest	0.180	Kouli et al. 2009
Vineyards	0.300	Kouli et al. 2009
Pastures	0.540	Kouli et al. 2009
Natural grassland	0.540	Kouli et al. 2009
Bare rocks	0.870	Kouli et al. 2009
Residential	0.003	Fu et al. 2006
Mixed rangeland	0.011	Fu et al. 2006
Cropland and pasture	0.150	Fu et al. 2006
Maize	0.420	Millward and Mersey 1999

1.4.2.5 Conservation practice (P)

The positive impact of runoff management controls that change the direction, speed, and amount of runoff, particularly the effect of contouring and tillage practices on soil erosion, is quantified by the P factor (Renard et al. 1997). Some traditional P factors used in agricultural practices are: buffer strips, filter strips, rotation strip cropping, terraces, contour tillage, and sub-surface drainage (Renard et al. 1997). The P factor is set to 1 where there are no erosion control practices.

1.5 Objectives

Most of the studies dealing with the prediction of soil erosion focus on crop lands throughout the World, whereas vineyards in the French Mediterranean area have been much less studied. The main objective of this study is to estimate the evolution in soil erosion in the Giscle catchment over time as vineyard areas have evolved (1950-2011) and are expected to change in the coming years (to 2025) using the RUSLE model.

2. Methods

2.1 Site description

The Giscle watershed is located in SE France and is described in Fox et al. (2012). It covers about 235 km² and has a sub-humid Mediterranean climate with a long dry season. Mean annual temperature reaches 27°C in the summer and 11°C in the winter, and the mean annual rainfall over the last 31 years was about 895 mm. Rainfall mostly occurs in spring and autumn, intensifies from October to January in the peak rainy season and a short season in April.

Grape production is the main agricultural activity in the catchment. Most of the vineyards in the study area are planted in straight rows and are oriented in the slope direction on steeper slopes and perpendicular to slope at gentler inclinations, as described below. Vineyards represent about 10% of catchment area (Roy et al. 2014b). They are located mostly in the sandy floodplain and have spread under urban pressure onto steeper slopes in recent years (from 2003) where soils are thin, slightly acidic, stony, and of sandy texture (Fox et al. 2006, Roy et al. 2014b). Soil texture in most of the vineyards is the following: 60-80% sand, 10-30% silt and 5-15% clay (De Coster 2013). Most of the vineyards in the catchment are affected by heavy rainfall in the winter as can be seen in Figure 0.1.

Figure 0.1: Vineyard affected by heavy rainfall (Photos: D. Fox)

2.2 Erosion estimation using RUSLE

Among the available models, RUSLE was applied in the study, data requirements are easier to satisfy compared to the deterministic models and it has been widely tested throughout the world, including in Mediterranean vineyards, as described above. The RUSLE module in IDRISI

estimates average annual soil loss and determines spatial patterns of soil loss (Eastman 2012). The model was run using a 25 m DEM. The soil erodibility (K), rainfall erosivity (R), land cover management (C), and conservation practice factors (P) were specified for 1950, 1982, 2003, and 2011 to estimate soil erosion. As described in earlier chapters, land cover maps of 1950, 1982, 2003, and 2011 were digitized from aerial photographs. Threshold values (described below) were held constant for all simulations. In addition, erosion rates were predicted for the simulated 2025 land cover map.

2.2.1 RUSLE parameters for soil erosion estimation

2.2.1.1 Rainfall-runoff erosivity (R)

In the absence of rainfall intensity data, R was estimated from mean annual rainfall. Daily rainfall recorded by a local weather station (Cogolin) from 1975 to 2005 (31 years) was used to estimate rainfall erosion index (R). Torri et al. (2006) calculated R for a region in Tuscany and his equation was used to compute R for this study; and then the value was converted to imperial units. Rainfall and runoff erosivity R-factor was estimated from the average annual rainfall of 895 mm in 1975-2005 which gave an R value of 107 MJ mm yr/ha/h.

2.2.1.2 Soil erodibility (K)

A soil map of the watershed was generated from soil data obtained from the local wine-making cooperative. In all, 24 soil samples were obtained, and soil structure and texture data were classified by De Coster (2013). The soil erodibility factor *K* was calculated for these plots following the equation described above from Wischmeier and Smith (1978). A point layer was created using calculated K values and then surface interpolation was applied using 'digital elevation model interpolate' option and the point layer to create a raster layer for the whole catchment area. K was expressed in SI units (T h MJ^{-1} mm^{-1}) then it was converted to imperial units (ton. acre $^{-1}$ per erosion index unit) by multiplying by 7.59 (Renard et al. 1997). The higher value of *K* shows less resistance to erosion and generates greater soil erosion rates.

2.2.1.3 Topographic factor (LS)

RUSLE in IDRISI calculates the LS factor automatically from the 25 m digital elevation model (DEM). Slope and aspect thresholds used were 5% and 180°. The maximum slope length

indicates the distance from the erosion starting point to the deposition point. Maximum slope length selected was 80 m. The slope and aspect thresholds were used to divide the whole surface into homogeneous topographic patches. The smallest patch size selected was 5000 m^2 for each date.

2.2.1.4 Cover management (C)

The cover management factor for vineyard was 0.3, following the scientific literature (Table 0.1).

2.2.1.5 Conservation practice (P)

The alignment of vineyard rows, which are perpendicular to slope in most of the vineyards in the catchment area. This arrangement of vineyard rows contributes to slow flow velocity, trap sediments, and reduce erosion compared to a bare surface. Therefore, the P value was set at 0.7 except for terraces. From field observations in study area, it was noted that terraces are found on most slopes above 10%. Therefore, vineyards at all slopes above 10% were considered as terraced and attributed a P value of 0.2.

2.2.2 Soil erosion mapping and validation

Soil erosion maps were predicted for 1950, 1982, 2003, 2011, and 2025, and erosion values were subsequently simplified into three categories: <10, 10-25, and >25 t/ha as low, medium, and high erosion, respectively.

During two consecutive rainy winters, field observations were made of erosion phenomena. Data were collected from different randomly selected vineyards, and the number and size of rills was noted as well as any signs of sediment deposition. Unfortunately, the data were lost in the time of my moving to Toronto. Results presented here are therefore not validated and their publication must await the renewal of field observations.

2.3 Land cover prediction for 2025

The module describing LCM was presented in Chapter 3 for prediction of 2011. To predict 2025, the historical images used were 2003 and 2011. Explanatory variables were the same as in Chapter 3 and correspond to driver variables identified in Chapter 2: altitude, slope, and distances

from roads, built area, and streams. In addition, the PLU was converted to a constraints/incentive layer where land cover restrictions (no building, protected agricultural, protected natural areas) were attributed conversion probabilities of 0; incentives (planned urban developed areas) were integrated by increasing the transition probabilities by 10 %. Only transition probabilities with accuracy rates greater than 70% were included in the model. These were the following: forest to vineyard, forest to grassland, forest to built area, vineyard to built area, and grassland to built area.

3. Results and discussion

The results are described in the following order: the overall trends in vineyard changes over the study period, soil erosion factors, description of soil erosion in the catchment and impact of land cover change on soil erosion.

3.1 Changes in vineyard area

Figure 0.2 shows that total vineyard area declined by around 35% in 1950-2011 due to urbanization in the plain (Roy et al. 2014b). Vineyard suddenly dropped in 1982-2003 by around 30% of its cover, and then it continued to decrease, but at a much slower rate.

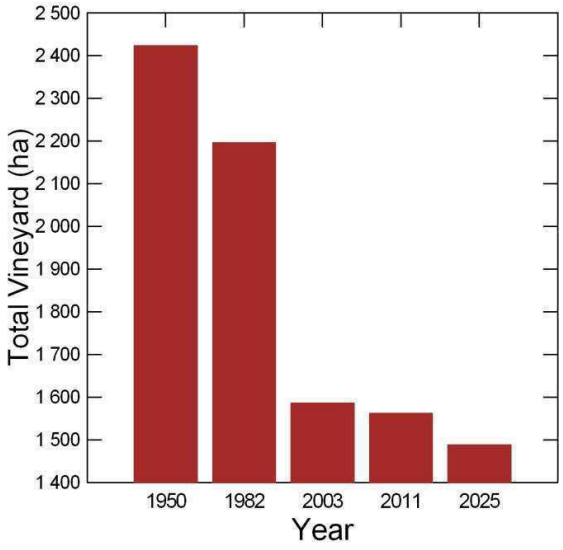

Figure 0.2: Vineyard changes in the study area in 1950-2025 (predicted)

3.2 Soil erosion factors in the catchment

The K and P factors for 2011 are presented in Figure 0.3a and 3b. Most of the soils of the catchment were similar: 22 soil samples were sandy and very sandy, and K factors ranged from 0.52 to 0.028 Mg h $MJ^{-1}mm^{-1}$ for these soils.

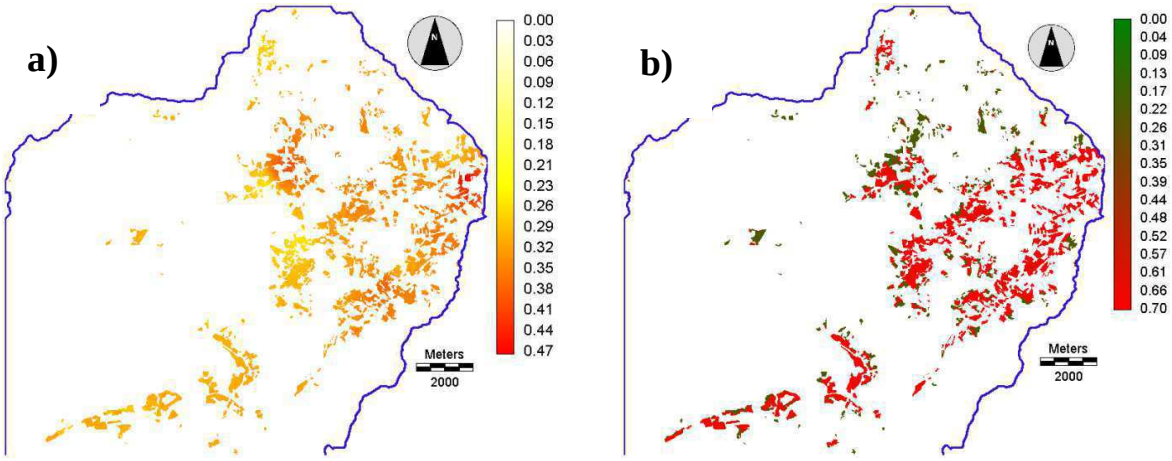

Figure 0.3: a) K factor and b) P factor for 2011

Mean slope was 5.9% in 1950 and increased to 6.9% and 8.1% in 1982 and 2003, respectively (Figure 0.4). However, it declined slightly to 7.1% in 2011 and increased to 7.6% in 2025 (median slope values followed similar trends). Increasing trends in the mean and median values justify that new vineyards were built in 1950-2003 on steeper slopes. In 2003-2011, change in slope was negligible. The 2025 prediction shows an increase in slope, but this value is probably overstated.

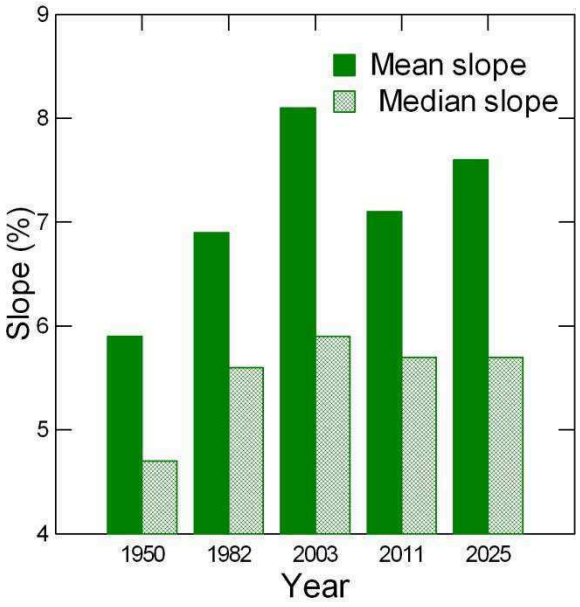

Figure 0.4: Mean and median slope values for different years

Mean and median slope lengths are presented in (Figure 0.5). Mean length declined rapidly from 197.6 m to 116.3 m in 1950-2003 and remained stable in 2003-2025. Median slope length decreased steadily from 125 m to 85.4 m in 1950-2025 (stable in 2003-2011). The difference in mean and median trends in 2025 suggests that slope lengths had more extreme values in the simulated land cover.

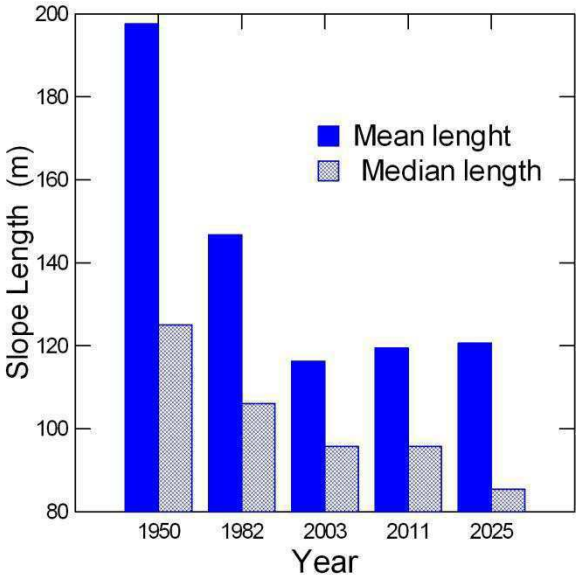

Figure 0.5: Mean and median slope length values for different years

Figure 0.6 presents terraced and non-terraced vineyards in different years. Terraces have a direct impact on the P factor where terraced slopes have a value of 0.2 and non-terraced fields are 0.7. Terraced area increased from 510 ha to 555 ha in 1950-1982, it decreased sharply to 458 ha as total vineyard area also dropped in 2003. After a drop to 410 ha in 2011, the predicted value rises sharply to 590 ha in 2025. Non-terraced area decreased sharply in 1950-2003 with the overall loss of vineyard area described in Chapter 2. Values are stable in 2003-2011 and simulated area decreases slightly in 2025. The percentage of terraced vineyard area (terraced area / total area * 100) increased from about 21% in 1950 to 25% and 29% in 1982 and 2003, respectively. In 2011 it was 26%, and the predicted 2025 value is estimated at 40% of vineyard area. Changes in the terraced vineyard shows the shift of vineyards under urban pressure (described in Chapter 2) from the alluvial plain to steeper slope areas. This is coherent with land cover change dynamics discussed in this thesis. However, the very high terraced area predicted for 2025 is clearly exaggerated and values for this prediction must be taken with circumspection.

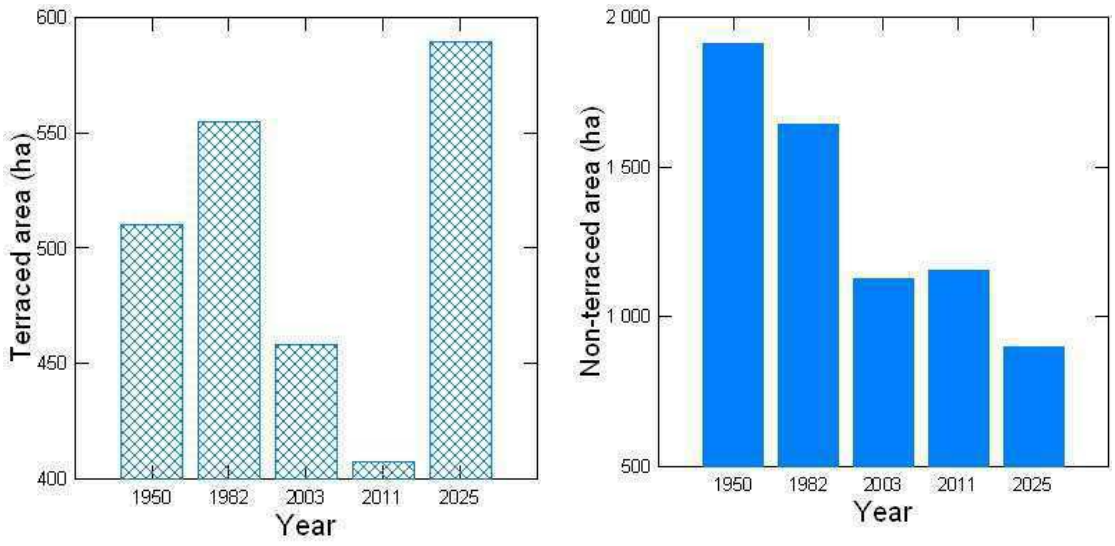

Figure 0.6: Terraced and non-terraced vineyard area in different years

3.3 Soil erosion in the catchment

The mean soil erosion rates for different years are presented in Figure 0.7. This value increased from 11.8 T ha^{-1} yr^{-1} to 13.2 T ha^{-1} yr^{-1} in 1950-1982, and it reached to 14.4 T ha^{-1} yr^{-1} in 2003. However, soil erosion rates dropped to 13.5 t/ha/yr and 11.8 t/ha/yr, in 2011 and 2025, respectively. These trends are related to both increases in slope inclination in the earlier period in particular (increasing S factor) and the proportion of slopes on terraced land described above. Values cited are comparable to those of Cerdan et al. (2010) who analysed soil erosion rates for both Mediterranean vineyards and in Europe globally. For vineyards, mean erosion was about 8.6 T ha^{-1} yr^{-1}.

Vineyard area in different soil erosion classes is presented in Figure 0.8a. The area of low erosion rate gradually decreased from 1238 ha to 646 ha in 1950-2003. However, it increased to 713 ha in 2025 as a greater proportion of the fields found itself on terraced slopes. The area of medium erosion rate also sharply declined from 956 ha to 717 ha in 1982-2003; it remains relatively stable afterwards. Decreasing trend in low and medium erosion rate might be occurred due to the depletion in vineyard in the plain land. The area of high soil erosion rate increased by around 35 ha (are you talking about how much it was increased, or you can give the actual increased amount like before or after values) in 1950-1982 from 209 ha in 1950, and then gradually decreased to 180.4 ha in 2011, respectively (not necessary here). However, it rapidly

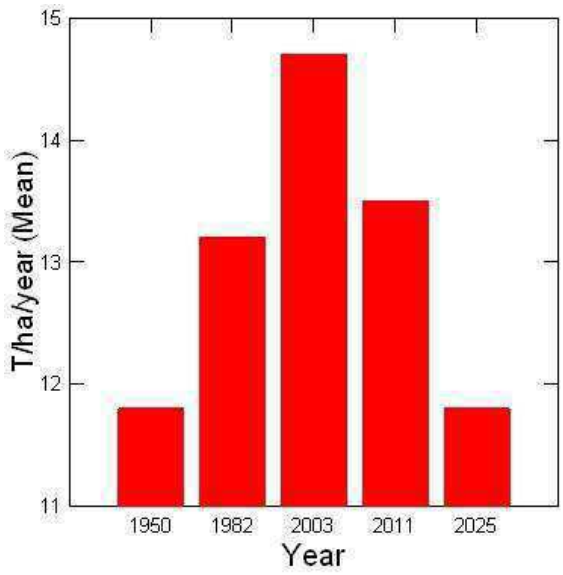

Figure 0.7: Erosion rate (t/ha/yr) in different years.

decreased to 71.6 ha in 2025. Use of terraces in vineyard played a significant role to decrease medium and high soil erosion rates after 1982.

The proportion of vineyard in each erosion class for different study years is presented in Figure 0.8b. The proportion of low erosion rate decreased from 51.1% to 40.8%, and the

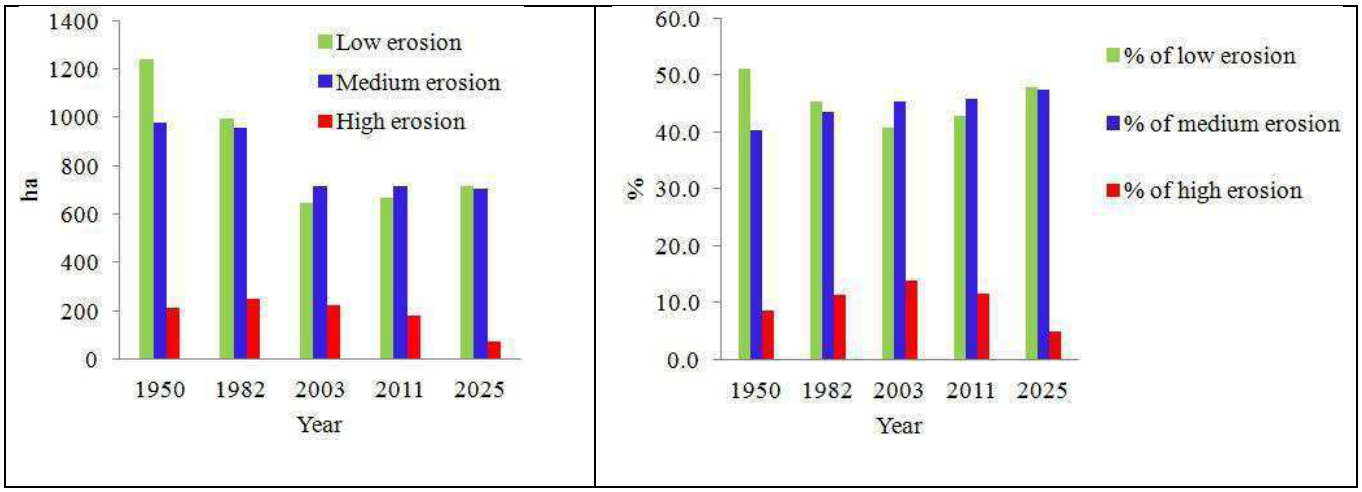

Figure 0.8: a) Area of soil erosion classes in different year, b) % of vineyard in different erosion classes.

proportion of medium and high erosion rate increased from 40.3% and 8.6% to 45.3% and 14%, respectively in 1950 to 2003. The high erosion rate shown in Figure 5.7 is therefore the result of the percentage of medium and high erosion rates in Figure 5.8b. The shift to lower rates after 2003 (Figures 5.7 and 5.8b) corresponds to the decrease in slope (Figure 5.4) noted above. The low erosion rates in Figure 5.7 and relatively low percentage of high erosion area shown in Figure 5.8b for 2025 result from the artificially high proportion terraced fields described above. The erosion rate for 2025 is certainly much lower than what could be expected.

The soil erosion maps in different years (1950, 1982, 2003, and 2011) are presented in Figure 0.9a-e. The eastern part remains dominated by low erosion rates between 1950 and 2011, and is characterized with low slope and high rates of conversion trend from vineyard to built area. Hence, the eroded area shrinks over time. Much of the ‘moderate’ and ‘high’ erosion area also decreased in 1950-2011 but to a lesser extent than the low erosion category. The moderate and high erosion areas tend to be concentrated on the periphery of the low class zone and in the north-central area.

Total erosion in different years is presented in Figure 0.10. Total soil loss represents the amount of sediment that can potentially be injected into the stream network, causing problems for aquatic biodiversity and channel navigation in the ports downstream. It is the product of the vineyard area times mean soil erosion rate. These two trends were opposite in 1950-1982, where vineyard area decreased substantially and mean erosion rate increased as fields were moved out of the alluvial plain and onto steeper foothills; therefore, total erosion remained constant in this period. After 1982, the great loss in vineyard area (Figure 5.2) outweighed the increase in mean erosion rate (Figures 5.7 and 5.8) and provoked a net loss in total soil erosion (Figure 5.10). After 2003, vineyard area remained stable and mean erosion rates decreased only slightly with less than a 10% decrease. Figure 5.10 shows a substantial decrease in total erosion for the simulated landscape of 2025, but as described above, this value is probably underestimated.

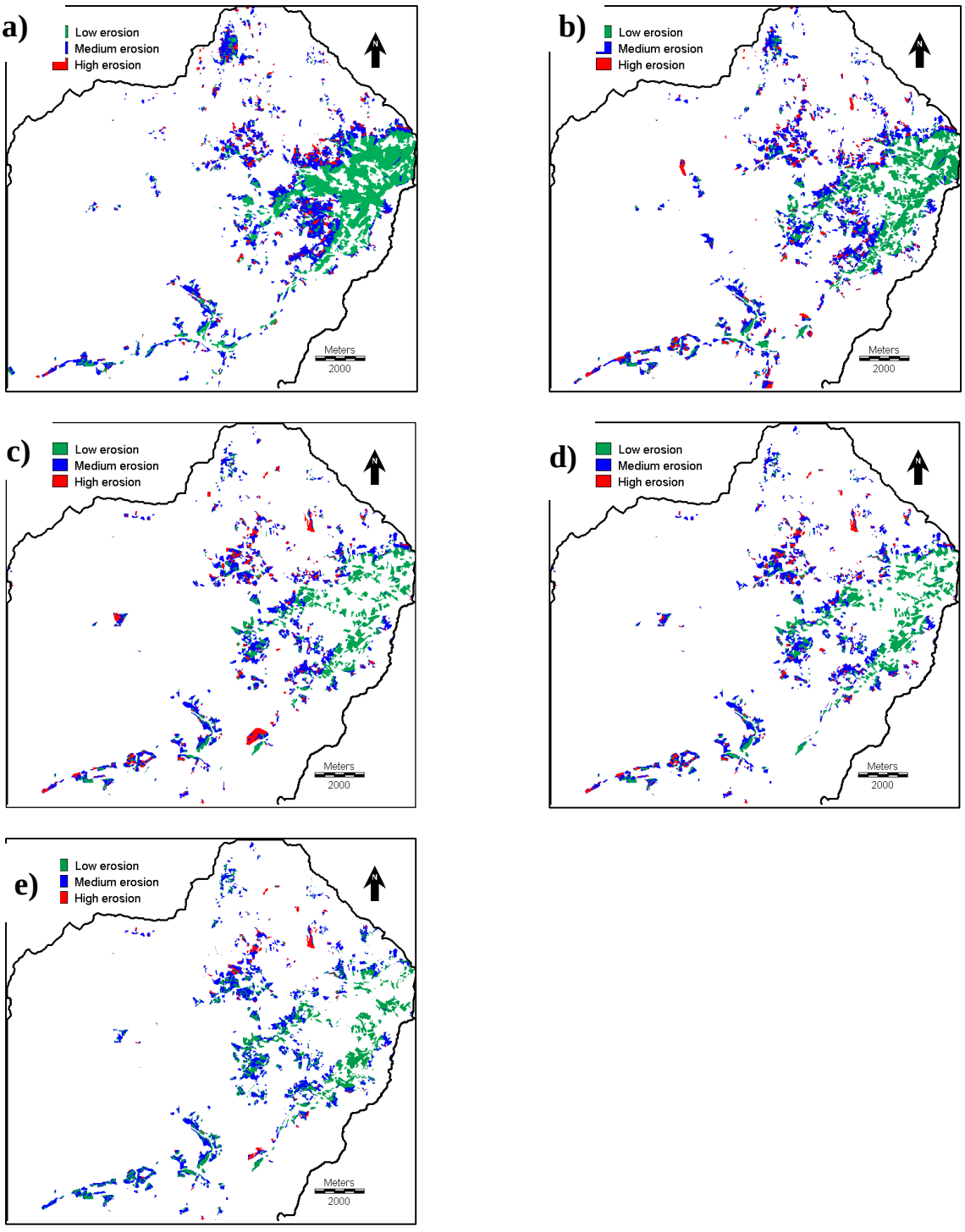

Figure 0.9: a) soil erosion map for 1950, b) soil erosion map for 1982 c) soil erosion map for 2003, d) soil erosion map for 2011, and e) soil erosion map for 2025.

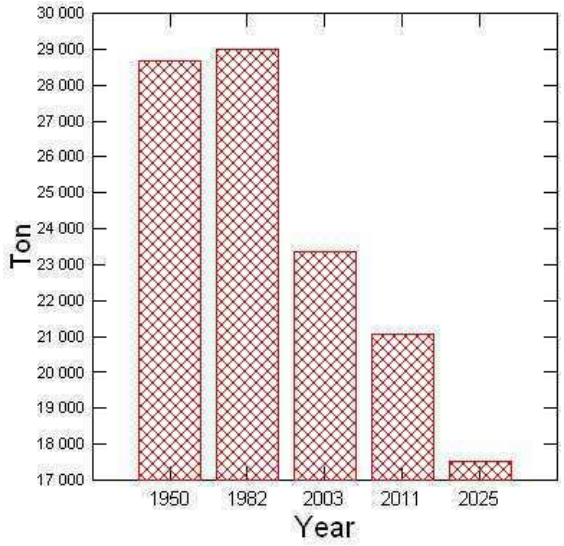

Figure 0.10: Total erosion in 1950-2025

4. Conclusions

The study quantified the impact of land cover change on soil erosion in vineyards in the Cogolin catchment in SE France in 1950-2011 where RUSLE was used in the IDRISI GIS environment to create and compare soil erosion maps of 1950, 1982, 2003, and 2011. Finally, a soil erosion map was created using predicted vineyard for 2025. Vineyard area decreased while mean erosion rates increased in the 1950 to 2003 time interval. This period represents the phase where change occurred rapidly due to strong urban pressure in the alluvial plain and a shift of vineyards to steeper slopes. Total erosion was stable in 1950-1982 and then decreased progressively, due mainly to the loss in vineyard area and a stabilization in the clearing of steeper slopes. Total erosion in 2011 represents about 75% of erosion in 1950-1982. Predicted erosion rates for 2025 are probably underestimated as the LCM model continued to move vineyards onto steeper slopes where terracing reduces estimated erosion rates.

GENERAL CONCLUSION

SYNTHESIS

This study makes a significant contribution to the current knowledge of land cover change in the Giscle catchment from 1950 to the present. A complex pattern of land cover change was observed in the catchment across various spatial and temporal dimensions. Marginal lands on steeper slopes were converted from forest to vineyard and vineyard terraces on foothills above the alluvial plain. This finding differs from the most frequently cited previous studies of land cover change in the Mediterranean region, which have tended to show the opposite, namely the abandonment of agriculture on marginal lands and their conversion to forest.

The tendency for cities to grow onto agricultural land is common throughout the world and in the Mediterranean area (Serra et al., 2008, Sluiter and de Jong, 2007). However, the conversion of vineyard to grassland in conjunction with urban expansion found in this study is much less common. Abandoned vineyard fields generally belonged to owners who did not produce their own wine, but brought their grapes to a winemaking cooperative. Grape production was therefore not necessarily as central to their livelihood as it would be for the winemaking *domaines*. When land is passed on from one generation to the next, grape production can be abandoned but the land retained. This explains some of the conversion from vineyard to grassland and then forest, and it also accounts for the paradoxical situation of agriculture expanding onto marginal lands on steep slopes, while at the same time abandoning fertile land in the alluvial plain to grassland and forest. In addition, the "prime à l'arrachement" in the 1980s contributed to eliminate small producers.

Altitude, slope, and distance from roads had the greatest impact on land cover change amongst all the variables tested. Projected land cover changes suggest that built area and grassland would increase in forest and vineyard areas following the previous historical trends in the catchment. The highest errors were observed in the long time scale prediction. Predicted maps were moderately accurate for the intermediate time scale and the most accurate for the short time scale. For all time scales, the greatest errors were observed in the prediction of grassland cover. The most accurate predictions were derived from the short time scale and the accuracy rate decreased with the increase in time scale. Therefore, the initial time period of 1982-2003 was selected to project land cover for 2011 in order to test the impact of spatial extent and cell size on

land cover change prediction. Then 2003-2011 was selected to predict land cover for 2025 in order to quantify the impact of land cover change on soil erosion.

Analysis of spatial extent found that land cover prediction appeared more accurate in the large zone than in the small. However, predicted land covers for the surface in the small zone are the same for both the small and large zone predictions. No significant impact of cell size on land cover change prediction was found in the study. However, when the downscaled predicted images are compared to the 25 m reference image from 2011, disagreement values respond differently. Quantitative disagreement varies little and even improves slightly at 100 m, but allocation disagreement rises sharply for the 50-25 m and 100-25 m land cover predictions for both the small and large study zones. Finally, a cell size of 25 m was selected to predict soil erosion.

The Giscle catchment was selected to assess the impacts of land use change on soil erosion because of its representative topography, climate, agriculture, and other human activites, which are typical of the Mediterranean region. Although the rate of erosion increased rapidly between 1950 and 2003, and then drops in the 2003-2025 period (actual and predicted), the total erosion was around the same between 1950 and 1982 and gradually decreases in the 2003-2025 period. This decreasing trend of total erosion should result in lower sediment loads in streams within the catchment area. This study shows that the spatial pattern of land cover change has a significant impact on soil erosion. In particular, vineyard areas in this catchment are highly vulnerable to soil erosion. This finding is consistent with other studies in the Mediterranean region (Kosmos et al., 1999; Cerdan et al., 2010). The ‘high’ and ‘moderate’ soil loss categories had increased by 2003 but then decreased by 2011. One explanation for this would be the gradual decrease in vineyard that occurred between 1950 and 2011. In addition, while new vineyards had appeared in the high slope areas by 2011, these were terraced and thus less prone to soil erosion.

In general, soil erosion prone areas increased in the central parts of the study area during the period of this study. By contrast, there was decreased soil erosion in the eastern part of the catchment due to land cover change from vineyard to built area in the alluvial plain area. Slope plays a significant role in soil erosion. Mean slope values increased moderately throughout the study period, whereas median slope remained more or less constant after 1982. This reflects the decrease of vineyard areas in the alluvial plain and the increase of vineyard areas in the upland valley and foothills between 1950 and 2003.

This issue has become very important, not only to researchers, but also to urban planners and environmentalists advocating and planning for sustainable land cover in the future.

LIMITATIONS OF THIS STUDY

The findings of this study on land cover change and soil erosion in the Gislce catchment can be helpful to government policy-makers, urban planners and activists advocating and planning for sustainable economic and social development and environmental protection in the future.

The limitations of this thesis include the following:

- The aerial photographs of 1950 were the first high quality post-WWII photos available when the area was still strongly rural. Intermediate dates (1982, 2003) were selected between 1950 and the most recent photographs (2008, 2011), due to the lack of aerial photographs from 1990 and 2000.
- The research findings presented in the soil erosion chapter are not yet validated and their publication must await field validation.

SUGGESTIONS FOR FUTURE RESEARCH

- Different land cover change and soil erosion models can be applied to this catchment and the entire PACA region taking into account individual land cover and multiple land cover categories.
- Additional plot-based research is needed to determine soil erosion to develop a sustainable erosion mitigation plan.
- The impact of land cover change on climate change in Southern France merits further research.

REFERENCES

Abu Hammad, A. and Tumeizi, A. 2012. Land degradation: socioeconomic and environmental causes and consequences in the eastern Mediterranean. *Land Degradation & Development,* 23(3), 216-226.

Agarwal, C.*, et al.*, 2002. *A review and assessment of land-use change models: dynamics of space, time, and human choice.* Newton Square, PA: United States Department of Agriculture.

Aguejdad, R., 2009. *Etalement urbain et évaluation de son impact sur la biodiversité, de la reconstitution des trajectoires à la modélisation prospective. Application à une agglomération de taille moyenne : Rennes Métropole.* (Ph. D.). Université Rennes 2 Haute-Bretagne.

Aguejdad, R. and Houet, T., Modeling of urban sprawl using the land change modeller on a French Metropolitan area (Rennes): Forsee the unpredictable. ed. *Symposium "Spatial landscape modelling: from dynamic approaches to functional evaluations"*, 2008 Toulouse, 2.

Ahmed, B. and Ahmed, R. 2012. Modeling Urban Land Cover Growth Dynamics Using Multi‐Temporal Satellite Images: A Case Study of Dhaka, Bangladesh. *ISPRS International Journal of Geo-Information,* 1(1), 3-31.

Aldwaik, S. Z. and Pontius Jr, R. G. 2012. Intensity analysis to unify measurements of size and stationarity of land changes by interval, category, and transition. *Landscape and Urban Planning,* 106(1), 103-114.

Alemayehu, T.*, et al.*, 2006. Land use change detection as a basis for analysing desertification processes: A case study in Tabernas (Almeria, Spain). *In:* Kepner, W.*, et al.* eds. *Desertification in the Mediterranean Region. A Security Issue.* Springer Netherlands, 341-352.

Alkharabsheh, M. M.*, et al.* 2013. Impact of Land Cover Change on Soil Erosion Hazard in Northern Jordan Using Remote Sensing and GIS. *Procedia Environmental Sciences,* 19(0), 912-921.

Alo, C. A. and Pontius Jr, R. G. 2008. Identifying systematic land-cover transitions using remote sensing and GIS: the fate of forests inside and outside protected areas of Southwestern Ghana. *Environment and Planning B: Planning and Design,* 35(2), 280-295.

Álvarez Martínez, J.-M., Suárez-Seoane, S. and De Luis Calabuig, E. 2011. Modelling the risk of land cover change from environmental and socio-economic drivers in heterogeneous and changing landscapes: The role of uncertainty. *Landscape and Urban Planning,* 101(2), 108-119.

Angima, S. D.*, et al.* 2003. Soil erosion prediction using RUSLE for central Kenyan highland conditions. *Agriculture, Ecosystems & Environment,* 97(1–3), 295-308.

Antrop, M. 2005. Why landscapes of the past are important for the future. *Landscape and Urban Planning,* 70(1–2), 21-34.

Araya, Y. H. and Cabral, P. 2010. Analysis and Modeling of Urban Land Cover Change in Setúbal and Sesimbra, Portugal. *Remote Sensing,* 2(6), 1549-1563.

Arnaez, J.*, et al.* 2007. Factors affecting runoff and erosion under simulated rainfall in Mediterranean vineyards. *Soil and Tillage Research,* 93(2), 324-334.

Baccaini, B. and Sémécurbe, 2009. *La croissance périurbaine depuis 1945.* INSEE.

Bakker, M. M.*, et al.* 2005. Soil erosion as a driver of land-use change. *Agriculture, Ecosystems & Environment,* 105(3), 467-481.

Baldock, D.*, et al.*, 1996. *Farming at the Margins: Abandonment Or Redeployment of Agricultural Land in Europe.* Institute for European Environmental Policy.

Balzter, H. 2000. Markov chain models for vegetation dynamics. *Ecological Modelling,* 126(2–3), 139-154.

Barredo, J. I.*, et al.* 2003. Modelling dynamic spatial processes: simulation of urban future scenarios through cellular automata. *Landscape and Urban Planning,* 64(3), 145-160.

Basharin, G. P., Langville, A. N. and Naumov, V. A. 2004. The life and work of A.A. Markov. *Linear Algebra and its Applications,* 386(0), 3-26.

Batty, M., Xie, Y. and Sun, Z. 1999. Modeling urban dynamics through GIS-based cellular automata. *Computers, Environment and Urban Systems,* 23(3), 205-233.

Benenson, I. and Torrens, P. M., 2004. *Geosimulation: Automata-based modeling of urban phenomena.* First ed. Chichester: John Wiley & Sons Ltd.

Benoit, G., 2001. *Urbanization in the Mediterranean Region from 1950-1995.* Sophia Antipolis: Plan Blue.

Benoit, G. and Comeau, A., 2005. *A Sustainable Future for the Mediterranean:The Blue Plan's Environment & Development Outlook.* London.

Berberoglu, S. and Akin, A. 2009. Assessing different remote sensing techniques to detect land use/cover changes in the eastern Mediterranean. *International Journal of Applied Earth Observation and Geoinformation,* 11(1), 46-53.

Bewket, W. and Teferi, E. 2009. Assessment of soil erosion hazard and prioritization for treatment at the watershed level: Case study in the Chemoga watershed, Blue Nile basin, Ethiopia. *Land Degradation & Development,* 20(6), 609-622.

Blavet, D.*, et al.* 2009. Effect of land use and management on the early stages of soil water erosion in French Mediterranean vineyards. *Soil and Tillage Research,* 106(1), 124-136.

Bohnet, I. C. and Pert, P. L. 2010. Patterns, drivers and impacts of urban growth—A study from Cairns, Queensland, Australia from 1952 to 2031. *Landscape and Urban Planning,* 97(4), 239-248.

Bonilla, C. A., Reyes, J. L. and Magri, A. 2010. Water Erosion Prediction Using the Revised Universal Soil Loss Equation (RUSLE) in a GIS Framework, Central Chile. *Chilean journal of agricultural research,* 70, 159-169.

Brady, N. C. and Weil, R. R., 1999. *The nature and properties of soils, 12th edition.* 12 ed. New Jersy: Prentice Hall/ Pearson Education.

Brauch, H. G., 2003. Urbanization and Natural Disasters in the Mediterranean – Population Growth and Climate Change in the 21st Century

In: Kreimer, A., Arnold, M. and Carlin, A. eds. *The Future of Disaster Risk: Building Safer Cities. December 2002.* Washington, 149-164.

Brunetta, G. and Rotondi, G. 1996. Migratory flows from southern to northern Mediterranean borders. *Social Geography,* 133, 65-80.

Cabral, P. and Zamyatin, A., Three land cover change models for urban dynamic analysis in Sintra-Cascais area. ed. *1st EARSeL Workshop of the SIG Urban Remote Sensing* 2006 Humboldt-Universität zu Berlin, 8.

Calvo-Iglesias, M. S., Fra-Paleo, U. and Diaz-Varela, R. A. 2009. Changes in farming system and population as drivers of land cover and landscape dynamics: The case of enclosed and semi-openfield systems in Northern Galicia (Spain). *Landscape and Urban Planning,* 90(3–4), 168-177.

Caraveli, H. 2000. A comparative analysis on intensification and extensification in mediterranean agriculture: dilemmas for LFAs policy. *Journal of Rural Studies,* 16(2), 231-242.

Casalí, J.*, et al.* 2010. Sediment production and water quality of watersheds with contrasting land use in Navarre (Spain). *Agricultural Water Management,* 97(10), 1683-1694.

Catalán, B., Saurí, D. and Serra, P. 2008. Urban sprawl in the Mediterranean?: Patterns of growth and change in the Barcelona Metropolitan Region 1993–2000. *Landscape and Urban Planning,* 85(3–4), 174-184.

Cerdan, O.*, et al.* 2010. Rates and spatial variations of soil erosion in Europe: A study based on erosion plot data. *Geomorphology,* 122(1–2), 167-177.

Chakroun, H., Bonn, F. and Fortin, J. P., 1993. Combination of single storm erosion and hydrological models into a geographic information system. *In:* Wicherek, S. ed. *Farm Land Erosion.* Amsterdam: Elsevier, 261-270.

Chaudhuri, G. and Clarke, K. C. 2014. Temporal Accuracy in Urban Growth Forecasting: A Study Using the SLEUTH Model. *Transactions in GIS,* 18(2), 302-320.

Chen, H. and Pontius, R., Jr. 2010. Diagnostic tools to evaluate a spatial land change projection along a gradient of an explanatory variable. *Landscape Ecology,* 25(9), 1319-1331.

Chen, H. and Pontius, R., Jr. 2011. Sensitivity of a Land Change Model to Pixel Resolution and Precision of the Independent Variable. *Environmental Modeling & Assessment,* 16(1), 37-52.

Chevigny, E.*, et al.* 2014. Lithology, landscape structure and management practice changes: Key factors patterning vineyard soil erosion at metre-scale spatial resolution. *CATENA,* 121(0), 354-364.

Ciampalini, R., Follain, S. and Le Bissonnais, Y. 2012. LandSoil: A model for analysing the impact of erosion on agricultural landscape evolution. *Geomorphology,* 175–176(0), 25-37.

Clarke, K. C. and Gaydos, L. J. 1998. Loose-coupling a cellular automaton model and GIS: long-term urban growth prediction for San Francisco and Washington/Baltimore. *International Journal of Geographical Information Science,* 12(7), 699-714.

Clarke, K. C., Hoppen, S. and Gaydos, L. 1997. A self-modifying cellular automaton model of historical urbanization in the San Francisco Bay area. *Environment and Planning B: Planning and Design,* 24(2), 247-261.

Cori, B. 1999. Spatial dynamics of Mediterranean coastal regions. *Journal of Coastal Conservation,* 5(2), 105-112.

Coulouma, G.*, et al.* 2006. Effect of deep tillage for vineyard establishment on soil structure: A case study in Southern France. *Soil and Tillage Research,* 88(1–2), 132-143.

Dadhich, P. N. and Hanaoka, S., 2010. Markov method integration with multi-layer perceptron classifier for simulation of urban growth of Jaipur city. *10th WSEAS/IASME international conference on electric power systems, high voltages, electric machines (power '10)) and 6th Wseas international conference on remote sensing (remote '10).* Iwate Prefectural University, Japan, 4-6.

Dangermond, J., 2012. *ESRI, ArcGIS Software* [online]. New York. Available from: http://www.esri.com.

De Coster, A., 2013. *Etude préliminaire de valorisation de compost de résidus verts dans les vignobles la Communauté de Communes de Saint Tropez.* (Master 1). Université Nice Sophia Antipolis.

de Jong, S. M.*, et al.* 1999. Regional assessment of soil erosion using the distributed model SEMMED and remotely sensed data. *CATENA,* 37(3–4), 291-308.

Dietzel, C. and Clarke, K. 2006. The effect of disaggregating land use categories in cellular automata during model calibration and forecasting. *Computers, Environment and Urban Systems,* 30(1), 78-101.

Dietzel, C. and Clarke, K. C. 2004. Spatial Differences in Multi-Resolution Urban Automata Modeling. *Transactions in GIS,* 8(4), 479-492.

Dietzel, C. and Clarke, K. C. 2007. Toward Optimal Calibration of the SLEUTH Land Use Change Model. *Transactions in GIS,* 11(1), 29-45.

Dunjó, G., Pardini, G. and Gispert, M. 2003. Land use change effects on abandoned terraced soils in a Mediterranean catchment, NE Spain. *CATENA,* 52(1), 23-37.

Dewan, A. M. and Yamaguchi, Y. 2009. Land use and land cover change in Greater Dhaka, Bangladesh: Using remote sensing to promote sustainable urbanization. *Applied Geography,* 29(3), 390-401.

EAA, 2011. *Annual report 2010 and Environmental statement 2011* [online]. Luxembourg: European Environment Agency. Available from: http://www.eea.europa.eu/publications/annual-report-2010.

Eastman, J. R., 2012. IDRISI Selva. *Version 17.02.* Worcester, MA.: Clark Labs, Clark University.

El Kateb, H.*, et al.* 2013. Soil erosion and surface runoff on different vegetation covers and slope gradients: A field experiment in Southern Shaanxi Province, China. *CATENA,* 105(0), 1-10.

Engelen, G.*, et al.*, 1999. Dynamic GIS and strategic physical planning support: a practical application. *Geographical information and planning.* Springer, 87-111.

Engelen, G., White, R. and Uljee, I., 1997. Integrating Constrained Cellular Automata Models, GIS and decision support tools for urban planning and policy making. *In:* Timmermans, H. P. J. ed. *Decision Support Systems in Urban Planning.* London: E & FN Spon, 125-155.

Urbanization and Desertification in European Mediterranean Coastal areas: A case study in North-Western Sardinia (Alghero, Italy), 2005. Human Settlement Development.

Evans, T. P. and Kelley, H. 2004. Multi-scale analysis of a household level agent-based model of landcover change. *Journal of Environmental Management,* 72(1–2), 57-72.

Falcucci, A., Maiorano, L. and Boitani, L. 2007. Changes in land-use/land-cover patterns in Italy and their implications for biodiversity conservation. *Landscape Ecology,* 22(4), 617-631.

Fox, D.*, et al.* 2006. Mapping erosion risk and selecting sites for simple erosion control measures after a forest fire in Mediterranean France. *Earth Surface Processes and Landforms,* 31(5), 606-621.

Fox, D. M. and Bryan, R. B. 2000. The relationship of soil loss by interrill erosion to slope gradient. *CATENA,* 38(3), 211-222.

Fox, D. M.*, et al.* 2012. A case study of land cover change (1950–2003) and runoff in a Mediterranean catchment. *Applied Geography,* 32(2), 810-821.

Fu, G., Chen, S. and McCool, D. K. 2006. Modeling the impacts of no-till practice on soil erosion and sediment yield with RUSLE, SEDD, and ArcView GIS. *Soil and Tillage Research,* 85(1–2), 38-49.

Fuller, D., Hardiono, M. and Meijaard, E. 2011. Deforestation Projections for Carbon-Rich Peat Swamp Forests of Central Kalimantan, Indonesia. *Environmental Management,* 48(3), 436-447.

García-Ruiz, J. M. 2010. The effects of land uses on soil erosion in Spain: A review. *CATENA,* 81(1), 1-11.

Geri, F., Amici, V. and Rocchini, D. 2010. Human activity impact on the heterogeneity of a Mediterranean landscape. *Applied Geography,* 30(3), 370-379.

Geri, F., Amici, V. and Rocchini, D. 2011. Spatially-based accuracy assessment of forestation prediction in a complex Mediterranean landscape. *Applied Geography,* 31(3), 881-890.

Guan, D.*, et al.* 2011. Modeling urban land use change by the integration of cellular automaton and Markov model. *Ecological Modelling,* 222(20–22), 3761-3772.

Haase, D., Lautenbach, S. and Seppelt, R. 2010. Modeling and simulating residential mobility in a shrinking city using an agent-based approach. *Environmental Modelling & Software,* 25(10), 1225-1240.

He, C.*, et al.* 2008. Modelling dynamic urban expansion processes incorporating a potential model with cellular automata. *Landscape and Urban Planning,* 86(1), 79-91.

He, C.*, et al.* 2006. Modeling urban expansion scenarios by coupling cellular automata model and system dynamic model in Beijing, China. *Applied Geography,* 26(3–4), 323-345.

Hernández, A. J., Lacasta, C. and Pastor, J. 2005. Effects of different management practices on soil conservation and soil water in a rainfed olive orchard. *Agricultural Water Management,* 77(1–3), 232-248.

Huang, J.*, et al.* 2012. Use of intensity analysis to link patterns with processes of land change from 1986 to 2007 in a coastal watershed of southeast China. *Applied Geography,* 34(0), 371-384.

Huang, Q.-h. and Cai, Y.-l. 2007. Simulation of land use change using GIS-based stochastic model: the case study of Shiqian County, Southwestern China. *Stochastic Environmental Research and Risk Assessment,* 21(4), 419-426.

IFEN, 2009. *LA France, Vue Par Corinne Land Cover.* Commissriat général au développment durable.

IFEN, 2012. *Trois quarts des rivages métropolitains sont non artificialisés.* Commissriat général au développment durable.

INSEE, 2011. [online]. Available from: http://www.insee.fr.

Jantz, C. A., Goetz, S. J. and Shelley, M. K. 2004. Using the SLEUTH urban growth model to simulate the impacts of future policy scenarios on urban land use in the Baltimore - Washington metropolitan area. *Environment and Planning B: Planning and Design,* 31(2), 251-271.

Jenerette, G. D. and Wu, J. 2001. Analysis and simulation of land-use change in the central Arizona – Phoenix region, USA. *Landscape Ecology,* 16(7), 611-626.

Jokar Arsanjani, J.*, et al.* 2013. Integration of logistic regression, Markov chain and cellular automata models to simulate urban expansion. *International Journal of Applied Earth Observation and Geoinformation,* 21(0), 265-275.

Kamusoko, C.*, et al.* 2009. Rural sustainability under threat in Zimbabwe – Simulation of future land use/cover changes in the Bindura district based on the Markov-cellular automata model. *Applied Geography,* 29(3), 435-447.

Kepner, W.*, et al.*, 2006. Desertification in the Mediterranean Region: A Security Issue. Dordrecht: Springer, 617.

Khoi, D. D., 2011. *Spatial modeling of deforestation and land suitability assessment in the Tam Dao National Park region, Vietnam.* (Ph. D.). University of Tsukuba.

Kok, K. and Veldkamp, A. 2001. Evaluating impact of spatial scales on land use pattern analysis in Central America. *Agriculture, Ecosystems & Environment,* 85(1–3), 205-221.

Kosmas, C.*, et al.* 1997. The effect of land use on runoff and soil erosion rates under Mediterranean conditions. *CATENA,* 29(1), 45-59.

Kouli, M., Soupios, P. and Vallianatos, F. 2009. Soil erosion prediction using the Revised Universal Soil Loss Equation (RUSLE) in a GIS framework, Chania, Northwestern Crete, Greece. *Environmental Geology,* 57(3), 483-497.

Koulouri, M. and Giourga, C. 2007. Land abandonment and slope gradient as key factors of soil erosion in Mediterranean terraced lands. *CATENA,* 69(3), 274-281.

Laflen, J. M.*, et al.* 1991. WEPP: Soil erodibility experiments for rangeland and cropland soils. *Journal of Soil and Water Conservation,* 46(1), 39-44.

Lambin, E. F.*, et al.* 2001. The causes of land-use and land-cover change: moving beyond the myths. *Global Environmental Change,* 11(4), 261-269.

Landis, J. R. and Koch, G. G. 1977. The Measurement of Observer Agreement for Categorical Data. *Biometrics,* 33(1), 159-174.

Leh, M., Bajwa, S. and Chaubey, I. 2013. Impact of land use change on erosion risk: an integrated remote sensing, geographic information system and modeling methodology. *Land Degradation & Development,* 24(5), 409-421.

Li, X. and Liu, X. 2008. Embedding sustainable development strategies in agent-based models for use as a planning tool. *International Journal of Geographical Information Science,* 22(1), 21-45.

Li, X. and Yeh, A. G.-O. 2000. Modelling sustainable urban development by the integration of constrained cellular automata and GIS. *International Journal of Geographical Information Science,* 14(2), 131-152.

Li, X. and Yeh, A. G.-O. 2002. Neural-network-based cellular automata for simulating multiple land use changes using GIS. *International Journal of Geographical Information Science,* 16(4), 323-343.

Ligtenberg, A.*, et al.* 2004. A design and application of a multi-agent system for simulation of multi-actor spatial planning. *Journal of Environmental Management,* 72(1–2), 43-55.

Liu, S. L.*, et al.* 2013. Effects of different terrace protection measures in a sloping land consolidation project targeting soil erosion at the slope scale. *Ecological Engineering,* 53(0), 46-53.

Liu, X.*, et al.* 2008. Simulating complex urban development using kernel-based non-linear cellular automata. *Ecological Modelling,* 211(1–2), 169-181.

Liu, Y., 2009. *Modelling Urban Development with Geographical Information Systems and Cellular Automata.* New York: CRC Press, Taylor & Francis Group.

López, E.*, et al.* 2001. Predicting land-cover and land-use change in the urban fringe: A case in Morelia city, Mexico. *Landscape and Urban Planning,* 55(4), 271-285.

Lu, D., *et al.* 2004. Mapping soil erosion risk in Rondonia, Brazilian Amazonia: using RUSLE, remote sensing and GIS. *Land Degradation & Development,* 15(5), 499-512.

Lufafa, A., *et al.* 2003. Prediction of soil erosion in a Lake Victoria basin catchment using a GIS-based Universal Soil Loss model. *Agricultural Systems,* 76(3), 883-894.

Macmillan, W. and Huang, H. Q. 2008. An agent-based simulation model of a primitive agricultural society. *Geoforum,* 39(2), 643-658.

Mahmoodabadi, M. and Cerdà, A. 2013. WEPP calibration for improved predictions of interrill erosion in semi-arid to arid environments. *Geoderma,* 204–205(0), 75-83.

MAP, 2008. *Mediterranean Action plan (MAP) Coastal Area Management Programme (CAMP) Slovenia: Final Integrated Report.* Athens.

Martínez-Casasnovas, J. A., Ramos, M. C. and Ribes-Dasi, M. 2005. On-site effects of concentrated flow erosion in vineyard fields: some economic implications. *CATENA,* 60(2), 129-146.

Martínez-Fernández, J., *et al.* 2013. Sustainability of Mediterranean irrigated agro-landscapes. *Ecological Modelling,* 248(0), 11-19.

Mas, J.-F., Pérez-Vega, A. and Clarke, K. C. 2012. Assessing simulated land use/cover maps using similarity and fragmentation indices. *Ecological Complexity,* 11(0), 38-45.

Mas, J. F., *et al.* 2004. Modelling deforestation using GIS and artificial neural networks. *Environmental Modelling & Software,* 19(5), 461-471.

Meusburger, K., *et al.* 2010. Soil erosion modelled with USLE and PESERA using QuickBird derived vegetation parameters in an alpine catchment. *International Journal of Applied Earth Observation and Geoinformation,* 12(3), 208-215.

Mhangara, P., 2011. *Land use/ cover change modeling and land degradation assessment in the Keiskamma catchment using remote sensing and GIS.* (Ph. D.). University of Nelson Mandela Metropolitan.

Miller, D. M., Kaminsky, E. J. and Rana, S. 1995. Neural network classification of remote-sensing data. *Computers & Geosciences,* 21(3), 377-386.

Millward, A. A. and Mersey, J. E. 1999. Adapting the RUSLE to model soil erosion potential in a mountainous tropical watershed. *CATENA,* 38(2), 109-129.

Mitasova, H., *et al.* 1996. Modelling topographic potential for erosion and deposition using GIS. *International Journal of Geographical Information Systems,* 10(5), 629-641.

Moravec, J. and Zemeckis, R., 2007. Cross Compliance and Land Abandonment: A research paper of the Cross Compliance Network.

Morschel, J. and Fox, D., 2004. Une methode de cartographie du risque erosif: application aux collines du terrefort lauragais. [online], m@ppemonde 76 (2004.4). Available from: http://mappemonde.mgm.fr/nun4/articles/art04404.html.

Muller, M. and Middleton, J. 1994. A Markov model of land-use change dynamics in the Niagara Region, Ontario, Canada. *Landscape Ecology,* 9(2), 151-157.

Müller, D., & Munroe, D. K., 2014. Editorial: Current and future challenges in land-use science. *Journal of Land Use Science*, 133-142. doi: http://dx.doi.org/10.1080/1747423X.2014.883731.

Munroe, D. K., & Müller, D., 2007. Issues in spatially explicit statistical land-use/cover change (LUCC) models: Examples from western Honduras and the Central Highlands of Vietnam. *Land Use Policy,* 521-530. doi: 10.1016/j.landusepol.2005.09.007.

Murayama, Y. and Thapa, R., 2011. *Spatial Analysis and Modeling in Geographical Transformation Process: GIS-based Applications.* Springer.

Nainggolan, D*., et al.* 2012. Afforestation, agricultural abandonment and intensification: Competing trajectories in semi-arid Mediterranean agro-ecosystems. *Agriculture, Ecosystems & Environment,* 159(0), 90-104.

Novara, A*., et al.* 2011. Soil erosion assessment on tillage and alternative soil managements in a Sicilian vineyard. *Soil and Tillage Research,* 117(0), 140-147.

Nunes, A. N., de Almeida, A. C. and Coelho, C. O. A. 2011. Impacts of land use and cover type on runoff and soil erosion in a marginal area of Portugal. *Applied Geography,* 31(2), 687-699.

Nyakatawa, E. Z., Reddy, K. C. and Lemunyon, J. L. 2001. Predicting soil erosion in conservation tillage cotton production systems using the revised universal soil loss equation (RUSLE). *Soil and Tillage Research,* 57(4), 213-224.

Oñate-Valdivieso, F. and Bosque Sendra, J. 2010. Application of GIS and remote sensing techniques in generation of land use scenarios for hydrological modeling. *Journal of Hydrology,* 395(3–4), 256-263.

Pacheco, F*., et al.* 2014. Soil losses in rural watersheds with environmental land use conflicts. *Science of The Total Environment,* 485, 110-120.

Parcerisas, L*., et al.* 2012. Land use changes, landscape ecology and their socioeconomic driving forces in the Spanish Mediterranean coast (El Maresme County, 1850–2005). *Environmental Science & Policy,* 23(0), 120-132.

Pelorosso, R., Leone, A. and Boccia, L. 2009. Land cover and land use change in the Italian central Apennines: A comparison of assessment methods. *Applied Geography,* 29(1), 35-48.

Pérez-Vega, A., Mas, J.-F. and Ligmann-Zielinska, A. 2012. Comparing two approaches to land use/cover change modeling and their implications for the assessment of biodiversity loss in a deciduous tropical forest. *Environmental Modelling & Software,* 29(1), 11-23.

Petrov, L. O., Lavalle, C. and Kasanko, M. 2009. Urban land use scenarios for a tourist region in Europe: Applying the MOLAND model to Algarve, Portugal. *Landscape and Urban Planning,* 92(1), 10-23.

Pontius, G. 2000. Quantification Error Versus Location Error in Comparison of Categorical Maps. *Photogrammetric Engineering and Remote Sensing,* 66(8), 1011-1016.

Pontius Jr, R. G., Shusas, E. and McEachern, M. 2004. Detecting important categorical land changes while accounting for persistence. *Agriculture, Ecosystems & Environment,* 101(2–3), 251-268.

Pontius, R., Jr., Thontteh, O. and Chen, H. 2008. Components of information for multiple resolution comparison between maps that share a real variable. *Environmental and Ecological Statistics,* 15(2), 111-142.

Pontius, R. G. and Millones, M. 2011. Death to Kappa: birth of quantity disagreement and allocation disagreement for accuracy assessment. *International Journal of Remote Sensing,* 32(15), 4407-4429.

Pontius, R. G. and Schneider L. 2001. Land-cover change model validation by an ROC method for the Ipswich watershed, Massachusetts, USA. Agriculture, Ecosystems & Environment 85:239-248.

Raclot, D.*, et al.* 2009. Soil tillage and scale effects on erosion from fields to catchment in a Mediterranean vineyard area. *Agriculture, Ecosystems & Environment,* 134(3–4), 201-210.

Ramos, M. C. and Martínez-Casasnovas, J. A. 2006. Nutrient losses by runoff in vineyards of the Mediterranean Alt Penedès region (NE Spain). *Agriculture, Ecosystems & Environment,* 113(1–4), 356-363.

Ramos, M. C. and Martínez-Casasnovas, J. A. 2004. Nutrient losses from a vineyard soil in Northeastern Spain caused by an extraordinary rainfall event. *CATENA,* 55(1), 79-90.

Renard, K. G.*, et al.* 1997. Predicting soil erosion by water: a guide to conservation planning with the revised universal soil loss equation (RUSLE). *Agriculture Handbook (Washington),* (703).

Renard, K. G. and Freimund, J. R. 1994. Using monthly precipitation data to estimate the R-factor in the revised USLE. *Journal of Hydrology,* 157(1), 287-306.

Roy, H., Fox, D. and Emsellem, K., 2014a. Predicting Land Cover Change in a Mediterranean Catchment at Different Time Scales. *In:* Murgante, B.*, et al.* eds. *Computational Science and Its Applications – ICCSA 2014.* Springer International Publishing, 315-330.

Roy, H. G., Fox, D. M. and Emsellem, K. 2014b. Spatial dynamics of land cover change in a Euro-Mediterranean catchment (1950–2008). *Journal of Land Use Science*, 1-21.

Royall, D. 2007. A comparison of mineral-magnetic and distributed RUSLE modeling in the assessment of soil loss on a southeastern U.S. cropland. *CATENA,* 69(2), 170-180.

Sala, O. E.*, et al.* 2000. Global Biodiversity Scenarios for the Year 2100. *Science,* 287(5459), 1770-1774.

Salome, C.*, et al.* 2014. Relevance of use-invariant soil properties to assess soil quality of vulnerable ecosystems: The case of Mediterranean vineyards. *Ecological Indicators,* 43(0), 83-93.

Salvati, L., Sateriano, A. and Bajocco, S. 2013. To grow or to sprawl? Land Cover Relationships in a Mediterranean City Region and implications for land use management. *Cities,* 30(0), 113-121.

Sang, L.*, et al.* 2011. Simulation of land use spatial pattern of towns and villages based on CA–Markov model. *Mathematical and Computer Modelling,* 54(3–4), 938-943.

Santé, I.*, et al.* 2010. Cellular automata models for the simulation of real-world urban processes: A review and analysis. *Landscape and Urban Planning,* 96(2), 108-122.

Schneider, A. and Woodcock, C. E. 2008. Compact, Dispersed, Fragmented, Extensive? A Comparison of Urban Growth in Twenty-five Global Cities using Remotely Sensed Data, Pattern Metrics and Census Information. *Urban Studies,* 45(3), 659-692.

Serra, P., Pons, X. and Saurí, D. 2008. Land-cover and land-use change in a Mediterranean landscape: A spatial analysis of driving forces integrating biophysical and human factors. *Applied Geography,* 28(3), 189-209.

Shafizadeh Moghadam, H. and Helbich, M. 2013. Spatiotemporal urbanization processes in the megacity of Mumbai, India: A Markov chains-cellular automata urban growth model. *Applied Geography,* 40(0), 140-149.

Silva, E. A. and Clarke, K. C. 2002. Calibration of the SLEUTH urban growth model for Lisbon and Porto, Portugal. *Computers, Environment and Urban Systems,* 26(6), 525-552.

Silva, T. S. and Tagliani, P. R. A. 2012. Environmental planning in the medium littoral of the Rio Grande do Sul coastal plain – Southern Brazil: Elements for coastal management. *Ocean & Coastal Management,* 59(0), 20-30.

Sluiter, R. and Jong, S. 2007. Spatial patterns of Mediterranean land abandonment and related land cover transitions. *Landscape Ecology,* 22(4), 559-576.

Susanna, C.*, et al.*, 2014. *Horizon 2020 Mediterranean report: Toward shared environmental information systems.* the European Environment Agency (EEA), the United Nations Environment Programme/Mediterranean Action Plan (UNEP/MAP)

Terranova, O.*, et al.* 2009. Soil erosion risk scenarios in the Mediterranean environment using RUSLE and GIS: An application model for Calabria (southern Italy). *Geomorphology,* 112(3–4), 228-245.

Tewolde, M. G. and Cabral, P. 2011. Urban Sprawl Analysis and Modeling in Asmara, Eritrea. *Remote Sensing,* 3(10), 2148-2165.

Torri, D.*, et al.*, 2006. Soil erosion in Italy: an overview. *In:* Boardman, J. and Poesen, J. eds. *Soil erosion in Europe.* New York: Wiley Online Library, 245-261.

Toy, T. J., Foster, G. R. and Renard, K. G., 2003. *Soil Erosion: Processes, Prediction, Measurement, and Control.* John Wiley & Sons Canada, Limited.

Turner, M.*, et al.* 1989. Effects of changing spatial scale on the analysis of landscape pattern. *Landscape Ecology,* 3(3-4), 153-162.

UNFPA, 2004. *The Cairo Consensus at Ten: Population, Reproductive Health and the Global Effort to End Poverty.*

Van Eetvelde, V. and Antrop, M. 2004. Analyzing structural and functional changes of traditional landscapes—two examples from Southern France. *Landscape and Urban Planning,* 67(1–4), 79-95.

Veldkamp, A. and Lambin, E. F. 2001. Predicting land-use change. *Agriculture, Ecosystems & Environment,* 85(1–3), 1-6.

Verburg, P. H.*, et al.* 2002. Modeling the Spatial Dynamics of Regional Land Use: The CLUE-S Model. *Environmental Management,* 30(3), 391-405.

Verburg, P. and Overmars, K. 2009. Combining top-down and bottom-up dynamics in land use modeling: exploring the future of abandoned farmlands in Europe with the Dyna-CLUE model. *Landscape Ecology,* 24(9), 1167-1181.

Verburg, P.*, et al.* 2004. Land use change modelling: current practice and research priorities. *GeoJournal,* 61(4), 309-324.

Verburg, P. H.*, et al.* 1999. A spatial explicit allocation procedure for modelling the pattern of land use change based upon actual land use. *Ecological Modelling,* 116(1), 45-61.

Verburg, P. H.*, et al.* 2006. Downscaling of land use change scenarios to assess the dynamics of European landscapes. *Agriculture, Ecosystems & Environment,* 114(1), 39-56.

Vliet, J. v., White, R. and Dragicevic, S. 2009. Modeling urban growth using a variable grid cellular automaton. *Computers, Environment and Urban Systems,* 33(1), 35-43.

Wainwright, J. 1996. Infiltration, runoff and erosion characteristics of agricultural land in extreme storm events, SE France. *CATENA,* 26(1–2), 27-47.

Wang, F.*, et al.* 2011. Identifying dominant factors for the calibration of a land-use cellular automata model using Rough Set Theory. *Computers, Environment and Urban Systems,* 35(2), 116-125.

Wang, S. Q., Zheng, X. Q. and Zang, X. B. 2012. Accuracy assessments of land use change simulation based on Markov-cellular automata model. *Procedia Environmental Sciences,* 13(0), 1238-1245.

Wang, Y. and Li, S. 2011. Simulating multiple class urban land-use/cover changes by RBFN-based CA model. *Computers & Geosciences,* 37(2), 111-121.

Weng, Q. 2002. Land use change analysis in the Zhujiang Delta of China using satellite remote sensing, GIS and stochastic modelling. *Journal of Environmental Management,* 64(3), 273-284.

Weng, Q. 2002. Land use change analysis in the Zhujiang Delta of China using satellite remote sensing, GIS and stochastic modelling. *Journal of Environmental Management,* 64(3), 273-284.

White, R. 1998. Cities and Cellular Automata. *Discrete Dynamics in Nature and Society,* 2, 111-125.

White, R.*, et al.*, Developing an urban land use simulator for European cities. ed. *In: Proceedings of the 5th EC-GIS Workshop*, 1999 Stresa, Italy, 8.

White, R. and Engelen, G. 1993. Cellular automata and fractal urban form: a cellular modelling approach to the evolution of urban land-use patterns. *Environment and Planning A,* 25(8), 1175-1199.

White, R. and Engelen, G. 2000. High-resolution integrated modelling of the spatial dynamics of urban and regional systems. *Computers, Environment and Urban Systems,* 24(5), 383-400.

Wischmeier, W. H. and Smith, D. D., 1978. *Predicting rainfall erosion losses: A guide to conservation planning.* Washington, DC: U.S. Department of Agriculture, Agriculture Handbook No. 537.

Wu, J. 2004. Effects of changing scale on landscape pattern analysis: scaling relations. *Landscape Ecology,* 19(2), 125-138.

Wu, J., Mohamed, R. and Wang, Z. 2011. Agent-based simulation of the spatial evolution of the historical population in China. *Journal of Historical Geography,* 37(1), 12-21.

Wu, X.*, et al.* 2009. Performance Evaluation of the SLEUTH Model in the Shenyang Metropolitan Area of Northeastern China. *Environmental Modeling & Assessment,* 14(2), 221-230.

Yeh, A. G.-O. and Li, X. 2003. Simulation of development alternative using Neural Networks, Cellular Automata, and GIS for urban planning. *Photogrammetric Engineering & Remote Sensing,* 69(9), 1043-1052.

Zhang, R.*, et al.* 2011. Using Markov chains to analyze changes in wetland trends in arid Yinchuan Plain, China. *Mathematical and Computer Modelling,* 54(3–4), 924-930.

Zhang, S., Liu, Y. and Wang, T. 2014. How land use change contributes to reducing soil erosion in the Jialing River Basin, China. *Agricultural Water Management,* 133(0), 65-73.

Zhou, P.*, et al.* 2008. Effect of vegetation cover on soil erosion in a mountainous watershed. *CATENA,* 75(3), 319-325.

APPENDIX 1

Résumé long en Français de

la thèse de Hari Gobinda Roy

« Long term prediction of natural risk evolution in a Mediterranean context of rapid urban growth and climate change »

INTRODUCTION GENERALE

Objectif de la thèse

La question du changement de la couverture terrestre est devenue importante dans le monde entier au cours des dernières années, non seulement pour les chercheurs, mais aussi pour les planificateurs urbains et les écologistes qui préconisent l'utilisation durable des terres dans l'avenir. En Europe méditerranéenne, les caractéristiques de couverture du sol ont considérablement changé depuis la Seconde Guerre mondiale en raison des activités humaines intensives, de la croissance de la population, et de l'étalement urbain et touristique.

La plupart des études antérieures sur les changements de l'occupation du sol dans la région méditerranéenne se sont centrées sur un problème particulier et / ou ont décrit un type spécifique de changement de la couverture terrestre. Peu de recherches ont pris en compte les transformations de plusieurs catégories d'occupation du sol en même temps. De même, rares sont les travaux qui considèrent plusieurs variables dans le changement de l'occupation du sol au cours du temps, au-delà des traditionnels effets de l'altitude et de la pente. Nous souhaitons ici intégrer la variété des catégories et des composantes d'évolution. En outre, si certaines études à propos de la modélisation des mutations de la couverture terrestre se concentrent sur les variables d'influence, peu se penchent sur l'influence de la période historique et des échelles de temps différentes sur la prédiction. Ainsi, dans cette thèse, les changements de l'occupation du sol ont été prédits en utilisant différentes échelles de temps pour évaluer les impacts de la période historique dans la prédiction de la carte de la couverture terrestre d'ici 2025. Enfin, si l'étendue spatiale varie dans les différentes recherches, il semble utile de s'interroger sur les effets de la taille du terrain d'étude et de la résolution des cellules prises en compte, dans la prédiction.

Les transformations de l'occupation du sol ont un impact significatif sur la dégradation des terres, y compris l'érosion des sols. La région méditerranéenne connaît une grande intensité de tempête sur un sol sec en été et en automne : à ce moment, les zones viticoles demeurent presque nues et un taux élevé d'érosion peut se produire (Blavet et al. 2009, Wainwright 1996, Ramos et Martínez-Casasnovas 2006). Or, la plupart des recherches sur la prédiction de l'érosion des sols se

concentrent sur les terres cultivées ailleurs dans le monde, alors que les vignobles de la région méditerranéenne française ont été beaucoup moins étudiés. C'est ce que nous souhaitons faire ici.

Enoncé du problème

Le principal objectif de cette thèse est de prédire les évolutions à long terme de l'occupation du sol, et de l'érosion des sols dans un contexte méditerranéen de croissance urbaine, à l'échelle du bassin versant.
Pour ce faire, les trois objectifs spécifiques suivants ont été formulés :
1. Identifier la dynamique spatiale du changement de la couverture terrestre dans un bassin versant méditerranéen, à savoir le bassin versant de la Giscle, dans le sud de France.
2. Pour déterminer les impacts des échelles temporelles, de l'étendue spatiale et de la taille des cellules sur l'utilisation des terres et les transformations de la couverture terrestre (LUCC), afin de prédire leurs évolutions.
3. Pour déterminer les modèles passés d'érosion des sols (1950, 1982, 2003, 2011), et d'avenir (2025) sur la base de la couverture terrestre projetée pour 2025.

Organisation de la thèse

Cette thèse se compose de sept parties, y compris les quatre chapitres de la recherche originale.
L'introduction décrit les motivations et les objectifs de l'étude, ainsi que les méthodes d'enquête.
Le chapitre 1 présente un examen approfondi de la documentation portant sur les études universitaires antérieures, à propos de la dynamique et de la modélisation de l'occupation du sol. Ces travaux sont issus du monde entier, et sont publiés entre 1994 et 2014.
Le chapitre 2 analyse les modèles de transformations de la couverture terrestre dans la zone d'étude, et en identifie les variables explicatives pour chaque catégorie d'occupation du sol. Le travail a d'abord porté sur la numérisation de l'occupation du sol en 5 catégories (forêt, prairie, vignoble, urbain, et suburbain), à partir de photographies aériennes orthorectifiées numériques, à trois dates (1950, 1982, et 2008) et donc à trois périodes temporelles d'évolutions (1950-1982, 1982-2008 et 1950-2008). Les dynamiques du sol ont été déterminées par la méthode de la couverture terrestre proposées par Ponce et al. (2004). Ainsi, les mutations de la couverture terrestre ont été quantifiées en utilisant la matrice de tableau croisé du module CROSSTAB et le module d'analyse de changement du Land Change Modeler (LCM) de IDRISI Selva Version 17.02 (Eastman 2012). On a ainsi mesuré la persistance, les gains, les pertes, le changement total (addition des gains et pertes), la variation nette, et l'échange entre toutes les catégories. Enfin, les influences des variables spatiales telles que l'altitude, la pente, les distances aux routes, aux cours d'eau, à la mer, et à la zone de construction sont présentées.
Le chapitre 3 traite de l'influence des échelles temporelles sur la modélisation des dynamiques de l'occupation du sol. La situation en 2011 a été prédite à partir de différentes échelles de temps (1950-1982, 1982-2003 et 2003-2008) à l'aide du Land Change Modeler (LCM), et comparées avec la carte de la couverture terrestre numérique de 2011 pour mesurer la précision du modèle. Différentes variables ont été prises en compte, et testées en utilisant le coefficient V de Cramer : des variables explicatives à composantes spatiales (l'altitude, la pente, et les distances des routes, aux cours d'eau, et aux zones bâties), et d'autres de planification.

Le chapitre 4 teste l'impact de l'étendue spatiale et la taille de la cellule sur la dynamique et la prévision de l'occupation du sol. Ces éléments peuvent avoir un impact important sur la qualité de la prévision, puisque les indices de comparaison entre la réalité et la prévision se basent sur le nombre de cellules. Des analyses ont été réalisées pour la prédiction en 2011 pour une grande (79,1 km²) et petite (36,6 km²) fenêtres en utilisant la taille des cellules de 25 m, 50 m et 100 m. Les effets de la résolution spatiale ont également été analysés par upscaling de 25 m à 50 m et 100 m, puis par downscaling retour à 25 m.
Enfin, le chapitre 5 mesure le degré d'érosion du sol, identifie les impacts des changements de la couverture terrestre sur l'érosion des sols, et prédit l'érosion des sols dans les vignobles pour 2025 à l'échelle du bassin versant en utilisant RUSLE. Différents paramètres ont été mesurés. L'indice de l'érosion des précipitations (R) a été estimé à partir des précipitations moyennes dans la période 1975-2005 suivant Torri et al. (2006). Le facteur d'érodabilité du sol K a été calculé suivant l'équation proposée par Wischmeier et Smith (1978). S'y ajoutent des facteurs de gestions des terres et de conservation en fonction du type d'occupation du sol. Des cartes d'érosion des sols ont été prévues pour 1950, 1982, 2003, 2011 et 2025. Pour les taux d'érosion estimés en 2025, la transition des cartes potentielles ont été créées pour toutes les transitions possibles en fonction des changements historiques réels au cours de la période de 1982 à 2003 et des variables explicatives en utilisant l'algorithme MLPNN de IDRISI (Eastman, 2012). Les taux d'exactitude de la prévision de plus de 70% étaient les suivants : de la forêt à la vigne, de la forêt en prairies, de la forêt en zone bâtie, de la vigne à la surface construite, et des prairies en zone bâtie.
Enfin, la thèse se termine par une dernière section qui présente une synthèse des résultats, une discussion sur les limites de cette étude, et des suggestions pour la recherche future.

CHAPITRE 1 : ETAT DE LA QUESTION SUR LES DYNAMIQUES D'OCCUPATION DU SOL ET LA MANIERE DE LES MODELISER

I. Etat de la question sur les changements d'occupation du sol

1.1 Introduction

La couverture terrestre est la couverture physique et biologique sur la surface de la terre, y compris l'eau, la végétation, le sol nu et structures artificielles (Ellis, 2011). L'occupation du sol et des terres est un terme plus complexe qui fait référence aux activités humaines telles que l'agriculture, la sylviculture, la construction de bâtiments et toute autre fonction qui modifie la surface de la terre ou la couverture terrestre. Les changements d'occupation du sol ont été particulièrement importants en Europe méditerranéenne, depuis la Seconde Guerre mondiale (Fox et al. 2012) en raison des activités humaines intensives (Geri et al., 2010). Ils sont en effet déterminés par l'interaction entre les activités humaines (croissance démographique, étalement urbain, développement industriel, tourisme et la politique environnementale, etc.) et des facteurs environnementaux (caractéristiques du sol, climat, topographie et végétation, etc.). Les changements d'occupation du sol (LUCC, « Land use / cover change ») sont importants à comprendre parce qu'ils témoignent de phénomènes plus globaux sur la biodiversité et les écosystèmes, la sécurité alimentaire, la santé humaine, la dégradation des sols, l'urbanisation et le changement climatique mondial

1.2. Les dynamiques majeures de changement de l'occupation du sol dans l'espace euro-méditerranéen

La zone côtière de la Méditerranée européenne a connu de profonds changements dans l'occupation du sol depuis 1950, à cause des révolutions industrielles et agricoles. En outre, la pression démographique élevée, le développement socio-économique très fort et surtout sa spécialisation dans des activités touristiques dans la région méditerranéenne, ont accentué l'urbanisation le long de la côté, à des rythmes très élevés (Cori 1999). Ces phénomènes se sont traduits sur les terres agricoles. Selon différentes études (Geri et al. 2011, Nunes et al., 2011), deux transformations majeures ont affecté l'occupation du sol de la région côtière de la Méditerranée, au cours des dernières décennies. Tout d'abord, dans les plaines alluviales, l'agriculture sèche et les terres forestières ont diminué, pendant que les vallons abandonnés et les escarpements étaient reboisés spontanément, signes de la décroissance des vignes et des oliviers. Ensuite, et parallèlement, l'urbanisation rapide s'est mise en place dans la plupart des plaines côtières, associée à une forte activité touristique et à une agriculture résiduelle. Puis, tout ceci a entrainé le développement des infrastructures et des réseaux de communication, ce qui a irrémédiablement conduit à l'abandon des terres agricoles sur des terres marginales. Serra et al. (2008) confirment ces propos pour le comté d'Alt Empordà (nord-ouest de la Catalogne, Espagne). Falcucci et al. (2007) signalent, au sujet de l'Italie, que l'agriculture a diminué dans les zones montagneuses et côtières, mais s'est étendue dans le reste du pays avec une transformation d'une culture traditionnelle en culture intensive basée sur la technologie moderne. Dans leurs travaux sur les transformations d'occupation du sol d'un bassin versant méditerranéen (province de Sienne, Italie) entre 1954-2000, Geri et al. (2010) ont révélé que ce sont essentiellement les terres semi-naturelles qui sont devenues des zones forestières ou des terres agricoles. En outre, les pertes de superficie forestière ont eu lieu principalement à des altitudes élevées et la conversion

des terres agricoles en semi naturel a eu lieu à des altitudes plus basses. Pour la France, Fox et al. (2012) ont mené une étude pour analyser l'impact des changements de la couverture terrestre sur écoulement total, dans un bassin versant méditerranéen entre 1950 et 2003. Ils ont montré que la couverture terrestre de la zone d'étude est fortement influencée par la topographie et que la plupart des changements d'occupation du sol ont eu dans la plaine et les contreforts du bassin, avec notamment une transformation des vignobles en zone urbaine

1.3 Les facteurs influents du changement d'occupation du sol

Les changements d'occupation du sol se produisent sous la pression d'une variété de facteurs socio-économiques qui interagissent avec l'environnement naturel pour déterminer la nature et la localisation de ces transformations.

- Le facteur majeur demeure la pression démographique et l'étalement urbain, qui se sont mis à en place à des rythmes effrénés. Selon Benoit (2001), les régions côtières de la Méditerranée sont plus urbanisées que les pays dans leur ensemble, et les populations urbaine et totale dans la région méditerranéenne ont augmenté de 2,7 et 1,9 fois, respectivement entre 1950 et 1995. Toujours selon ces travaux, la côte méditerranéenne européenne est maintenant presque entièrement urbanisée, avec une distance moyenne entre les zones urbaines d'environ 10 km, 17 km et 18 km en Italie, en Espagne et en France, en 1995. Plus encore, 34% des zones côtières méditerranéennes espagnoles ont été urbanisées depuis 1999 et ce chiffre était de 43% pour la côte italienne (Serra et al., 2008). Cette artificialisation des sols (urbanisation, routes, parkings, jardins, pelouses, etc.) s'est essentiellement développée au détriment des zones agricoles ou forestières.
- Le second facteur est bien évidemment le tourisme, puisque la Méditerranée est la première destination touristique au monde (MAP 2008). Van Eetvelde et Antrop (2004) expliquent que les valeurs naturelles, culturelles et panoramiques des paysages euro-méditerranéens sont des éléments importants pour le développement du secteur du tourisme dans ces lieux. Comme décrit par EAA 2011, le nombre de résidences secondaires a augmenté de 10% entre 1990 et 1999 en France, créant une pression intensive sur l'environnement, en particulier dans les zones côtières et montagneuses. Selon Cori 1999), la moitié des résidences secondaires en France sont situées dans la zone côtière de la Méditerranée. Ainsi, les infrastructures à destination des touristes (logement, routes, divertissement, etc.) sont construites de façon permanente, ce qui contribue à accélérer la croissance urbaine, et donc à modifier l'occupation du sol.
- Le troisième facteur concerne l'intensification de l'agriculture. Globalement, deux modèles de changement agricole de la couverture terrestre dans les régions méditerranéennes européennes au cours des cinquante dernières années peuvent être définis (Baldock et al., 1996). D'une part, les lieux les plus appropriés et productifs ont été convertis à des usages agricoles plus intensifs depuis les années 1950, souvent avec une expansion des terres arables au détriment des prairies permanentes, les zones humides, et de la forêt. D'autre part, les zones marginales avec des barrières physiques et socio-économiques comme les pentes abruptes, les petites terrasses, les zones humides sans systèmes de drainage, et les régions montagneuses reculées ont été abandonnées ou remplacées par des systèmes agricoles spécialisés, plantations forestières ou la succession naturelle.
- L'abandon des terres peut être considéré comme le quatrième facteur. Il s'applique à la terre où l'utilisation agricole traditionnelle ou récente a cessé. La plupart des études (Geri

et al. 2010, Koulouri et Giourga 2007, Sluiter et de Jong 2007, Van Eetvelde et Antrop 2004) sur l'abandon des terres en Europe méditerranéenne montrent que les zones de collines montagneuses ou semi montagneuses ont été abandonnées en raison de petites parcelles de vignes et oliviers non rentables. La plupart des abandons de terres ont eu lieu au cours des dernières décennies en raison de l'urbanisation et de l'intensification agricole (fertilité du sol, pente, altitude, disponibilité en eau etc. qui définissent le potentiel agricole), mais aussi de l'évolution technologique des systèmes et politiques agricoles pour la commercialisation ou encore de la population agricole vieillissante.

- Puis, les facteurs économiques interviennent pour expliquer les changements d'occupation du sol. Selon certaines études (Baldock et al 1996), tout s'explique derrière le terme de concurrence : d'autres zones agricoles, d'autres couvertures terrestres, d'autres types d'emploi, et d'autres systèmes de production.
- Enfin, les politiques et la planification jouent aussi. Nunes et al. (2011) décrivent la façon dont les domaines de l'environnement et de la forêt ont bénéficié de la réforme de la PAC en 1992. Par exemple, cette politique agricole a encouragé les grandes entreprises agricoles et cultures subventionnées dans les grands champs. En conséquence, l'abandon des terres agricoles s'est déroulé dans des zones moins favorables pour ces grands champs, en vertu également des politiques de boisement pour réduire la désertification et l'érosion des sols.

En outre, ces changements d'occupation des sols ont diverses conséquences en Europe méditerranéenne : déclin de la diversité et de la complexité des paysages, augmentation de certains risques tels que les incendies de forêt, les inondations et les sécheresses. Mais il peut y avoir aussi des effets positifs. Ainsi, dans ce cas, Koulouri et George (2007) ont observé que la diminution de l'érosion des sols est due à la régénération de la végétation qui a amélioré la structure du sol en ajoutant de la matière organique.

II. Etat de la question sur la modélisation du changement d'occupation du sol

2.1 Introduction

Les changements d'occupation du sol (« Land use / cover change », LUCC) sont devenus un enjeu très important pour les chercheurs et gestionnaires, y compris les planificateurs, les écologistes, les économistes, en raison de leur relation avec les modifications de l'environnement mondial et le développement durable (Dietzel et Clarke 2006, Guan et al. 2011, Lambin et al., 2001). En effet, ils sont liés à l'interaction entre les activités humaines et l'environnement naturel. Leur modélisation permet d'en identifier la localisation, d'en mesurer les niveaux, de prévoir les modifications futures compte tenu des transformations passées et actuelles, et d'en tester des variables explicatives. En conséquence, des chercheurs ont créé un vaste ensemble d'outils de modélisation opérationnelle pour mettre en œuvre la prédiction et l'exploration de trajectoires possibles des changements d'occupation du sol (Verburg et al., 2006). Mais très peu d'études portent sur les dynamiques modélisées de l'occupation du sol dans la région méditerranéenne (Geri et al. 2011, Oñate-Valdivieso et Bosque Sendra 2010, Petrov et al., 2009). Il s'agit dans ce chapitre de présenter un aperçu des méthodes de modélisation des transformations d'occupation du sol, et de justifier notre choix d'utiliser l'approche « Land Change Modeler » (LCM) du logiciel IDRISI comme outil de modélisation pour notre étude.

2.2. Les modèles de couverture terrestre et d'occupation du sol

Différentes techniques de modélisation ont été conçues pour saisir l'état et l'évolution de l'occupation du sol, en utilisant les potentiels biophysiques et les caractéristiques socio-économiques (Guan et al. 2011, Kamusoko et al., 2009, Barredo et al., 2003, He et al., 2008). Certains ont une approche plus statistique, d'autres plus spatiale comme les automates cellulaires (CA) ou le modèle de SLEUTH (Clarke et Gaydos 1998). Quatre types peuvent être distingués.

- Premièrement, les automates cellulaires fonctionnent à partir d'un ensemble d'états cellulaires possibles, qui évoluent à partir de règles de transition prenant en compte la situation des cellules environnantes. En quelque sorte, les automates cellulaires sont des systèmes spatiaux, dont les cellules sont situées et interconnectées dans l'espace, et qui évoluent dans le temps et dans l'espace. Plus précisément, appliqué à notre cas, un automate cellulaire se compose (Liu 2009, White et al., 1999) d'un ensemble de cellules, unité spatiale de base, définies par des états en fonction d'attributs (type de couverture du sol, statut socio-économique, densité de population, etc.), et qui évoluent dans le temps en fonction de règles de transition élaborées (probabilités de transformation des cellules, calculées à partir de l'accessibilité, du zonage, et des effets de voisinage, etc.) qui s'appliquent à l'échelle d'un quartier.

  De nombreuses modélisations à travers les automates cellulaires ont été développées dans la dernière décennie, en raison de leur puissance technique et modélisatrice (Dietzel et Clarke 2004, Wu et al., 2009), particulièrement dans les études urbaines pour simuler l'expansion urbaine dans l'espace (Clarke et Gaydos 1998, Liu 2009, Santé et al. 2010, blanc de 1998, White et Engelen 2000). De telles approches ont également été mises en œuvre pour simuler plusieurs types d'utilisation des terres, montrer leurs dynamiques, et analyser la croissance urbaine locale et régionale (Jantz et al., 2004). Ainsi, par exemple, White et al. (1997) ont modélisé la croissance urbaine, grâce aux automates cellulaires : les cellules représentaient les couvertures terrestres, les règles de transition exprimaient la potentialité temporelle de chaque type de couverture terrestre, et le réseau routier, les plans d'eau, et les chemins de fer étaient utilisées comme des contraintes spatiales pour le développement urbain de l'utilisation des terres.

  Deux exemples d'application d'automates cellulaires – particulièrement utilisés - sont à signalés. D'une part, le modèle SLEUTH intègre six types d'éléments, essentiellement locaux, dans les règles de croissance d'une grille de cellules : la pente, l'occupation du sol, l'exclusion, l'urbanisation, le transport, et la topographie. D'autre part, l'unité de gestion des terres de l'Institut pour l'environnement et le développement durable (MOLAND) a mis au point un cadre de modélisation intégrée basée sur le CA développé par White et al. (1997) pour évaluer, surveiller, et les politiques de gestion de l'environnement spatial, urbain, régional et durable modèle passés, présents et futurs en Europe. Ce modèle se distingue donc par sa prise en compte des politiques spatiales existantes (Barredo et al., 2003).

  Au-delà de ces exemples, nous avons identifié les avantages et les limites de ce type de modélisation par automates cellulaires. Ces modèles sont explicitement spatiaux (Blanc et Engelen 2000), dans la localisation et le comportement des cellules, dans leurs capacités à représenter des processus spatiaux, et dans leurs facilités d'intégration de données spatiales raster dérivées de plates-formes de télédétection. Ils sont en outre capables de représenter des dynamiques spatio-temporelles. C'est pourquoi ces modèles sont

couramment utilisés dans la connaissance et la simulation du développement urbain (White et Engelen 2000, Murayama et Thapa 2011, Li et Liu 2008). Cependant, ces modèles avec automates cellulaires ont certaines limites pour saisir les processus d'urbanisation complexes (Verburg et al., 2004), et notamment calibrer les multiples catégories d'utilisation des terres (Li et Yeh, 2002). En outre, ils n'arrivent pas à intégrer les influences de facteurs humains tels que les politiques publiques.

- Deuxièmement, la modélisation de la chaîne de Markov est une technique de simulation, introduite en Géographie en 1965 pour étudier la dynamique des zones résidentielles dans le centre-ville par Clark (1965). Depuis, le développement des outils de télédétection et de SIG ont élargi leur utilisation aux études environnementales : dynamique de la végétation (Balzter 2000), évaluation des grands investissements publics tels que les barrages et leurs impacts sur l'occupation du sol (Muller et Middleton, 1994), ou encore prévision des différentes catégories de mutations de l'occupation du sol (Weng 2002). En effet, la modélisation de la chaine de Markov évalue les changements récents dans l'espace et les utilise comme conditions initiales pour les intégrer dans des matrices de probabilité de transition pour simuler l'avenir (Zhang et al., 2011). Par exemple, on peut construire des matrices de probabilité de transition, en calculant à partir de 2 cartes d'utilisation du sol à 2 temps, le passage d'un état (terres cultivées, par exemple) à un autre état (zones bâties) dans une période de temps donnée (Benenson et Torrens 2004, Jokar Arsanjani et al. 2013).

  On peut combiner un modèle de Markov, pour déterminer les changements temporels des types d'occupation du sol au fil du temps sur la base de matrices de transition de probabilité, avec un automate cellulaire, pour contrôler la configuration spatiale du changement grâce à des règles de voisinage en fonction du potentiel de transition de chaque pixel (Araya et Cabral 2010, He et al., 2008).
- Troisièmement, LCM (Modèle de changement d'occupation du sol ou « Land Change Modeler ») est un module d'analyse écologique dans le logiciel IDRISI, développé par Clark Labs. Il est recommandé pour évaluer et prévoir les changements d'occupation du sol, puisqu'il calcule des potentiels de transition entre deux images d'entrée, sur la base de réseaux de neurones (méthode statistique non linéaire, qui se compose d'un réseau connecté d'unités de traitement). Ce modèle a donc l'avantage de modéliser des transitions de groupe et les relations complexes entre de nombreuses variables. Par exemple, Mas et al. (2012) ont mené une étude visant à saisir et prévoir l'occupation du sol. Ils ont utilisé la répartition des phénomènes fonciers de 1986 et 1994, et cinq variables explicatives (distance aux zones urbaines, distance aux routes, pente, distance à la perturbation, et altitude), pour simuler une future occupation du sol, en se basant sur des cartes de potentiels de transition dans IDRISI, avec une matrice de Markov. Les conclusions de l'étude ont révélé d'assez bonnes prédictions de changement du sol.
- Enfin, dernièrement, la modélisation multi-agents (SMA) est constituée d'un ensemble d'agents qui interagissent entre eux et avec leur environnement pour répondre aux objectifs de l'utilisateur en utilisant l'information et les états des objets dans l'environnement (Ligtenberg et al., 2004). Cette approche de modélisation est capable de tenir compte à la fois de l'état précis de chaque occupation du sol, des interactions spatiales et donc de la concurrence entre les différentes couvertures terrestres (Verburg et Overmars 2009). Il s'agit d'une modélisation spatialement explicite, et les agents représentent, par exemple, les ménages qui déménagent leurs foyers ou des individus qui

utilisent des systèmes de transport (Miller et al., 2004). Dans le contexte qui nous intéresse, un agent peut représenter les caractéristiques de l'occupation du sol, les composants et la qualité du sol, l'état topographique, et également intégrer des choix de gestion des terres plus sociaux (politique foncière, dynamique des populations, niveau de revenus)

2.3. Justification du choix d'étude

Au final, différents types de modélisation ont été présentés et discutés. La modélisation par automates cellulaires, principalement utilisée dans la simulation de croissance urbaine, a montré ses limites dans la prédiction de l'occupation du sol multiple et complexe. Par ailleurs, peu d'études ont réussi avec succès à utiliser la modélisation par chaine de Markov. Cependant, plusieurs travaux ont mis au point une prédiction acceptable en combinant ces deux approches précédentes (Araya et Cabral 2010, Guan et al. 2011, Jokar Arsanjani et al. 2013, Kamusoko et al . 2009). En outre, les modèles multi-agents sont largement utilisés pour intégrer fortement la composante spatiale et des variables explicatives humaines et sociales. Enfin, nous avons montré que le modèle LCM (Land Change Modeler, modélisation du changement de l'occupation du sol) d'IDRISI, basé sur la combinaison automates cellulaires / Markov, était un outil performant pour évaluer et prédire les changements spatiaux de l'occupation du sol. En outre, il dispose de différents indicateurs qui en font une technique très puissante. En conséquence, dans notre étude, nous avons utilisé des variables explicatives topographiques combinées avec des éléments de planification spatiale pour simuler les changements d'occupation du sol, sans tenir compte de certains attributs sociaux (population et données socio-économiques) ; notre choix ne s'est donc pas orienté vers une modélisation à base d'agent. Nous nous sommes alors orientés vers une modélisation de transformation d'occupation du sol (LCM) sous IDRISI, un modèle qui couple automates cellulaires avec chaine de Markov, pour simuler des tendances temporelles et spatiales.

CHAPITRE 2 : DYNAMIQUE SPATIALE DE L'OCCUPATION DU SOL DANS UN BASSIN VERSANT EURO-MÉDITERRANÉEN (1950-2008)

I. Introduction

Nous nous situons un contexte où la région euro-méditerranéenne connaît une très forte croissance urbaine depuis les années 1970, du fait du développement du tourisme mais aussi de l'attraction migratoire générale de ces espaces. Dans ce cadre, l'agriculture traditionnelle méditerranéenne est composée principalement de vignes, d'oliviers et de blé cultivés dans l'arrière-pays à proximité, souvent sur des terrasses. De nombreux auteurs ((Serra et al., 2008) ont montré que les vignes et les oliviers ont diminué dans les zones montagneuses et les sous-régions de transition, ce qui entraîne l'abandon des terres et l'augmentation de la superficie des terres en forêt. La vigne a essentiellement diminué à proximité des routes et des zones urbaines en raison de l'étalement urbain.

La plupart des études sur le changement de l'occupation du sol dans la région méditerranéenne mettent en évidence un problème particulier ou décrivent un changement de la couverture individuelle de la terre, comme la forêt, l'agriculture ou l'expansion urbaine (Calvo-Iglesias et al. 2009, Pelorosso et al., 2009) ; seuls quelques travaux prennent en compte tous ces changements en même temps. En outre, la répartition spatiale des transformations de l'occupation du sol est souvent réalisée, mais l'identification des variables clés qui influencent ces changements se limite principalement à l'altitude ou la pente (Geri et al. 2010, Serra et al., 2008) ; quelques rares auteurs (Sluiter et de Jong 2007) prennent les variables de distance en compte. De plus, si de nombreuses recherches s'intéressent à la dynamique de la population urbaine et à l'expansion du tourisme dans la zone côtière méditerranéenne française, en termes d'intensification et de littoralisation, très peu de travaux décrivent précisément les changements d'occupation du sol dans la région.

Le premier objectif de ce chapitre est de quantifier la modélisation des dynamiques de l'occupation du sol en termes de gains, de pertes, de changement total et de transition dans un bassin versant méditerranéen, caractérisé par une activité viticole forte, et à proximité d'une zone côtière bien connue pour son tourisme. Le deuxième objectif est de mesurer les impacts des variables topographiques et de distance sur les transformations de la couverture terrestre pour chaque catégorie d'occupation du sol.

II. Aspects méthodologiques

2.1. Présentation de la zone d'étude

La zone d'étude (environ 235 km²) est située dans le département du Var, dans le Sud-Est de la France, près du golfe de Saint-Tropez (figure 2.1). Elle est caractérisée par un climat méditerranéen avec des étés chauds et secs et des hivers pluvieux. Les températures moyennes varient entre 22° C à 26° C en été et de 5° C à 10° C en hiver. La pluviométrie moyenne annuelle est d'environ 900 mm, et la principale saison des pluies est d'octobre à janvier et en avril (Fox et al. 2012).

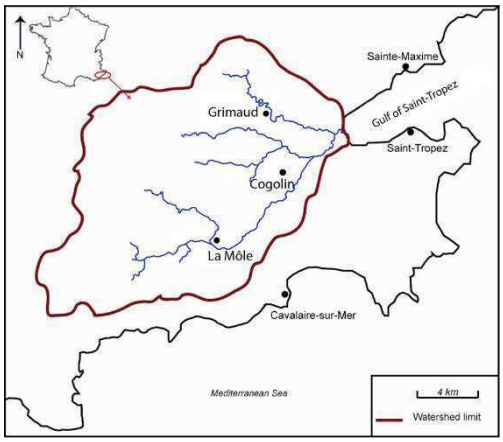

Figure 2.1: Localisation de la zone d'étude.

La zone d'étude comprend deux unités topographiques : la partie supérieure avec les collines du bassin versant (environ 70% du bassin versant), et la partie inférieure du bassin, située près du golfe, qui se finit en pente douce sur une plaine alluviale (Fox et al. 2012). La partie occidentale du bassin versant est constituée de forêt, et la topographie y est inégale, avec des altitudes pouvant aller jusqu'à 650 mètres. Plusieurs affluents (la Môle, la Grenouille, la Tourre, Verne) se jettent dans la rivière principale qu'est le Giscle.

L'activité agricole et l'urbanisation modérée à dense sont les types dominants de l'occupation du sol, dans la partie inférieure du bassin versant. Les vignobles représentent environ 10% de la superficie du bassin versant (Roy et al. 2014). Ils sont, pour la plupart, situés dans la plaine inondable de sable, mais se sont également étendus sur des pentes depuis 2003, là où les sols sont minces, légèrement acides et pierreux (Fox et al. 2006, Roy et al. 2014).

La région est devenue une destination touristique majeure de la France méditerranéenne dans la seconde moitié du XXe siècle, avec le développement de la « Côte d'Azur", et ceci a généré une forte croissance de l'urbanisation. Trois principaux lieux de peuplement existent. Ils sont situés dans le bassin versant : Cogolin, Grimaud et La Môle. Cogolin est la commune la plus peuplée (11 000 hab en 2011), et Grimaud est de plus petite taille (4000 hab) (INSEE 2011). La Môle est un petit village avec une population d'environ 950 habitants (INSEE 2011). La population totale du bassin versant augmente très fortement en été, allant jusqu'à être multipliée par 10, du fait de l'activité touristique et des résidences secondaires. Sur la population permanente, les variations de population sont très faibles. Contrairement à d'autres zones côtières de la Méditerranée, le front de mer est confiné par le golfe et la topographie, et les changements de l'occupation du sol sont limités à la zone côtière

2.2. Descriptions des données utilisées et classification de l'occupation du sol

Des cartes de l'occupation du sol ont été numérisées, à partir de photographies aériennes numériques orthorectifiées (1950 et 1982 en panchromatique ; 2008 en couleur). La résolution initiale des photographies aériennes était de 0.5 m, mais cela a réduit à 1 m pour faciliter la manipulation des données. Les photographies aériennes de 1950 étaient les premières photos de haute qualité de la Seconde Guerre mondiale disponibles, à un moment où la région était encore fortement rurale ; une date intermédiaire (1982) a été choisie entre 1950 et les plus récentes photographies de 2008. L'année 1982 représente également la couverture terrestre au début de l'étalement urbain rapide (Baccaini et Sémécurbe 2009, Salvati et al. 2013).

Les surfaces ont été classées en cinq catégories en fonction de l'interprétation visuelle réalisée (cf. figure 2.2) : la forêt, les prairies, les vignes, les zones urbaines et périurbaines (distinguées en fonction de leur densité). La classification de la couverture terrestre a été facilitée par de nombreuses visites sur le terrain. Les routes principales et les réseaux de cours d'eau ont ensuite été numérisés à partir des photographies aériennes de 2008. La taille des cellules de toutes les cartes numérisées a été changée de 1 m à 25 m, afin de les rendre compatibles avec l'échelle du MNT (25 mètres), utilisé pour la création des variables topographiques et de la distance.

2.3. Les matrices de dynamiques temporelles (1950-1982, 1982-2008 et 1950-2008)

Les mutations de l'occupation du sol ont été quantifiées en utilisant la matrice de tableau croisé du module Land Change Modeler (LCM) d'IDRISI Selva, qui est un outil permettant de mesurer les changements entre images à dates différentes. Trois périodes temporelles ont été distinguées : 1950-1982, de 1982 à 2008, 1950 à 2008. Pour chacune d'elles, nous avons calculé et spatialisé différents indicateurs : les gains, les pertes, le changement total (addition des gains et pertes), la variation nette, et l'échange (échanges entre les classes de couverture terrestre).

III. Résultats

3.1. Les tendances générales des dynamiques de l'occupation du sol

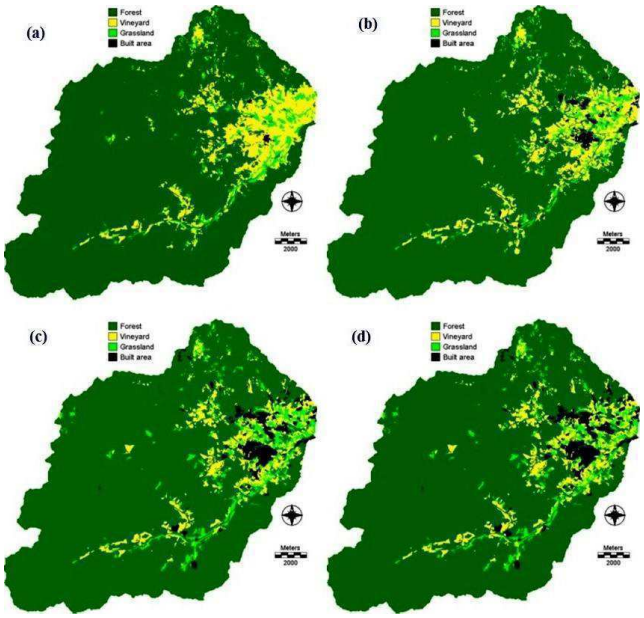

Figure 0.2 : Les types d'occupation du sol (a) 1950, (b) 1982, (c) 2008, (d) 2011.

La figure 2.3. présente l'occupation du sol sous formes de cartes numérisées, à partir de photos aériennes. La forêt est la couverture terrestre dominante dans le bassin versant, passant de 86% de la surface totale à 85% entre 1950 et 2008. Classé en deuxième place, le vignoble a perdu plus d'un quart de sa couverture initiale, surtout depuis 1982. Puis, les prairies ont augmenté de manière significative sur toute la période (+50% entre 1950 et 2008), mais ne se placent qu'en troisième position. Enfin, en ce qui concerne les zones construites (urbaines et péri-urbaines), elles sont de plus en plus présentes sur le territoire (50 ha en 1950, 700 ha en 2008). La plupart de

ces changements d'occupation du sol se sont concentrés dans la partie orientale du bassin versant, sur la plaine alluviale.

Ensuite, nous avons réalisé une analyse détaillée des mutations de l'occupation du sol pour trois périodes (1950-1982, 1982-2008, 1950- 2008), en utilisant des tableaux croisés, qui indiquent 2 phases différentes en ligne et en colonne.

- Entre 1950 et 1982 (Tableau 2.2), la forêt a la plus grande persistance (surface similaire à 97%), et ses terres perdues se transforment en vignobles (407 ha). En parallèle, les vignes se maintiennent de manière modérée (67%), et l'occupation du sol devient alors surtout de la prairie (362 ha). Mais la compensation des pertes de la vigne n'est que partielle, puisque une partie des sols en activité viticole se transforme en forêt (234 ha). La catégorie urbaine est stable, et son expansion se réalise majoritairement sur le vignoble. En conséquence, entre 1950 et 1982, le vignoble est l'occupation du sol qui a subi le plus de changements et de transferts, en particulier sur les zones urbaines et avec les forêts et les prairies. A l'inverse, les espaces urbains gagnent du terrain, mais ont de faibles échanges.
- Les tendances en cours entre 1950 et 1982 se sont poursuivies entre 1982 et 2008. La superficie forestière a diminué légèrement, mais a maintenu une persistance élevée (96,6%) en raison de sa grande surface. Une grande partie du vignoble a continué à se convertir en prairies (445 ha) ; mais au cours de cette période, l'effet compensateur de la forêt sur la vigne a été plus faible que précédemment (237 ha contre 407 ha) : l'activité viticole est donc devenue moins pérenne (61%).En parallèle, entre 1982 et 2008, les prairies constituent l'occupation du sol qui bouge le plus, et interagit le plus avec les autres catégories, même si elle ne représente qu'une faible part du bassin versant (4,8% de la superficie totale en 2008). Les zones urbaines et périurbaines connaissent une forte croissance sur cette période
- Au final, sur 60 ans, entre 1950 et 2008, on observe des changements majeurs dans l'occupation du sol (Tableau 2.6). La forêt est restée la catégorie vraiment dominante, mais de grandes zones forestières ont été converties en vignoble (458 ha) et de prairies (320 ha). Ces pertes ont été partiellement compensées par des gains de vignoble (331 ha) et de prairies (191 ha). La vigne est la catégorie qui a contribué le plus à tous les autres, et plus particulièrement aux prairies (518 ha). La majorité de l'expansion urbaine a eu lieu sur le vignoble tandis que la croissance des zones périurbaines a eu lieu plus ou moins également sur le vignoble et la forêt. Dans l'ensemble, 3 catégories ont montré leur fragilité : vignoble, prairies et péri-urbain. Mais les échanges sont complexes entre les catégories.

Land cover type	Forest	Vineyard	Grassland	Urban	Suburban	Total
Forest	19569 (95.3)	331	191	0	0	20091
Vineyard	458	1015 (45.3)	144	0	0	1616
Grassland	320	518	302 (40.1)	0	0	1140
Urban	69	241	66	19 (100)	8	402
Suburban	123	137	51	0	5 (40.8)	316
Total	20538	2241	754	19	13	23565

Tableau 0.1: Mutations entre les occupations du sol en 1950 (colonnes) et 2008 (lignes)

3.2. Les dynamiques spatiales influençant les changements d'occupation du sol

On s'intéresse d'abord à la localisation des dynamiques de l'occupation du sol, entre 1950 et 2008. Pour la forêt, la majeure partie des terres perdues se situe dans les contreforts à proximité de la plaine alluviale, tandis que la forêt progresse dans l'espace principalement dans la partie sud-est de la plaine alluviale. Pour la vigne, la zone perdue dépasse nettement les gains, et les pertes se sont concentrées dans la plaine alluviale. Les gains en terrain viticole ont tendance à se trouver en dehors de la zone plaine alluviale de l'Est, soit dans les contreforts à proximité ou sur le sol alluvial à l'extrême sud-ouest du bassin versant. En revanche, pour la catégorie des prairies, il n'y a pas de forte structure spatiale des gains et des pertes puisque ceux-ci se localisent tous les deux dans la plaine alluviale. Enfin, l'expansion des zones urbaines s'est réalisée exclusivement dans la plaine alluviale, et à partir des centres urbains existants (Grimaud, Cogolin).

Si l'on étudie l'impact des variables spatiales, on peut mettre en évidence les faits suivants :

- L'influence de l'altitude est majeure (Figure 2.8). Toutes les catégories d'occupation du sol ont une dynamique qui décroît exponentiellement avec l'altitude, et se concentre essentiellement dans les altitudes de moins de 25 m. Une certaine organisation spatiale apparait ainsi en fonction de l'altitude : à moins de 25 mètres, les vignes déclinent de manière importante et laissent la place à des couvertures forestières ou à l'expansion urbaine ; à plus de 200 mètres, les pertes du couvert forestier s'intensifient ; et les altitudes intermédiaires voient se développer les zones de construction.
- La pente et l'altitude sont bien évidemment corrélées dans le bassin versant, et on aboutit à des conclusions similaires à propos de leurs effets dans l'espace. La majeure partie des mutations se concentrent sur des pentes inférieures à 10%. Quelques apports supplémentaires mineurs apparaissent, comme par exemple, l'absence de progression de la forêt sur les pentes les plus raides.
- La distance aux cours d'eau apparaît comme un facteur important (Figure 2.10), toutes les catégories d'occupation du sol diminuant de manière exponentielle en fonction d'elle. Entre 1950 et 1982, les progressions majeures des vignes se situent proches des cours d'eau ou à distance intermédiaire (moins de 900 mètres). Des processus similaires se produisent pour les prairies, dans la dernière période. A l'inverse, la forêt gagne de la surface près des cours d'eau entre 1950 et 1982, et en perd dans la même localisation entre 1982 et 2008. En ce qui concerne les zones construites, l'effet de la distance au cours d'eau se joue non pas à proximité immédiate, mais dans des distances intermédiaires (environ 100-800 m).

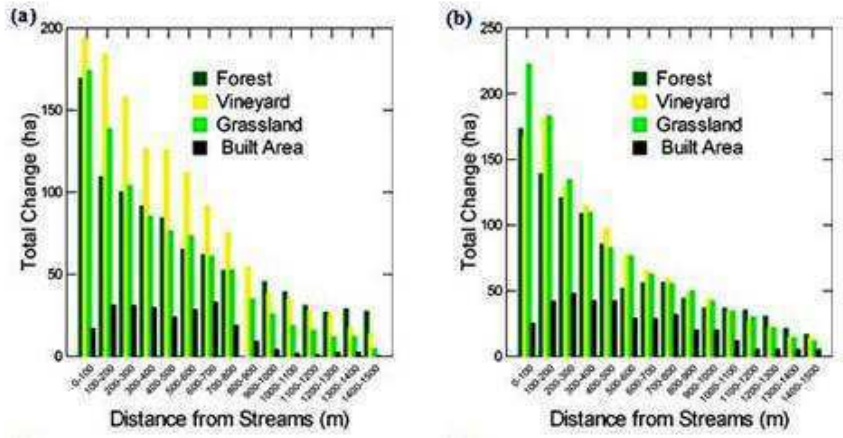

Figure 0.3: Types d'occupation du sol et distance aux cours d'eau, en (a) 1950-1982, (b) 1982-2008

- Les variations des types d'occupation du sol mises en relation avec la distance à la route suivent la tendance exponentielle décroissante de la plupart des variables prises en considération. Environ 40% à 50% des dynamiques totales de la forêt, de la vigne, et des prairies ont lieu à moins de 100 m d'une route. Cette valeur est supérieure à 95% pour la zone construite. Entre 1982 et 2008, la distance à la route s'élargit, et c'est plutôt la gamme 100-300 mètres qui joue un rôle.
- La relation entre les transformations des types d'occupation du sol et la distance aux zones construites (Figure 2.12) est fortement dépendante du temps. Entre 1950 et 1982, la relation n'existe pas, malgré une tendance pour les couvertures de végétation (forêt, vignes, prairies) à montrer un plus grand changement à des distances intermédiaires de la zone construite (300-1300 m), et la zone construite à changer de manière plus proche de la zone précédemment construite (0-100 m). Entre 1982-2008, le modèle est totalement différent. Pour le vignoble et les prairies, les dynamiques totales augmentent d'abord en fonction de la distance à la surface construite, avec des pics à environ 100-200 m, puis diminuent au-delà. Les variations de la couverture forestière sont à peu près constantes entre 0-300 m avant de diminuer avec de plus grandes distances

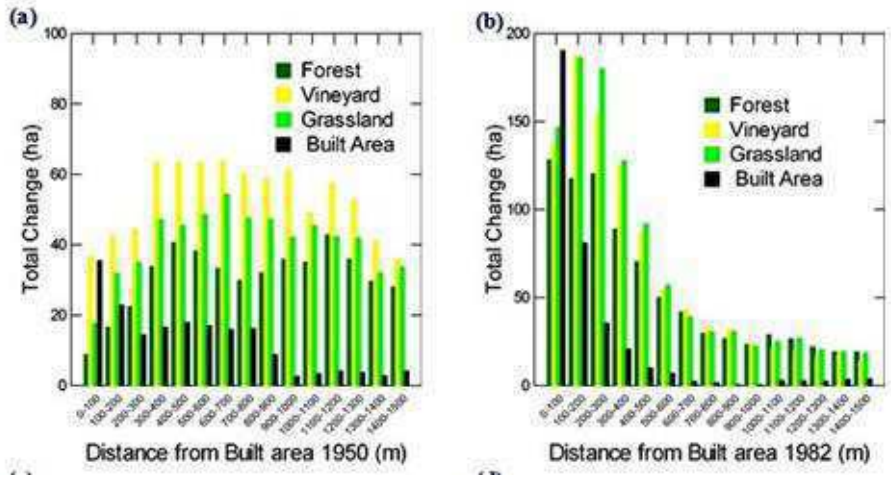

Figure 0.4: Types d'occupation du sol et distance aux zones construites, en (a) 1950-1982, (b) 1982-2008

- L'influence de la distance à la mer sur les types d'occupation du sol est distincte de tous les autres modèles examinés jusqu'ici. Avant de l'examiner, il convient de noter que le front bassin versant de la mer est limité à une bande étroite près de la sortie dans le Golfe de St Tropez (Figure 2.1). Les variations majeures des vignes, des prairies et de la zone construite se localisent à environ 3 à 5 km du front de mer. Cette distance correspond à peu près au centre de la plaine alluviale et est proche des noyaux de Cogolin et Grimaud. Les changements dans la couverture forestière se situent à une plus grande distance (environ 7-9 km) et cela correspond à peu près à un pic secondaire dans le changement des vignes et de prairies.

IV. Discussions

Il convient de noter que les variables topographiques et de distance sont souvent corrélées, mais peuvent avoir des effets distincts. L'altitude et la pente sont corrélées et les deux reflètent une plus grande distance de la mer; tous influencent les coûts et donc les niveaux de construction. La distance à la mer reflète également l'impact de la distance aux zones construites, les grandes villes de Ste Maxime et St Tropez étant situées de chaque côté du golfe de St Tropez.

Dans la littérature scientifique, la transition de la couverture terrestre la plus fréquemment citée dans les régions méditerranéennes est l'abandon des pratiques agricoles sur les terres marginales et sa conversion en forêt (Falcucci et al. 2007, Geri et al. 2010, Parcerisas et al. 2012, Pelorosso et al., 2009, Serra et al., 2008). Cela n'a pas été observé dans ce bassin versant. Au contraire, les terres marginales sur des pentes plus raides ont été converties de forêt en vignoble, comme on peut le voir sur la figure 2.14 montrant les vignobles en terrasses sur les contreforts des dessus de la plaine alluviale. En ce qui concerne les vignobles, de vastes zones de la plaine ont été converties en prairies, en zone bâtie, et en forêt. Ceci a été compensé en partie (mais seulement en partie puisque le résultat net est une perte de 28% de couverture du vignoble entre 1950 et 2008) en replantant sur des pentes à proximité de la plaine. Ces champs se trouvent donc à l'interface entre la forêt étendue sur un côté et la plaine de l'autre.

Dans les différents travaux, une autre tendance commune citée est l'intensification de l'agriculture dans les plaines (Falcucci et al. 2007, Geri et al. 2010, Van Eetvelde et Antrop 2004). Dans la région étudiée, les récoltes de vin se réalisent mécaniquement et non plus manuellement, et témoignent donc d'une intensification de l'agriculture. Mais l'un des résultats majeurs de notre étude montre que le vignoble a tendance à se convertir de manière plus fréquente en prairies qu'en zone construite. Cela témoigne de l'abandon temporaire de ces vignes, soit par des grands propriétaires dont la production de raisin n'est pas au centre de leurs moyens de subsistance (cf. les grands domaines), soit par des agriculteurs qui jouent sur la valeur foncière de leur propriété. Cela explique en partie la conversion de la vigne à la prairie et rend compte de la situation paradoxale de l'agriculture conquérant des terres marginales sur les pentes abruptes tout en abandonnant les terres fertiles dans la plaine en prairies et forêts.

Les dynamiques des prairies sont particulièrement complexes dans le bassin versant. Comme indiqué plus haut, une partie de la croissance des prairies est due à l'abandon des terres dans la plaine alluviale fertile. Cependant, plusieurs autres facteurs entrent en jeu. Le premier est la reconversion des vignobles en prairies (principalement des pâturages) le long des cours d'eau, ce qui est probablement lié à des risques d'inondation. Ensuite, une partie de la transition vignoble-prairies est liée à la création d'activités d'équitation au cours des dernières années. Le tourisme est une industrie locale importante et la proximité de grandes étendues de forêt avec des sentiers et des chemins de terre transforme l'équitation en une activité touristique attrayante.

V. Conclusion

Comme dans une grande partie de l'Europe méditerranéenne, des changements importants de la couverture terrestre se sont produits dans 1950-2008. La forêt est restée la couverture terrestre dominante à tous les temps. Et les changements relatifs à la couverture forestière étaient faibles

pour plusieurs raisons: sa grande surface (plus de 85% du bassin versant) et l'emplacement à des altitudes plus élevées et sur des pentes raides. Malgré cela, les mutations de la forêt vers les vignes et les prairies étaient élevées. Le vignoble a perdu une superficie considérable. Il a été converti principalement en prairies, en milieu urbain. La catégorie prairie était très dynamique et a connu de grandes pertes et gains en raison de l'abandon du vignoble et la création de coupe-feu et des pâturages. La plupart des changements de l'occupation du sol se sont produits à basse altitude et à plat ou en pente douce, dans des zones de la partie orientale du bassin versant. Toutes les variables de distance (de cours d'eau, aux routes, à la zone bâtie, et à la mer) ont eu un impact significatif sur la dynamique des changements de la couverture terrestre.

CHAPITRE 3 : PREVISIONS DE CHANGEMENT D'OCCUPATION DU SOL, EN MEDITERRANEE, A DIFFERENTES ECHELLES

I. Introduction

La sélection des intervalles de prédiction et le temps de validation ont un grand impact sur la précision de la prédiction (Chen et Ponce 2010). Ainsi, la modélisation du changement de l'occupation du sol en utilisant une échelle temporelle grossière peut entraver la performance du modèle (Álvarez Martínez et al., 2011). De nombreuses études sur la modélisation de l'occupation du sol prennent en compte des échelles de temps courtes qui permettent d'atteindre une meilleure prédiction (Ahmed et Ahmed 2012, He et al., 2006, Li et Yeh 2002 Sang et al., 2011). Rares sont les travaux qui combinent plusieurs échelles de temps.
L'objectif de ce chapitre est d'étudier l'impact des échelles temporelles sur la modélisation et la prévision des transformations de la couverture terrestre dans un bassin versant méditerranéen SE France. Des cartes de l'occupation du sol en 2011 ont été ici prédites à partir de différentes échelles de temps (1950-1982, 1982-2003 et 2003-2008) et comparées avec la réalité pour mesurer la précision du modèle.

II. Méthodologie adoptée

La modélisation mise en place (LCM, Land Change Modeler) a permis d'identifier les variables explicatives, d'évaluer les changements de couverture terrestre, afin de créer des potentiels de transition, pour prédire les répartitions futures de l'occupation du sol. Puis les prédictions sont validées en comparant avec la réalité. La figure 3.2. présente les principales étapes de ce modèle LCM – IDRISI.

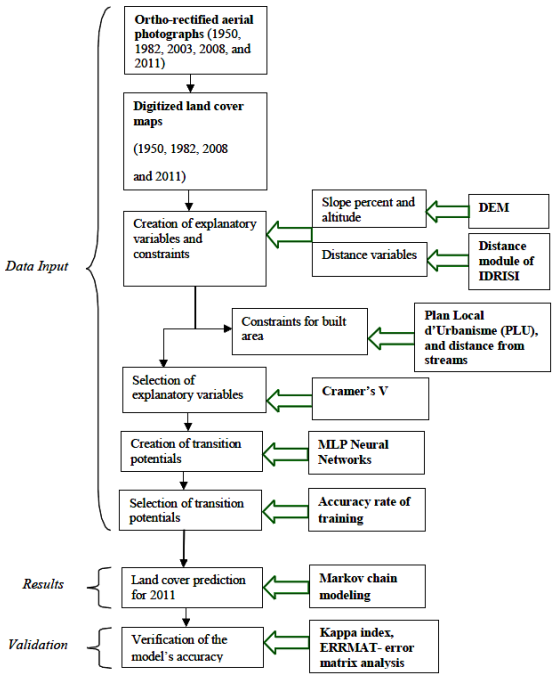

Figure 0.5: Les étapes du modèle

Notre travail se base toujours sur la numérisation de photographies aériennes à différentes dates (1950, 1982, 2003, 2008 et 2011), sur lesquelles ont été définies 4 catégories d'occupation du sol (forêt (F), vigne (V), prairies (G), et bâti (B)), validées par des visites sur le terrain. Nous avons ensuite intégré dans la prédiction différentes variables explicatives précédemment identifiées comme étant fondamentales pour les transformations passées (et mesurées à partir du test V de Cramer) : la pente, l'altitude, la distance aux routes, la distance à la surface construite (de première année), et la distance au cours d'eau. Des contraintes et des incitations de localisation ont été aussi incluses dans le processus de prédiction ; il s'agit de variables construites à partir de documents d'aménagement (PLU et SCOT) qui interdissent la transformation de toute occupation du sol (forêt, vigne, prairies) en zone bâtie.
Des cartes de potentiel de transition ont été créées pour chaque possibilité de transition (F à V, F à G, F à B, V à F, V à G, V à B, G à F, G à V, et G à B) sur la base historique les changements et les variables explicatives. L'algorithme Multi-Layer Perceptron Neural Network (MLPNN) d'IDRISI (Eastman 2012) a été utilisé pour créer des potentiels de transition. Pour toutes les transitions à différentes périodes de temps, 10.000 itérations ont été réalisées, et des modes dominants et persistants d'occupation du sol ont été déterminés.

La prédiction des transformations d'occupation du sol comporte deux aspects. D'une part, LCM fournit la quantité de changement à travers la matrice de Markov qui compare la première (T1) et deuxième couverture terrestre (T2) et qui construit ainsi une probabilité de conversion pour chaque catégorie, puis LCM prédit la couverture terrestre future (T3) en utilisant cette matrice de probabilité de transition pour l'avenir. D'autre part, les distributions spatiales du changement sont indiquées par les cartes de potentiel de transition générées en utilisant MLPNN. Ainsi, les répartitions d'occupation du sol prévues pour 2011 ont été prévues en utilisant des cartes de transition potentiels de plusieurs périodes historiques (1950-1982, 1982-2003, 2003-2008) (tableau 3.3). Enfin, la validation de la modélisation pour 2011 a été réalisée en comparant avec la carte numérisée réelle de la même année, et des erreurs quantitatives et de localisation ont été mesurées, à travers l'indice Kappa et l'analyse de la matrice d'erreur (Eastman 2012).

III. Résultats

Différents résultats ont été produits, à propos :

- Les transformations de l'occupation du sol à différentes périodes de temps. Deux tendances générales peuvent être identifiées dans le changement de la couverture terrestre depuis 1950 : la forêt et le vignoble ont diminué tandis que les prairies et les zones urbaines ont augmenté. Et la plupart de ces modifications se sont produites dans la plaine alluviale. Mais au-delà de ces tendances, des fluctuations peuvent exister. Ainsi, par exemple, si le vignoble a connu une baisse marquée en 1950 et 2003, il a de nouveau augmenté entre 2003 et 2008, puis a repris sa tendance à la baisse dans la dernière période 2008-2011.
- La prise en compte des variables explicatives. Le niveau de l'association entre les variables explicatives et les types de couverture terrestre dans les différentes périodes de temps est mesuré par l'indicateur V de Cramer. La variable explicative la plus forte est l'altitude, sauf avec la catégorie forêt. La distance aux routes montre un niveau

d’association élevé avec la vigne à toutes les périodes de temps, et un bon niveau d'association avec les forêts et les prairies pour les périodes intermédiaires (1982-2003) et longues (1950-1982). La distance aux flux est la variable la plus faible : elle montre une relation relativement limitée avec les couvertures terrestres existantes, et ne dispose d'un bon niveau d'association qu’avec la vigne dans toutes les périodes de temps.

- Les potentiels de transition pour les différentes périodes de temps. Ils présentent des profils similaires pour les différents pas de temps, et indiquent tous une forte concentration principalement dans la plaine alluviale (Figure 3.8). La plupart des zones d'altitude et celles de pentes douces ont montré une haute potentialité de transformation de la forêt à la vigne et aux prairies. La plupart des prairies loin des cours d'eau et des routes ont un potentiel plus élevé pour se transformer en forêt, et celles à proximité des routes et des cours d'eau ont un potentiel plus élevé de se convertir en vignoble. Certains vignobles éparpillés au bord de la zone bâtie existante ont montré une possibilité plus forte de transition vers la forêt, ce qui n’est pas le cas des vignes de la plaine. Enfin, toutes les occupations du sol ont une forte probabilité de se transformer en zone bâtie, quand elles sont à proximité du réseau routier et des surfaces construites existantes. En outre, un taux d’exactitude a été calculé pour tous ces transferts (tableau 3.7). Il est élevé pour plusieurs transitions dans toutes les périodes : la forêt pour toutes les autres catégories, et la vigne et les prairies en zone bâtie
- Les prévisions des changements de l’occupation du sol. Les matrices de transition sont présentées dans le tableau 3.8, avec en colonne la situation résultante simulée à la période d’après. Elles sont calculées sur la base de l'historique des changements de la couverture terrestre aux cours des périodes 1950-1982, 1982 à 2003, et 2003-2008. La forte probabilité de stabilité de la forêt à toutes les périodes apparait. En revanche, une probabilité de 0.72 associée à la persistance de la vigne indique sa vulnérabilité face à la progression des autres catégories, même si cette fragilité diminue dans le temps. De même, une probabilité de stabilité de 0.51 pour la prairie montre clairement son instabilité, et une haute possibilité de changement vers les autres types de couverture terrestre en 1982-2011. Enfin, la surface bâtie reste quasiment constante. En outre, il faut modérer ces probabilités par les superficies transformées. Et également par les périodes de temps : sur une phase courte de temps, les transformations sont moins fortement probables. Néanmoins, les tendances demeurent les mêmes sur les temps long et court.

Initial time period	Land cover types	Forest	Vineyard	Grassland	Built area
1950-1982	Forest	**0.97 (19,626)**	0.02 (404)	0.01 (202)	0.00 (0)
	Vineyard	0.08 (174)	**0.72 (1,571)**	0.15 (327)	0.049 (109)
	Grassland	0.21 (184)	0.23 (202)	**0.51 (448)**	0.048 (43)
	Built area	0.00 (0)	0.00(0)	0.00(0)	**1.000 (255)**
1982-2003	Forest	**0.98 (19,709)**	0.01 (201)	0.01 (201)	0.00 (00)
	Vineyard	0.01 (15)	**0.79 (1,224)**	0.18 (227)	0.02 (31)
	Grassland	0.14 (177)	0.07 (108)	**0.73 (458)**	0.06 (76)
	Built area	0.00 (0)	0.00(0)	0.00(0)	**1.000 (627)**
2003-2008	Forest	**1.00 (20,091)**	0.00 (0)	0.00(0)	0.00 (0)
	Vineyard	0.00 (0)	**0.98 (1,585)**	0.14 (11)	0.01 (16)
	Grassland	0.02 (23)	0.05 (81)	**0.91 (639)**	0.02 (23)
	Built area	0.00(0)	0.00(0)	0.00(0)	**1.000 (702)**

Tableau 0.2. Matrices de probabilité de transition en 1982-2011, 2003-2011, et 2008-2011, en utilisant différentes périodes (1950-1982, 1982-2003, et 2003-2008, respectivement). Les superficies potentielles de changement sont indiquées en ha entre parenthèses

- La validation des occupations du sol prévues. Des simulations pour 2011 ont été exécutées à l'aide des potentiels de transition 1950-1982, 1982-2003 et 2003-2008, respectivement (Figure 3.9). Des écarts sont observés principalement dans la partie orientale du bassin versant. Les indices Kappa (tableau 3.9) montrent que la prédiction s'améliore avec la réduction de l'échelle du temps. Ainsi, l'indice Klocation (qui donne la précision spatiale globale d'une simulation) est assez correct sur la longue période, mais augmente avec les temps intermédiaires et courts. Le tableau 3.10 présente l'analyse de la matrice d'erreur de l'occupation du sol en 2011, entre ce qui est réel (colonne) et prévu (ligne), pour différentes échelles de temps. Il indique également que toutes les erreurs ont diminué avec la réduction des échelles de temps. Les plus faibles erreurs ont été observées pour la forêt, et en réduction avec le raccourcissement de l'échelle de temps. Des écarts sont à noter dans le vignoble, sur l'échelle de temps longue. De très fortes erreurs sont observées pour les prairies, particulièrement à l'échelle de temps long. Des quantités importantes de vignes et de prairies ont été attribuées à tort en forêt.

Initial time period		Forest	Vineyard	Grassland	Built area	Total	Error of commission (%)
1950-1982 (long)	Forest	19,277	158	236	113	19,784	**2.6**
	Vineyard	438	1,305	488	156	2,387	**45.3**
	Grassland	295	113	403	118	930	**56.6**
	Built area	20	27	25	378	450	**16**
	Total	20,030	1,603	1,152	765	23,550	
	Error of Omission (%)	**3.8**	**18.6**	**65**	**50.6**		**9.3**
1982-2003 Iinterme-diate)	Forest	19,716	45	52	51	19,864	**0.7**
	Vineyard	68	1,413	80	30	1,590	**11.2**
	Grassland	204	119	965	37	1,326	**27.2**
	Built area	42	26	54	647	770	**15.9**
	Total	20,030	1,603	1,152	765	23,550	
	Error of Omission (%)	**1.6**	**11.9**	**16.2**	**15.4**		**3.4**
2003-2008 (short)	Forest	19,953	30	45	27	20,055	**0.5**
	Vineyard	16	1,496	94	15	1,621	**7.7**
	Grassland	44	68	997	17	1,127	**11.5**
	Built area	16	9	16	706	747	**5.4**
	Total	20,030	1,603	1,152	765	23,550	
	Error of Omission (%)	**0.4**	**6.7**	**13.4**	**7.7**		**1.69**

Table 0.3: La matrice d'erreur entre l'occupation du sol actuelle en 2011 (colonne) et prévue, pour différentes périodes de temps. Les valeurs sont exprimées en ha, et les erreurs en %.

IV. Discussions

Les dynamiques passées et récentes de l'occupation du sol ont un impact sur sa simulation future. Comme il est décrit dans les résultats, la forêt est facile à prédire, et obtient des écarts entre réalité et prévision faibles avec le meilleure Kquantity, à différentes échelles de temps, en raison de sa couverture dominante dans la zone d'étude et de sa localisation hors de la plaine alluviale là où les transformations majeures ont eu lieu. A l'inverse, les simulations des vignes et des prairies sont extrêmement difficiles à prévoir, et provoquent des précisions les plus faibles et des erreurs importantes, en raison essentiellement des mutations de ces catégories, de leurs variations aléatoires en début de période. S'y ajoutent également l'absence de prise en compte de certaines contraintes, notamment en termes de structures foncières (existence de Domaines viticoles, plus stables (Roy et al. 2014b)) et d'activités réelles sur les prairies (fonctions touristiques pratiquées sur les prairies et qui amènent à une plus forte stabilité). La prédiction exacte de l'expansion urbaine est difficile, en raison de la complexité de l'urbanisation qui dépend de plusieurs variables spatiales (planification urbaine, choix individuels d'installation, etc. (He et al., 2008)), mais également d'une croissance urbaine exceptionnellement rapide, et qui s'est parfois déroulée dans des lieux dispersés, loin de la zone bâtie existante.

Les échelles de temps ont un impact significatif sur la simulation de l'occupation du sol. La quantité est mieux prédite que la localisation, probablement en raison de la couverture forestière dominante dans la zone d'étude. Par conséquent, Kquantity est presque parfait dans toutes les échelles de temps. En revanche, les transformations complexes de l'occupation du sol génèrent

des niveaux moins parfaits d'entente pour Klocation que Kquantity, et les valeurs augmentent avec la diminution des échelles de temps.

CHAPITRE 4 : PREVISIONS DE CHANGEMENT D'OCCUPATION DU SOL : EFFETS DES CATEGORIES ET DES TAILLES DE CELLULE

I. Introduction

Plusieurs techniques de modélisation ont été développées pour explorer et prévoir les changements de l'occupation du sol (Barredo et al. 2003, He et al., 2008), et les facteurs topographiques et socio-économiques sont considérés comme importants dans la compréhension et la prédiction de la couverture terrestre (Munroe et Müller 2007). Cependant, la qualité de la prédiction ne dépend pas seulement de la pertinence des variables explicatives, mais aussi de plusieurs autres éléments, qu'il faut désormais prendre en compte : le type et le nombre de catégories de l'occupation du sol, les intervalles historiques et la période temporelle à atteindre (Roy et al de 2014a.), et l'étendue spatiale et la résolution (Chen et Ponce 2011). Ainsi, une étude comparative bibliographique nous montre que si les transformations de l'occupation du sol sont distribuées de façon homogène dans l'espace, l'étendue spatiale n'a que peu d'impact sur la prévision et sa qualité. Cependant, ce cas est rare, et l'augmentation de l'étendue spatiale se traduit souvent par l'augmentation de l'instabilité de catégories et donc par une difficulté à prévoir le phénomène. De même, d'autres travaux (Dietzel et Clarke 2004) ont montré que des résolutions plus fines, inférieures à la taille des parcelles (<10m) – alors que la résolution de 30m est la plus souvent utilisée -, pouvaient augmenter les erreurs de prévision, du fait de la création de petits changements non significatifs. A l'inverse, beaucoup d'études suggèrent que la modélisation des transformations de l'occupation du sol pouvait être améliorée en utilisant des tailles de cellules grossières, tout en réduisant le temps de calcul.
Les effets des échelles de temps (long, court, intermédiaire) ont été discutés dans les chapitres précédents. Dans ce chapitre, nous souhaitons mettre en évidence le rôle de l'étendue spatiale et celui de la taille des cellules, dans la modélisation A partir de photos aériennes de 1950, 1982 , 2003, et 2011, la dynamique de l'occupation du sol a d'abord été analysée à travers des mesures d'intensité ; puis, sur cette base, la couverture terrestre a été prédit pour 2011 pour une grande (79,1 km²) et petite (36,6 km²) fenêtres en utilisant la taille des cellules de 25 m, 50 m, 100 m. Les effets de la résolution spatiale ont également été analysés, en faisant varier les échelles dans les deux sens (de 25 m à 50 m et 100 m, puis retour à 25 m).

II. Méthodologie adoptée

Notre territoire d'étude est toujours le bassin versant de la Giscle. La partie ouest du bassin versant est boisée et a peu changé depuis 1950 environ (Fox et al. 2012, Roy et al. 2014A, Roy et al. 2014b), et une grande partie du changement de la couverture terrestre est concentrée dans la plaine alluviale vers l'est, près de la côte. La première aire d'étude sélectionnée pour ce chapitre est une superficie de 33.6 km² (petite zone), et comprend la principale zone peuplée dans la plaine alluviale et le noyau de la plupart des dynamiques de l'occupation du sol dans le bassin versant. Une seconde zone, plus grande 79.1 km², contient cette zone précédente et une extension vers l'ouest pour inclure une grande étendue de la couverture forestière stable. Les altitudes et les pentes sont plus douces et moins fortes dans la petite que dans la grande fenêtre. Le point

fondamental est que la plupart des transformations se produisent dans la petite fenêtre, alors que la grande reste plus stable.
On choisit ici de travailler sur des taux relatifs de changements de l'occupation du sol, comme mesure de l'intensité des transformations. On mesure aussi, pour chaque intervalle de temps, des taux de transformations annuels (St), et des taux annuels moyens calculés pour tous les intervalles de temps (U), pour déterminer des rythmes de mutations (Aldwaik et Ponce Jr 2012). Pour les gains et les pertes de chaque catégorie d'occupation du sol, on calcule aussi des variations relatives en fonction de superficie de départ. Les transitions entre catégories ont été aussi calculées de manière relative.
Nous avons utilisé la procédure LCM (Land change Modeler) d'IDRISI pour prédire l'occupation du sol de 2011. L'échelle de référence de traitement des catégories est de 1 mètre. Afin d'étudier l'impact de la taille des cellules sur la modélisation des transformations de l'occupation du sol, la taille des cellules a été successivement convertie à 25 m et 50 m et 100 m, puis réduite en sens inverse (upscaling et downscaling). Pour étudier l'influence de l'étendue spatiale, deux zones de tailles différentes ont été sélectionnées
Différentes variables ont été intégrées dans la procédure de modélisation : l'altitude, la pente et les distances des routes, à la surface construite initiale, et aux cours d'eau. Des contraintes et des incitations ont été également incluses dans le processus de prédiction, à partir des documents d'aménagement (PLU et SCOT) : zones où le développement urbain est restreint (réserve forestière et des zones agricoles) ou au contraire privilégié (à proximité des zones bâties, à proximité des cours d'eau, etc.). Le test V de Cramer a été utilisé pour évaluer l'impact de l'étendue spatiale et de la taille de la cellule sur l'importance des variables explicatives. Grâce aux potentiels de transition significative (probabilité d'évolution d'une catégorie à une autre), des cartes ont été créées pour toutes les transitions possibles en fonction des changements historiques au cours de 1982 à 2003 et les variables explicatives en utilisant l'algorithme MLPNN de IDRISI (Eastman 2012). Puis des indices de validation sont établis.

III. Résultats

L'analyse de la comparaison entre la petite et la grande zone d'étude donne les résultats suivants (tableau 4.3). Dans la petite zone, la forêt et le vignoble occupent des superficies équivalentes en 1950 (environ 43%), bien que cet équilibre change considérablement au fil du temps puisque la vigne perd du terrain au profit d'autres types d'occupation du sol. Toujours dans cette petite zone, l'espace bâti subit une augmentation relativement importante. A l'inverse, dans la grande zone, la forêt domine largement et reste stable à environ 74%. La plupart des changements se produisent donc dans la petite fenêtre, dans la plaine alluviale.

		Change (ha)			% of change in small window		
	Category	**1950-1982**	**1982-2003**	**2003-2011**	**1950-1982**	**1982-2003**	**2003-2011**
Small	Forest	387	398	137			
	Vineyard	703	550	168			
	Grassland	504	577	231			
	Built area	164	271	93			
	TOTAL	1,758	1,796	630			

Large	Forest	491	514	153	78.8	77.4	89.5
	Vineyard	781	631	180	90.0	87.2	93.3
	Grassland	549	653	246	91.8	88.4	93.9
	Built area	164	274	94	100	98.9	98.9
	TOTAL	1,985	2,071	673	88.6	86.7	93.6

Tableau 0.4: Les différentes catégories d'occupation du sol, en valeurs absolues et relatives, à différentes périodes de temps.

L'influence de l'intervalle de temps sur les caractéristiques d'occupation du sol indique, en règle générale, des intervalles de temps plus longs aboutissent à des variations absolues plus grandes : ainsi, les transformations relativement faibles observées pour 2003-2011 résultent principalement de l'intervalle de temps court (8 ans) par rapport aux autres périodes (32 et 21 ans, respectivement). Cependant, si l'on étude cette dynamique en valeur relative, on voit bien que la période la plus active a été 1982-2003, suivie de 2003-2011 puis 1950-1982. En outre, comme la plupart des changements sont concentrés dans la plaine alluviale, les changements relatifs dans la petite zone sont environ 2 fois plus élevés que dans la fenêtre plus grande. Ceci est particulièrement vrai en ce qui concerne la zone bâtie.

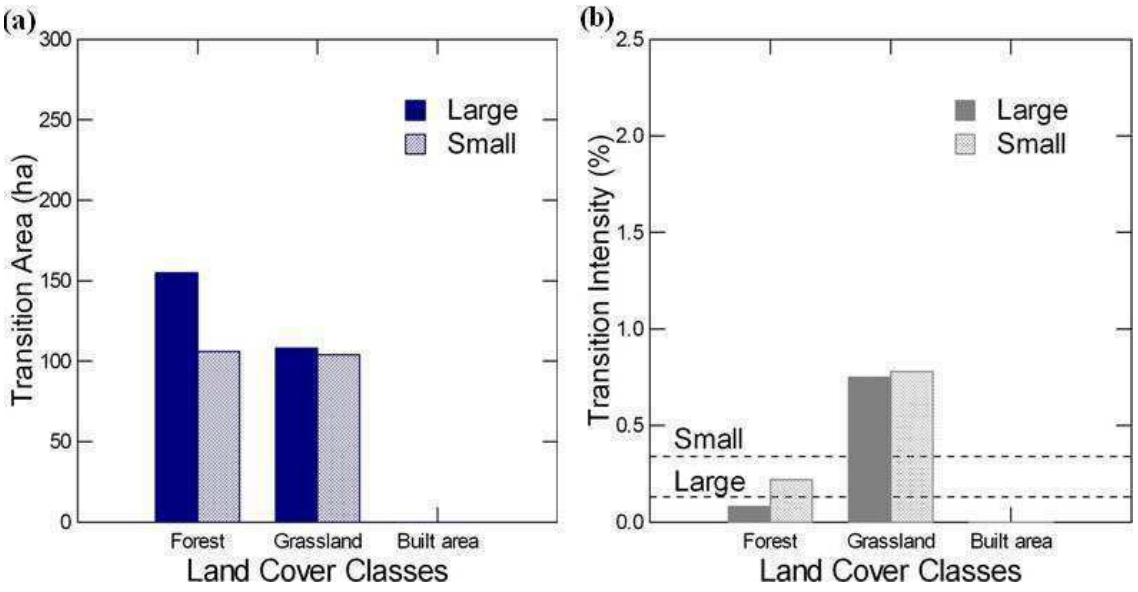

Figure 0.6: Modalités de transition de la vigne aux autres catégories, en ha, en %, entre 1950 et 1982

Si l'on se concentre sur l'évolution de la vigne (Figure 4.7), on constate des conversions des forêts en vigne, plus importantes que les mutations des prairies en vignes, et ceci entre 1950 et 2003 ; et ce phénomène s'inverse dans la dernière période. Ces phénomènes se produisent essentiellement dans notre petite zone d'étude. De même, c'est essentiellement dans cette zone, que se concentrent les gains de surface construite sur la vigne.

Les indices de Cramer permettent de mesurer les impacts de l'étendue spatiale et de la taille des cellules (ici 25m dans un premier temps) sur les dynamiques de l'occupation du sol. On constate ainsi que les valeurs V de Cramer sont généralement 1,3 à 1,7 fois plus élevées pour la grande zone que pour la petite fenêtre, et cela vaut pour toutes les catégories et les variables explicatives,

sauf pour la zone de construction et les deux prédicteurs de changement de surface construite (distances aux routes et à la zone bâtie). Les indices de désaccords témoignent d'une meilleure prédiction de l'occupation du sol pour la grande fenêtre. En ce qui concerne la taille des cellules, elle apparaît d'abord n'avoir aucune incidence sur le V de Cramer, puisque ces valeurs sont presque identiques pour les trois tailles de cellules dans les deux étendues spatiales. Ceci fait exception pour les deux variables explicatives les plus fortement liées à l'évolution de la zone construite (distances aux routes et à la zone de construction) : le V de Cramer est systématiquement plus grand pour la zone construite que pour la forêt dans la petite fenêtre, mais pas dans la grande fenêtre. Les pouvoirs explicatifs de la distance sur les routes et à la zone construite augmentent considérablement lorsque l'étendue spatiale est réduite. Les mêmes calculs ont été faits avec les résolutions de 50 m et de 100 m, et les relations entre les variables explicatives et la catégorie restent les mêmes. L'absence d'un impact de la taille des cellules sur la modélisation est également apparemment confirmée par les valeurs de désaccord similaires entre les résolutions spatiales de 25 m, 50 m et 100 m

IV. Discussions

Nos résultats ont montré, à travers l'analyse de l'intensité, que la variation de la catégorie d'occupation du sol dépend en partie de l'étendue spatiale. Sur la base des valeurs absolues des terres converties, la forêt était modérément réactive à l'étendue spatiale ; mais en valeurs relatives, elle était beaucoup moins active que les petites catégories qui subissent moins de changement en termes de superficie absolue, mais beaucoup plus en relatif. La vigne est apparue particulièrement active à la grande échelle, mais beaucoup moins dans la petite fenêtre. Dans cette étude, les deux catégories prairies et zone bâtie sont particulièrement actives en ce qui concerne leurs surfaces respectives, ce qui tend à réduire l'importance relative des changements de la vigne, quand une catégorie dominante (la forêt) est exclue de l'étude en passant de la grande à la petite fenêtre. Ainsi, les taux de variation des catégories sont sensibles à l'étendue spatiale et peuvent tout à fait différents quand une grande catégorie de dominante est présente.
En ce qui concerne l'étendue spatiale, un facteur entre en jeu dans la détermination des variations des catégories. Ainsi, si une quantité importante d'une couverture terrestre se trouve en dehors de la petite zone, mais que la plupart du changement est dans la petite fenêtre (comme pour la forêt), alors les valeurs absolues seront plus importantes à la grande échelle, mais les taux relatifs seront inférieurs dans la fenêtre plus petite. En outre, le pouvoir prédictif des variables explicatives est fortement affecté par l'étendue spatiale, et la présence de la couverture forestière persistante a donné l'impression que les variables explicatives étaient de meilleurs prédicteurs à grande échelle que pour la petite fenêtre. De plus, l'ajout d'une grande zone de couverture terrestre persistante semble réduire la quantité et la répartition des erreurs : ainsi, la quantité et la répartition des désaccords sont plus importantes dans la petite fenêtre en raison de changements dans les trois valeurs différentes utilisées pour calculer ces indices (superficie totale, variation absolue totale, et la zone correctement prédite). Ceci est en accord avec les observations de Chen et Ponce (2010) et Ponce et Spencer (2005) qui montrent que la persistance est plus facile à prévoir que le changement. Mais pourquoi le V de Cramer s'améliore t il, dans l'ensemble, si fortement avec l'étendue spatiale ? L'une des raisons possibles serait que quand la taille de la fenêtre augmente, la variabilité des valeurs explicatives augmente aussi. Ainsi, par exemple, les plages d'altitude

sont 237 m et 663 m pour les petites et grandes fenêtres, respectivement. Ces petites différences peuvent avoir un impact important sur la valeur du chi carré utilisé pour calculer le V de Cramer. Au total, e choix de l'étendue spatiale dans la modélisation des transformations de la couverture terrestre peut être lié au processus étudié, aux contraintes de données (fonction des unités administratives, par exemple), ou à une décision arbitraire. Dans tous les cas, il faut chercher au maximum à la présence de grandes catégories dormantes afin d'éviter d'augmenter artificiellement les résultats de prédiction.

La taille des cellules de la grille est entraînée par de nombreux facteurs et peut être sujette à des interprétations différentes. Elle peut dépendre de la taille initiale de la cellule de données d'entrée (par exemple 30 m Landsat vs 10 m images SPOT) ou elle peut être liée à des procédures d'harmonisation, d'expansion et de contraction. Dans cette étude, nous avons adopté une échelle fine de numérisation de la couverture terrestre (1 mètre), afin de créer une meilleure classification des types d'occupation du sol et pas nécessairement une carte plus détaillée de la couverture terrestre. Les premiers résultats semblent montrer que la taille de la cellule n'a pas d'impact sur la modélisation du changement de la couverture terrestre, sur la base du test V en changeant d'échelle. Toutefois, la procédure upscaling / downscaling montre que pendant la progression vers une plus grande échelle, une grande partie des informations ont été perdues. Les impacts de l'étendue spatiale et de la résolution des cellules sur les données du paysage sont discutés dans Turner et al. (1989), où les chercheurs montrent que la probabilité de perte d'information augmente avec la taille de la cellule. En effet, comme la taille des cellules augmente, le détail est perdu, les pixels isolés disparaissent, et le paysage devient à la fois plus simple et moins représentatif de la réalité. Cependant, la réduction de l'échelle ne restaure pas l'information initiale, mais elle permet au modélisateur d'avoir une certaine mesure de la quantité d'informations perdues par des changements dans les valeurs de désaccord.

V. Conclusions

L'étendue d'un territoire et la taille des cellules sont deux questions fondamentales de la modélisation des dynamiques de la couverture terrestre. Dans cette thèse, l'étendue spatiale a un impact majeur sur la perception de la dynamique des changements de la couverture terrestre, où de relativement grandes catégories dormantes peuvent masquer les mutations de catégories plus dynamiques et plus petites. En conséquence, il est plus difficile de modéliser les petites zones avec plusieurs types de couverture terrestre en mutation rapide que les zones stables plus grandes. Les quantités et les répartitions des mesures de désaccord sont plus dans la petite fenêtre que dans la grande fenêtre, car la plupart des changements se produisent dans la petite zone et la partie étendue de la grande fenêtre composée de la forêt persistante et la persistance génère une plus grande précision de la prédiction.

CHAPITRE 5 : EVOLUTION DE L'EROSION DU SOL DANS UN BASSIN VERSANT MEDITERRANEEN ENTRE 1950 ET 2025

I. Introduction

1.1.Cadrage sur l'érosion du sol

Le sol est une ressource non renouvelable vitale formée par divers processus biologiques physiques, chimiques, et dans le milieu naturel. La dégradation des sols due à l'érosion est devenue un grave problème environnemental à travers le monde en raison de la croissance rapide du surpâturage, de la déforestation, de pratiques agricoles inadaptées, de la surexploitation du bois de feu, des feux de forêt, et d'autres activités humaines (Alkharabsheh et al. 2013, Brady et Weil 1999, Terranova et al., 2009). Dans de nombreuses régions du monde, les taux d'érosion du sol dépassent la formation du sol et produisant ainsi une dégradation grave du sol (Toy et al., 2003). L'érosion du sol peut causer plusieurs problèmes environnementaux et économiques : la perte de la productivité agricole, la pollution de l'eau (envasement des ruisseaux, rivières, réservoirs), et la perte de la biodiversité, etc. (Lu et al 2004, Zhang et al 2014.). Brady et Weil (1999) décrivent trois étapes fondamentales de l'érosion des sols : détachement de particules du sol, transport des particules détachées par différents processus et dépôt des particules transportées à basse altitude. Trois formes d'érosion par l'eau sont également décrites dans Brady et Weil (1999) : l'érosion en nappe, l'érosion des rigoles, et le ravinement. L'érosion en nappe peut être observée lorsque l'écoulement de l'eau élimine le sol plus ou moins uniformément ; elle se transforme en érosion des rigoles lorsque le débit se concentre dans de petits canaux. Lorsque le ruissellement se concentre, des ravines peuvent être formées.

Le risque d'érosion du sol varie en fonction de plusieurs paramètres : la topographie (gradient et longueur pentes), les caractéristiques du sol, le climat local, le type de végétation, l'occupation du sol, et les pratiques de gestion des terres (Alkharabsheh et al 2013.). Par conséquent, le terrassement peut diminuer l'érosion du sol puisque les deux facteurs topographiques sont réduits (Liu et al. 2013). Mais celui-ci doit être combiné à l'occupation du sol (terres arables, progression de la foret, etc.). Bakker et al. (2005) ont identifié une bonne relation entre l'érosion des sols et l'utilisation des terres dans la partie ouest de Lesbos, Grèce. Pour identifier la relation, une régression logistique a été réalisée en utilisant la dynamique de l'occupation du sol comme variable à expliquer et la profondeur du sol, l'érosion et la pente comme variables explicatives. En outre, un impact significatif de la végétation a été mesuré dans Mohammad et Adam (2010) : la couverture de la végétation ajoute de la matière organique à la surface du sol, ce qui peut empêcher l'érosion des sols par le développement de la structure du sol et l'amélioration de la stabilité des agrégats. Et, le couvert végétal protège la surface du sol de la pluie et réduit l'énergie de ruissellement. Ce que conforme une autre étude sur le Portugal (Nunes et al. (2011)).

1.2.Ampleur de l'érosion en Europe méditerranéenne

L'érosion du sol par le ruissellement est une question importante pour la France méditerranéenne. Plusieurs études ont déjà été menées pour mesurer l'érosion du sol et d'identifier les facteurs d'érosion des sols pour différents bassins versants dans la région méditerranéenne (Blavet et al. 2009, Kosmas et al., 1997, Ramos et Martínez-Casasnovas 2006, Torri et al. 2006, Wainwright 1996). Les régions méditerranéennes sont particulièrement vulnérables à l'érosion des sols en

raison de l'intensité des précipitations élevées, des activités agricoles sur les pentes raides, de la faible teneur en matière organique, de faibles teneurs en éléments nutritifs et des rapides changements d'utilisation des terres (García-Ruiz 2010, Novara et al. 2011). Kosmas et al. (1997) ont révélé, à partir d'une étude sur l'Europe méditerranéenne dont les Pyrénées, que les terres cultivées dans les zones montagneuses des régions méditerranéennes sont très sensibles à l'érosion due à un sol peu profond et au manque de couverture végétale. En outre, l'abandon des terres agricoles, l'expansion de la vigne dans les forêts de montagne et les champs de céréales ont également accéléré le risque d'érosion du sol dans ce domaine. Arnaez et al. (2007) décrit les différents facteurs de l'érosion du sol et utilise l'USLE pour estimer l'érosion d'un bassin méditerranéen espagnol dominé par les vignobles (La Penedès et Rioja). L'étude a révélé que le gradient de pente, la taille des gouttes de pluie, les capacités d'infiltration et de stockage de l'eau ont des impacts directs sur les processus d'érosion. Elle a en outre montré que l'érosion du sol peut être diminuée en augmentant la densité de la vigne, en changeant le système de travail du sol (à angle droit au gradient de pente maximale pour favoriser l'infiltration), et en installant des terrasses de construction le long des lignes de contour.

Les vignobles dans la région méditerranéenne ont les plus hauts taux d'érosion du sol (Kosmas et al., 1997). La région méditerranéenne connaît de fortes intensités de tempête, sur le sol sec en été, et à l'automne lorsque les vignes sont souvent nues ; c'est donc sur ces périodes que se produisent des taux élevés d'érosion (Blavet et al. 2009, Wainwright 1996, Ramos et Martínez-Casasnovas 2006). En outre, les agriculteurs utilisent de nombreux traitements herbicides chimiques, afin que les champs soient nus pour un temps plus long et que moins d'herbe poussent en hors-saison. Les raisins sont récoltés en août-septembre, et les fortes pluies commencent peu après et continuent d'octobre à mars. Ces pratiques sont populaires pour obtenir des raisins de qualité à rendement élevé et de meilleure qualité. Au total, les vignes sont donc fortement vulnérables à l'érosion, à l'épuisement de la matière organique du sol, à la pollution et à la perte de la biodiversité (Coulouma et al. 2006, Raclot et al., 2009).

Novara et al. (2011) ont réalisé une étude pour estimer les pertes de sol dans une vigne irriguée à Sambuca di Sicilia, dans le sud-ouest Sicile sous labour conventionnel. L'étude a estimé un taux d'érosion du sol moyen de 124,1 T ha-1y-1 en utilisant le modèle USLE et les taux d'érosion les plus élevés ont été observés sur les pentes plus raides. D'un autre côté, Ramos et Martínez-Casasnovas (2006) ont calculé les pertes de nutriments dans les vignobles et leur relation avec l'érosion des sols dans la région viticole Alt Penedès (nord-est de l'Espagne). Dans leur zone d'étude, 80% de la superficie cultivée a été occupée par les vignes, et l'érosion des sols a augmenté en raison de l'intensification et la mécanisation de la culture de la vigne.

1.3.Modélisation de l'érosion des sols

Différents modèles d'érosion ont été interfacés avec les SIG pour évaluer et prédire l'érosion des sols. Les modèles les plus fréquemment cités sont les suivants : le modèle RUSLE (Equation revisitée de l'érosion du sol universelle) (Renard et al 1997), le programme de prédiction de l'érosion par l'eau (WEPP) (Laflen et al., 1991), et LANDSOIL (Ciampalini et al. 2012). Les modèles d'érosion des sols sont importants pour mesurer et identifier les processus de détachement, le transport et le dépôt de l'érosion des sols à l'aide d'un ensemble d'équations mathématiques liées aux précipitations, aux caractéristiques du sol, à a topographie, à la végétation et à la gestion des sols d'un site (Brady et Weil 1999).

Le modèle LANDSOIL est basé sur l'étanchéité et le transfert par ruissellement et l'érosion liée à la gestion agricole (STREAM) ; et la distinction principale de ce modèle est de considérer les caractéristiques du sol (rugosité du sol, encroûtement de surface, et la couverture végétale d'évaluation) comme le principal processus d'érosion des sols et de redistribution dans un paysage agricole (Ciampalini et al. 2012). Les modèles LANDSOIL traitent de processus de redistribution des sols dans différents paysages topographiques et agricoles, et ils facilitent la conception de paysage à l'échelle du bassin versant pour la conservation des sols en utilisant différents types de couverture terrestre dans le sud de France (Ciampalini et al. 2012). De la même manière, Evrard et al. (2010) ont identifié l'impact des précipitations saisonnières et l'utilisation des terres sur l'érosion des sols au cours des 40 dernières années en utilisant le modèle STREAM pour un bassin versant dans le sud de la France. L'étude a révélé que l'exportation de sédiments a augmenté de 168% après la consolidation de la terre en raison de la diminution de la couverture de la prairie et l'augmentation de la taille du champ.
Le projet de prévision de l'érosion de l'eau (PPS) prédit la perte de sol et le dépôt en utilisant une approche spatialement et temporellement distribuée et peut intégrer différentes couvertures terrestres (pâturages, forêts, terres agricoles, et la zone urbaine) (Mahmoodabadi et Cerdà 2013). Il est également en mesure de décrire les processus de ruissellement et d'érosion, et d'évaluer les impacts de l'intervention de la direction et les changements environnementaux.

1.4.Le modèle USLE

Le modèle USLE a été utilisé dans le monde entier depuis les années 1970 et il a été mis à jour au début des années 1990 pour créer un outil de prévision de l'érosion nommé : Equation revisitée de l'érosion du sol universelle (RUSLE) (Brady et Weil 1999). RUSLE est un modèle à base de facteur qui estime le taux d'érosion globale des sols, et qui quantifie un ou plusieurs processus et interactions à travers les facteurs (Millward et Mersey, 1999). Il est facile à utiliser et pratique pour quantifier l'érosion du sol en tenant compte des précipitations, de la topographie, du sol, de la végétation, de l'utilisation des terres et de la gestion des terres (Zhou et al., 2008). La première version de ce modèle a été développée pour les champs agricoles, et la version mise à jour récente est modifiée sur la base de la théorie de la puissance du courant qui est adapté aux conditions topographiques complexes (Mitasova et al. 1996, Chakroun et al., 1993). Toutefois, ce modèle ne peut pas envisager de dépôt (Terranova et al., 2009). Le modèle USLE et sa version améliorée, RUSLE, sont les modèles plus couramment utilisés pour estimer et prévoir l'érosion du sol à différents endroits géographiques. Il a été appliqué sur différentes occupation du sol (végétation, vignoble, etc.) et à des échelles différentes (parcelles, bassin versant, etc.).
RUSLE est conçu pour prédire l'érosion annuelle moyenne du sol (Alkharabsheh et al. 2013, Nyakatawa et al., 2001). Il est construit à partir d'une équation basée sur les principaux facteurs qui influent sur l'érosion des sols (Renard et al., 1997). Il calcule une perte moyenne du sol par unité de surface en fonction des facteurs : d'érosivité des pluies (R), d'érodabilité (K), de longueur (L) et d'inclinaison (S) de la pente, de gestion de l'occupation du sol (C), et de pratique d'entrainement (P). Les facteurs R, K et LS déterminent le taux d'érosion tandis que P et C sont des facteurs de réduction, compris entre 0 et 1 (Meusburger et al., 2010).
R est le facteur d'érosivité des pluies qui représente une valeur annuelle moyenne de l'agressivité de la pluie pour provoquer l'érosion (Lal, 1990, (Kouli et al., 2009). Il traduit l'énergie de la tempête totale (E) pour une intensité maximale de 30 minutes (I30) calculée pour chaque tempête de pluie pour une période donnée (Kouli et al. 2009, Renard et al., 1997). Cependant, il pourrait

être calculé à partir de la pluviométrie annuelle moyenne, en raison de l'absence de données de pluie détaillée. Ce facteur R est considéré comme le plus influent de l'érosion des sols dans les différentes études utilisant RUSLE à travers le monde (Kouli et al. 2009, Wischmeier et Smith 1978).

Le facteur K est le facteur d'érodabilité du sol. Il indique le taux de perte du sol par unité d'indice d'érosion pour une parcelle spécifique du sol, qui est de 22,1 m de longueur avec une pente uniforme de 9% en continu, et labouré ou en jachère (Renard et al., 1997). Il reflète le processus de détachement du sol qui est généré par l'impact des éclaboussures ou des flux de surface, et il estime l'influence des propriétés du sol. K dépend de la texture du sol (M), de la matière organique (OM), de la structure du sol (1 <s <4), et de la perméabilité ou de la capacité d'infiltration (1 <p <6) (Morschel et Fox 2004, Renard et al., 1997). La texture du sol a un impact significatif sur K. Les sols à teneurs élevées en argile ont de faibles valeurs de K, en raison de leur haute résistance au détachement. Cependant, les sols à texture grossière, comme les sols sablonneux ont de faibles valeurs de K. En outre, des teneurs élevées en matières organiques peuvent diminuer l'érodabilité du sol, en réduisant la sensibilité au détachement et au ruissellement.

Les facteurs LS décrivent les effets combinés de la longueur de la pente (G) et la pente elle-même (S). Ces facteurs reflètent les effets de la topographie sur l'érosion des sols (Fu et al., 2006). La longueur de la pente (L) peut être mesurée comme la distance horizontale de l'origine de l'écoulement de surface à l'endroit où le dépôt commence ou bien où le ruissellement se concentre (Wischmeier et Smith 1978, Renard et al., 1997). La forme d'une pente affecte également la perte moyenne du sol qui peut être de 30% supérieure pour une pente convexe que pour une pente uniforme avec la même pente (Renard et al., 1997).

C est le facteur de la gestion de la couverture terrestre, utilisé pour estimer les effets de la culture et des pratiques de gestion sur les taux d'érosion (Renard et al., 1997). Ce facteur tient compte de divers systèmes de travail du sol, de la rotation des cultures, des traitements de fertilité, et de la gestion des résidus de récolte (Renard et al., 1997). En outre, il met en évidence l'effet des plans de conservation des sols

Enfin, le facteur P quantifie l'impact positif des contrôles de gestion des eaux de ruissellement qui changent la direction, la vitesse, et la quantité des eaux de ruissellement, à travers certaines pratiques agricoles (contournement, bandes tampons, bandes filtrantes, bandes de rotation des cultures, terrasses, le drainage du sous-sol, etc.) (Renard et al., 1997).

1.5.Le modèle USLE

La plupart des études portant sur la prédiction de l'érosion des sols mettent l'accent sur les terres cultivées dans le monde, alors que les vignobles de la région méditerranéenne française ont été beaucoup moins étudiés. L'objectif principal de ce chapitre est d'estimer l'évolution de l'érosion des sols dans le bassin versant de la Giscle, alors que les zones viticoles ont évolué (1950 à 2011) et devraient changer dans les prochaines années (jusqu'en 2025) en utilisant le modèle de RUSLE.

II. Méthodologie adoptée

Le bassin versant de la Giscle est toujours notre terrain d'étude. La production de raisin est la principale activité agricole dans le bassin versant. La plupart des vignobles y sont plantés en rangées droites et sont orientés dans le sens de la pente sur des pentes raides, et perpendiculaires à la pente lors d'inclinaisons plus douces. Les vignes représentent environ 10% de la superficie du bassin versant (Roy et al. De 2014b). Elles sont situées principalement dans la plaine inondable de sable et se sont propagées sous la pression urbaine sur des pentes plus fortes au cours des dernières années (de 2003), là où les sols sont minces, légèrement acides, pierreux et de texture sableuse (Fox et al. 2006, Roy et al. 2014b). La texture du sol dans la plupart des vignobles est la suivante : 60-80% de sable, 10-30% de limon et 5-15% d'argile (De Coster 2013). La plupart des vignobles dans le bassin versant sont touchés par de fortes précipitations en hiver, comme on peut le voir à la figure 5.1.

Figure 0.7: Les vignes affectées par de fortes précipitations (Photos: D. Fox)

Le module RUSLE implanté en IDRISI estime la perte annuelle moyenne du sol et détermine la répartition spatiale de la perte de sol (Eastman 2012). Le modèle a été exécuté à l'aide d'un 25 m DEM. L'érodabilité du sol (K), l'érosivité des pluies (R), la gestion de la couverture terrestre (C), et les facteurs de pratiques de conservation (P) ont été spécifiés pour 1950, 1982, 2003, et 2011. En outre, les taux d'érosion ont été prévus pour 2025, à partir de cartes simulées de la couverture terrestre.

En l'absence de données sur l'intensité des précipitations, R a été estimé à partir des précipitations annuelles moyennes, enregistrées par une station météo locale (Cogolin) de 1975 à 2005. R a été calculé sur la base d'une équation mise en place pour une région en Toscane. Les précipitations et le ruissellement érosif R-facteur ont été estimées à partir de la pluviométrie annuelle moyenne de 895 mm en 1975-2005, qui a donné une valeur de R de 107 MJ mm an / ha / h. Pour le coefficient K, une carte des sols du bassin versant a été générée à partir des données du sol obtenues à partir de la coopérative vinicole locale. Puis, ensuite, on a appliqué l'équation décrite dans Wischmeier et Smith (1978), et les points obtenus ont été interpolés. Le modèle RUSLE dans IDRISI calcule automatiquement le facteur LS à partir du modèle numérique d'élévation de 25 m (DEM). Le facteur de gestion de la couverture terrestre (C) pour le vignoble est de 0,3, choix établi d'après la littérature scientifique. La valeur P a été fixée à 0.7, compte tenu du choix de culture de l'alignement des rangées de vigne, perpendiculaire à la pente, ce qui contribue à ralentir la vitesse d'écoulement, à piéger les sédiments, et à réduire l'érosion par rapport à une surface nue. Pour les terrasses, on a choisi la valeur de P=0.2.

Les cartes d'érosion du sol ont été estimées pour 1950, 1982, 2003, 2011, et 2025. Les valeurs d'érosion ont ensuite été simplifiées en trois catégories: <10, 10-25 et> 25 t / ha comme faible, moyen et élevé, respectivement. Pendant deux hivers pluvieux consécutifs, des observations sur le terrain ont été faites des phénomènes d'érosion. Les données ont été recueillies auprès de différents vignobles choisis au hasard, et le nombre et la taille des ruisselets ont été notés, ainsi que les signes de dépôt de sédiments. Malheureusement, ces données ont été perdues durant mon déplacement à Toronto. Les résultats présentés ici ne sont donc pas validés et leur publication doit attendre le renouvellement des observations sur le terrain. Pour prédire l'occupation du sol en 2025, nous avons utilisé les données réelles de 2003 et 2011, combinées aux variables explicatives définies dans les chapitres 2 et 3. En outre, le PLU a été converti en contraintes (zones protégées, zones agricoles), et en incitations (développement de zones urbaines). Seules les probabilités de transition avec des taux supérieurs à 70% d'exactitude ont été incluses dans le modèle. Elles étaient les suivantes : de la forêt à la vigne, de la forêt à la prairie, de forêt à la zone bâtie, de la vigne à la surface bâtie, et des prairies en zone bâtie.

III. Résultats et discussions

La figure 5.2 montre que la superficie totale du vignoble a diminué d'environ 35% entre 1950 et 2011, en raison de l'urbanisation dans la plaine (Roy et al. 2014b). Les vignobles ont soudainement baissé entre 1982 et 2003, d'environ 30% de leur superficie, puis ont continué à diminuer, mais à un rythme beaucoup plus lent.

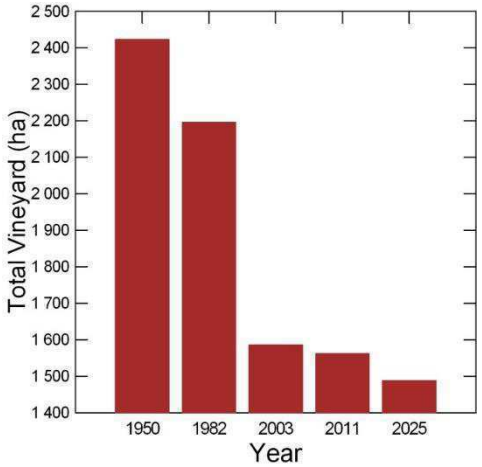

Figure 0.8: Evolution des vignes entre 1950 et 2025 (prévision)

En ce qui concerne les facteurs d'érosion des sols dans le bassin versant, on remarque que la plupart des sols du bassin versant étaient semblables : 22 échantillons de sol étaient sableux et très sablonneux, et les facteurs de K varient de 0,52 à 0,028 Mg h MJ-1mm-1 pour ces sols. La pente moyenne était de 5,9% en 1950 et a augmenté à 6,9% et 8,1% en 1982 et 2003. Cependant, elle a légèrement diminué à 7,1% en 2011 et a augmenté à 7,6% en 2025. L'augmentation des valeurs moyennes entre 1950 et 2003 peut se justifier par la construction de nouveaux vignobles entre 1950 et 2003, sur les pentes raides. En 2003-2011, le changement de pente est négligeable.

La prédiction 2025 montre une augmentation de la pente, mais cette valeur est probablement surestimée.
L'évolution des vignobles en terrasses est la suivante : ils sont passés de 510 ha à 555 ha en 1950-1982, et ont fortement diminué à 458 ha en 2003. Après une baisse de 410 ha en 2011, la valeur prédite augmente fortement à 590 ha en 2025. Les vignobles non installés sur des terrasses ont décliné entre 1950 et 2003, puis les valeurs sont stables en 2003-2011 et la zone simulée diminue légèrement en 2025. Ces changements sont essentiellement liés au déplacement des vignes sous pression urbaine, de la plaine alluviale à des zones en pente raide (cf. chapitre 2).

Les taux moyens d'érosion des sols pour différentes années sont présentés à la figure 5.7. Les valeurs sont passées de 11,8 T ha-1 an-1 à 13,2 T ha-1 an-1 en 1950-1982, et ont atteint 14,4 T ha-1 an-1 en 2003. Cependant, les taux d'érosion du sol ont chuté à 13,5 t / ha / an et 11,8 t / ha / an, en 2011 et 2025, respectivement. Ces tendances sont liées à la fois aux augmentations d'inclinaison de la pente et à la proportion des pentes en terrasses décrite ci-dessus. Les valeurs citées sont comparables à celles de Cerdan et al. (2010) qui a analysé les taux d'érosion des sols pour les vignobles méditerranéens.

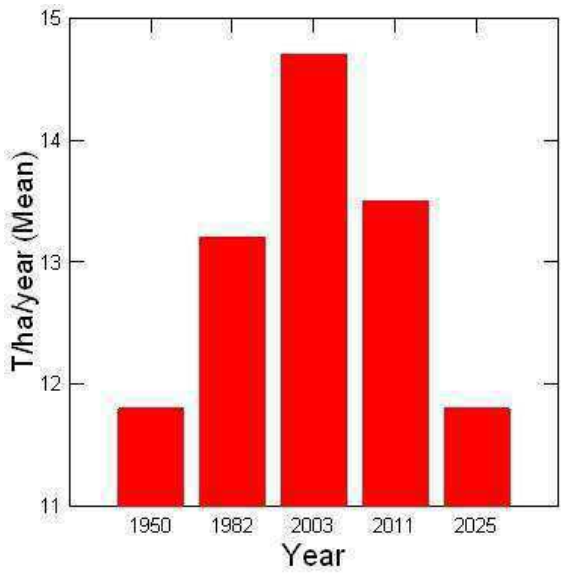

Figure 0.9: Taux d'érosion par différentes années

Pour les vignes, différentes classes d'érosion des sols sont présentées. La zone à faible taux d'érosion a diminué progressivement à partir de 1238 ha à 646 ha entre 1950-2003. Cependant, elle a augmenté à 713 ha en 2025, puisqu'une plus grande proportion des champs se trouve sur les pentes en terrasses. La zone à taux d'érosion moyen a également fortement diminué, passant de 956 ha à 717 ha en 1982-2003; mais elle reste relativement stable par la suite. Ces tendances à la baisse du taux d'érosion pourraient être liées à l'épuisement de la vigne sur la terre ordinaire. La zone à haut taux d'érosion des sols a augmenté d'environ 35 ha en 1950-1982 à partir de 209 ha en 1950, puis progressivement a diminué à 180,4 ha en 2011. Cependant, il a rapidement diminué à 71,6 ha en 2025. L'utilisation de terrasses dans le vignoble a joué un rôle important pour réduire les taux d'érosion élevés du sol.

Les cartes d'érosion des sols dans les années différentes (1950, 1982, 2003, et 2011) sont présentées dans la figure 5.9a-e. La partie orientale reste dominée par les taux d'érosion faibles entre 1950 et 2011, et se caractérise avec une faible pente et des taux élevés de conversion du vignoble à la zone bâtie. Par conséquent, la zone érodée se rétrécit au fil du temps. Une grande partie de la zone d'érosion «modérée» et «élevée» a également diminué en 1950-2011, mais dans une moindre mesure que la catégorie d'érosion faible. Les zones d'érosion modérée et élevée ont tendance à se concentrer sur la périphérie de la zone de basse classe et dans la région du centre-nord.

L'érosion totale évalue de manière différente. Entre 1950 et 1982, la superficie viticole a considérablement diminué et le taux moyen d'érosion s'accru du fait que les champs ont été déplacés hors de la plaine alluviale et sur les contreforts raides ; par conséquent, l'érosion totale est restée constante durant cette période. Après 1982, la grande perte dans la zone de vignoble l'emporte sur l'augmentation du taux d'érosion moyen et a provoqué une perte nette de l'érosion totale du sol. Après 2003, la superficie viticole est restée stable, et les taux d'érosion ont diminué légèrement avec moins d'une baisse de 10%.

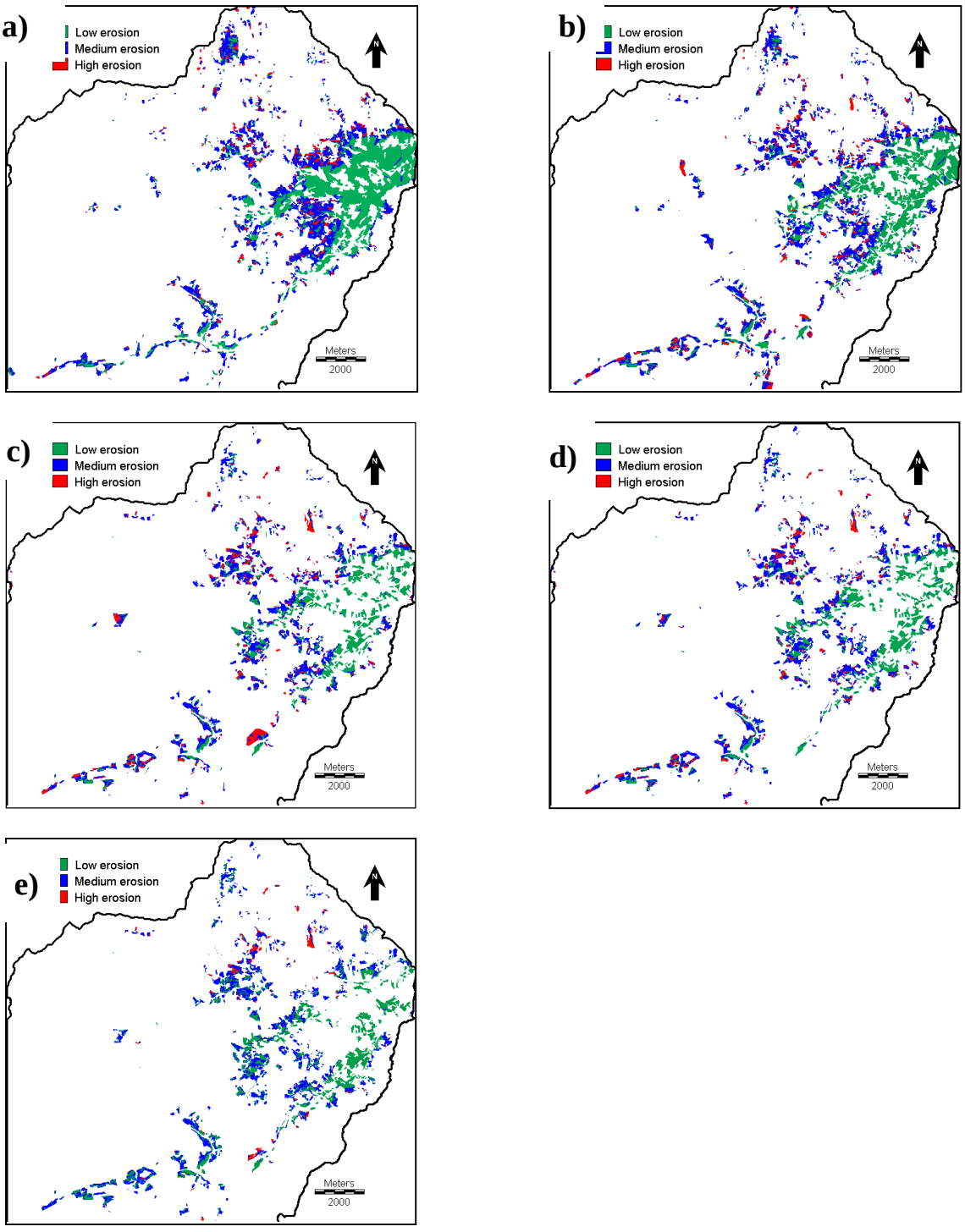

Figure 0.10: Niveaux d'érosion du sol a) 1950, b) 1982 c) 2003, d) 2011, e) 2025.

IV. Conclusions

L'étude a quantifié l'impact des changements de la couverture terrestre sur l'érosion des sols dans les vignobles dans le bassin versant de Cogolin au SE France entre 1950-2011. Le modèle RUSLE a été utilisé dans l'environnement SIG IDRISI et a permis de créer et de comparer l'érosion des sols sur des cartes en 1950, 1982, 2003, et 2011. Enfin, une carte de l'érosion des sols a été créée en utilisant la vigne prévue pour 2025. Les vignobles ont diminué, tandis que les taux d'érosion moyen ont augmenté dans l'intervalle de temps 1950-2003. Cette période représente la phase où le changement a eu lieu rapidement en raison de la forte pression urbaine dans la plaine alluviale et a conduit à un déplacement des vignes à des pentes plus raides. L'érosion totale a été stable entre 1950-1982, puis a progressivement diminué, principalement en raison de la perte dans la zone viticole et à une stabilisation dans la clairière des pentes plus raides. L'érosion totale en 2011 représente environ 75% de l'érosion dans 1950 à 1982. Les taux d'érosion prédits pour 2025 sont probablement sous-estimés, puisque le modèle de LCM a continué à déplacer des vignobles vers les pentes les plus raides où le terrassement réduit les taux d'érosion estimés.

CONCLUSION GÉNÉRALE

SYNTHÈSE

Cette étude apporte une contribution importante à la connaissance actuelle du changement de la couverture terrestre dans le bassin versant Giscle de 1950 à nos jours. Des modalités complexes des dynamiques de l'occupation du sol ont été observées dans le bassin versant à travers différentes dimensions spatiales et temporelles. Les terres marginales sur des pentes plus raides ont été converties de la forêt à la vigne, et des vignobles en terrasses sont apparus sur les contreforts au-dessus de la plaine alluviale. Cette constatation diffère des recherches précédemment menées, sur les transformations de l'occupation du sol, dans la région méditerranéenne, qui ont eu tendance à montrer le contraire, à savoir l'abandon de l'agriculture sur des terres marginales et leur conversion en forêt.

Certes, la tendance à l'expansion urbaine sur les terres agricoles est répandue dans le monde et dans la région méditerranéenne (Serra et al., 2008, Sluiter et de Jong, 2007). Cependant, la conversion de la vigne à la prairie, en conjonction avec l'expansion urbaine, trouvée dans cette étude est beaucoup moins fréquente. En effet, les champs de vignes abandonnés appartenaient généralement à des propriétaires qui ne produisaient pas leur propre vin, mais apportaient leurs raisins à une coopérative de vinification. La production de raisin n'était donc pas forcément au centre de leur vie, comme cela pouvait être le cas pour les Domaines viticoles. Et lorsque la terre est transmise d'une génération à l'autre, la production de raisin peut être abandonnée, mais la terre retenue. Cela explique une partie de la conversion de la vigne à la prairie, puis en forêt. En outre, la « prime à l'arrachement » dans les années 1980 a contribué à éliminer les petits producteurs.

L'altitude, la pente et la distance aux routes ont eu l'impact le plus grand sur le changement de la couverture terrestre parmi toutes les variables testées. Les transformations de l'occupation du sol projetées suggèrent que la zone bâtie et les prairies augmenteraient dans les zones forestières et viticoles, suivant les tendances historiques précédentes dans le bassin versant. Les erreurs les plus élevées ont été observées dans la prévision d'échelle de temps. Les cartes prédites étaient modérément précises pour l'échelle de temps intermédiaire et plus précises pour l'échelle de temps courte. Pour toutes les échelles de temps, les plus grandes erreurs ont été observées dans la prédiction de la couverture des prairies. Les prévisions les plus précises ont été tirées de l'échelle de temps court et le taux d'exactitude a diminué avec l'augmentation de l'échelle de temps. Par conséquent, la période initiale de 1982-2003 a été choisie pour projeter l'occupation du sol en 2011, dans le but de tester les influences de l'étendue spatiale et de la taille de la cellule sur la prévision des changements de la couverture terrestre. Puis 2003-2011 a été sélectionné pour prédire la couverture terrestre en 2025 afin de quantifier l'impact des transformations de l'occupation du sol sur l'érosion des sols. L'analyse de l'étendue spatiale a montré que la prédiction de la couverture terrestre est apparue plus précise dans la grande zone que dans la petite. Aucun impact significatif de la taille des cellules sur la prévision des changements de l'occupation du sol n'a été trouvé dans l'étude. Cependant, lorsque les images prédites à échelle réduite sont comparées à l'image de 25 m de référence à partir de 2011, les valeurs de désaccord réagissent différemment. Enfin, une taille de cellule de 25 m a été choisie pour prédire l'érosion des sols.

Le bassin versant Giscle a été choisi pour évaluer les impacts de l'utilisation des terres sur l'érosion des sols en raison de sa topographie, du climat, de l'agriculture et d'autres activités humaines, qui sont typiques de la région méditerranéenne. Bien que le taux d'érosion ait

augmenté rapidement entre 1950 et 2003, puis décliné dans la période 2003-2025 (réelle et prévue), l'érosion totale est environ la même entre 1950 et 1982 et diminue progressivement dans la période 2003-2025. Cette tendance à la baisse de l'érosion totale devrait se traduire par des charges de sédiments dans les cours inférieurs dans la zone de chalandise. Cette thèse montre que la répartition spatiale des changements de la couverture terrestre a un impact significatif sur l'érosion des sols. En particulier, les zones viticoles de ce bassin sont très vulnérables à l'érosion des sols. Cette constatation est conforme à d'autres études dans la région méditerranéenne (Kosmos et al., 1999; Cerdan et al., 2010). Les catégories de perte de sol «haute» et «modéré» ont augmenté en 2003, mais ensuite diminué de 2011. Une explication de ceci serait la diminution progressive de la vigne entre 1950 et 2011. De plus, les nouveaux vignobles qui sont apparus dans les hauteurs des pentes de pente à partir 2011, sont en terrasse et donc moins sujets à l'érosion des sols.

En général, les zones sujettes à l'érosion des sols ont augmenté dans les parties centrales de notre territoire pendant la période de cette étude. En revanche, l'érosion des sols a diminué dans la partie orientale du bassin, en raison de modification du couvert végétal, du vignoble vers la zone bâtie dans la plaine alluviale. La pente joue un rôle important dans l'érosion des sols. Les valeurs moyennes de la pente ont augmenté modérément pendant toute la période d'étude, alors que la pente moyenne est restée plus ou moins constante après 1982. Cela reflète la diminution des zones viticoles dans la plaine alluviale et l'augmentation des surfaces viticoles dans la vallée de montagne et les contreforts entre 1950 et 2003. Ce problème est devenu très important, non seulement pour les chercheurs, mais aussi pour les planificateurs et les écologistes urbains prônant et de la planification pour la couverture durable des terres dans l'avenir.

LIMITES DE CETTE THESE

Les limites de cette thèse concernent deux points. D'une part, les photographies aériennes de 1950 ont été les premières photos d'après-guerre de haute qualité disponibles lorsque la région était encore fortement rurale. Les dates intermédiaires (1982, 2003) ont été sélectionnées du fait de leur situation médiane entre 1950 et les photographies les plus récentes (2008, 2011), en raison de l'absence de photographies aériennes de 1990 et 2000. Le choix des dates a donc été largement contraint par les disponibilités de l'information. D'autre part, les résultats de recherche présentés dans le chapitre de l'érosion des sols ne sont pas encore validés et leur publication doit attendre la validation sur le terrain.

PISTES POUR LA RECHERCHE FUTURE

Différentes directions de recherche pourraient être envisagées. Premièrement, on pourrait envisager d'appliquer la modélisation établie, à l'échelle de la région PACA. Deuxièmement, on pourrait intégrer des parcelles complémentaires, pour déterminer l'érosion du sol afin d'élaborer un plan d'érosion d'atténuation durable. Troisièmement, l'influence des transformations de la couverture terrestre sur le changement climatique dans le sud de la France mérite des recherches plus poussées.

APPENDIX 2

Published and submitted articles from this thesis.

Journal of Land Use Science

Publication details, including instructions for authors and subscription information:
http://www.tandfonline.com/loi/tlus20

Spatial dynamics of land cover change in a Euro-Mediterranean catchment (1950–2008)

Hari Gobinda Roy[a], Dennis M. Fox[a] & Karine Emsellem[a]

[a] Department of Geography, UMR 7300 ESPACE CNRS, Université de Nice Sophia Antipolis, Nice 06204, France

Published online: 24 Mar 2014.

To cite this article: Hari Gobinda Roy, Dennis M. Fox & Karine Emsellem (2014): Spatial dynamics of land cover change in a Euro-Mediterranean catchment (1950–2008), Journal of Land Use Science, DOI: 10.1080/1747423X.2014.898105

To link to this article: http://dx.doi.org/10.1080/1747423X.2014.898105

Journal of Land Use Science, 2014
http://dx.doi.org/10.1080/1747423X.2014.898105

Spatial dynamics of land cover change in a Euro-Mediterranean catchment (1950–2008)

Hari Gobinda Roy, Dennis M. Fox* and Karine Emsellem

Department of Geography, UMR 7300 ESPACE CNRS, Université de Nice Sophia Antipolis, Nice 06204, France

(*Received 17 August 2013; final version received 5 February 2014*)

The Euro-Mediterranean area has experienced widespread land cover change since 1950, but few studies of land cover change explicitly explore spatial constraints on land cover change patterns. The main objective of this study was to analyze the spatial dynamics of land cover change from 1950 to 2008 in a French Mediterranean catchment. Aerial photographs (1950, 1982, and 2008) were screen digitized, and surfaces were classified into five categories: forest, vineyard, grassland, urban, and suburban. Land cover changes were concentrated mainly in the alluvial plain. Although forest remained the dominant land cover in the catchment (>85.0%), it underwent significant swapping with vineyard and grassland. Vineyard decreased (34% of initial loss) while grassland increased (43% of initial). Urban and suburban areas remained minor in the catchment (0.2% in 1950 and 3.0% in 2008), but showed a dramatic relative increase (about 20×). Changes occurred mainly at low altitudes and slopes. Vineyard located near streams was converted mainly to grassland. Built areas were dependent on roads and former built areas for expansion but expanded little near streams due to flooding risks. The rate of change was greater during the latter part of the study (1982–2008) than in the earlier phase (1950–1982).

Keywords: land cover change; urban expansion; vineyard conversion; topographic drivers; distance drivers

1. Introduction

Land cover changes represent major human alterations of the Earth's land surface (Lambin et al., 2001), and land cover conversion processes in Europe have accelerated since the Second World War (Antrop, 2005; Geri, Amici, & Rocchini, 2010; Serra, Pons, & Saurí, 2008). Land cover change has occurred through the interaction of environmental and socioeconomic characteristics, including population growth, urban sprawl, industrial development, and political and environmental policies. In addition, rapid expansion of tourism during the last six decades has caused important socioeconomic changes (Dunjó, Pardini, & Gispert, 2003) driving land cover alterations in Euro-Mediterranean areas (Geri, Amici, & Rocchini, 2011). Land cover changes affect biodiversity and ecosystems, food security, human health, urbanization, and global climate change (Falcucci, Maiorano, & Boitani, 2007; Geri et al., 2011; Sala et al., 2000). They can also be responsible for environmental change, water pollution, and soil degradation (Dunjó et al., 2003).

Several studies have described land cover changes in the Mediterranean area. Mediterranean countries from Spain to Greece experienced strong urban growth from

*Corresponding author. Email: fox@unice.fr

the 1970s onwards, and a moderate growth rate is projected to continue (Benoit & Comeau, 2005). Serra et al. (2008) reveal that about 34% of Spanish Mediterranean coastal areas were urbanized between 1989 and 1999. In France's Provence Alpes Côte d'Azur region (SE France), about 40% of shorelines were built in 2006 (IFEN, 2012). Migration from other European countries tends to concentrate in the Mediterranean coastline area (Brunetta & Rotondi, 1996), since the quality of life in Mediterranean cities seems to be greater than average in European countries (Cori, 1999). Aging population in Europe has a typical migration trend towards the Mediterranean coastal zone (Van Eetvelde & Antrop, 2004). In addition, internal migration also favors coastal areas, increasing urban pressure land cover changes in these areas (IFEN, 2009). For example, Van Eetvelde and Antrop (2004) analyzed the characteristics and mechanisms of land cover change in southern France (Tavernes) and identified a pattern where arable land decreased in foothills while urban areas expanded near the coast. They also found that residential and secondary houses occupied traditional terraced foot slopes.

Traditional Mediterranean agriculture was comprised mainly of vineyards, olive trees, and wheat grown in the nearby hinterland, often on terraces. Serra et al. (2008) reported that vineyards and olive trees decreased in mountainous areas and transitional subregions, resulting in land abandonment and increased shrub land area. Vineyard area decreased near roads and urban areas due to urban sprawl and industrialization in moderately mountainous to flat valley areas in Peyne, France (Sluiter & de Jong, 2007). Under these conditions, farmland is sacrificed to urban expansion (Martínez-Fernández, Esteve-Selma, Baños-González, Carreño, & Moreno, 2013). Nainggolan et al. (2012) identified several biophysical and socioeconomic factors (demography, markets, and subsidies on agriculture) responsible for the change in Torrealvilla catchment of South-eastern Spain: population decreased in 1960–1980 due to migration from villages to the coastal area, and rain fed agricultural, the main landscape feature in 1940–1960, was abandoned. However, in 1980–2005, intensification of agriculture occurred on flat to gentle slopes and near main roads due to subsidies for agriculture and the European highway infrastructure. Other authors have found that land cover change affected the overall environment, resulting in deforestation (Kepner, Rubio, Mouat, & Pedrazzini, 2003), land abandonment (Serra et al., 2008), and increased runoff and soil erosion in Portugal and Greece (Koulouri & Giourga, 2007; Nunes, de Almeida, & Coelho, 2011).

From a spatial point of view, Falcucci et al. (2007) describe three common major land cover changes in the Mediterranean area of Italy: the expansion of tourism that promotes rapid urbanization along the coastline, spatial concentration of agriculture on alluvial plains and low lands (except in the coastal area), and abandonment of agricultural terraced land in mountainous steep slopes resulting in their transformation to forest. According to Geri et al. (2011) and Nunes et al. (2011), four general trends of land cover change took place during the last decades in the coastal Mediterranean area. First, dry farming and forest land cover decreased in alluvial coastal plains while reforestation occurred in hilly areas. Second, urbanization occurred rapidly in most of the coastal plains where the tourism industry flourished. Third, population growth and socioeconomic development caused agricultural intensification that increased irrigated crops. Fourth, the development of infrastructure, communication networks, and technological advances resulted in socio-economic development that was the main reason of agricultural land abandonment on marginal lands.

Most of the studies on land cover change in the Mediterranean area highlight a particular issue or describe an individual land cover change such as forest, agriculture, or urban expansion (Calvo-Iglesias, Fra-Paleo, & Diaz-Varela, 2009; Pelorosso, Leone, &

Boccia, 2009), and few studies take into account all these changes concurrently. In addition, spatial patterns of land cover change and identification of driver variables influencing change are sometimes taken into consideration, but they tend to focus mainly on altitude or slope (Geri et al., 2010; Serra et al., 2008), and few authors (Sluiter & de Jong, 2007) take distance variables into account. Urban population growth and expansion of tourism occurred more in the French Mediterranean coastal area than on average for European Mediterranean coasts in the last decades (Blue Plan Papers, 2001). This resulted in significant land cover change in this region, but very few studies describing land cover change in the area can be found. Fox et al. (2012) analyzed the impact of land cover change on total runoff between 1950 and 2003 in the upper part of the study catchment. They noted a small increase in runoff due to a complex pattern of land cover change, but much of the lower alluvial plain, where most changes occurred was ignored, and spatial controls on these changes were not examined.

The first objective of this study is to quantify land cover change patterns in terms of gains, losses, total change and swapping in a Mediterranean catchment with a strong vineyard activity in proximity to a coastal area well known for its tourism. The second objective is to quantify the impacts of topographic and distance variables on land cover change for each land cover category.

2. Methods

2.1. The study area

The Giscle watershed has a surface area of about 235 km^2 and is situated in the Var department of SE France near the Gulf of St. Tropez (outlet coordinates 43°16′30″N, 6°34′24″E). It is characterized by a Mediterranean climate with hot dry summers that extend from June to August, and cooler rainier winters. Average temperatures range between 22°C and 26°C in summer and 5°C to 10°C in winter. The mean annual rainfall is about 900 mm, and the main rainy seasons are from October to January and then in April (Fox et al., 2012). The study area includes two topographic units: the hilly upper part of the catchment (roughly 70% of the catchment) is made up of metamorphic rocks, mostly schist and gneiss, while the lower part of the catchment, located near the gulf, is a gently sloping alluvial plain (Fox et al., 2012).

The western (upper) part of the watershed is mostly forest (pine and oaks), and the topography of the area is uneven with the highest elevation at about 650 m. Vineyard and moderate to dense urban areas are the dominant land cover types of the lower part of the catchment. The region became a major tourist destination of Mediterranean France in the second half of the twentieth century, with the 'Côte d'Azur' development, and this generated a strong growth in urbanization. Three main municipalities are located within the catchment: Cogolin, Grimaud, and La Môle. Cogolin and Grimaud are situated in the eastern part of the catchment, about 5 km from the Mediterranean coast. They represent the main populated areas with total populations of around 11,000 and 4000, respectively (INSEE, 2011). La Môle is a small urban area with a total population of around 950 (INSEE, 2011). The total population of the catchment increases by several times (perhaps as many as 10) in the summer due to tourism and secondary homes. Unlike many Mediterranean coastal areas, the sea front is confined by the gulf and topography, and land cover change is restricted to the inner near coastal area.

2.2. Data description and land cover classification

Land cover maps were screen digitized from acquired (Institut Géographique National) digital orthorectified aerial photographs (1950 and 1982 were panchromatic; 2008 was color), using ArcGIS (ESRI, 2012). Initial spatial resolution for all aerial photographs was 0.5 m, and this was reduced to 1 m to facilitate data manipulation. The aerial photographs of 1950 were the first high-quality post-Second World War photos available when the area was still strongly rural; an intermediate date (1982) was selected between 1950 and the most recent 2008 photographs. Aerial photographs of 1982 may represent land cover conditions at the beginning of rapid urban sprawl (Baccaini & Semécurbe, 2009; Salvati, Sateriano, & Bajocco, 2013).

Surfaces were classified into five categories based on visual interpretation: forest, prairie or grassland, vineyard, urban and suburban areas. High-density urban, industrial, and commercial areas were classified as urban, and moderate- to low-density built areas were classified as suburban. Urban and suburban areas were distinguished by the density of buildings and other infrastructures as described below. Isolated housing was ignored. To avoid creating a small isolated category, the Verne water dam (built in 1989–1991) was ignored and left as forest; its surface area is negligible compared to total forest cover. Similarly, a small recreational port built on the sea at the outlet of the catchment was ignored. After digitization, land cover maps were imported into IDRISI (Eastman, 2012). Main roads and stream networks were then digitized from the aerial photographs of 2008. Main roads were about the same in aerial photographs of 1982 and 2008, so this layer did not change over time. Cell size of all digitized maps was changed to 25 m to make land cover layers compatible with the 25 m digital elevation model (DEM) used for the creation of topographic and distance variables.

Land cover layers were identified visually. Most of the forest areas found in the aerial photographs were evergreen and were clearly identified by their deep gray color in the black-and-white aerial photographs (1950 and 1982) and deep green color in color aerial photographs (2008). Vineyards were differentiated by their blocky, geometric shapes and linear texture created by the rows of planted vines. Unmanaged or abandoned agricultural areas, new shrub lands with small and scattered trees, and pasture land for sheep and horses were all classified as grassland, even though some of it could more appropriately be called shrubland. Densely to moderately built areas, including residential, commercial, and industrial areas, were identified as urban. Urban areas were distinguished from suburban by the density of buildings and absence of trees and open area. Suburban area is essentially low-density residential housing. Some small denser communities were considered suburban areas. The presence of trees and open spaces were common in the suburban area. Land cover classification was facilitated by numerous field visits

2.3. Cross-tabulation analysis in 1950–1982, 1982–2008, and 1950–2008

Land cover change was quantified using the cross-tabulation matrix of the CROSSTAB module and the change analysis module of the land change modeler (LCM) of IDRISI Selva (version 17.02 (Eastman, 2012)). The cross-tabulation matrix is a fundamental process in land cover change analysis (Pontius, Shusas, & McEachern, 2004) to show land cover changes between two images of different dates. Persistence and pixel numbers of each category from earlier to later classified images are displayed through images and tables. After creating land cover maps of 1950, 1982, and 2008, land cover changes in three temporal periods were investigated: 1950–1982, 1982–2008, and 1950–2008. Cross-

tabulation of 1950–1982 represents the historical land cover change shortly after the Second World War; 1982–2008 represents more recent changes in land cover from the beginning of the urban sprawl period. The net 58 year change is provided by the 1950–2008 analysis. The land cover change determining method proposed by Pontius et al. (2004) was applied for all temporal periods to quantify persistence, gains, losses, total change (addition of gains and losses), net change, and swapping (exchanges between land cover classes, equal to the difference between total change and absolute net change).

2.4. Spatial dynamics

To describe spatial dynamics in land cover change, surfaces were simplified into four categories: forest, vineyard, grassland, and built area. Urban and suburban areas were combined into built area due to their small individual coverage compared to other land cover categories. Although data were available for all time periods cited above, maps of losses and gains for individual categories were simplified to show the spatial pattern of net 1950–2008 change since spatial patterns did not vary significantly between 1950–1982 and 1982–1950. Histograms were used to display quantitative losses and gains of each land cover class as a function of topographic (altitude and slope) and distance (from streams, roads, built area, and the sea) variables for the 1950–1982 and 1982–2008 periods. However, since this analysis alone generated 36 figures, only summary figures of total change will be presented here and gains and losses will be described in the text. Altitude and slope were obtained from a 25 m DEM. Only main roads (created by screen digitization) were taken into consideration, and smaller roads and dirt paths were ignored. Main stream channels were also digitized manually due to errors in the automatic tracing of the hydrologic network from the 25 m DEM: in the plain, where topography is nearly flat, errors of up to 300 m could be observed between the modeled and actual channels. Finally, for changes in land cover occurring in 1950–1982, distance from built area in 1950 was used. For changes taking place in 1982–2008, distance from built area in 1982 was calculated.

3. Results

The steps in describing the results are the following: overall trends in land cover change over the study period, detailed analysis of land cover change patterns for three periods (1950–1982, 1982–2008, and 1950–2008) using CROSSTAB, spatial trends of land cover change, and topographic and distance controls on land cover change.

3.1. Areal trends in land cover change

Figure 1a–c shows land cover maps digitized from the air photos, and Table 1 provides the corresponding surface areas and changes in surface area for each category and time period. Forest remained by far the dominant land cover in the catchment (Figure 1a–c), accounting for more than 85% of land cover at all times (Table 1). Forest cover decreased by only 34 ha in 1950–1982, represents a change of only about 0.2% of its catchment cover. This increased slightly to 0.7% loss in catchment cover in 1982–2008. Vineyard was the second dominant land cover and it too declined from about 2457 –2183 ha (a loss of 274 ha, almost 11% of the catchment area) between 1950 and 1982 (Table 1). This trend accelerated in 1982–2008 to reduce vineyard area to about 1616 ha (almost 26% lost). Over the 1950–2008 period, vineyard lost more than a third (34.2%) of its initial

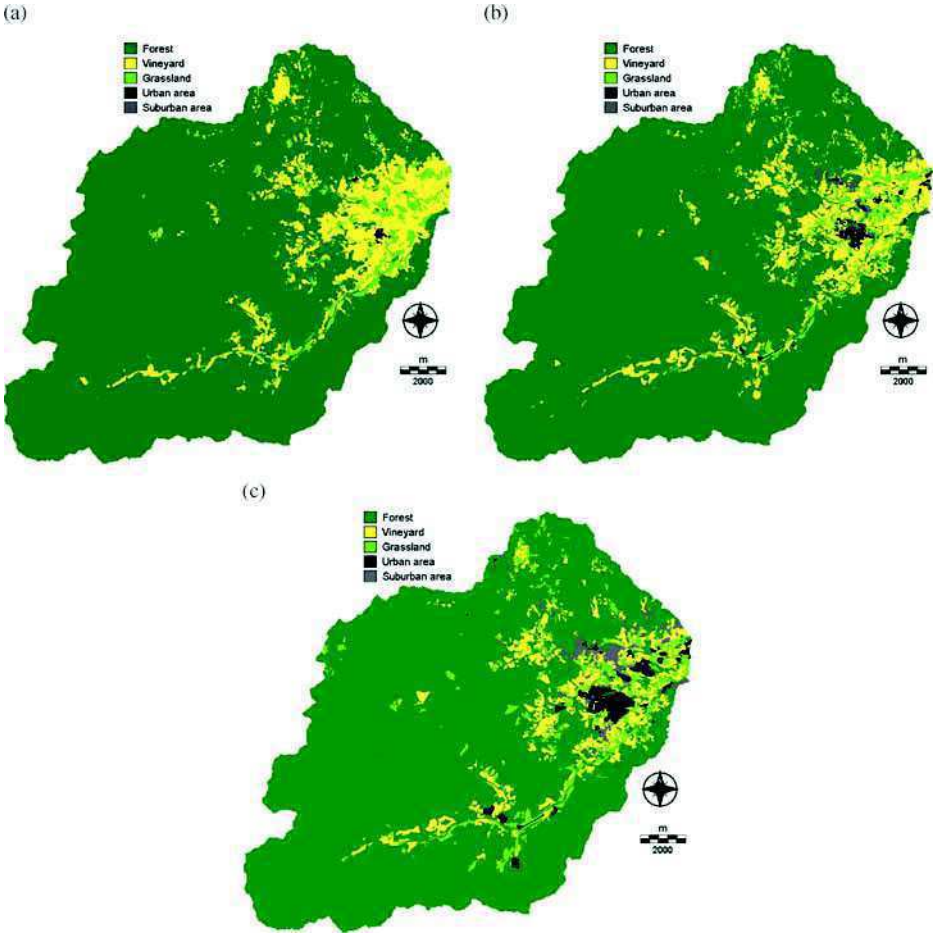

Figure 1. (a) Land cover map of 1950. (b) Land cover map of 1982. (c) Land cover map of 2008.

Table 1. Surface area of land cover types for 1950, 1982, and 2008, and changes in area for 1950–1982, 1982–2008, and 1950–2008.

Land cover type	Surface area in ha (% of catchment)			Change in surface area in ha (% of initial cover)		
	1950	1982	2008	1950–1982	1982–2008	1950–2008
Forest	20,267 (86.1)	20,233 (85.9)	20,091 (85.3)	−34 (−0.2)	−142 (−0.7)	−176 (−0.9)
Vineyard	2457 (10.4)	2183 (9.3)	1616 (6.9)	−274 (−11.2)	−566 (−25.9)	−840 (−34.2)
Grassland	794 (3.4)	879 (3.7)	1140 (4.8)	84 (10.6)	261 (29.7)	345 (43.5)
Urban	19 (0.1)	140 (0.6)	387 (1.7)	121 (645.0)	247 (176.2)	368 (1957.8)
Suburban	13 (0.1)	115 (0.5)	316 (1.3)	102 (787.0)	200 (173.8)	303 (2328.3)

cover. Grassland was the third dominant cover in 1950, though its surface area amounted to less than a third of vineyard. Contrary to forest and vineyard, grassland increased significantly during the study period, showing an overall 43.5% increase between 1950

Table 2. Cross-tabulation of land cover in 1950 (columns) and in 1982 (rows). Values are in ha, persistence (diagonal) is also expressed in % of total area in initial year (1950).

	Forest	Vineyard	Grassland	Urban	Suburban	Total
Forest	**19,777 (97.6)**	270	186	0	0	20,336
Vineyard	337	**1660 (67.5)**	186	0	0	2183
Grassland	105	394	**379 (47.7)**	0	0	879
Urban	12	83	22	**19 (100.0)**	5	140
Suburban	36	50	21	0	**8 (59.1)**	115
Total	20,267	2457	794	19	13	23,565

and 2008. These first three land cover categories covered 97% (in 2008) of the catchment (Table 1). Rapid changes occurred in built area (both urban and suburban), which increased steadily to over 700 ha in 2008 from below 50 ha in 1950 (Table 1). Moreover, urban and suburban areas each covered only 0.1% of the catchment in 1950, and they increased to about 1.7% and 1.3% of the catchment in 2008, respectively.

As can be seen in Figure 1a–c, most of the changes occurred in the eastern part of the catchment. This area corresponds to the alluvial plain where altitudes and slopes are gentler. For the vegetation land covers (forest, vineyard, and grassed areas), the rate of change, expressed as % of initial cover, was greater in 1982–2008 than in 1950–1982 (Table 1). Calculated on an annual basis, the difference would be even greater since the latter period showed greater change in a shorter time, 26 years versus 32 for the initial period. Although the contrary appears to be true for urban and suburban categories, where % change was greater in 1950–1982 than in 1982–2008, it should be noted that the latter period experienced greater absolute change, and small absolute differences in 1950–1982 generate an artificially large % change due to the very small initial area. The built categories showed the greatest % change of all land cover types during the 1950–2008 study period with an increase of more than 2000% each.

3.1.1. Cross-tabulation analysis 1950–1982

Cross-tabulation for 1950–1982 (Table 2) was used to explain persistence, losses, and gains in land cover. In Table 2, columns display time 1 (1950) and rows display time 2 (1982). Persistence represents the amount of unchanged land cover between 1950 and 1982; this is highlighted in bold in diagonal, and values are presented in both ha, and % of initial (1950) area in parentheses. As for % change, persistence is often correlated with initial land cover, where extensive land covers tend to have greater persistence (Pontius et al., 2004). The sum of each column shows total area in 1950 for each land cover type. The sum of each row shows total area in 1982. The cross section of each column–row shows the area converted from one land cover to another between 1950 and 1982. For example, 337 ha were converted from forest to vineyard between 1950 and 1982; in terms of losses/gains, this therefore corresponds to a loss of 337 ha of forest to vineyard and, of course, a gain of 337 ha of vineyard from forest.

Forest had the greatest persistence (97.6%), and most of its loss was conversion to vineyard. Vineyard, on the other hand, had moderate persistence (67.5%), and its greatest loss was conversion to grassland. In this initial period (1950–1982), the dominant trends among the vegetated land covers are a conversion from vineyard to grassed areas (394 ha) and forest to vineyard (337 ha). This apparent compensation in vineyard loss is only

partial since there is also considerable loss of vineyard to forest (270 ha). Among the different land cover types, swapping is greatest for forest and vineyard. Although grassland gained in surface area, it had low persistence (47.7%) and greater susceptibility to change, showing high losses to both forest and vineyard as well as significant gains from these two land cover types, especially from vineyard (394 ha). The urban category reflects an 'end state' which cannot easily evolve into another land cover type, though suburban can evolve into urban. Both urban and suburban gained from all vegetated land cover types. The greatest gains in the built categories were from vineyard. Therefore, although all land cover types contributed to the growth of urban and suburban areas, the major trend was expansion of built area on vineyard.

Forest, vineyard, and grassland experienced the most significant gains and losses (Tables 1 and 2). Among these, vineyard underwent the greatest total change within the catchment, even though its initial surface area in 1950 was only about 12% that of forest (2457 ha vs. 20,267 ha). It also exhibited the highest rate of swapping, demonstrating extensive exchanges with other land cover types, especially forest and grassland. Of the five land cover types, vineyard was the most active, gaining and losing the most area and exchanging the most land with other land covers. Built areas had low total change, but especially very low swapping since these land covers gain from others but do not lose in exchange.

3.1.2. *Cross-tabulation analysis 1982–2008*

As can be seen in Table 3, trends during 1950–1982 continued in 1982–2008. Forest area decreased slightly but maintained high persistence (97.0%) due to its high surface area. A large area of vineyard continued to convert to grassland (457 ha), but during this period the compensating effect of forest to vineyard was weaker than in 1950–1982 (169 ha vs. 337 ha), and vineyard persistence decreased (61.5%). The conversion of forest to grassland was greater in 1982–2008 than in 1950–1982 (279 ha vs. 105 ha). As in 1950–1982, urban expansion occurred mainly at the expense of vineyard. However, during the latter period, suburban growth took place on forest cover before vineyard. Grassed area showed the lowest persistence (46.0%) as significant areas converted to forest and vineyard.

During 1982–2008, grassland surpassed vineyard in both total change and swapping, even though it still accounted for only 4.8% of the catchment in 2008 (Table 1). The significance of grassland dynamics will be discussed below. Total change in 1982–2008 was greater than in 1950–1982 for all categories except vineyard, though vineyard had the greatest net change (−2.4% of catchment area). This was particularly true of urban and suburban areas for which total change in 1982–2008 was more than double the values for

Table 3. Cross-tabulation of land cover in 1982 (columns) and in 2008 (rows). Values are in ha, persistence (diagonal) is also expressed in % of total area in initial year (1982).

	Forest	Vineyard	Grassland	Urban	Suburban	Total
Forest	**19,636 (97.0)**	215	240	0	0	20,091
Vineyard	179	**1344 (61.5)**	104	0	0	1617
Grassland	279	457	**404 (46.0)**	0	0	1140
Urban	51	105	63	**140 (100.0)**	27	387
Suburban	99	62	67	0	**88 (76.4)**	316
Total	20,233	2183	879	140	115	23,550

1950–1982. Overall, the 1982–2008 period experienced more land cover change than in 1950–1982 (16.5% of catchment compared to 14.5%).

3.1.3. Cross-tabulation analysis 1950–2008

Table 4 shows the results of almost 60 years (1950–2008) of land cover change in the catchment. Forest remained the dominant category by far and had high persistence (96.1%), but large areas of forest were converted to vineyard (358 ha) and grassland (247 ha). These losses were only partially compensated by gains from grassland (216 ha) and vineyard (39 ha). Vineyard is the land cover type that contributed most to all others, and more particularly to grassland (577 ha). The majority of urban and suburban expansion occurred on vineyard, though significant suburban growth was also at the cost of forest. Overall, three land cover types showed low persistence: vineyard (45.2%), grassland (39.7%), and suburban (40.9%), where the low persistence of suburban can be explained by its conversion to urban.

The greatest land cover change between 1950 and 2008 was experienced by vineyard which lost an equivalent of 3.5% of the catchment area or 34.2% of its initial area (or 840 ha out of an initial 2457 ha, Table 1) in the 58 year time frame. This, however, was not a simple loss in land but corresponds to a complex pattern of exchanges with other land cover types since vineyard has a swapping value of 4.3% (greatest swapping was for forest, 5.2%). Major swapping trends were a net gain in vineyard from forest of 319 ha and a net loss in vineyard to grassland of 431 ha, so grassland progressed significantly within this context of land cover swapping. Total and net change were smallest for urban and suburban land covers, but these values are high for land covers which had very low initial values (Table 1). Urban and suburban area increased by about more than 20 times in 1950–2008.

3.2. Spatial dynamics influencing land cover change

The spatial dynamics of land cover change will be investigated in two steps. In the first, land cover change maps will be used to highlight specific locations. In the second, the impact of spatial variables (altitude, slope, and distance from roads, streams, sea, and built area) will be presented. As described in the methods, urban and suburban are grouped together into a single ‘built’ category. Histograms showing total change will be described first, and then significant gains and losses will be detailed; however, histograms showing gains and losses are not included here due to the very large number of figures involved.

Table 4. Cross-tabulation of land cover 1950 (columns) and land cover 2008 (rows) (ha).

Land cover type	Forest	Vineyard	Grassland	Urban	Suburban	Total
Forest	**19,477 (96.1)**	39	216	0	0	20,091
Vineyard	358	**1111 (45.2)**	146	0	0	1617
Grassland	247	577	**316 (39.7)**	0	0	1140
Urban	69	228	64	**19 (100)**	8	387
Suburban	118	143	50	0	**5 (40.9)**	316
Total	20,267	2457	794	19	13	23,550

3.2.1. General spatial trends

Although the rates of change between 1950–1982 and 1982–2008 were different, spatial patterns for losses and gains were similar, so only the net 58 year (1950–2008) differences are shown here. Gains and losses for each land cover type are shown in Figure 2a–d; low altitudes are portrayed in white while higher values are in black to enable better visualization of gains and losses. Losses and gains in forest (Figure 2a) indicate that much of the lost land was in foothills in proximity to the alluvial plain (white patch in eastern part of catchment). Area lost was almost twice the area gained. Gains in forest occurred mainly in the south-eastern portion of the alluvial plain.

Whether in terms of percent of initial area (Table 1), absolute area (Table 1), or percent of catchment area, vineyard was the major loser of all land cover types. Lost area clearly outstrips gains and was concentrated almost entirely in the alluvial plain (Figure 2b). Only about half the land lost was compensated by gains elsewhere, and these tend to be found outside the eastern alluvial plain area, either in nearby foothills or on alluvial soil to the extreme SW of the catchment.

In terms of absolute area and percent of catchment (Table 1), grassland gained the most land, just ahead of urban areas. There is no strong spatial pattern to the gains and

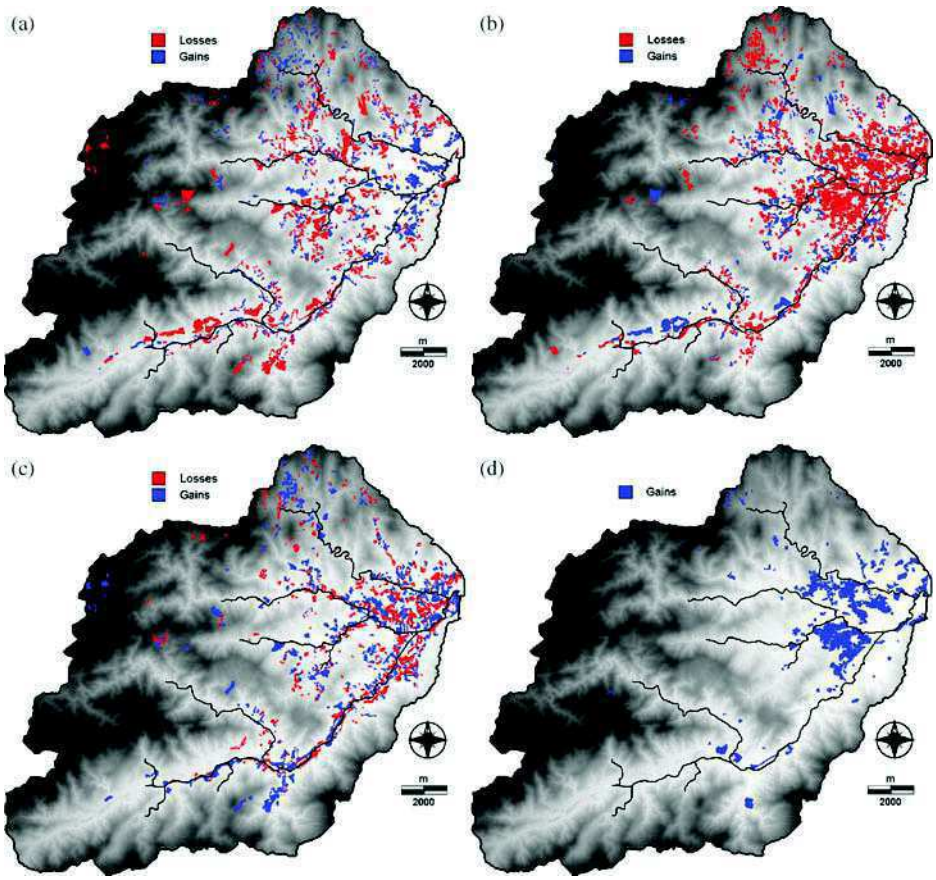

Figure 2. (a) Forest change in 1950–2008. (b) Vineyard change in 1950–2008. (c) Grassland change in 1950–2008. (d) Built area change in 1950–2008.

losses in grassland (Figure 2c) with gains and losses both occurring in the alluvial plain. There is a weak tendency for grassland losses to be absent from higher altitudes (Figure 2c).

The combined gains in urban and suburban covers outstrip individual gains and losses of all other land covers (Table 1). Built area expansion (Figure 2d) occurred almost exclusively in the alluvial plain, and much of it was in close proximity to the core city centers of Grimaud and especially Cogolin (Figure 1a–c).

3.2.2. *Altitude*

The impact of altitude on total change for each land cover type is shown in Figure 3a (1950–1982) and 3(b) (1982–2008), respectively, where it can be seen that total change in all land cover types decays exponentially with increasing altitude. The decrease in change with increasing altitude is the least pronounced for forest, for which about 30% of total change occurs in the 0–25 m range in both time periods. For the other land cover types, the 0–25 m range accounts for about 50% to 65% of total change according to the specific cover and time period. Grassland has the highest percentage of total change in the 0–25 m for both periods: 64.4% and 58.4% for 1950–1982 and 1982–2008, respectively.

The relationship between gains and losses in forest cover and altitude over time is complex. In both time periods, gains outstrip losses in the lowest altitude range (0–25 m); this corresponds to the overall increase in forest noted in Figure 2a in the SE portion of the alluvial plain. At greater altitudes, losses are greater than gains, and in intermediate altitudes (50–100 m), lost forest area tends to be greater in 1982–2008 than in 1950–1982. Unlike the other land cover types, losses in forest cover tend to increase slightly at the highest altitudes (greater than about 200 m). This loss tends to benefit grassland and then vineyard most.

Vineyard changes tend to be the opposite of forest trends noted above. For both time periods, the 0–25 m altitude experienced significant loss in vineyard cover. Although gains at greater altitudes (≥25 m) compensate a small part of the losses in vineyard in

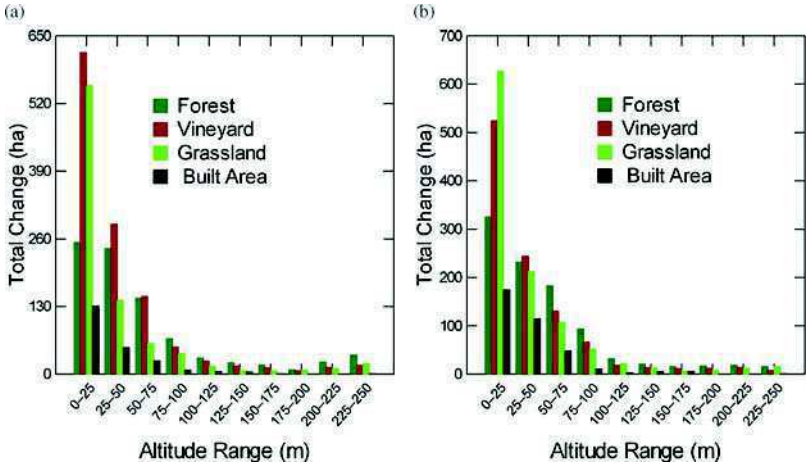

Figure 3. (a) Land cover changes in 1950–1982 with altitude (m). (b) Land cover changes in 1982–2008 with altitude (m).

1950–1982, this is no longer true in 1982–2008 where losses remain significantly greater than gains in the 25–50 m range.

Grassland gains and losses with altitude are quite different from both forest and vineyard. In 1950–1982, gains are slightly greater than losses for all altitude ranges. Although the trend remains the same in 1982–2008, the gap between gains and losses is greater. Finally, built area increases at all altitudes and more particularly in the lower range, as for the other land cover types. The 1982–2008/1950–1982 gain ratio is substantially greater in the intermediate altitude range (25–75 m) than in the 0–25 m range, indicating that higher altitudes were preferentially built in the later time period.

3.2.3. *Slope*

Slope and altitude are correlated in the catchment as higher altitudes tend to have steeper slopes. Changes in land cover as a function of slope (Figure 4a and b) are therefore similar to the trends with altitude, and only noteworthy differences will be highlighted here. Overall trends are sensitive to the choice of range and in this case, there is an intermediate range (5%–15%) where values in two categories (5%–10% and 10%–15%) remain constant (Figure 4a and b); there seem to be no significant exceptions to this trend. Roughly 30% of changes in forest occur on slopes less than 5%, and this value ranges from about 50%–60% for the other land covers. For slopes less than 10%, these values increase to about 50% (forest) and 60%–70% (others), respectively. Changes in land cover for the 0–25 m altitudes (Figure 3a and b) correspond closely to values for the 0%–5% slope range (Figure 4a and b). Unlike altitude, where forest cover loss increased at higher altitudes, there is no increase in land cover loss on steepest slopes. Thus, the loss experienced at higher altitudes probably corresponds to level ground or topslope convexities with low slope inclinations.

3.2.4. *Distance from streams*

Total change in the vegetation covers (forest, vineyard, and grassland) all decrease exponentially with distance from streams (Figure 5a and b). In the initial period (1950–

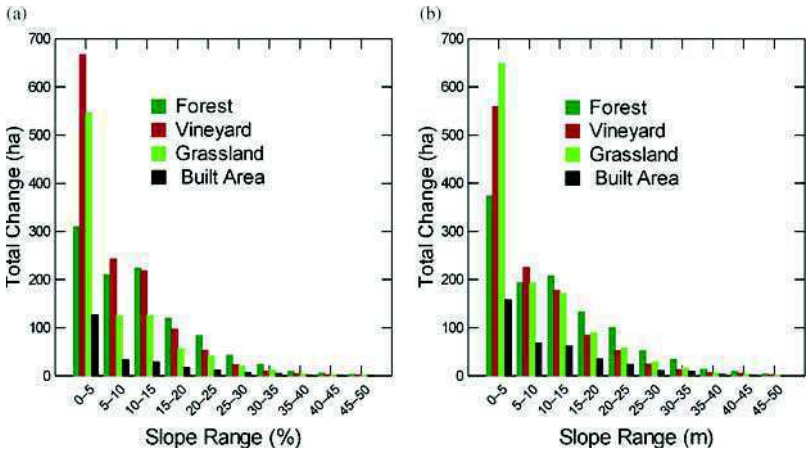

Figure 4. (a) Land cover changes in 1950–1982 with slope (%). (b) Land cover changes in 1982–2008 with slope (%).

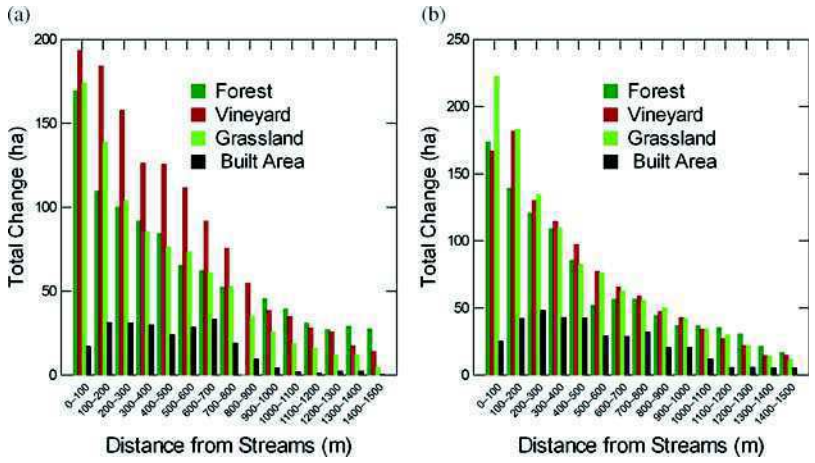

Figure 5. (a) Land cover changes in 1950–1982 with distance from stream. (b) Land cover changes in 1982–2008 with distance from stream.

1982), the greatest total change near streams concerns vineyards most, and this continues on into intermediate distances of up to about 900 m (Figure 5a). In the latter period (1982–2008), grassland experiences the greatest total change near streams, but there is little difference with vineyard or forest beyond about 100 m and 200 m, respectively (Figure 5b). The relationship between total change in built area and distance from stream (Figure 5a and b) is unlike any other so far: very little change close to the stream, moderate change at intermediate distances (roughly 100–800 m), and then little change again at greater distances.

In 1950–1982, forest gains more than twice the surface lost close to streams, but this trend is reversed in 1982–2008. For all other distances and in both periods, forest generally loses more land than it gains. In the initial period (1950–1982), lost land tends to peak at about 200–300 m from streams whereas it is greatest close to streams in 1982–2008 and decreases with distance. Vineyard loses more land than it gains at all times and distances, except for the 1950–1982 period when gains are slightly greater than losses at distances greater than about 800 m. At intermediate distances in 1950–1982 (100–400 m), the difference between losses and gains is progressively minimized by greater gains, but this no longer holds in the 1982–2008 period.

Gains and losses in grassland are the general opposite of those noted for forest, though the gains in grassland cannot be accounted for entirely by forest and significant areas of vineyard must have contributed to grassland growth close to streams. The greatest gains in grassland close to streams (<400 m) occur in 1982–2008. Before then, gains and losses are roughly equivalent except at intermediate distances (400–600 m) where gains are greater than losses. In the latter period (1982–2008), gains become greater than losses again at distances beyond about 1000 m.

Built area gains relatively little land immediately next to streams (<100 m). Gains in built area are then relatively stable between distances of 100–700 m and 100–800 m for 1950–1982 and 1982–2008, respectively. For almost all distances, gains in 1982–2008 were greater than in 1950–1982, with the exception of roughly equivalent values in the 500–700 m range.

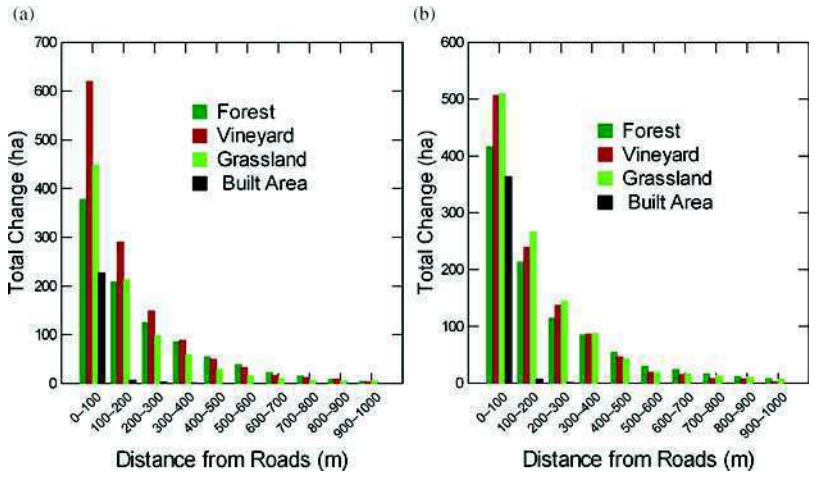

Figure 6. (a) Land cover changes in 1950–1982 with distance from road. (b) Land cover changes in 1982–2008 with distance from road.

3.2.5. *Distance from roads*

Total change in land cover with distance from roads (Figure 6a and b) follows the decaying exponential trend of most variables taken into consideration. Roughly 40%–50% of total change in forest, vineyard, and grassland occurred within 100 m of a road. This value was greater than 95% for built area. In 1950–1982, vineyard was most affected close to roads (0–100 m), but in 1982–2008, vineyard and grassland were approximately equal.

For both time periods and almost all distance ranges, loss in forest cover was greater than gains, and the greatest overall difference was in the 0–100 m range in 1982–2008. Vineyard trends are similar to forest but greatly exaggerated. Losses outweigh gains significantly close to roads (0–100 m), but differences are small beyond this distance. Grassland gains are greater than losses at all distances, though the land gained and lost decreases with distance from roads. Major gains are registered more particularly in the 0–100 m range for 1950–1982 and in the 100–300 m range for 1982–2008. Built area clearly distinguishes itself from the other land cover types since almost all of its gain occurs within 100 m of a main road.

3.2.6. *Distance from built area*

The relationship between total land cover change and distance from built area (Figure 7a and b) is strongly time dependent. In 1950–1982 (Figure 7a), there is little evolution in land cover change with distance from built area despite a tendency for the vegetation covers (forest, vineyard, grassland) to show greater change at intermediate distances (300–1300 m) and built area to change more close to earlier built area (0–100 m). In 1982–2008, the pattern is totally different (Figure 7b). For vineyard and grassland, total change first increases with distance from built area, peaks at about 100–200 m, and then decreases with further distance from built area. Total change in forest cover is roughly constant between 0 and 300 m before decreasing with greater distances. Built area change is greatest within 0–100 m, where more than 50% of total change takes place in 1982–2008. For comparison, the value for the other land cover types in this distance range is

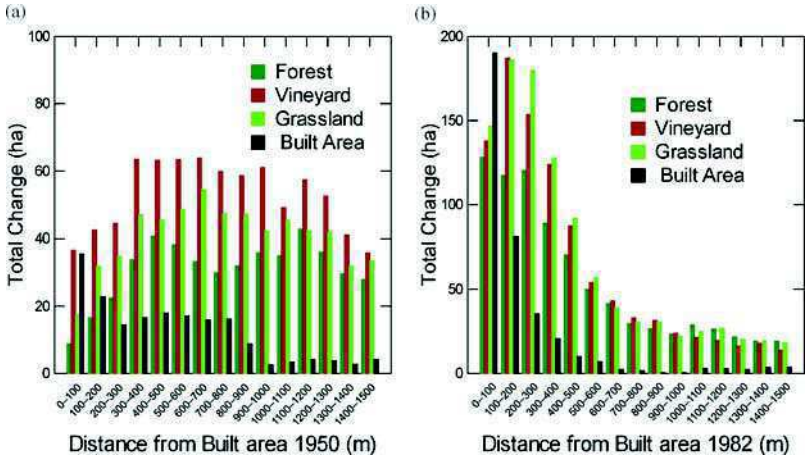

Figure 7. (a) Land cover changes in 1950–1982 with distance from built area 1950. (b) Land cover changes in 1982–2008 with distance from built area 1982.

approximately 15%. It should be noted that built area was limited to only 32 ha in 1950 and expanded to almost 270 ha in 1982 (Table 1); built area expansion was particularly important in the 1982–2008 period (Table 1).

Gains and losses in forest vary with time: in 1950–1982, gains and losses are relatively small and tend to occur far from built area. In 1982–2008, forest land is lost close to built area (within 200 m) and gained at intermediate distances (200–500 m). Vineyard clearly loses significant area near built area. The trend is particularly strong in 1982–2008 within about 300 m to 400 m from built area. In this range, losses are 3 to 10 times greater than gains. Although total changes are similar for vineyard and grassland (Figure 7b), the relationship with distance from built area is quite different: in grassland, losses and gains are better balanced in the estimation of total change. In the 0–100 m range, grassland experiences a net loss, but beyond this distance, grassland gains are generally greater than losses, even though losses can remain substantial, especially in the 100–400 m range. Where vineyard systematically lost area, grassland both lost and gained land. Built area expansion in 1982–2008 occurred close to former built area. Almost 75% of the land gained in 1982–2008 was located within 200 m of 1982 built land.

3.2.7. Distance from sea

Trends for changes in land cover with distance from the sea (Figure 8a and b) are distinct from all other patterns examined thus far. Before examining these, it should be noted that the catchment sea front is restricted to a narrow band near the outlet into the Gulf of St Tropez. Total change in vineyard, grassland, and built area covers tends to be greatest at about 3–5 km from the sea front in 1950–1982 (Figure 8a). This distance corresponds roughly to the center of the alluvial plain and is close to the city cores of Cogolin and Grimaud. Changes in forest cover peak at a greater distance (about 7–9 km) and this corresponds roughly to a secondary peak in change for vineyard and grassland. This distance is situated near the foothills peripheral to the alluvial plain. Finally, there appears to be a third smaller peak in change around 10–12 km and this corresponds roughly to the area near the town of La Môle in the western part of the catchment. Trends for 1982–2008

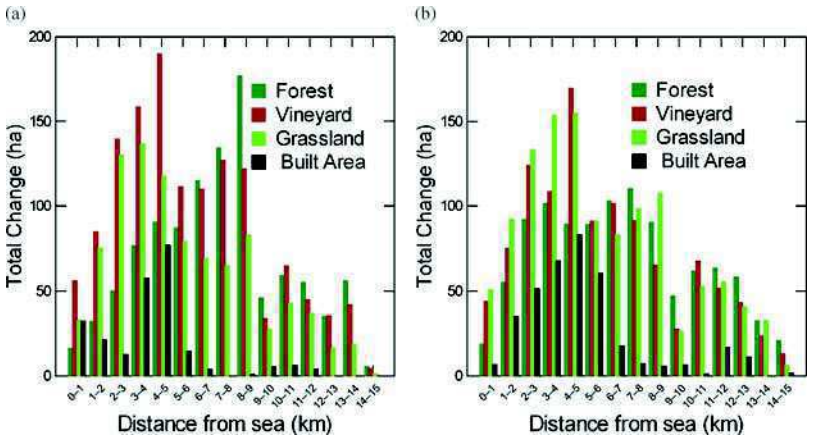

Figure 8. (a) Land cover changes in 1950–1982 with distance from sea. (b) Land cover changes in 1982–2008 with distance from sea.

(Figure 8b) are generally similar to 1950–1982 (Figure 8a), but changes in forest are concentrated within closer distances to the sea, vineyard changes are less great at intermediate distances (5–9 km), grassland peaks are greater at both near (3–5 km) and intermediate (7–9 km) distances, and built area changes are significantly greater in the 1–4 km range especially.

Forest gains and losses are sensitive to distance from the sea. Gains outweigh losses close to the sea (within about 2–3 km for both periods and 3–4 km for 1950–1982), but losses are generally greater beyond about 5 km. The greatest difference in gain–loss occurs at about 7–9 km. Vineyard losses and gains are strikingly simple. Losses outstrip gains at all distances up to 6 km, and gains outweigh losses at all distances beyond 6 km. Peak lost land is situated about 3–5 km from the sea, and the peak gained land occurs at a distance of around 6–9 km. Grassland trends are more complex and vary less systematically as a function of either time period or distance. Three approximate distance peaks can be identified. The first is in the 2–5 km range; here, grassland gains more land than it loses in 1950–1982, but the trend is reversed in 1982–2008. The second is in the 7–9 km range; gains are greater than losses for both time periods. The third is in the 10–13 km range where land gained is also greater than lost. Finally, the major peak in gained land for built area is about 3–5 km from the sea in 1950–1982 and 2–6 km in 1982–2008. For the initial 1950–1982 period, significant gains were made close to the seafront but these do not persist in 1982–2008. Finally, built area shows growth in the distant (11–13 km) range in the latter period.

4. Discussion

The results above detail land cover changes for the 235 km^2 Giscle catchment over two time periods and describe spatial patterns and topographic/distance variables influencing these changes. The spatial and temporal dimensions create a complex pattern of change that will be simplified in the discussion to highlight the major findings of the study. Before this, it should be noted that the topographic and distance variables are often correlated, but may have distinct impacts. Altitude and slope are correlated and both reflect a greater distance from the sea; in addition, slope influences building costs as it is

cheaper to build on flat land than steep slopes. Distance from the sea also reflects the impact of built area, as described in the results. The major cities of Ste Maxime and St Tropez are located on either side of the Gulf of St Tropez, so distance from the sea also represents distance from larger urban centers, seafront tourism, and major road and rail transportation networks. Behind all these variables are economic considerations that are impossible to isolate and quantify here.

Perhaps the most frequently cited land cover transition in Mediterranean regions in the scientific literature is the abandonment of agricultural practices on marginal land and its conversion to forest (Falcucci et al., 2007; Geri et al., 2010; Parcerisas et al., 2012; Pelorosso et al., 2009; Serra et al., 2008). This was not observed in this catchment. On the contrary, marginal lands on steeper slopes were converted from forest to vineyard, as can be seen in Figure 9 showing vineyard terraces on foothills above the alluvial plain. A forest fire in the catchment in 2003 (Fox, Berolo, Carrega, & Darboux, 2006) revealed extensive terracing on steep slopes, but marginal subsistence farming was probably abandoned in the region before 1950, as was the case elsewhere in Mediterranean France (Sluiter & de Jong, 2007). The Maures mountains ('Massif des Maures') are highly prone to forest fires and this clearly explains the prevalence of cork oak (*Quercus suber*) as the dominant tree species in the catchment. The thick bark of cork oak protects the heart of the tree from intense heat, and most trees survive even high severity fires. Exceptions are the very young or old trees, and trees which have recently been harvested for their cork bark. Pine (*Pinus pinaster*) trees, on the other hand, are systematically killed by high severity fires. With regard to vineyards, large areas in the plain were converted to grassland, built area, and some forest. This was compensated in part (but only partially since the net result is a 28% loss in vineyard cover between 1950 and 2008) by planting on steeper slopes in proximity to the plain. These fields therefore find themselves at the interface between the extensive forest on one side and the plain on the other. During the large fires of 2003, vineyards served as effective fire breaks; as forest fires penetrated into the vineyard, the lack of combustible vegetation extinguished the fire after the first few vine rows were burned or dried out.

A second common trend cited is the intensification of agriculture on plains (Falcucci et al., 2007; Geri et al., 2010; Van Eetvelde & Antrop, 2004). The term 'intensification' is ambiguous as it can imply either the clearing of land to plant crops or an increase in

Figure 9. Clearing and terracing of foothills for vineyard.

mechanization in crop production. The latter is true here; wine producers are more mechanized and most harvest grapes mechanically and no longer manually in the catchment, as has been the trend elsewhere in southern France (Sluiter & de Jong, 2007). However, the first interpretation of land clearing does not hold since vineyard experienced the greatest loss (−34.2% of initial cover, Table 1) in the alluvial plain of all land cover types. Much of this was to built area as urban centers expanded onto adjoining land. The tendency for cities to grow onto agricultural land is common throughout the world and the Mediterranean area (Serra et al., 2008; Sluiter & de Jong, 2007), but the conversion of vineyard to grassland in conjunction with urban expansion is less common (Falcucci et al., 2007; Serra et al., 2008). In this case, abandoned vineyard fields generally belonged to owners who did not produce their own wine but brought their grapes to a winemaking cooperative. Grape production was therefore not necessarily central to their livelihood as it is for the winemaking 'domaines'. Furthermore, when land is passed on from one generation to the next, grape production can be abandoned but the land retained. Property values are known to increase in the region, so land represents a secure financial investment. This explains some of the conversion from vineyard to grassland and then forest, and it accounts for the paradoxical situation of agriculture conquering marginal lands on steep slopes while abandoning fertile land in the plain to grassland and forest.

The shift in agriculture from the alluvial plain to fields located on bedrock soils is probably specific to vineyard production since vines adapt better to cultivation on steeper slopes than most crops. In addition, steeper slopes with thin soils brought into cultivation are generally terraced, and soil depths are significantly improved by terracing. Upland slopes are dominated by schist and gneiss which tend to generate slightly acidic sandy soils. In an unpublished analysis of 24 soil samples from vineyards from both the plain and foothills, there was very little variation within the catchment in texture and pH. Clay contents were low for all samples (mean and median of 7.6% and 6.6%, respectively), coarse sand contents were high (mean and median of 45.3% and 48.4%, respectively), and pH values were all slightly acidic (mean and median of 6.6 and 6.7, respectively). Hence, soil attribute differences generated by different geological substrates were minor, and the French notion of 'terroir' in wine production can be considered preserved despite the move of some fields from the plain to the foothills. It is, however, probable that the alluvial plain soils benefit from better soil moisture conditions in the summer, but there are no data available to support this.

Grassland dynamics are particularly complex in the catchment. As discussed above, some of the growth in grassland is due to land abandonment in the fertile alluvial plain. However, several other factors come into play. One is the conversion of vineyard to grassland (mostly pasture) along stream channels and this is probably related to flooding risks (Figure 10) where lowland areas along stream channels experience regular flooding. This probably also accounts for the relatively low gains in built area close to stream channels. With time, abandoned vineyard evolves into grassland (or shrubland) first (Serra et al., 2008), then forest afterwards, accounting for grassland–forest transitions and the increase in forest area in the alluvial plain in 1982–2008 (Figure 2a). Although the reverse is intuitively unlikely, clearing of forest to create fire breaks was a priority after the 2003 fires that ravaged >4000 ha, and some fire breaks were present before then. Finally, some of the vineyard–grassland transition is related to the creation of horseback riding activities in recent years. Tourism is a major local industry and the proximity of large expanses of forest with paths and dirt roads makes horseback riding an attractive tourism activity. Cori (1999) explains that rapid growth of the tourism industry increased dramatically in the last few decades and influenced the land cover change on the northern shores of the

Figure 10. Flooding in vineyard close to stream channel.

Mediterranean. He reported that agricultural land decreased and nonagricultural land increased in the Spanish, French, and Italian Mediterranean regions due to the spread of touristic activities. And Nainggolan et al. (2012) found significant land cover change over 72% of their study area in a Mediterranean catchment due to biophysical and socio-economic factors, most of which were associated directly or indirectly with rapid urbanization and tourism. The combination of all these dynamics explains the high swapping of land between forest, vineyard, and grassland.

Built area increased substantially between 1950 and 2008. During the initial period, about 223 ha were added to the catchment in 32 years (7.0 ha y^{-1}); this value increased to 448 ha in 1982–2008 (17.2 ha y^{-1}). Other authors (Antrop, 2005; Salvati et al., 2013) have also found that urban sprawl accelerated in Euro-Mediterranean countries in the 1980s. Permanent population for the three main cities grew faster in 1982–2007 (about 296 pers. y^{-1}) than in 1962–1982 (about 229 pers. y^{-1}), but built area growth in the region probably depends as much on the nonpermanent population. Many new secondary homes were built during the past two decades (EAA Annual Report, 2010) near Mediterranean beaches to attract European and French populations (Blue Plan Papers, 2001). In addition, French and immigrated foreign retirees tend to settle in Mediterranean cities or use their coastal house as a secondary home. According to Cori (1999), half of total secondary homes in France are situated in the Mediterranean coastal area. Spatially, previously built area had a stronger impact on newly built area location in 1982–2008 than in 1950–2008, and urban expansion occurred almost exclusively within 100 m of roads and was concentrated mainly at low altitudes and on low to intermediate slopes. This agrees well with the findings of Schneider and Woodcock (2008) on the growth trends in 25 cities across the world in 1990–2000.

5. Conclusion

As in much of Mediterranean Europe, significant land cover changes occurred in 1950–2008. Forest remained the dominant land cover at all the times, and relative changes in forest cover were small for several reasons: its large surface (more than 85% of the catchment) and location at higher altitudes and on steeper slopes. Despite this, forest swapping with vineyard and grassland were high. Vineyard lost considerable area. It was

converted mainly into grassland, urban, and suburban land covers. Grassland was highly dynamic and experienced large losses and gains due to vineyard abandonment and the creation of fire breaks and pasture land. Grassland expanded mainly on abandoned vineyards. Most land cover changes occurred at lower altitudes and on flat to gently sloping areas in the eastern part of the catchment. All distance variables (from streams, roads, built area, and the sea) had significant impacts on land cover change dynamics.

Acknowledgments

We express our sincere thanks to the European Commission and the EMMA consortium of the University of Nice Sophia-Antipolis (UNS).

Funding

This research was funded in part by Erasmus Mundus Program (EMMAsia) from the EACEA acting for the European Commission, under reference 2010-2374/001-001-EMMA2.

References

Antrop, M. (2005). Why landscapes of the past are important for the future. *Landscape and Urban Planning, 70*, 21–34. doi:10.1016/j.landurbplan.2003.10.002

Baccaini, B. S. (2009). La croissance périurbaine depuis 1945. *Insee Première, 1240*, 1–4.

Benoit, G., & Comeau, A. (2005). A sustainable future for the Mediterranean. In *The Blue Plan's environment & development outlook* (464p.). London: Earthscan.

Blue Plan Papers. (2001, October). *Urbanization in the Mediterranean region from 1950–1995*. Nice: Sophia Antipolis, n.-1.

Brunetta, G., & Rotondi, G. (1996). Migratory flows from southern to northern Mediterranean borders. *Social Geography, 133*, 65–80.

Calvo-Iglesias, M. S., Fra-Paleo, U., & Diaz-Varela, R. A. (2009). Changes in farming system and population as drivers of land cover and landscape dynamics: The case of enclosed and semi-openfield systems in Northern Galicia (Spain). *Landscape and Urban Planning, 90*, 168–177. doi:10.1016/j.landurbplan.2008.10.025

Cori, B. (1999). Spatial dynamics of Mediterranean coastal regions. *Journal of Coastal Conservation, 5*, 105–112. doi:10.1007/BF02802747

Dunjó, G., Pardini, G., & Gispert, M. (2003). Land use change effects on abandoned terraced soils in a Mediterranean catchment, NE Spain. *Catena, 52*, 23–37. doi:10.1016/S0341-8162(02)00148-0

EAA Annual Report. (2010). Retrieved from http://www.eea.europa.eu/publications/annual-report-2010

Eastman, J. R. (2012). *IDRISI selva help system*. Worcester, MA: Clark Labs, Clark University.

ESRI. (2012). ArcGIS software. Retrieved from http://www.esri.com

Falcucci, A., Maiorano, L., & Boitani, L. (2007). Changes in land-use/land-cover patterns in Italy and their implications for biodiversity conservation. *Landscape Ecology, 22*, 617–631. doi:10.1007/s10980-006-9056-4

Fox, D., Berolo, W., Carrega, P., & Darboux, F. (2006). Mapping erosion risk and selecting sites for simple erosion control measures after a forest fire in Mediterranean France. *Earth Science Processes and Landforms, 31*, 606–621.

Fox, D. M., Witz, E., Blanc, V., Soulié, C., Penalver-Navarro, M., & Dervieux, A. (2012). A case study of land cover change (1950–2003) and runoff in a Mediterranean catchment. *Applied Geography, 32*, 810–821. doi:10.1016/j.apgeog.2011.07.007

Geri, F., Amici, V., & Rocchini, D. (2010). Human activity impact on the heterogeneity of a Mediterranean landscape. *Applied Geography, 30*, 370–379. doi:10.1016/j.apgeog.2009.10.006

Geri, F., Amici, V., & Rocchini, D. (2011). Spatially-based accuracy assessment of forestation prediction in a complex Mediterranean landscape. *Applied Geography, 31*, 881–890. doi:10.1016/j.apgeog.2011.01.019

IFEN. (2009). LA France, Vue Par Corinne land cover. *Le point sur, 10*, 4.

IFEN. (2012). Trois quarts des rivages métropolitains sont non artificialisés. *Le point sur, 153*, 4.
INSEE. (2011). Retrieved from http://www.insee.fr
Kepner, W., Rubio, J. L., Mouat, D. A., & Pedrazzini, F. (2003). *Desertification in the Mediterranean region: A security issue* (617p). Springer (ebook).
Koulouri, M., & Giourga, C. (2007). Land abandonment and slope gradient as key factors of soil erosion in Mediterranean terraced lands. *Catena, 69*, 274–281. doi:10.1016/j.catena.2006.07.001
Lambin, E. F., Turner, B. L., Geist, H. J., Agbola, S. B., Angelsen, A., Bruce, J. W., … Xu, J. (2001). The causes of land-use and land-cover change: Moving beyond the myths. *Global Environmental Change, 11*, 261–269. doi:10.1016/S0959-3780(01)00007-3
Martínez-Fernández, J., Esteve-Selma, M. A., Baños-González, I., Carreño, F., & Moreno, A. (2013). Sustainability of Mediterranean irrigated agro-landscapes. *Ecological Modelling, 248*, 11–19. doi:10.1016/j.ecolmodel.2012.09.018
Nainggolan, D., de Vente, J., Boix-Fayos, C., Termansen, M., Hubacek, K., & Reed, M. S. (2012). Afforestation, agricultural abandonment and intensification: Competing trajectories in semi-arid Mediterranean agro-ecosystems. *Agriculture, Ecosystems and Environment, 159*, 90–104. doi:10.1016/j.agee.2012.06.023
Nunes, A. N., de Almeida, A. C., & Coelho, C. O. A. (2011). Impacts of land use and cover type on runoff and soil erosion in a marginal area of Portugal. *Applied Geography, 31*, 687–699. doi:10.1016/j.apgeog.2010.12.006
Parcerisas, L., Marull, J., Pino, J., Tello, E., Coll, F., & Basnou, C. (2012). Land use changes, landscape ecology and their socioeconomic driving forces in the Spanish Mediterranean coast (El Maresme County, 1850–2005). *Environmental Science & Policy, 23*, 120–132. doi:10.1016/j.envsci.2012.08.002
Pelorosso, R., Leone, A., & Boccia, L. (2009). Land cover and land use change in the Italian central Apennines: A comparison of assessment methods. *Applied Geography, 29*, 35–48. doi:10.1016/j.apgeog.2008.07.003
Pontius, R. G., Jr., Shusas, E., & McEachern, M. (2004). Detecting important categorical land changes while accounting for persistence. *Agriculture, Ecosystems and Environment, 101*, 251–268. doi:10.1016/j.agee.2003.09.008
Sala, O. E., Chapin, F. S., III, Armesto, J. J., Berlow, E., Bloomfield, J., Dirzo, R., … Wall, D. A. (2000). Global biodiversity scenarios for the year 2100. *Science, 287*, 1770–1774. doi:10.1126/science.287.5459.1770
Salvati, L., Sateriano, A., & Bajocco, S. (2013). To grow or to sprawl? Land cover relationships in a Mediterranean city region and implications for land use management. *Cities, 30*, 113–121. doi:10.1016/j.cities.2012.01.007
Schneider, A., & Woodcock, C. E. (2008). Compact, dispersed, fragmented, extensive? A comparison of urban growth in twenty-five global cities using remotely sensed data, pattern metrics and census information. *Urban Studies, 45*, 659–692. doi:10.1177/0042098007087340
Serra, P., Pons, X., & Sauri, D. (2008). Land-cover and land-use change in a Mediterranean landscape: A spatial analysis of driving forces integrating biophysical and human factors. *Applied Geography, 28*, 189–209. doi:10.1016/j.apgeog.2008.02.001
Sluiter, R., & de Jong, S. M. (2007). Spatial patterns of Mediterranean land abandonment and related land cover transitions. *Landscape Ecology, 22*, 559–576. doi:10.1007/s10980-006-9049-3
Van Eetvelde, V., & Antrop, M. (2004). Analyzing structural and functional changes of traditional landscapes-two examples from Southern France. *Landscape and Urban Planning, 67*, 79–95. doi:10.1016/S0169-2046(03)00030-6

Predicting Land Cover Change in a Mediterranean Catchment at Different Time Scales

Hari Gobinda Roy, Dennis M. Fox*, and Karine Emsellem

UMR 7300 CNRS ESPACE, Université de Nice Sophia Antipolis, BP 3209,
06204 Nice cedex 3, France
roy.hari.gobinda@etu.unice.fr,
{fox,Karine.Emsellem}@unice.fr

Abstract. Land cover has been changing rapidly throughout the world, and this issue is important to researchers, urban planners, and ecologists for sustainable land cover planning for the future. Many modeling tools have been developed to explore and evaluate possible land cover scenarios in future and time scales vary greatly from one study to another. The main objective of this study is to test land cover change prediction at different time scales in a Mediterranean catchment in SE France. Land cover maps were created from aerial photographs (1950, 1982, 2003, 2008, and 2011) of the Giscle catchment (235 Km^2) and surfaces were classified into four land cover categories: forest, vineyard, grassland, and built area. Explanatory variables were selected through Cramer's coefficient. Different time scales were tested in the study: short (2003-2008), intermediate (1982-2003), and long (1950-1982). To test the model's accuracy, Land Change Modeler (LCM) of IDRISI was used to predict land cover in 2011 and predicted images were compared to a real 2011 map. Kappa index and confusion matrix were used to evaluate the model's accuracy. Altitude, slope, and distance from roads had the greatest impact on land cover changes among all variables tested. Good to perfect level of spatial and perfect level of quantitative agreement were observed in long to short time scale simulations. Kappa indices ($K_{quantity}$ = 0.99 and $K_{location}$ = 0.90) and confusion matrices were good for intermediate and best for short time scale. The results indicate that shorter time scales produce better predictions. Time scale effects have strong interactions with specific land cover dynamics, in which stable land covers are easier to predict than cases of rapid change and quantity is easier to predict than location for longer time periods.

Keywords: Time scale, Land cover change modeling, Mediterranean Europe, Land change Modeler (LCM).

1 Introduction

1.1 Land Cover Change Modeling

Land cover is changing rapidly throughout the world, and it has become an important issue for urban planners, ecologists, economists, and resource managers to evaluate

* Corresponding author.

B. Murgante et al. (Eds.): ICCSA 2014, Part IV, LNCS 8582, pp. 315–330, 2014.

environmental change and establish sustainable development planning [7, 10, 17]. Land cover change models are able to identify location and quantity of change, predict land cover change considering past changes, test explanatory variables, and simulate management policies. For this reason, many interdisciplinary research projects have been initiated for land cover change modeling, measuring regional and global land cover change, forecasting future conditions, and planning for sustainable development [28]. As a result, researchers have created a large set of operational modeling tools to implement prediction and exploration of possible land cover change trajectories and land cover planning and policy in recent years [29]. Moreover, land cover change, urban growth, and spatial modeling have drawn considerable interest in the last two decades due to better computing power, availability of spatial data, and the need for innovative planning tools for decision support [7]. Advanced urban and land cover change modeling techniques have been included in many GIS software package.

1.2 The Role of Time Scale in Land Change Prediction

The selection of prediction and validation time intervals has a great impact on prediction accuracy [6]. Prediction accuracy can depend on the rate and process of transitions in both time intervals. Modeling of land cover change using a coarser temporal scale may fail to understand landscape change patterns properly and can hamper model performance [2], so most studies on future land cover change use short to intermediate historical time scales (5–15 years). Many studies on urban land cover change modeling use short time scales that achieve better prediction [1, 11, 18, 24]. Some studies use intermediate time scales [13, 14, 15, 20, 25, 26, 27] and very few studies use long time scales to simulate urban land cover [4] and multiple land cover change [10, 21]. Average historical and prediction time periods are about 10 and 12 years, respectively, analyzing 25 recent studies on land cover change using CA-Markov and Multi-Layer Perceptron (MLP).

Very few studies were found on the comparison of the impact of historical time periods on land cover prediction using different time scales. To investigate the impact of time interval on prediction accuracy in Gorizia-Nova Gorica (Italy), urban area was predicted for different years (2005 to 2010) from initial conditions in 1985 and 2004 [5]. The authors found that prediction accuracy increased with decreasing prediction time period.

1.3 Objectives

The objective of this paper is to explore the impact of temporal scales on land cover change modeling for predicting land cover change in a Mediterranean catchment in SE France. Land cover maps of 2011 were predicted from different time scales (1950-1982, 1982-2003, and 2003-2008) and compared with the digitized land cover map of 2011 to measure model accuracy. The study is part of a larger program to evaluate the impacts of land cover change on runoff and soil erosion at the catchment scale.

2 Methods

Study area, land change modeling steps, and data are discussed in this section.

2.1 Site Description

The study area (about 235 km²) is situated in the Var department of SE France near the Gulf of St. Tropez. The western part of the watershed (about 70% of the catchment) is forest (mostly pine and oaks), and the topography is uneven with the highest elevation at about 650 m. The lower part of the catchment is a gently sloping alluvial plain. The catchment area is characterized by a Mediterranean climate with hot dry summers, and cooler rainier winters. Average temperatures range between 22°C to 26°C in summer and 5°C to 10°C in winter. The mean annual rainfall is about 900 mm, and the main rainy season is from October to January [9]. Several tributaries flow into the Giscle main channel, including the Môle, the Grenouille, the Tourre, and the Verne. Three main municipalities are located within the catchment: Cogolin, Grimaud, and La Môle.

2.2 Land Change Modeling Procedure

Land Change Modeler (LCM) in IDRISI [8] was originally designed to manage impacts on biodiversity, and analyze and predict land use and land cover changes. Only thematic raster images with the same land cover categories listed in the same sequential order can be inputted in LCM for analysis, and background areas must be identified on maps coded with 0. LCM evaluates land cover changes between Time 1 (initial time) and Time 2 (second time). It calculates the changes, and displays the results with various graphs and maps. Finally, it predicts future (Time 3) land cover on the basis of relative transition potential maps. LCM was used in this study to identify explanatory variables, create transition potentials, and predict future land cover maps.

Digital Data and Land Cover Categories

Land cover maps were digitized from grey scale ortho-rectified aerial photographs of 1950 and 1982, and color ortho-photos of 2003, 2008, and 2011. Spatial resolution for all aerial photographs was reduced to 1 m from 0.5 m to facilitate data manipulation during digitization. Surfaces were initially characterized into five categories: forest (F), vineyard (V), grassland (G), urban (U) and suburban (S), but the last 2 categories were collapsed into a single built area (B) class to improve category attribution as described below. Methods of land cover digitization, classification, and characteristics of land cover classes were discussed in [23]. Land cover classification was facilitated by numerous field visits, and validation was carried out through a group of 15 third year Geography students of the University of Nice Sophia Antipolis. Each student was provided with a sample of 20 selected cells to identify land cover class; each sample had a roughly equal number of cells in each category, and there were 5

students for each year (1950, 1982, and 2003). This was the students' first contact with digital air photos, so the validation is considered a worst case scenario.

Slope was created from a 25 m Digital Elevation Model (DEM). Road and stream networks were screen digitized from the aerial photographs of 2008. Only major roads were taken into account, so road network was considered constant for all time periods. In order to make the land cover maps compatible with the explanatory variables, celle size was converted to 25 m.

Explanatory Variables and Constraints

Topographic and distance variables have been used to simulate land cover change studies throughout the world [16, 18, 19, 27]. In an earlier study [23], major topographic and distance variables were identified. These include the following: slope, altitude, distance from roads, distance from built area (initial year), and distance from streams. In addition, three constraints and incentives (forest to built area, vineyard to built area, and grassland to built area) were included in the prediction process. These were created from the "Plan Local d'Urbanisme" (PLU) and "Schéma de Coherence Terrtoriale" (SCOT). The PLU is the local urban plan in France; it determines land use guidelines. The SCOT integrates different policies regarding urban planning: social and private housing, communication infrastructure and public transport, commercial infrastructure, and environment protection. Constraints and incentives are multiplied by the corresponding transition potential during modeling. In this study, values of 0 on the map were used to define absolute constraint, and 1.1 was used for incentives to emphasize the expansion of built areas in suitable selected zones for development according to the regional plan. In addition, distance from streams was also added with above mentioned constraints. Disincentive areas situated within a distance from streams of 0-25 m, and 25-50 m were defined by values of 0.6 and 0.8, respectively to maintain the historical trend of less urbanization near stream networks in the study area according to [23].

Selection of Explanatory Variables

The simulation of multiple categories of land cover change depends on several explanatory variables [18]. Explanatory variables that were drivers of past land cover change are expected to be an influential force in future changes and are selected based on available data and their explanatory abilities. DEM, slope, and distance from road represent the accessibility of a neighborhood, and distance from built area highlights the proximate location of urbanization. The significance of explanatory variables was tested using Cramer's V which measures the strength of association between two categorical variables based on Chi-square statistics [21]. In this study, land cover change in a historical time period and explanatory variables are taken into account to test Cramer's V for a particular variable. LCM calculates Cramer's V automatically and displays the association level of explanatory variables with land cover categories. Variables with greater values are considered more important than other variables. Cramer's V values of ≥ 0.4 and ≥ 0.15 are considered good and useful, respectively; and values <0.15 should be removed from the model [8].

Transition Potentials

Transition potential maps were created for each transition possibility (F to V, F to G, F to B, V to F, V to G, V to B, G to F, G to V, and G to B) based on historical changes and selected explanatory variables. The Multi-Layer Perceptron Neural Network (MLPNN) algorithm of IDRISI [8] was employed to create transition potentials. Each transition potential was modeled individually using the same explanatory variables, but only transition potentials with an accuracy rate greater than 70% were utilized for land cover prediction.

Land Cover Prediction and Time Scales Test

Land cover change prediction has two aspects: the quantity of change is provided by the Markov change model matrix and the spatial distribution of change is given by MLPNN. LCM provides the quantity of change by evaluating the Markov matrix comparing the initial (T1) and second land cover (T2), and then predicts the future land cover (T3) using a transition probability matrix for the future. The transition probability matrix displays the probability of each land cover category changing into another category. A value close to 0 indicates a low conversion probability, and 1 indicates a high conversion probability for the target land cover. Land cover maps were predicted for 2011 using transition potential maps from several historical time periods (1950-1982, 1982-2003, 2003-2008) (Table 1). The same variables and constraints were incorporated in all simulations.

Table 1. Historical time periods, prediction and validation dates for different scales

Historical time period	Prediction date	Historical time interval	Validation time interval
1950-1982	2011	32	29
1982-2003	2011	21	8
2003-2008	2011	5	3

Land Cover Prediction Validation

Validation of a model is needed in order to assess its accuracy. To do this, simulated land cover maps of 2011 created using different time scales were compared with a digitized map of the same year. Kappa indices and error matrix analysis were used in the study for model validation. The standard 'Kappa index' is a comparative analytical process that measures spatial and non-spatial aspects between predicted and reference maps [8]. Kappa values were characterized as excellent over 0.75, 0.40 to 0.75 as fair to good, and below 0.40 as poor [8].

Several components of Kappa indices are described in [22]: Kappa standard ($K_{standard}$), Kappa for location ($K_{location}$), and Kappa for quantity ($K_{quantity}$). They [22] define *"$K_{standard}$ as an index of agreement that attempts to account for the expected agreement due to random spatial reallocation of the categories in the comparison map, given the proportions of the categories in the comparison and reference maps, regardless of the size of the quantity disagreement"*. $K_{quantity}$ is a ratio of quantitative difference between the categories in the comparison map and reference map, and $K_{location}$ is the spatial allocation agreement between them.

The confusion matrix was analyzed using the ERRMAT module of IDRISI [8] to assess the fitness of spatial cell allocation between predicted and true values. ERRMAT outputs an error matrix containing a tabulation of the number of cells found in each possible combination of true and mapped categories and a summary of statistics [8]. Error of omission estimates the proportion of the area of a particular land cover that is omitted by the model. Error of commission represents the proportion of wrongly attributed land cover of a particular category that is overestimated by the model for each category.

3 Results

3.1 Land Cover Change Analysis during Different Time Periods

The classification validation procedure revealed that classifying land cover into five categories was difficult from grey scale photographs and simpler for the 2003 color air photos. For 1950, classification error was 27%, and sources of error were either a confusion between vineyard and grassland or urban and suburban. The classification error decreased to 20% when urban and suburban were collapsed into a single built category. For 1982, category error was 10% and 20% for 4 and 5 categories, respectively. Finally, for 2003, the error was only 4% for 4 categories, down from an initial 15% due to confusion between urban and suburban classes (by one student). It should be noted that the exercise was for unexperienced undergraduates just introduced to digital air photos. The actual classification was carried out by an experienced user over several months and verified thoroughly by a second experienced user, so the actual classification accuracy can be considered much greater than the values cited above.

Fig. 1a-d show land cover maps (1950, 1982, 2003, and 2008) digitized from the air photos. Most of the land cover changes occurred in the alluvial plain (East), where most of the vineyard, grassland and built areas are concentrated.

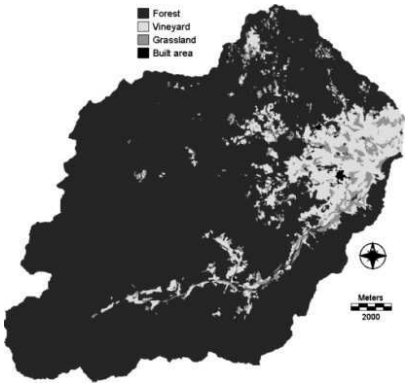

Fig. 1a. Land cover map of 1950

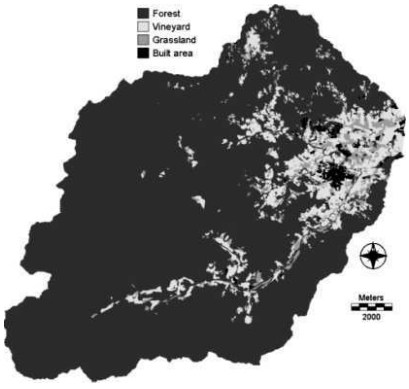

Fig. 1b. Land cover map of 1982

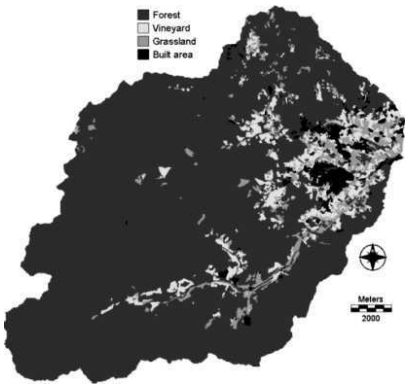

Fig. 1c. Land cover map of 2003

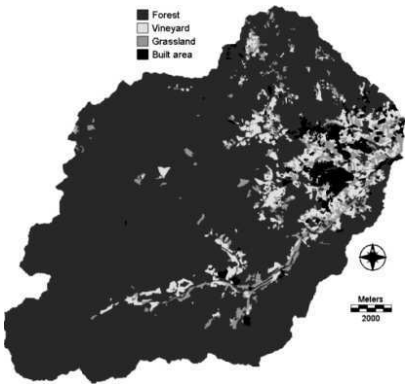

Fig. 1d. Land cover map of 2008

Fig. 2 a-d present land cover changes (ha) in all categories of the study area, and Table 2 shows the percentage of total surface area of each land cover category in different years. Two general trends can be identified in land cover change since 1950: forest and vineyard decreased while grassland and built area increased. Some changes in forest occurred in 1982-2003 as it lost about 120 ha (Fig. 2 a). A marked decrease was observed in vineyard (28% of the initial year) that lost 854 ha between 1950 and 2003 (Fig. 2 b). Then, it increased 67 ha in 2003-2008 and resumed its decreasing trend in the last time period 2008-2011. Vineyard was 10.4% of the catchment in 1950 and decreased to 6.6% in 2003 and then remained more or less stable till 2011. Grassland increased from 3.4% to 5.4% of the catchment in 1950-2003 and decreased slightly to 4.9% in 2011. It increased greatly (383 ha) in 1982-2003, decreased 122 ha in the next time period (2003-2008) but resumed the increasing trend again in 2008-2011 (Fig. 2 c). Built area remained a minor component of the catchment, and increased rapidly from only 0.1% to 3.2% of the catchment during the study period (Table 2).

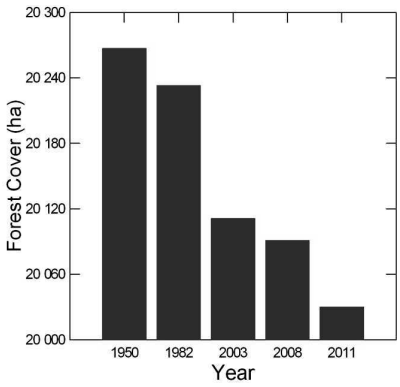

Fig. 2a. Forest change in 1950-2011

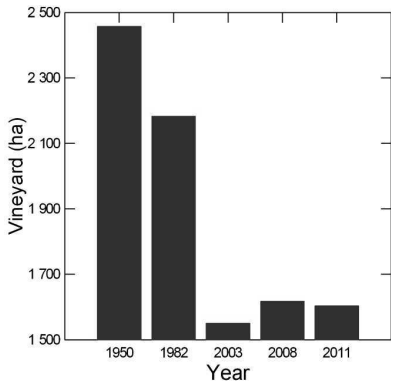

Fig. 2b. Vineyard change in 1950-2011

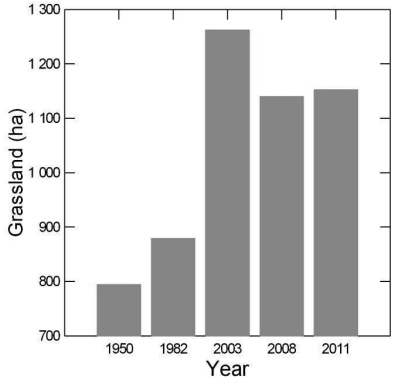

Fig. 2c. Grassland change in 1950-2011

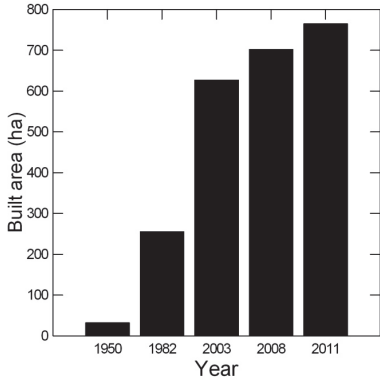

Fig. 2d. Built area change in 1950-2011

Table 2. Percentage of the catchment area for each category

	Total surface area (% of the catchment)				
	1950	1982	2003	2008	2011
Forest	86.1	85.9	85.4	85.3	85.1
Vineyard	10.4	9.3	6.6	6.9	6.8
Grassland	3.4	3.7	5.4	4.8	4.9
Built area	0.1	1.1	2.7	3.0	3.2

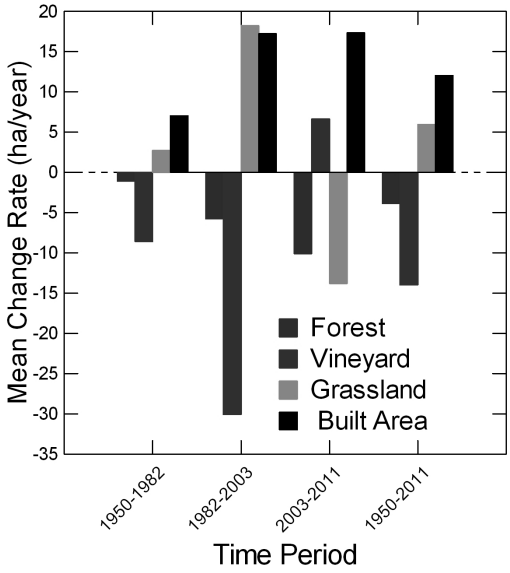

Fig. 3. Mean rates of land cover change (ha) in different time periods

Fig. 3 summarizes the mean rate of change of each land cover category in the different time periods. Forest loss was -1.1 ha yr^{-1} and -5.8 ha yr^{-1} in 1950-1982 and 1982-2003, respectively, it lost -10.1 ha yr^{-1} in the recent time period 2003-2011. The average forest depletion rate was -3.9 ha yr^{-1} in 1950-2011. The greatest rate of vineyard loss was -30.1 ha yr^{-1} in 1982-2003, and the average overall rate of vineyard depletion was -14 ha yr^{-1}. The rate of grassland expansion was 2.7 ha yr^{-1} in 1950-1982; it increased to 18.2 ha yr^{-1} in 1982-2003, and then to 13.8 ha yr^{-1} in 2003-2011. Grassland gained an average of 5.9 ha yr^{-1} in the study period. The rate of built area expansion was 7 ha yr^{-1} in 1950-1982 and increased to 17.6 ha yr^{-1} in the recent time period 2003-2011. So, the average rate of built area expansion was 12 ha yr^{-1} in 1950-2011.

3.2 Selection of Explanatory Variables

The association level between explanatory variables and land cover types in different time periods is shown in Table 3. It is measured through Cramer's V. All variables have a Cramer's V value ≥0.15 with all land cover types except forest in the long time period (1950-1982).

Table 3. Cramer's V coefficient (relationship between land cover change and explanatory variables). Values ≥ 0.40 are highlighted in bold

Time period		Altitude	Slope	Dist. Road	Dist. Built area	Dist. stream
1950-1982	Forest	0.20	0.15	0.31	**0.40**	0.12
	Vineyard	**0.69**	**0.65**	**0.59**	**0.46**	**0.41**
	Grassland	**0.52**	**0.50**	**0.44**	0.33	0.32
	Built area	0.39	0.36	0.28	0.22	0.20
1982-2003	Forest	0.30	0.22	**0.49**	**0.60**	0.16
	Vineyard	**0.67**	**0.63**	**0.59**	**0.59**	**0.41**
	Grassland	**0.40**	**0.40**	0.36	0.33	0.27
	Built area	**0.44**	**0.42**	0.30	0.30	0.25
2003-2008	Forest	0.30	0.22	**0.49**	**0.64**	0.16
	Vineyard	**0.67**	**0.62**	**0.59**	**0.60**	**0.41**
	Grassland	**0.41**	**0.41**	0.36	0.34	0.27
	Built area	0.39	0.38	0.27	0.29	0.25

The strongest explanatory variable is altitude, which has a good association level (Cramer V ≥0.40) with all land covers except forest for all time periods. A good association level is also observed in slope with all land covers in all time periods, especially with vineyard and grassland. Distance from roads shows a high association level with vineyard in all time periods, and has good association level with forest and grassland in the intermediate (1982-2003) and long (1950-1982) time periods, respectively. Distance from built area also has a good association level with forest and vineyard in all time periods. Distance from streams is the weakest variable; it shows comparatively limited association with existing land covers and has only a good level of association with vineyard in all time periods. The lowest association is observed

for forest with all variables except distances from road and built area, indicating that the dominant forest category (about 85%) is less influenced by topographic variables.

3.3 Transition Potentials

Transition potentials for different time periods present similar patterns and the same explanatory variables were used in all simulations for the different time scales. Table 4 presents the accuracy rate of all transition potentials for different time periods. Accuracy rate represents the agreement between a particular transition and selected explanatory variables. A high accuracy rate is observed for several transitions in all time periods: forest to all other categories, and vineyard and grassland to built area. Transition from vineyard to forest in 2003-2008 also shows high accuracy. Therefore, transition potentials from forest to all and vineyard and grassland to built area are good. All transitions from vineyard and grassland to other land covers except built area have low to intermediate accuracy rate.

Table 4. Accuracy rate (%) of transition potentials in different time periods (F-Forest, V-Vineyard, G-Grassland, B-Built area)

	Accuracy rate (%)								
Time period	F-V	F-G	F-B	V-F	V-G	V-B	G-F	G-V	G-B
1950-1982	85	86	99	64	58	97	63	58	97
1982-2003	83	81	97	64	60	85	62	57	83
2003-2008	91	97	98	100	63	85	63	64	82

3.4 Validation of Predicted Land Cover

Simulations for 2011 were executed using transition potentials from 1950-1982, 1982-2003, and 2003-2008, respectively. Simulated and actual land cover maps of 2011 are presented in Fig. 4a-d. Dissimilarities are observed mainly in the plain land

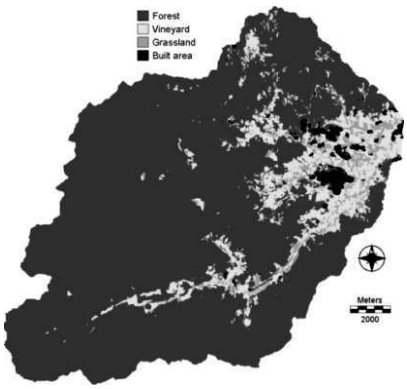

Fig. 4a. Predicted land cover map of 2011 from transition potentials 1950-1982

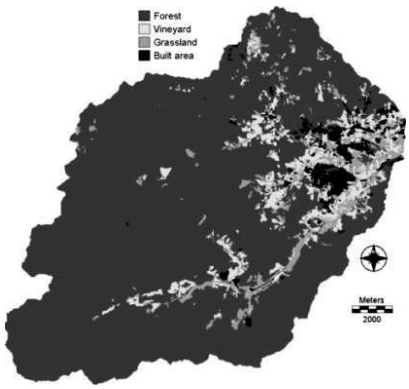

Fig. 4b. Predicted land cover map of 2011 from transition potentials 1982-2003

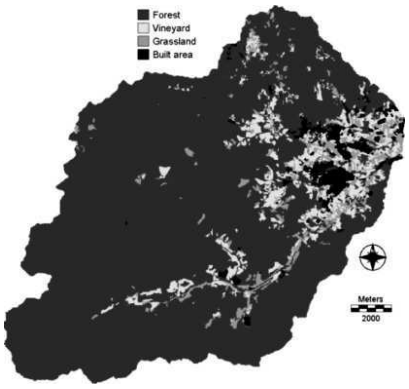

Fig. 4c. Predicted land cover map of 2011 from transition potentials 2003-2008

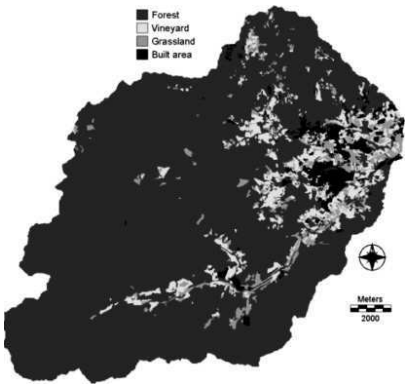

Fig. 4d. Land cover map 2011 (actual)

of the eastern part of the catchment where most of the conversion took place as described in [23]. Visual interpretation (Fig. 4 a-c) suggests the simulated maps from intermediate (Fig. 4 b) and short (Fig. 4 c) time scales are reasonably similar to the actual map of that year (Fig. 4 d).

Kappa Indices for Predicted Land Cover from Different Time Periods

The summary of the Kappa indices at different time scale simulations is presented in Table 5. These indices are acquired from the VALIDATION module of IDRISI [8] and can also be obtained using the Pontius matrix following [22]. Results show that all Kappa components increase with decreasing time scale up to the near perfect level of agreement for the short time scale. However, simulation from long time scale also achieved a perfect level for $K_{quantity}$ and a reasonable level of agreement for $K_{location}$, and $K_{standard}$.

Values of $K_{quantity}$ were observed in the perfect level of agreement in all three simulations, and these values increased a little from 0.95 to 1.00 for long to short time scale simulations. $K_{location}$ gives the overall spatial accuracy of a simulation. Spatial accuracy was difficult to achieve from the long time simulation. Values of $K_{location}$ varied greatly from long to short time scale though the simulation for the long time scale also had a good level of agreement (0.75); this increased to 0.87 and 0.94 for intermediate and short time simulations, respectively. The greatest changes were also observed in $K_{standard}$ for different time scales which increased from 0.66 to 0.94 with decreasing time scale.

Table 5. Summary of Kappa indices

	Initial time period		
	1950-1982	1982-2003	2003-2008
$K_{quantity}$	0.95	0.99	1.00
$K_{location}$	0.75	0.90	0.94
$K_{standard}$	0.66	0.87	0.94

Error Matrix Analysis for Predicted Land Cover from Different Time Periods

Table 6 presents the error matrix analysis of the actual land cover map 2011 (column) against predicted land cover (row) for different time scales. The table contains three 6 x 6 matrices for the 1950-1982, 1982-2003, and 2003-2008 time periods. In addition to overall errors, this table also shows where errors occur. For example, 158 ha of vineyard was wrongly attributed to forest, and 438 ha of vineyard was omitted that should be forest.

Table 6. Error matrix analysis of actual land cover map 2011 (column) against predicted (row) land cover from transition potentials for different time periods. Values are expressed in hectares (ha) and errors of commission and omission are expressed in % and in bold.

Initial time period		Forest	Vineyard	Grassland	Built area	Total	Error of commission (%)
1950-1982 (long)	Forest	19,277	158	236	113	19,784	**2.6**
	Vineyard	438	1,305	488	156	2,387	**45.3**
	Grassland	295	113	403	118	930	**56.6**
	Built area	20	27	25	378	450	**16.0**
	Total	20,030	1,603	1,152	765	23,550	
	Error of Omission (%)	**3.8**	**18.6**	**65.0**	**50.6**		**9.3**
1982-2003 (interme-diate)	Forest	19,716	45	52	51	19,864	**0.7**
	Vineyard	68	1,413	80	30	1,590	**11.2**
	Grassland	204	119	965	37	1,326	**27.2**
	Built area	42	26	54	647	770	**15.9**
	Total	20,030	1,603	1,152	765	23,550	
	Error of Omission (%)	**1.6**	**11.9**	**16.2**	**15.4**		**3.4**
2003-2008 (short)	Forest	19,953	30	45	27	20,055	**0.5**
	Vineyard	16	1,496	94	15	1,621	**7.7**
	Grassland	44	68	997	17	1,127	**11.5**
	Built area	16	9	16	706	747	**5.4**
	Total	20,030	1,603	1,152	765	23,550	
	Error of Omission (%)	**0.4**	**6.7**	**13.4**	**7.7**		**1.69**

Errors for all land covers decreased with decreasing time scales. The lowest commission and omission errors were observed in forest for all time scales and these decreased slightly with decreasing time scales. Errors of commission and omission were 2.6% and 3.8%, respectively, for forest in the long time scale prediction, and these decreased to 0.7% and 1.6% in the intermediate and 0.5% and 0.4% in the short time scale predictions, respectively. High error of commission (45.3%) was observed in vineyard in the long time scale where the greatest amount of vineyard (1,082 ha) was wrongly attributed, and commission error decreased markedly in intermediate and short time scales. However, error of omission was relatively low in the long time scale simulation for vineyard. The highest errors of commission and omission were observed in grassland in all time scale simulations, particularly the long time scale where errors of commission and omission were 56.6% and 65%, respectively. Errors for this land cover also decreased greatly with decreasing time scale (Table 6). Considerable amounts of vineyard and grassland were wrongly attributed to forest, and considerable areas of vineyard and grassland were omitted by the model in the long

time scale simulation; this occurred mainly due to high swapping of these land covers with forest. For this reason, high errors of commission and omission were generated for vineyard and grassland in the long time scale; errors decreased considerably in the intermediate and short time scale simulations. In long time simulation, errors of commission of built area were lower than for vineyard and grassland due to its small coverage in the catchment, and it was wrongly attributed 72 ha of other land covers. However, high error of omission was observed in the same simulation because much built area (388 ha) was omitted.

4 Discussion

Land cover dynamics and changes in individual land covers have an important impact on land cover simulation. As it is described in the results, forest is easy to predict, and it obtains the best level of agreement and the lowest error in all simulations using different time scales due to its dominant coverage in the study area. It is the least probable to change in all transition potentials of forest to other land covers, so $K_{quantity}$ is better for all time scales.

Simulations of vineyard and grassland are extremely difficult to predict: accuracy is lower and errors greater due to the dynamic changes in different time periods and high swapping between these covers. Hence, high commission and omission errors are observed in vineyard and grassland simulations, particularly in the long time scale. These errors may occur due to different rates of change in initial and prediction time periods and the selection of transition potentials where transition potentials from vineyard to forest and grassland, and grassland to forest and vineyard were avoided due to their limited accuracy rate (<70%). Simulations of vineyard and grassland may improve using constraints for vineyard and grassland. Vineyard fields belonging to the wine making "domaines" tend to remain stable and convert to other covers less [23], so a "domaine" layer could be used as a constraint for vineyard. This information, however, was not available in this study. In addition, fire breaks, horseback riding, and other tourism related activity zones that are classified as grassland could perhaps be taken as a constraint for grassland.

Accurate prediction of urban expansion is difficult due to the complexity in urbanization which depends on several spatial variables, urban planning, and land use demand [12]. The rapid relative rate of urban growth impacted the urban prediction. For example, the model predicts (for 2011) about 40% less built area than the actual map of 2011 using the long time scale because the rate of built area expansion increased by more than double in the latter time period (1982-2011) compared to the initial period (1950-1982) (Fig. 3). However, intermediate and short time periods perform better since increasing trends in the initial time periods are about the same as in the prediction time periods (2003-2011 and 2008-2011). In addition, several scattered urban areas are developed exceptionally far away from existing built area in the recent year, and these remain difficult to predict because the model is based on historical trends. Earlier trials showed the use of constraints for the transitions to built area from other land covers reduced error in built area in all simulations.

Time scales have a significant impact on land cover simulation. Quantity was predicted better than location, probably due to the dominant forest cover in the study area. Therefore, $K_{quantity}$ is nearly perfect in all time scales. However, complex land cover changes and swapping between land covers generate less perfect levels of agreement for $K_{location}$ than $K_{quantity}$, and values increase with decreasing time scales.

Although different indexes are used, there is a general trend for Shorter time scales to Produce better prediction results [1, 15, 16, 20, 21, 24, and 27], as found in this study was. The values of $K_{quantity}$ and $K_{location}$ are in acceptable ranges for different time scales in this study. Maximum commission and omission errors observed in crops and grassland [27] were also noted in this study since complex changes in grassland and vineyard are difficult to simulate.

5 Conclusion

Studies of the temporal and spatial distribution of land cover change have become an important issue due to the rapid conversion of land cover and its impact on environment change. Time scale has a significant impact on prediction. Near perfect quantitative accuracy was achieved in all time scales but spatial accuracy varied with different time scales. High quantitative and location accuracy were found in forest prediction due to its large surface area, in which changes are relatively small and swapping does not impact prediction. Prediction of vineyard and grassland were difficult due to high swapping with one another and forest, and prediction of built area was complicated by the dramatic relative growth that increased in the recent time periods and the emergence of urban lots far from historic centers. Cell size and catchment area may also impact land cover change simulation and this is under study now.

References

1. Ahmed, B., Ahmed, R.: Modeling urban land cover growth dynamics using multi-temporal satellite images: A case study of Dhaka, Bangladesh. ISPRS International Journal of Geo-Information 1, 3–31 (2012), doi:10.3390/ijgi1010003
2. Álvarez-Martínez, J.M., Suárez-Seoane, S., Luis Calabuig, E.D.: Modelling the risk of land cover change from environmental and socio-economic drivers in heterogeneous and changing landscapes: The role of uncertainty. Landscape and Urban Planning 101, 108–119 (2011), doi:10.1016/j.landurbplan.2011.01.009
3. Araya, Y.H., Cabral, P.: Analysis and Modeling of Urban Land Cover Change in Setúbal and Sesimbra, Portugal. Remote Sensing 2, 1549–1563 (2010), doi:10.3390/rs2061549
4. Bohnet, I., Pert, P.L.: Pattern, drivers and impacts of urban growth- A study from Cairns, Queensland, Australia from 1952 to 2031. Landscape and Planning 97, 239–248 (2010), doi:10.1016/j.landurbplan.2010.06.007
5. Chaudhuri, G., Clarke, K.C.: Temporal accuracy in urban growth forecasting: A study using the SLEUTH model. Transactions in GIS 18, 302–320 (2014), doi:10.1111/tgis.12047
6. Chen, H., Pontius Jr., R.G.: Diagnostic tools to evaluate a spatial land change projection along a gradient of an explanatory variable. Landscape Ecology 25, 1319–1331 (2010), doi:10.1007/s10980-010-9519-5

7. Dietzel, C., Clarke, K.: The effect of disaggregating land use categories in cellular automata model calibration and forecasting. Computers, Environment and Urban Systems 30, 78–101 (2006), doi:10.1016/j.compenvurbsys.2005.04.001
8. Eastman, J.R.: IDRISI Selva Help System. Clark Labs, Clark University, Worcester (2012)
9. Fox, D.M., Witz, E., Blanc, V., Soulié, C., Penalver-Navarro, M., Dervieux, A.: A case study of land cover change (1950-2003) and runoff in a Mediterranean catchment. Applied Geography 32, 810–821 (2012), doi:10.1016/j.apgeog.2011.07.007
10. Guan, D., Li, H., Inohae, T., Su, W., Nagaie, T., Hokao, K.: Modeling urban land use change by the integration of cellular automata and Markov model. Ecological Modelling 222, 3761–3772 (2011), doi:10.1016/j.ecolmodel.2011.09.009
11. He, C., Okada, N., Zhang, Q., Shi, P., Zhang, J.: Modeling urban expansion scenarios by coupling cellular automata model and system dynamic model in Beijing, China. Applied Geography 26, 323–345 (2006), doi:10.1016/j.apgeog.2006.09.006
12. He, C., Okada, N., Zhang, Q., Shi, P., Li, J.: Modelling dynamic urban expansion processes incorporating a potential model with cellular automata. Landscape and Urban Planning 86, 79–91 (2008), doi:10.1016/j.landurbplan.2007.12.010
13. Huang, Q., Cai, Y.: Simulation of land use change using GIS-based stochastic model: The case study of Shiqian County, Southwestern China. Stochastic Environment Research Risk Assessment 21, 419–426 (2007), doi:10.1007/s00477-006-0074-1
14. Jenerette, G.D., Wu, J.: Analysis and simulation of land -use change in the central Arizona Phonix region, USA. Landscape Ecology 16, 611–626 (2001)
15. Kamusoko, C., Aniya, M., Adi, B., Manjoro, M.: Rural sustainability under threat in Zimbabwe-Simulation of future land use/cover change in the Bindura district based on the Markov-cellular automata model. Applied Geography 29, 435–447 (2009), doi:10.1016/j.apgeog.2008.10.002
16. Khoi, D.D.: Spatial modeling of deforestation and land suitability assessment in the Tam Dao National Park region. University of Tsukuba, Vietnam. Ph. D. thesis (2011)
17. Lambin, E.F., et al.: The cause of land-use and land-cover change: moving beyond the myths. Global Environment Change 11, 261–269 (2001)
18. Li, X., Yeh, A.G.O.: Neural network based cellular automata for simulating multiple land use change using GIS. International Journal of Geographical Information Science 16, 323–343 (2002), doi: 10.108 0/13658810210137004
19. Mas, J.F., Pérez-Vega, A., Clarke, K.C.: Assessing simulated land use/cover maps using similarity and fragmentation indices. Ecological Complexity 11, 38–45 (2012), doi:10.1016/j.ecocom.2012.01.004
20. Mhangara, P.: Land use/ cover change modeling and land degradation assessment in the Keiskamma catchment using remote sensing and GIS. University of Nelson Mandela Met-ropolitan. Ph. D. thesis (2011)
21. Pérez-Vega, A., Mas, J.F., Ligmann-Zielinska, A.: Comparing two approaches to land use /cover change modeling and their implications for the assessment of biodiversity loss in a deciduous tropical forest. Environmenta Modelling & Software 29, 11–23 (2012), doi:10.1016/j.envsoft.2011.09.011
22. Pontius Jr., R.G., Millones, M.: Death to Kappa: birth of quantity disagreement and allocation disagreement for accuracy assessment. International Journal of Remote Sensing 32, 4407–4429 (2011), doi:org/10.1080/01431161.2011.552923
23. Roy, H.G., Fox, D.M., Emsellem, K.: Spatial dynamics of land cover change in a Mediterranean catchment (1950-2008). Journal of Land use Science (2014)

24. Sang, L., Zhang, C., Yang, J., Zhu, D., Yun, W.: Simulation of land use spatial pattern of towns and villages based on CA-Markov model. Mathematical and Modelling 54, 938–943 (2011), doi:10.1016/j.mcm.2010.11.019
25. Silva, T.S., Tanliani, P.R.A.: Environment planning in the medium littoral of the Rio Grand do Sul coastal plain - Southern Brazil: Elements for coastal management. Ocean and Coastal Management 59, 20–30 (2012), doi:10.1016/j.ocecoaman.2011.12.014
26. Tewolde, M.G., Cabral, P.: Urban sprawl analysis and modeling in Asmara, Eritrea. Remote Sensing 3, 2148–2165 (2011), doi:10.3390/rs3102148
27. Valdivieso, F.O., Sendra, J.B.: Application of GIS and remote sensing techniques in generation of land use scenarios for hydrological modeling. Journal of Hydrology 365, 256–263 (2010), doi:10.1016/j.jhydrol.2010.10.033
28. Verburg, P.H., de Koning, G.H.J., Kok, K., Veldkamp, A., Bouma, J.: A spatial explicit allocation procedure for modellling the pattern of land use change based upon actual land use. Ecological Modelling 116, 45–61 (1999)
29. Verburg, P.H., Schulp, C.J.E., Witte, N., Veldkamp, A.: Downscaling of land use change scenarios to assess the dynamics of European landscapes. Agriculture, Ecosystem and Environment 114, 39–56 (2006), doi:10.1016/j.agee.2005.11.024

LAND COVER CHANGE IN A MEDITERRANEAN CATCHMENT: IMPLICATIONS FOR SOIL EROSION

8th International Geomorphology Conference, Paris, 27-31 August, 2013

H. G. ROY, D. M. FOX, K. EMSELLEM
UMR 7300 ESPACE CNRS, Université de Nice Sophia Antipolis, NICE, FRANCE. (roy.hari.gobinda@etu.unice.fr)

1. INTRODUCTION

The Mediterranean landscape has changed greatly since 1950. Changes in vineyard area and slope have major repercussions on soil erosion. Erosion (**Figs. 1 & 2**) impoverishes the soil and contributes to sedimentation in channels and ports. The study objective was to analyze land cover changes from 1950 to 2008 and evaluate their implications for soil erosion.

Fig. 1: Rills in vineyard

Fig. 2: Severe inter-row erosion

2. SITE DESCRIPTION AND METHODS

The 235 km² Giscle catchment is located in SE France (**Fig. 3**). Roughly 70% of the catchment is upland forest, the remainder is an alluvial plain occupied mainly by vineyards and built areas. Air photos (1950, 1982, and 2008) were digitized to produce land cover maps with 4 categories: forest, vineyard, grassland (mixed pasture & shrubland), and built areas. These data were complemented by a 25 m DEM and field observations. The red line in **Fig. 3** delimits the watershed, the green line shows the window used for land cover maps in **Fig. 4**; most changes occurred in this zone. Land cover results cited are for entire catchment.

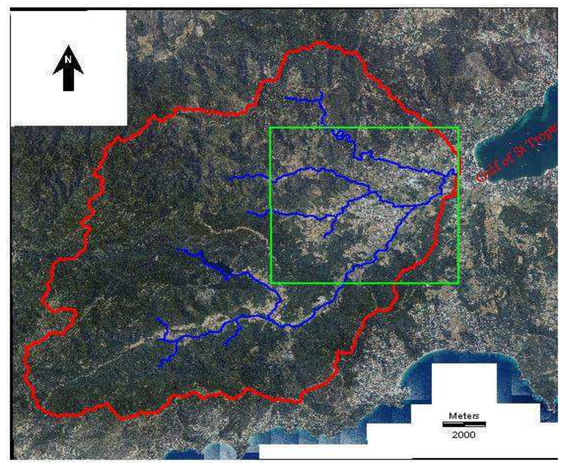

Fig. 3: Catchment location

3. RESULTS AND DISCUSSION

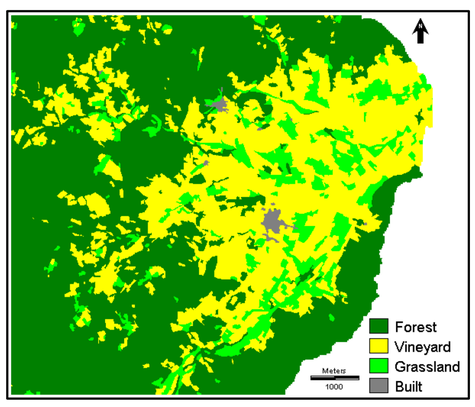

Fig. 4a: Land cover map 1950

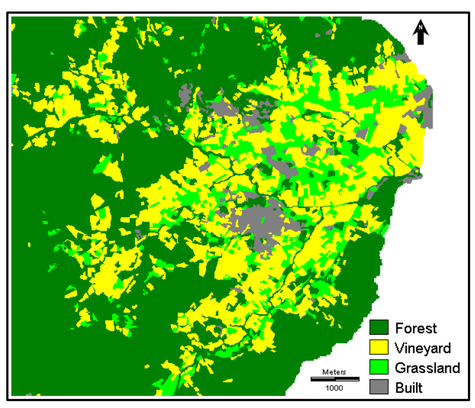

Fig. 4b: Land cover map 1982

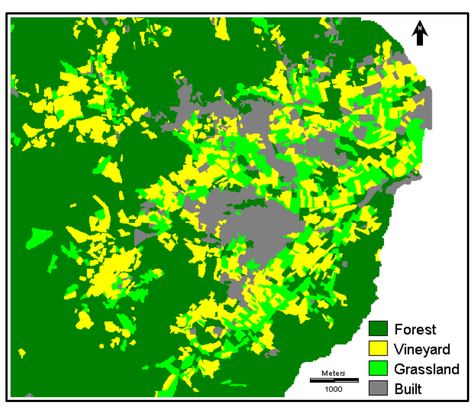

Fig. 4c: Land cover map 2008

3.1 LAND COVER CHANGES

Temporal land cover maps for the alluvial plain are presented in **Figs. 4a-c**. Vineyards decreased from 2,240 ha to 2,089 ha (-151 ha) in 1950-1982, and lost a further 473 ha in 1982-2008 (**Table 1**). Vineyard evolved mainly into grassland and built area.

Grassland increased by 386 ha in 1950-2008. Built area was 32 ha in 1950 and increased to 268 ha in 1982 and then 718 ha in 2008 (net gain of 686 ha).

Fig. 5a: Land cover 1950

Fig. 5b: Land cover 1982

Fig. 5c: Land cover 2008

Figs. 5a-c show examples of land cover change between 1950 and 2008 for a selected site within the alluvial plain. Although built area expansion began before 1982, the rate of expansion accelerated greatly in 1982-2008. Grassland increased overall in 1950-1982, though there was considerable swapping with vineyards and forest over time.

3.2 CHANGES IN VINEYARD SLOPE

Slope is one of the most important factors affecting soil erosion. **Figs. 6a-b** illustrate that vineyard lost most of its area in 1950-1982 on gentle slopes (0-5%), but some of this was compensated on steeper slopes (>5%). In 1982-2008, losses were once again greatest on 0-5% slopes but without any compensation elsewhere. The net 1950-2008 change was a significant loss in area and a shift to steeper slopes (**Table 1**).

Table 1: Changes in vineyard slope and area

	1950	1982	2008
Mean slope (%)	5.5	6.6	7.4
Median slope (%)	3.9	4.5	5.6
Vineyard area (ha)	2,240	2,089	1,616

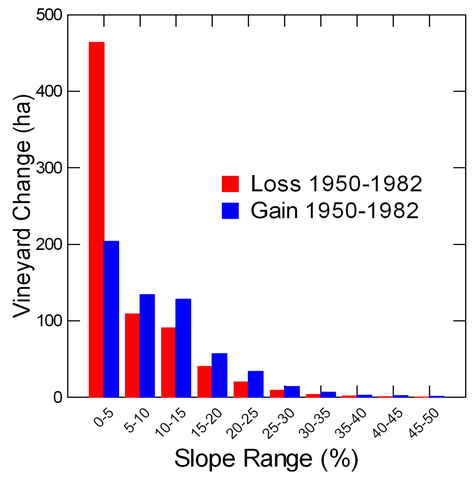

Fig. 6a: Changes in vineyard with slope (%) in 1950-1982

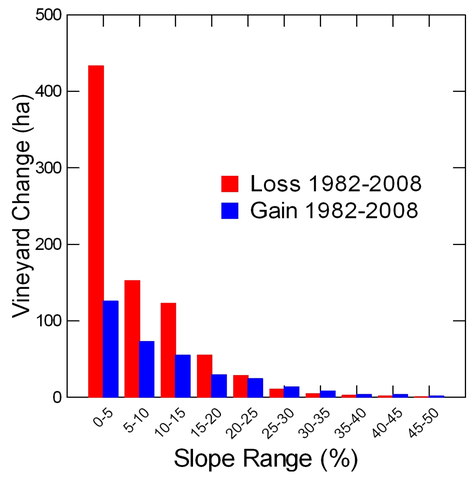

Fig. 6b: Changes in vineyard with slope (%) in 1982-2008

4. DISCUSSION AND CONCLUSION

Vineyard area decreased by 28% in 1950-2008. Under urban pressure, vineyards were converted to built areas and grassland. Mean and median vineyard slopes increased by 34% and 44%, respectively. However, slopes were calculated from a 25 m DEM which does not take terracing (**Fig. 7**) into account, so actual change in vineyard slope is certainly smaller than calculated. The net effect is a probable decrease in overall erosion rate at the catchment scale over time. Attempts to model erosion for each period are currently underway.

Fig. 7: Expansion on steeper slopes accompanied by terracing.